P.G. DEMIDOV YAROSLAVL STATE UNIVERSITY
RUSSIAN ACADEMY OF SCIENCES
VALIEV INSTITUTE OF PHYSICS AND TECHNOLOGY,
YAROSLAVL BRANCH
CENTER FOR COLLECTIVE USE
"DIAGNOSTICS OF MICRO- AND NANOSTRUCTURES"

IV INTERNATIONAL CONFERENCE
ON

MODERN PROBLEMS IN PHYSICS OF SURFACES AND NANOSTRUCTURES

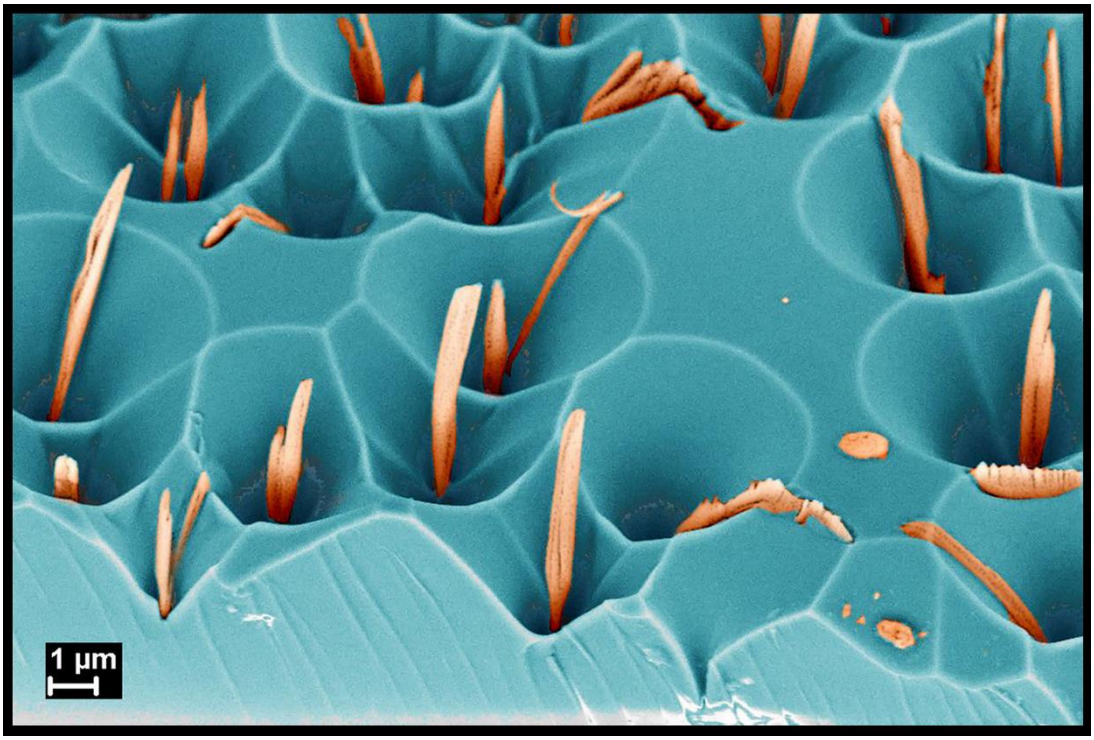

BOOK OF ABSTRACTS

YAROSLAVL, RUSSIA
26-29 AUGUST 2019

International Advisory Board:

Alexander Rusakov, rector of the P.G. Demidov Yaroslavl State University, Yaroslavl, Russia
Vladimir Lukichev, director of Valiev IPT RAS*, Moscow, Russia
Konstantin Rudenko, deputy director of Valiev IPT RAS, Moscow, Russia
Tapio Ala-Nissial, Aalto University, Helsinki, Finland
See-Chen Ying, Brown University, Providence, USA
Talat Rahman, University of Central Florida, Orlando, USA
Enzo Granato, Institute of Space Research, San Jose dos Campos, Brasil
Oleg Trushin, Valiev IPT RAS , Yaroslavl Branch, Yaroslavl Russia
Ildar Amirov, deputy director of Valiev IPT RAS, Yaroslavl Branch, Yaroslavl Russia
Vladimir Bachurin, Valiev IPT RAS , Yaroslavl Branch, Yaroslavl Russia
Alexander Prokaznikov Valiev IPT RAS , Yaroslavl Branch, Yaroslavl Russia

The Local Organizing Committee:

Alexander Rudy (head of orginizing committee), head of Valiev IPT RAS**,
Yaroslavl Branch, Yaroslavl Russia
Oleg Trushin (dep. head of orginizing committee), Valiev IPT RAS , Yaroslavl Branch,
Yaroslavl Russia
Ildar Amirov, deputy director of Valiev IPT RAS , Yaroslavl Branch, Yaroslavl, Russia
Vladimir Bachurin, Valiev IPT RAS , Yaroslavl Branch, Yaroslavl, Russia
Anatoly Churilov, Valiev IPT RAS , Yaroslavl Branch, Yaroslavl, Russia
Alexander Kupriyanov, Valiev IPT RAS , Yaroslavl Branch, Yaroslavl, Russia
Alena Novozhilova, Valiev IPT RAS , Yaroslavl Branch, Yaroslavl, Russia
Tatiana Shalaeva, Valiev IPT RAS , Yaroslavl Branch, Yaroslavl, Russia
Anastasya Pestova, P.G. Demidov Yaroslavl State University, Yaroslavl, Russia

* - Valiev Institute of Physics and Technology, Russian Academy of Sciences

** - Valiev Institute of Physics and Technology, Russian Academy of Sciences, Yaroslavl Branch

Image on the cover – quartz etched in fluorine-containing plasma

Contents

I1-1: Spin-based Electronics: Recent Developments and Trends

Viktor Sverdlov

Christian Doppler Laboratory for Nonvolatile Magnetoresistive Memory and Logic
Institute for Microelectronics, TU Wien, Gusshausstr. 27-29, 1040 Vienna, Austria
E-Mail: Sverdlov@iue.tuwien.ac

Continuous miniaturization of semiconductor devices is the key driving force ensuring breathtaking increase of performance of modern integrated circuits. With chips based on 5nm technology approaching production, the semiconductor industry is focusing on the 3nm technology node [1]. To sustain the growing demand for high performance small area CPUs and high-capacity memory, an introduction of a disruptive technology employing conceptually new computing principles becomes paramount. At the same time, the critically high power consumption becomes incompatible with the global demands of sustaining and accelerating the vital industrial growth, prompting an introduction of new solutions for energy efficient computations. An attractive path to dramatically reduce the power consumption and eliminate leakages in modern integrated circuits is to introduce non-volatility. Magnetic tunnel junctions (MTJs) with large magnetoresistance ratio are perfectly suited as key elements of nonvolatile CMOS-compatible magnetoresistive embedded memory. MTJs possess a simple structure and are characterized by long retention time. A MTJ is a sandwich made of two ferromagnetic layers separated by a thin tunnel barrier. The information can be encoded into two relative magnetization states with parallel (P) or anti-parallel (AP) orientations. Due to the tunneling magnetoresistance effect the resistances of the two states are different and the information can be sensed. The relative configuration of the two layers can switch by means of the spin transfer torque (STT) due to the current passing through the structure. All major FABs claimed to begin production of embedded STT MRAM production in the near future, with the most recent report from Intel [2].

To further reduce the energy consumption, it is essential to replace static RAM in modern hierarchical multi-level processor memory caches with a non-volatile memory. Although STT-MRAM can in principle be used in L3 cache [3], the switching current floating through the tunneling oxide becomes very large at an access time of 5ns and faster. This prevents STT-MRAM from entering in L2 and L1 caches currently mastered by static RAM (SRAM). Three-terminal spin-orbit torque (SOT) MRAM is an electrically addressable non-volatile memory combining high speed, high endurance, and long retention. Recently, IMEC presented a technology to integrate SOT-MRAM on a 300mm CMOS wafer using CMOS compatible processes [18]. For SOT-induced deterministic switching of a perpendicular free magnetic layer a static magnetic field is required. A scheme employing the two orthogonal current pulses is suitable for achieving the sub-ns deterministic switching without an external magnetic field [5].

The electron spin offers an additional functionality to digital switches based on field effect transistors. SpinFETs and SpinMOSFETs are promising devices, with the nonvolatility introduced through the relative magnetization orientation between the ferromagnetic source and drain. Several fundamental problems including spin injection from a metal ferromagnets to a semiconductor, spin propagation and relaxation, as well as spin manipulation by the gate voltage were resolved in order to demonstrate such devices. However, boosting the spin injection efficiency as well as increasing efficient electrical spin control represents the challenges to be resolved before these devices appear on the market.

The introduction of non-volatility to data processing offers outstanding advantages over standard CMOS-based computing. This paves the way for a new low power and high-performance computation paradigm based on logic-in-memory and in-memory computing architectures, where the same nonvolatile elements are used to store and to process the information.

1. G. Bae et al., “3nm GAA Technology Featuring Multi-Bridge-Channel FET for Low Power and High Performance Applications”, IEDM Proc., pp.656-659, Dec. 2018.
2. O. Golonzka et al., “MRAM as Embedded Non-Volatile Memory Solution for 22FFL FinFET Technology”, IEDM Proc., pp.412-415, Dec. 2018.
3. S. Sakhare et al., “Enablement of STT-MRAM as Last Level Cache for the High Performance Computing Domain at the 5nm Node”, IEDM Proc., pp.420-423, Dec. 2018.
4. K.Garello et al., “SOT-MRAM 300mm Integration for Low Power and Ultrafast Embedded Memories”, VLSI Technology and Circuits, 2018, p.C8-2, 2018.
5. V. Sverdlov et al., “Two-pulse Sub-ns Switching Scheme for Advanced Spin-Orbit Torque MRAM”, Solid-State Electron., DOI: 10.1016/j.sse.2019.03.010, in press, 2019.

I1-2: Functional GMR multilayers

M. Milyaev, L. Naumova, N. Bannikova, V. Proglyado, V. Ustinov

M.N. Miheev Institute of Metal Physics of the Ural Branch of the Russian Academy of Sciences, Ekaterinburg, Russia e-mail: milyaev@imp.uran.ru

The exchange-coupled multilayers with giant magnetoresistance (GMR) are one of modern types of functional nanomaterials widely used in different practical applications. Functional characteristics of these nanomaterials can be changed considerably by the choice of multilayer composition, by using of different types of magnetic and nonmagnetic materials and by optimization of a preparation method. The distinguishing feature of functional multilayers is a presence of combination of a number of optimal characteristics being useful for concrete practical applications. The most important functional characteristics include the GMR ratio, saturation magnetic field, sensitivity, hysteresis, temperature stability and linearity of the GMR magnetic field dependence.

The results of experimental researches of different types of GMR multilayers prepared by the magnetron sputtering method will be shown. Namely, the next types of multilayers will be considered: CoFe/Cu with GRM ratio above 80% at room temperature [1, 2], CoFeNi/Cu(~1 nm) with linear change of magnetoresistance for current sensors, CoFeNi/Cu(~2 nm) with different types of ferromagnetic alloys [3], CoFeNi/Cu(~2 nm) with the saturation magnetic field about 100–200 Oe, GMR ratio 25%, high linearity and weak hysteresis (Fig.1). It will be paid attention to the question about an influence of different types of buffer layers on multilayers structure and hysteresis on magnetoresistance curves [4].

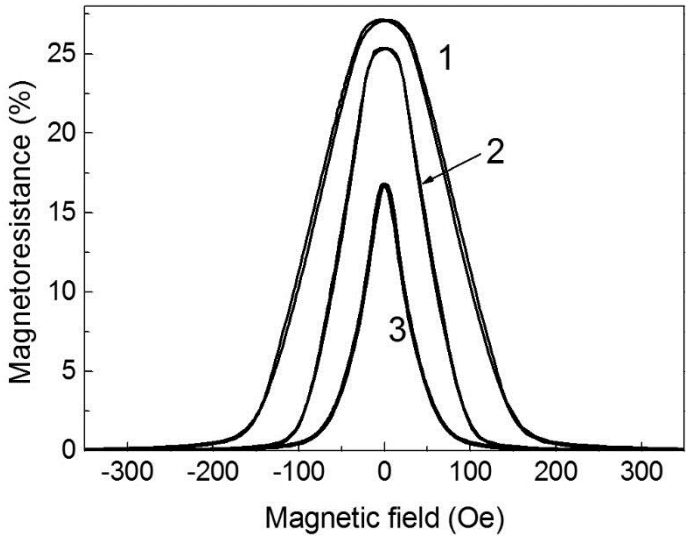

Fig.1. Magnetoresistance curves for CoFe(Ni)/Cu(~2 nm) multilayers with different ferromagnetic alloys: (1) – $Co_{90}Fe_{10}$, (2) – $Co_{70}Fe_{20}Ni_{10}$, (3) – $Co_{23}Fe_{31}Ni_{46}$.

The research was carried out within the theme “Spin” AAAA-A18-118020290104-2 and supported in part by RFBR project No. 19-02-00057.

1. M. Milyaev, L. Naumova, V. Proglyado, T. Krinitsina, N. Bannikova, V. Ustinov, “High GMR Effect and Perfect Microstructure in CoFe/Cu Multilayers”, IEEE Trans. On Magn., **50**, No 4, pp. 2300904(1-4), 2019.
2. N.S. Bannikova, M.A. Milyaev, L.I. Naumova et al., “Giant Magnetoresistance and Hysteresis Phenomena in CoFe/Cu Superlattices with Highly Perfect Crystallographic Texture”, Phys. Met. Metallogr., **119**, No 11, pp. 1073-1078, 2018.
3. M.A. Milyaev, N.S. Bannikova et al., “Magnetoresistance of CoFeNi/Cu superlattices with various composition of ferromagnetic layer”, Phys. Met. Metallogr., 2019 – *in press*.
4. V.V. Ustinov, M.A. Milyaev, L.I. Naumova, “Giant Magnetoresistance of Metallic Exchange-Coupled Multilayers and Spin Valves”, **118**, No. 13, pp. 1300-1360, 2017.

O1-1: Modification of PLD-grown GaAs:Mn layers by pulse excimer laser annealing

Yu. Danilov[1], R. Kryukov[1], A. Kudrin[1], V. Lesnikov[1], A. Nezhdanov[1], A. Parafin[2], S. Plankina[1], O. Vikhrova[1], A. Zdoroveishchev[1], B. Zvonkov[1]

1. *N.I. Lobachevsky State University, Nizhny Novgorod, Russia, E-mail address: danilov@nifti.unn.ru.*
2. *Institute for Physics of Microstructures, Russian Academy of Sciences, Nizhny Novgorod, Russia.*

Highly Mn-doped III-V compounds gain unusual magnetic properties and retain main semiconductor characteristics. Such ferromagnetic semiconductors (FS) can be integrated into spintronics devices, for example, as injectors of spin-polarized current carriers. Mn concentrations, needed for achievement of ferromagnetic behavior, are of several atomic percent (much higher than the equilibrium solubility limit of Mn in GaAs). Therefore, some non-equilibrium methods must be used to create the GaAs:Mn layers. The technique of low-temperature molecular-beam epitaxy is most used. The GaAs:Mn layer, fabricated by this technique, are standard for FSs; typically, these layers have Curie temperature $T_C \leq 110$ K. One another technique combines two non-equilibrium stages: (a) high-fluence implantation of Mn^+ ions into GaAs, and (b) pulse laser annealing (PLA) for restoration of crystal structure and for electrical activation of Mn atoms.

In this work we examine possibilities of a new combination of two non-equilibrium methods: pulse laser deposition (PLD) for fabrication of highly Mn-doped GaAs and pulse excimer laser annealing for augmentation of electrically active Mn portion.

The GaAs layers heavily doped with Mn were grown on GaAs(100) semi-insulating substrates by pulsed laser sputtering of a target composed of undoped GaAs and high-purity Mn. Q-switched YAG:Nd laser with a wavelength of 532 nm and pulse duration of 10-12 ns was used for sputtering. The thickness of the deposited GaAs:Mn layer was ~40 nm. We varied growth temperature (T_g) and Mn concentration (Y_{Mn}).

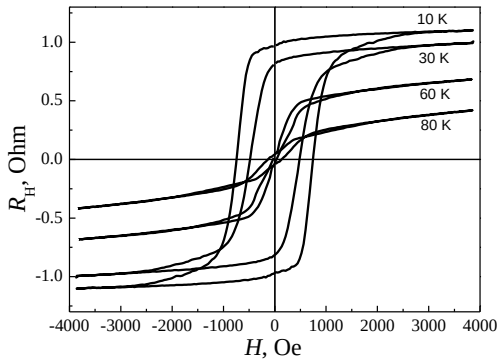

Fig.1. The Hall effect at different temperatures for GaAs:Mn layer (T_g = 350°C, Y_{Mn} = 0.13), annealed by excimer laser pulse (E = 0.29 J/cm^2).

For as-grown PLD layers, the best results were obtained at T_g = 350°C. The layers had p-type conductivity. Low-temperature anomalous Hall effect and negative magnetoresistance (NMR) was observed for $Y_{Mn} \geq 0.13$. The Curie temperature increased to 40 K at Y_{Mn} = 0.23. Concentration of holes in GaAs:Mn layers up to 1×10^{19} cm^{-3} indicates small activation of the Mn atoms.

Experiments on PLA of the deposited GaAs:Mn layers were performed with a KrF excimer laser (wavelength of 248 nm, pulse duration of ~30 ns, pulse energy density E of up to 0.5 J/cm^2). Single pulse laser annealing leads to significant changes in electrical behavior: for $E > 0.23$ J/cm^2, the hole concentration increases by more than an order of magnitude and reaches ~3×10^{20} cm^{-3} in GaAs:Mn annealed at E = 0.27 J/cm^2. On the Raman spectra for annealed GaAs:Mn layer instead of the lines corresponding to LO and TO phonons in as-grown samples, the mode with peak at 259 cm^{-1} dominates. This mode was identified as a coupled phonon-plasmon mode, the emergence of which also indicates a high concentration of free carriers. The results of measuring the Hall effect for excimer laser annealed samples are presented in Fig.1. It can be seen that an anomaly of the ferromagnetic type with a hysteresis loop is observed up to sufficiently high temperatures (250 K – not shown). At low temperatures the hysteresis loop has an almost rectangular shape with a coercive field of ~800 Oe. The NMR occurs up to 250 K. Evaluation of the Curie temperature in excimer laser annealed GaAs:Mn layers gives value of 80 K.

We discuss the reasons of relatively low hole concentration in as-grown PLD GaAs:Mn layer and processes involved at excimer laser annealing. It can be assumed that during the excimer laser pulse the heating and generation of Ga vacancies occurs. Due to the capture of Mn atoms, initially located in interstices, concentration of free holes significantly increases that provokes an augmentation of Curie temperature.

This work was supported by the Russian Science Foundation (grant № 19-19-00545).

O1-2: Problems of quality control at different stages of MTJ fabrication

O. Trushin[1], A. Pestova[2]

[1]*Valiev Institute of Physics and Technology of RAS, Yaroslavl Branch, Yaroslavl, Russia, otrushin@gmail.com*

[2]*P.G. Demidov Yaroslavl State University, Yaroslavl, Russia*

In this work we discuss different experimental methods used for quality control during the process of Magtnetic Tunneling Junctions fabrication. MTJ is an importants ingredient of moderm MRAM cell[1]. As an example case we consider here complete technological cycle from blank wafer to micropatterning of MTJ. We have done analysis of multilayer magnetoresistive structure of the following composition: Ta/CuN/Ta/NiFe/IrMn/CoFe/Ru/CoFeB/MgO/CoFeB/Ta/Ru been deposited using magnetron sputtering on Singulus Timaris cluster tool. On the first stage we carried out complex layer-by-layer chemical and structural analysis of that structure using combination of methods, including cross section TEM, SIMS ION TOF and XRD[2]. On the second stage of the quality control we measured different functional characteristics of multilayer stack, such as magnetization reversal and magnetoresistance. We used home made transverse Kerr effect magnetometer for measurements of magnetization reversal curve of the multilayer structure. Corresponding curve is shown in Fig.1A. Another important characteristic of the multilayer structure is its tunneling magnetoresistance. Direct measurement of this parameter might be done only in CPP (Current Perpendicular Plane) geometry after micropatterning of the structure with creating insulated contacts to the top and bottom layers of the film. However for the purpose of intermediate control the tunneling magnetoresistance can be measured in CIP (Current In Plane) geometry as it has been shown in paper[3]. We performed such measurements with varying the distance between two contacts to the surface of the structure. The results are shown in Fig.1B.

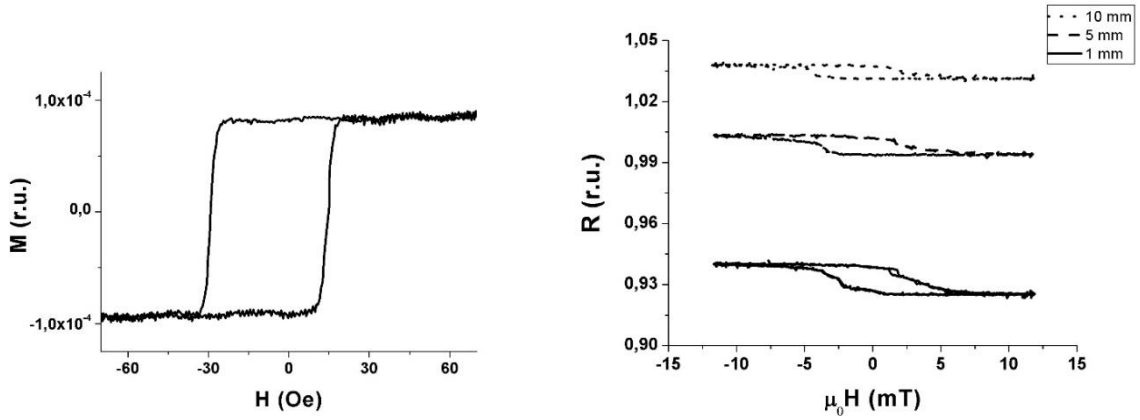

Fig.1 (A) Magnetization reversal measured using Kerr magnetometry, (B) magnetoresistance of unpatterned multilayer structure measured using CIP geometry with different distances between contacts/

As it was expected the magnitude of magnetoresistance is growing with reducing the distance between contacts. From comparing the figures (Fig1A and B) we also observe similar values of switching field obtained by these two methods. In such a way, it might be concluded that combination of different analytical methods gives valuable information about multilayer structures, that might be on demand for quality control in the process of MRAM fabrication. The work has been done under State Programs #0066-2019-0003 of the Ministry of Science and Higher Education of Russia.on the equipment of the center for collective use of the scientific equipment «Diagnostics of micro- and nanostructures»

1. H. Yoda MRAM Fundamentals and Devices in *Handbook of Spintronics*. Edited Yongbing Xu, David D. Awschalom, Junsaku Nitta, pp. 1031-1064, Springer Reference: Heidelberg-New York-London. 2016.

2. O. S. Trushin, S. G. Simakin, S. V. Vasiliev and E. A. Smirnov, “Quality Control of a Multilayer Spin-Tunnel Structure with the Use of a Combination of Analytical Methods”, Russian Microelectronics, 47, pp. 381–387, 2018.

3. D. C. Worledge and P. L. Trouilloud “Magnetoresistance measurement of unpatterned magnetic tunnel junction wafers by current-in-plane tunneling”, Appl. Phys. Lett. 83, pp. 84-86, 2003.

O1-3: Magnetooptical properties of structured surfaces

A. Prokaznikov[1], V. Paporkov[2], N. Zvezdin [2]
1. Yaroslavl Branch of the Institute of Physics and Technology, Russian Academy of Sciences, 150007 Yaroslavl, Universitetskaya, 21
2. P.G. Demidov Yaroslavl State University, 150007 Yaroslavl, Sovetskaya, 14
E-mail: prokaznikov@mail.ru, pva@uniyar.ac.ru, gudzon-88@mail.ru

In the present time, magnetic structures with a complex topology of the formed surface are of special interest due to their potential use in contemporary information technology. This interest is aroused by the connection of special magnetic properties (in particular, chirality, polarity etc.) with the curvature of space. Three-dimensional structures whose dimensions are in the nanometer range are of particular interest. Special properties of such structures make them important to study systems suitable for creating compact 3D magnetic memory. The density of the packing of information increases significantly when the topological objects called skyrmions are used in these devices.
In the present work, the magnetooptical (MO) studies of the magnetic nanostructures created on the surface of a specially treated silicon are presented. The three-dimensional magnetic nanostructures were created by the method of cosputtering two targets with the subsequent deposition of the cobalt layer. We compared the results of the angular dependences and loops of magnetooptical hysteresis for the equatorial magnetooptical Kerr effect obtained on three-dimensional magnetic nanostructures with the results of measurements on nanostructured samples and test samples with uniform nanofilms. These results demonstrate a different behavior. The topological picture of the distribution of magnetic moments in the presence of nonmagnetic defects, as well as in the case of curved surfaces, was plotted by the method of micromagnetic modeling. The defects were demonstrated to promote retention of the boundaries of the domains. The spherical surface contributes to the formation of a vortex structure, which, in addition to a clearly pronounced nucleus, reveals an additional vortex confocal with the original one and partially compensating for it.
The magnetooptical hysteresis loops and the angular dependences of the amplitude values of the transverse magneto-optical Kerr effect (TMOKE) were investigated. The investigations were carried out at room temperature.

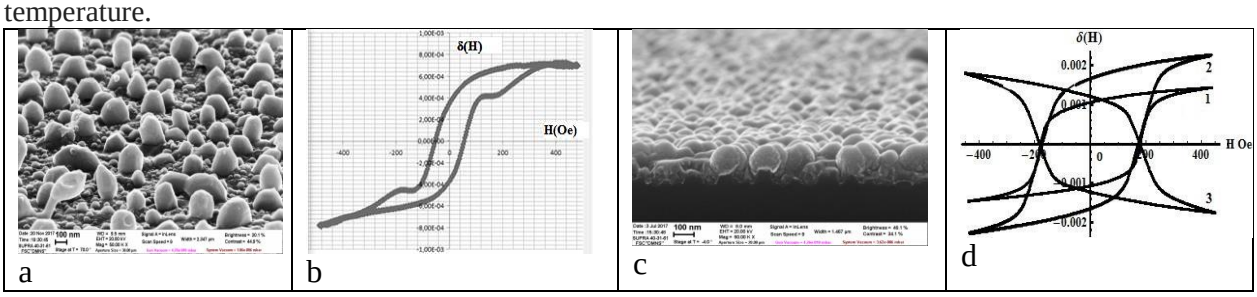

Figure 1. General view of the structure formed after 120 s plasmochemical PbSe etching – (a). TMOKE loop for the structure in (a) with Co film – (b). General view of the structure formed after plasmochemical etching of two spattering targets and Co evaporation– (c). TMOKE loops for the structure in (c) with Co film.

A typical manifestation of occurrence of vortex magnetic structures is appearance of a characteristic plateau at the hysteresis of magneto-optical loop (see Fig. 1b), and the flatter the plateau is, the more stable is the vortex configuration of topological magnetic structure. Investigations have shown that magnetic vortices are observed at a certain ratio between the thickness of the magnetic metal layer and the characteristic size of the structure. In our case, at a thickness of 20 nm the transverse dimensions were 200 nm (see Fig. 1a), and at a thickness of 30 nm the transverse dimensions were about 400 nm. To study the details of formation of magnetic structures in a curved cobalt-based magnetic shell, a micromagnetic simulation was carried out, which relies on a mathematical description of the relaxation process of the magnetic subsystem using the Landau-Lifshitz equation taking into account various mechanisms of interaction of magnetic moments. A vortex domain structure and multivortex states are observed on the spherical surface of nanoobjects obtained by computer simulation with a common center for different vortex domains.
Reported study was carried out under State Programs #0066-2019-0003 of the Ministry of Science and Higher Education of Russia.

I1-3: Multiscale Modeling of 2D Materials with the Phase Field Crystal Method

Tapio Ala-Nissila

Quantum Technology Finland Center of Excellence and Department of Applied Physics, Aalto University, FIN-00076 Aalto, Espoo, Finland, and Interdisciplinary Centre for Mathematical Modelling and Department of Mathematical Sciences, Loughborough University, Loughborough, Leicestershire LE11 3TU, United Kingdom. E-mail address: Tapio Ala-Nissila@aalto.fi

Novel 2D materials have unusual properties, many of which are coupled to their large scale mechanical and structural properties. Modeling is a formidable challenge due to a wide span of length and time scales. I will review recent progress in structural multiscale modeling of 2D materials and thin heteroepitaxial overlayers [1], and graphene and h-BN [2,3], based on the Phase Field Crystal (PFC) model combined with Molecular Dynamics and Quantum Density Functional Theory. The PFC model allows one to reach diffusive time scales at the atomic scale, which facilitates quantitative characterization of domain walls, dislocations, grain boundaries, and strain-driven self-organization up to micron length scales. This allows one to study e.g. thermal conduction and electrical transport in realistic multi-grain systems [3,4].

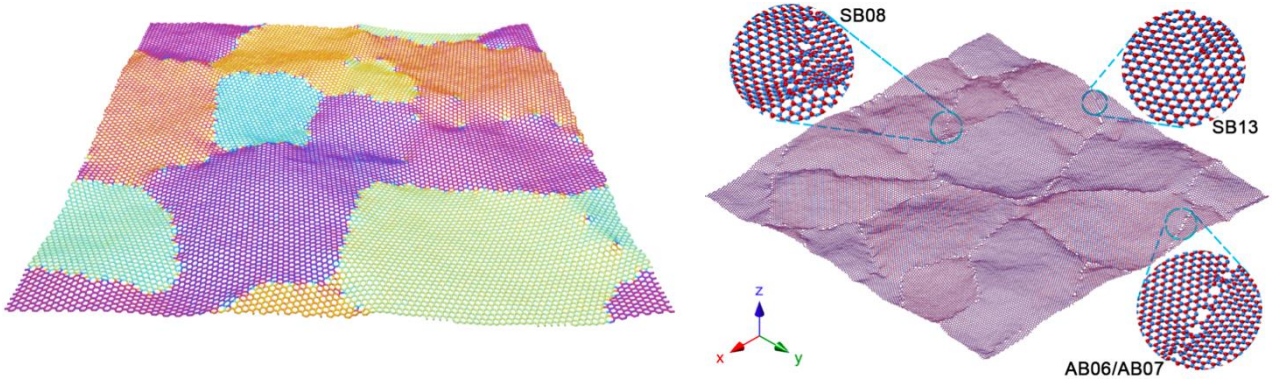

1. K. R. Elder *et al*., Phys. Rev. Lett. **108**, 226102 (2012); Phys. Rev. B **88**, 075423 (2013); J. Chem. Phys. **144**, 174703 (2016).
2. P. Hirvonen *et al*., Phys. Rev. B **94**, 035414 (2016).
3. H. Dong *et al*., Chem. Phys. Phys. Chem. **20**, 4263 (2018).
4. Z. Fan *et al*., Phys. Rev. B **95**, 144309 (2017); Nano Lett. 7b172 (2017); K. Azizi *et al*., Carbon **125**, 384 (2017).

I1-4: Bragg-Laue diffraction excitation of a waveguide mode inside a plane periodic array of magnetic microelements

M. Yu. Barabanenkov[1,2], Yu.N. Barabanenkov[3] , S.A. Nikitov[3]

1.Molecular Electronics Research Institute, Zelenograd, Moscow, Russia 2. Institute of Microelectronics Technology, Russian Academy of Sciences, 142432 Chernogolovka, Moscow Region, IMT RAS, barab@iptm.ru, 3. Kotelnikov Institute of Radio-engineering and Electronics of RAS, Moscow, Russia

We have considered the electromagnetic (EM) wave multiple scattering by the plane periodic array of magnetic microelements in free space, characterizing each element by its magnetic susceptibility tensor and shape. A waveguide mode excitation inside this periodic array is considered analytically by subdividing the EM wave into the averaged and fluctuation components.

We started with an integral equation for the magnetic field vector inside the array and verified that this magnetic field has the form of the Floquet -- Bloch (FB) wave, provided that the incident magnetic field has a similar form. An exact Dyson integral equation was derived for the FB amplitude of in-plane magnetic field averaged over a unit cell of magnetic elements periodic array. We also derived, for the first time, an exact quadrature to calculate magnetic field deviations (fluctuations) from their averaged value. The averaged magnetic field inside the array was determined by solving the Dyson equation and was presented as superposition of eigenwaves with their eigenvalues in dependence on the perpendicular to the array plane coordinate; the Dyson equation solution also describes the reciprocal and nonreciprocal averaged magnetic field reflection from and transmission through the array. We showed that magnetic field fluctuations are generated by the Bragg-Laue diffraction of an averaged magnetic field by the periodic array and are described inside the array as waves propagating with the Laue wave vectors equal to the difference between the in-plane wave vector of the incident magnetic field and the reciprocal lattice wave vector.

These general results were illustrated by the simple Born approximation, which corresponds to the model of mutual dipolar interaction of magnetic nanodots. We made use of an additional supposition concerning the quasi-static approach to the case where an incident EM wavelength is much greater than the sizes of magnetic elements and periods of the array. The case of normal EM wave incidence on the periodic array was also considered.

For numerical estimations we choose after [1] an array of vertically oriented identical cylindrical nanowires with the length of 30 μm, radius of 60 nm, and arranged in a square lattice with the lattice constant of 200 nm. It is assumed that the wires were made of Permalloy with the saturation magnetization of M_s = 800 kA/m and the Gilbert damping constant of α_G = 0.01. Also we choose the diagonal and off-diagonal elements μ and μ_a of the magnetic permeability tensor of wires in close vicinity $\omega \approx \omega_0$ of the ferromagnetic resonance frequency (FMR) ω_0 were according [2] $\mu - 1 \approx \mu_a \approx \frac{\omega_M / \omega_0}{2(1 - \omega / \omega_0 - i\alpha_G)}$ where $\omega_M = \gamma 4\pi M_s$, γ is the gyromagnetic ratio. We put the FMR linear frequency $\omega_0 / 2\pi \approx 3.5$ GHz with corresponding wavelength of the EM plane wave in the free space 8.5 cm. Then, ω_M as $\omega_M / 2\omega_0$ = 0.2.

On this way we found the averaged magnetic field inside the array to be close to the incident magnetic field and the small averaged magnetic field reflection from the array and the value of transmitted averaged magnetic field through the array to be close to the incident magnetic field.

The novel results were obtained in this case of magnetic fluctuations and electric fields accordingly. These fluctuations have the form of waves propagating inside the magnetic elements array with reciprocal lattice wave vectors. These waves excited inside the micro discrete waveguide can be characterized as specific TE modes, with a transverse to the reciprocal lattice wave vector component of electric field fluctuations being of big amplitude because of the evanescent wave nature of EM field fluctuations outside the discrete waveguide. Thus, we revealed a mechanism of discrete waveguide excitation by an incident plane EM wave via the averaged EM wave Brag-Laue diffraction on magnetic microelements.

1. I. Lisenkov *et al*, "Electrodynamic boundary conditions for planar arrays of thin magnetic elements," Appl. Phys. Lett., 107, pp. 082405, 2015.

2. Yu. Barabanenkov *et al*, "Spin wave bound modes in a circular array of magnetic inclusions embedded into a metallized ferromagnetic thin-film matrix," Phys. Rev. B, 91, pp. 214419, 2015.

O1-4: A Monte-Carlo modeling of surface structure of epitaxial Si layers grown using MBE

L. V. Arapkina

Prokhorov General Physics Institute of the Russian Academy of Sciences, Moscow, Russia, arapkina@kapella.gpi.ru

In the report, I present results of investigation of structural properties of epitaxial Si layers grown using molecular beam epitaxy on the Si(001) substrates with miscut from 0.12° to 0.9° toward [110] and [001]. The transfer from the structure with prevailing T_b terraces to the structure with equal T_a and T_b terraces [1] with the increase of the Si(001) substrate miscut has been observed using STM for samples with the miscut towards [110]. The Monte-Carlo simulation of the growth surface structure is provided. The model is based on the assumption that a long-range strain field existing on the surface [2] influences the step permeability. Quantity of ad-atoms Si attaching to a step edge determines the step permeability. In the thermodynamic equilibrium conditions, the strain potential has a symmetric shape (it is usually considered between neighboring steps of the same type (e.g., S_a) and its minimum corresponds to the position of a step of another type (e.g., S_b) [1]) that leads to the formation of terraces with equal areas. S_a and S_b steps are known to have unequal spread rates during the growth. The S_b step spread rate is greater and its edge is a better sink for ad-atoms in comparison with that of an S_a step [3,4]. During the growth, this must lead to forming biatomic D_b steps. If Si(001) substrate miscuts is below ~2° it is typical that monoatomic steps form on the growth surface. For surface structure to be stable during the growth, the spread rates of S_b and S_a steps (quantity of ad-atoms attaching to the edge of a S_b or S_a step per unit time) must be equal. In the proposed growth model, I simulate the influence of the elastic interaction between neighboring S_a and S_b steps on the process of Si ad-atom attachment to step edges. The STM data confirm the modeling results. The samples for STM were grown by MBE (Riber EVA 32) in the step-flow mode; the growth temperature was 650°C. The samples did not leave UHV since they were examined using STM (GPI-300) connected with the MBE chamber.

1. D. J. Chadi, "Stabilities of single-layer and bilayer steps on Si(001) surfaces," Phys. Rev. Lett., 59(4), p. 1691, 1987.
2. O. L. Alerhand, D. Vanderbilt, R. D. Meade, J. D. Joannopoulos, "Spontaneous formation of stress domains on crystal surfaces," Phys. Rev. Lett., 61, p. 1973, 1988.
3. H. J. Zandvliet, "Energetics of Si(001)", Rev. Mod. Phys., 72 (2), p. 593, 2000.
4. Y.-W. Mo, B. S. Swartzentruber, R. Kariotis, M. B. Webb, M. G. Lagally, "Growth and equilibrium structures in the epitaxy of Si on Si(001)," Phys. Rev. Lett., 63(21), p. 2393, 1989.
5. B. S. Swartzentruber, N. Kitamura, M. G. Lagally, M. B. Webb, "Behavior of steps on Si(001) as a function of vicinality," Phys. Rev. B, 47, p. 13432, 1993.

O1-5: Energetics of domain wall in magnetic nanowire

O. Trushin, N. Barabanova
Valiev Institute of Physics and Technology of RAS, Yaroslavl Branch, Yaroslavl, Russia, otrushin@gmail.com

Magnetic nanowires (MN) have attracted new interest in recent years due to rich physics related to the nucleation and propagation of domain walls (DW) in them. Such systems represent good framework for studies of magnetic phenomena at nanoscale. From other side MN is of perspective object for the development of new generation of spintronic devices, such as racetrack memory. While a lot of works have already been published devoted to studies of DW dynamics, not so much is known about energetics of those processes. Physics of DW nucleation and motion can be described within framework of micromagnetic theory. In this work micromagnetic modeling is used to study the energetics of magnetic switching of single-layer permalloy nanowire. The energy landscape of the system is studied using Nudged Elastic Band method. We considered here only relatively narrow magnetic nanowires with in plane magnetization where only Transverse Domain Walls exist. Our model system representing magnetic nanowire consists of rectangular shape single Permalloy nanowire with the following dimensions: length 200 nm, width 20 nm and thickness 5 nm. All calculations were done using standard formulation micromagnetic theory. The following parameters for permalloy film were used: $A=13{,}0*10^{-12}$ J/m, uniaxial anisotropy constant K1=0 J/m3 , saturation magnetization $Ms=8.0\times10^{5}$ A/m , damping constant $\alpha=0.5$. Mesh sizes were 2*2*5 nm. There is complete description of the application of the NEB method within micromagnetic theory given in the paper[1]. This formalism has been implemented on the base of our program code MICROMAG written in Intel Visual Fortran language with the use of elements of object oriented programming. As a result, the program code NEB_MICROMAG has been created[2].

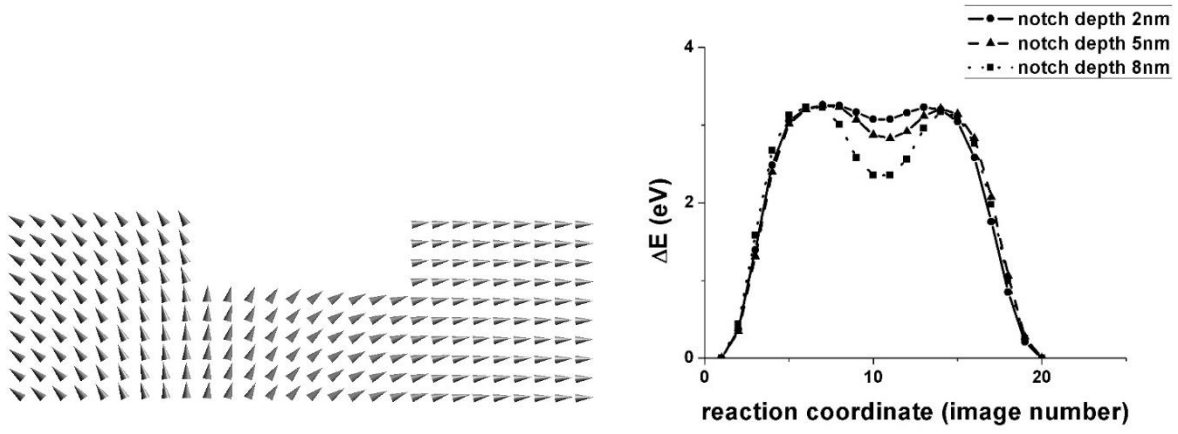

A B

Fig1. (A)Nanowire with rectangular shape notch and (B)corresponding energy profiles along MEP for single DW nucleation and propagation through it with the notches of different depths.

This numerical technique let us explore different minimal energy paths for DW nucleation and motion in magnetic nanowire. For single DW nucleation path we studied dependence of the energy barrier on nanowire geometry. We observed the effect of constant external magnetic field bias on the magnetization switching. Finally, we explored the effect of nanowire imperfections on the energetics of magnetization switching. In particular presence of the rectangular shape notch on the nanowire leads to formation of additional local minimum on the energy profile. This energy minimum corresponds to the pinning of DW (Fig1).

Reported study was carried out under State Programs #0066-2019-0003 of the Ministry of Science and Higher Education of Russia.

1. D. Suess, et al., Phys. Rev. B 75, pp.174430 (1-11), 2007.
2. O.S. Trushin, N.I. Barabanova, “Peculiarities of the Energy Landscape of a Rectangular Magnetic Nanoisland”, Russian Microelectronics 46, pp, 309-315, 2017.
3. O.S. Trushin, E. Granato, S.C. Ying, “Energetics of domain wall in magnetic nanowire”, Proc. SPIE, 11022, p. 110221L, 2019.

O1-6: Surface halogenation of Si crystallites as an efficient means of slowing down internal Auger and radiative processes

N.V. Derbenyova, A.A. Konakov, A.E. Shvetsov, V.A. Burdov
Lobachevsky State University of Nizhny Novgorod, Nizhny Novgorod, Russia, burdov@phys.unn.ru

For more than two past decades, silicon crystallites have been the subject of extensive study, especially, from the standpoint of their use in optical applications. Research activity was traditionally concentrated on searching the ways for increasing the rates of radiative interband recombination and enhancement of the photoluminescence intensity in Si crystallites. Certain success was achieved in this way – many research groups, indeed, reported on the theoretical predictions or the experimental observations of the increase of the radiative recombination rates [1,2], the photoluminescence intensity [3,4], or the quantum efficiency of the photon generation [5]. Nevertheless, the obtained increase of the radiative recombination rates was, as a rule, insufficient to provide highly efficient light emission, because the nanocrystals inherit from bulk silicon its basic property – indirect band gap. At the same time, silicon indirect gap can turn into a positive factor for photovoltaics, where the key process of multiple exciton generation is realized [6]. In this case the indirect band gap could reduce the rates of the main undesirable (for photovoltaic applications) processes – Auger recombination and radiative transitions – lowering the number of electron-hole pairs in a crystallite. Evidently, weakening of both these processes, which are alternative ones with respect to the carrier multiplication, is extremely desirable. It is quite clear that the surface chemistry is one of possible effective methods for modification of the electronic structure and optical properties of crystallites, especially, in the case of their small sizes – of the order of a nanometer. Here, we present the *ab-initio* study of 1 – 2 nm in diameter Si crystallites with fully Cl- or Br-passivated surfaces. It has been shown that halogenation straightens the band structure of Si crystallites in momentum space but strongly separates electron densities of the states above and below the fundamental gap (the so-called LUMO and HOMO states, respectively) in real space. This causes a substantial slowdown, up to several orders of magnitude in the rate values, of the radiative electron-hole transitions whose rates were computed with the use of a time-dependent Density Functional Theory. Similar effect takes place for the Auger recombination – the rates of the Auger process become one-two orders smaller compared to the case of the hydrogen passivation. In contrast to the radiative and Auger recombination, the process of multiple exciton generation is not, in fact, strongly affected by the halogen surface passivation. As our calculations show, typical rates of this process remain at the same level as in the case of hydrogen passivation. Consequently, an essential rise of the internal quantum efficiency (up to the values close to 2 in its maximum) of the multiexciton generation takes place. Such a rise allows one to consider halogenated Si crystallites as very attractive objects for photovoltaics. It should be noted also that saturation of the surface dangling bonds with Cl or, essentially, Br strongly decreases the HOMO-LUMO gap of Si crystallites. This implies that electron-hole pairs can be generated in Cl- and Br-coated silicon crystallites by the photons with lower energies than in H-coated ones or, otherwise, the threshold energy for multiple exciton generation becomes less due to the halogenation. This as well widens opportunities for the use of halogen-passivated silicon crystallites in photovoltaic applications.

1. K. Dohnalova, et al., “Surface brightens up Si quantum dots: direct bandgap-like size-tunable emission”, Light: Sci. Appl., 2, p.e47, 2013
2. N.V. Derbenyova, V.A. Burdov, “Effect of Doping with Shallow Donors on Radiative and Nonradiative Relaxation in Silicon Nanocrystals: Ab-Initio Study”, J. Phys. Chem. C, 122, pp.850-858, 2018
3. V.A. Belyakov, et al., “Improvement of the photon generation efficiency in phosphorus-doped silicon nanocrystals: Γ-X mixing of the confined electron states”, J. Phys.: Condens. Matter, 21, p.045803, 2009
4. K. Nomoto, et al., “Microstructure analysis of silicon nanocrystals formed from silicon rich oxide with high excess silicon: Annealing and doping effects”, J. Appl. Phys. 122, p.025102, 2017
5. F. Sangghaleh, I. Sychugov, Z. Yang, J.G.C. Veinot, J. Linnros, “Near-Unity Internal Quantum Efficiency of Luminescent Silicon Nanocrystals with Ligand Passivation”, ACS Nano 9, pp.7097-7105, 2015
6. I. Marri, M. Govoni, S. Ossicini, “Red-Shifted Carrier Multiplication Energy Threshold and Exciton Recycling Mechanisms in Strongly Interacting Silicon Nanocrystals”, J. Am. Chem. Soc. 136, pp.13257-13266, 2014

I1-5: Memristor and opto-memristor effects in films of non-stoichiometric germanosilicate glasses with nanocrystals and amorphous Ge and GeSi clusters

V.A. Volodin[1,2], G.N. Kamaev[1,2]

1. *Rzhanov Institute of Semiconductor Physics, Russian Academy of Sciences, Novosibirsk, Russia, E-mail volodin@isp.nsc.ru.*
2. *Novosibirsk State University, Pirogova Str. 2, Novosibirsk 630090, Russia.*

Modern information technologies require the development of mega-data centers. The capacity of memory matrices grows exponentially, and the degree of integration of memory elements is already reaching physical limits, which stimulates research and development of new physical principles and new materials for memory elements, the most promising of which are "memristors". With a giant capacity, the energy that needed for re-writing of memristors supposed to be very small. The ideas of optical control of memristor states were proposed several years ago. The possibility of optically stimulated switching of memristors is very promising for creating "optical" computers, simulating human vision and neuron networks [1].

The memristor effect is based on controlled switching of dielectrics to high and low resistance states (HRS and LRS, correspondingly) and is observed in a wide class of different materials [2]. Several years ago the industrial ReRAM based on TaO_x films was developed [3]. Most researchers are studying the memristor effect in metal oxides, but it is very important to develop memristors based on materials that are fully compatible with simple silicon planar technology, such as materials like silicon oxide or germanium oxide.

The advantage of germanosilicate glasses ($Si_xGe_yO_z$ solid alloys) is that the technology of its deposition is simple, not expensive and fully compatible with silicon technology. The peculiarities of these solid alloys are the two possibilities of nanoscale fluctuations of the potential (parameters of the energy bands). The widths of the band gaps in SiO_2 (8-9 eV) and GeO_2 (4-5 eV) differ significantly. It allows modulating the parameters of the traps of the following type - the inclusion of germanium oxides in silicon oxide. Another possibility is the controlled formation of precipitates with excess of germanium atoms (or oxygen deficit regions), which are also charge traps, as well as amorphous nanoclusters and/or germanium nanocrystals.

The studied $Si_xGe_yO_z$ solid alloys films (50 nm) were obtained by simultaneous evaporation of GeO_2 and SiO_2 (or SiO) powders in high vacuum (10^{-8} Torr) and deposition onto n-type, p-type Si(001), or quartz substrates heated up to 100°C. Two types of films were deposited: by evaporation of GeO_2 and SiO_2 sources, with accordance to chemical composition we will mark it as GeO[SiO_2]; and by evaporation of GeO_2 and SiO sources, with accordance to chemical composition it is GeO[SiO] film. The transparent ITO contacts were used as top electrode. The stoichiometry and structure of the samples was determined using electron microscopy, X-ray photoelectron spectroscopy, transmittance and reflectance and Fourier transform infrared (FTIR) absorption spectroscopy. The presence of Ge-clusters in the films was detected from analysis of the Raman spectra. Dark and light-illuminated current-voltage (I-V) characteristics were measured using ammeter and voltmeter setup at room temperature in air atmosphere.

It was found, that as-deposited GeO[SiO] films contain amorphous Ge nanoclusters. It is quite surprising that at such a low temperature of deposition, the following chemical reaction probably occurs: $GeO(solid)+SiO(solid) \rightarrow Ge(solid)+SiO_2(solid)$. The furnace annealings lead to further forming of a-Ge clusters and its crystallization at temperatures 550 °C and higher. The optical gap (absorbance edge) of the films was varied in range 500-700 nm with changing of its structure due to annealing. Better stability of switching was observed in films containing germanium nanoclusters.

So, reversible (many-cycles) resistive switchings from HRS to LRS (memristor effect) were observed for the semiconductor-dielectric-metal structures, namely p-Si (or n-Si)/ GeO[SiO_2] (or GeO[SiO]) /ITO structures in air atmosphere. The structures are "forming-free" and fully compatible with simple silicon planar technology. The effect of light illumination on I-V characteristics of the structures is discussed.

1. S. Chen, Z. Lou, D. Chen, and G. Shen. Adv. Mater., 30, pp.1705400, 2018.
2. D.B. Strukov, G.S. Snider, D.R. Stewart and R.S. Williams, "The missing memristor found", Nature, 453, pp.80, 2008.
3. Panasonic Starts World's First Mass Production of ReRAM Mounted Microcomputers. http://news.panasonic.com/global/press/data/2013/07/en130730-2/en130730-2.html, 2013.

I1-6: Perspective directions of non-volatile memory FeRAM and ReRAM based on thin HfOx layers and their features

O. Orlov [1], G.Krasnikov[1]

1. SC "Research Institute of Molecular Electronics", 124460, Moscow, Zelenograd, , Russia, oorlov@niime.ru

The thin doped HfO_x layers obtained by the atomic layer deposition (ALD) method are a promising material in the capacitor cells of FeRAM and ReRAM memory. FeRAM based on HfO_x has a large number of rewriting cycles up to 10^{11}-10^{12}. But FeRAM has a lesser degree of integration: the minimum size of topological elements is ~ 0.5 μm, which is 2-3 orders of magnitude worse than ReRAM (~ 5 nm). This is due to the fact that the minimum size of topological elements (the area of the ferroelectric capacitor) is determined by the sensitivity of the reading circuits flowing charge during switching. In addition, the FeRAM or ReRAM cell, in contrast to the flash memory cell, has a simpler structure. For today, the achievement of the minimum size of ReRAM topological elements up to 9 nm has been demonstrated, and the miniaturization forecast is 5 nm [2]. Formation of required level of oxygen vacancies of the HfOx layer for ReRAM, (for example-by forming) and the use of an electrode from the oxygen-active material TiN (possibly Ta etc.) on the one hand and the inert electrode Pt on the other hand effectively controls the concentration of oxygen vacancies in the oxide layer and to obtain a stable effect of resistive switching.
In 2011, the ferroelectric effect in hafnium oxide was first discovered, which was considered as a paraelectric material for over a hundred years [3,4]. This effect was observed in thin films of thickness ~ 6-10 nm under the condition of their doping with various elements, including Si, Al, Y, Gd and La, and subsequent high-temperature annealing (~ 1000°C). It is noted that for $Hf_{0.5}Zr_{0.5}O_2$ high-temperature annealing is not required [5]. Ferroelectricity in these materialsis associated with the possibility of stabilization in them of a nonequilibrium central asymmetric orthorhombic phase Pbc21. It is important to note that materials based on hafnium oxide have a number of advantages over traditional ferroelectrics, such as PZT etc., relative to compatibility with traditional processes of modern microelectronics. FeRAM test samples studied in work [6,7] were $TiN/Hf_{0.5}Zr_{0.5}O_2/TiN$. $Hf_{0.5}Zr_{0.5}O_2$ films with a thickness of 10 nm were grown by atomic layer deposition at a temperature of 240°C with the use of $Hf[N(CH_3)(C_2H_5)]_4$ (TEMAH) and $Zr[N(CH_3)(C_2H_5)]_4$ (TEMAZ) precursors and the oxidizer H_2O. The 1T-1C cells with a storage element size of 2 x 2 μm^2 and a thickness of the SE layer of ~ 10 nm demonstrated residual polarization at the level of ~ 15-20 $\mu C / cm^2$ and ~ 10^{10} cycles of state switching . An unsolved problem in the way of development of FRAM-based memory are is a reason of memory window of FeRAM instability during endurance. One of the possible reasons for these effects is the presence of defects in $Hf_{0.5}Zr_{0.5}O_2$ thin films.
Thus, ferroelectric HfO_x is a very attractive candidate for nonvolatile memory applications due to its compatibility with standard complementary metal-oxide-semiconductor (CMOS) [1] processes and high scalability. Thus, the discovery of ferroelectric effect in these materials gave an impetus for the development of the universal memory concept which may lead to a significant breakthrough in the development of memory devices. Comparing FeRAM and ReRAM based on thin doped HfOx layers obtained by ALD we can see that FeRAM is preferable for achievments the maximum number of FeRAM write-rewrite cycles and ReRAM for large packing density.

1. G.Ya. Krasnikov et al. J. Russian Nanotechnologies, 2008, 3, N 7 - 8, p.124-128
2. http://www.itrs.net/ International Technology Roadmap of semiconductors. Редакция 2011 г
3. T. S. Boscke, J. Muller, D. Brauhaus, U. Schroder, andU. Bottger, Appl. Phys. Lett. 99, 102903 (2011)
4. S. Mueller et al., Adv. Function.Mater. 22, 2412 (2012)
5. A. Chernikova et al., J.Microelectron. Eng.147, 15 (2015)
6. O.M.Orlov et al. J.Russian Micr., 46,5,2017, DOI 10.1134/S1063739717050067
7.O.M.Orlov et al., J.Russian Micr., 45,4, 2016, p. 262-269

I1-7: Deep Silicon Plasma Etching: from Bosch process to Polymer-free Approaches for Different Applications

K.V. Rudenko[1], I.I. Amirov[2], A.V. Miakonkikh[1], S.N. Averkin[1], and V.F. Lukichev[1]

1 - Valiev Institute of Physics and Technology of RAS, Nakhimovsky av. 34, 117218, Moscow, Russia,

2- Valiev Institute of Physics and Technology of RAS, Yaroslavl Branch, Universitetskaya str 21, 150007, Yaroslavl, Russia

Deep silicon plasma etching (DSE) processes are in-demand for fabrication of a variety devices including MEMS and NEMS microstructures; Silicon elements of X-ray optics, trench capacitors in DRAMs, and capacitors in RF ICs; isolation trenches for HV devices, TSVs in interposers for 3D-integration of ICs, and others. Each case requires own specification for etched structures but common condition for DSE technologies is relatively high anisotropic etch rate (3 – 20 um/min) of Si and process selectivity to mask > 50:1. Structures for micro- and nanoelectronic application require clean sidewalls to minimize leakage currents and vertical or tapered etching profiles with minimal scalloping or roughness . From other hand the trace polymer contaminations is not issue for MEMS/NEMS devices where the possibility of etching depth up to hundreds microns with high aspect ratio and vertical profile is main demand. Present talk overviews existent and newly developed DSE technologies offering optimal choice for specific demands. Under consideration there are four types of deep silicon etching processes: cyclic original Bosch process [1] and modified one, continuous cryoetch process [2], cyclic STiGer process [3], and new Ox-Etch process [4] developed in Valiev IPT RAS. All processes designed with fluorine chemistry of SF_6 based plasma that provides fastest etch reaction with Silicon enhanced by ion bombardment from plasma. The differences are in approach used to suppress the isotropic etching of the structure sidewalls to achieve required anisotropy and of etch process parameters. Bosch process consisting of sequential alternating steps of etching and polymer sidewalls passivation gives typically scalloping profile and polymer contamination of sidewalls (Fig 1a). The SF_6 plasma step etches the Silicon, and the C_4F_8 plasma steps deposits protection layer. The control of step durations within cycle and *in situ* controlling the wafer bias during etch provides significant reducing scalloping effect up to nanoscale size (~ 10 nm) (Fig. 1b). The price paid for this improvement is a drop in the average etch rate.. More clean cryogenic DSE processes utilizes $Si_xF_yO_z$ passivation layer stable only at cryogenic temperature (< -80ºC). First version is continues regime with SF_6+O_2 plasma, and the second one is gas chopping process SiF_4+O_2/SF_6 which is patented as STiGer etch process. The first gives minimal sidewall roughness (< 5 nm) (Fig. 1c) with control of profile angle, and the second is more fast, also clean but gives scalloping profile similar Bosh process. An alternative clean process was proposed [4] where the layer of stable SiO_x formed as a result of the oxidation of the silicon surface in oxygen plasma is used as a passivant; the etch step is then carried out in SF_6 plasma. As a result new DSE process with clean low roughed sidewalls was designed (Fig. 1d).

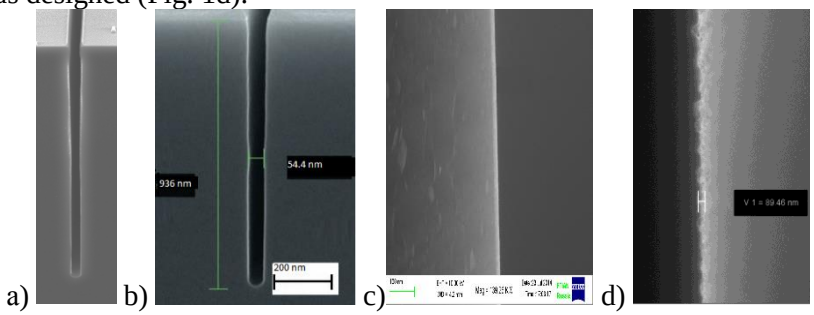

Fig. 1. Etched structures for (a) advanced Bosh process (b) nanoscale Bosch process modified at Valiev IPT RAS (c) sidewall for cryo DSE < 5 nm roughness (d) sidewall roughness in polymer-free Ox-Etch process < 0.1 um

Observed technologies were used to etch trenches for microelectronic applications, TSVs, capacitors, MEMS. Reported study was carried out under State Programs #0066-2019-0002 and #0066-2019-0004 of the Ministry of Science and Higher Education of Russia.

1. Laermer F and Schilp A 1996 U.S. Patent 5501893

2. Tillocher T, Dussart R, Mellhaoui X, et al. Microelectronic Engineering **84 (**2007) 1120-1123.

3 Tillocher T, Dussart R, Overzet L J, et al. J. Electrochem. Soc. **155 (**2008) D187

4. Аверкин С.Н., Мяконьких А.В., Руденко К.В. и др. Положит. решение от 07.05.2019 по заявке №2018130004/28(048577) на выдачу патента РФ.

O1-7: Layer metal nanowires: synthesis, investigation and possible applications

D. Zagorskiy[1] , I. Doludenko[1] , S.Bedin[1] , D. Trushina[1], T. Bukreeva[1], T. Borodina[1],V. Kanevski [1], A. Muslimov [1] , D. Bizyaev[2], A. Shatalov[1], S. Chigarev[3]

1. *Center of Crystallography and Photonics of RAS, Moscow, Russia, dzagorskiy@gmail.com.*
2. *Zavoisky Physical-Technical Institute (KPhTI), Kazan, Tatarstan, Russia. 3*
3. *Kotelnikov Institute of Radioengineering and Electronics of RAS, Fryazino, Russia*

It is known that method of matrix synthesis is one of the ways to create nanoscale structures.The method consists in the galvanic filling of the pores of the matrix with the required material. In this work, polymer track membranes were used, the pores in which were filled with metals (copper and iron group metals) by electroplating. It is important that the matrix synthesis method makes it possible to obtain structures of various types due to successive growth in different electrolytes or by alternating of deposition potentials. The possible applications of the obtained structures consisting of alternating layers of different metals - "layered" nanowires (NWs) -are discussed below.

DRUG DELIVERY. Of great interest is the introduction of magnetic nanowires into capsules for drug delivery. With this, the problem of mechanical destruction of the capsule shell can be solved by rotating the particle in a low-frequency magnetic field. Such a destruction of the shell can be used to "open" the capsule and release the encapsulated medicinal substance. In this paper, a method is proposed for obtaining magnetic particles of a certain composition and a given elongated shape. This is done by synthesizing a heterogeneous NWs from alternating layers of magnetic and nonmagnetic material. After synthesis, the non-magnetic material is removed, resulting in the formation of cylindrical nanoparticles (CNP) of a calibrated size

GMR. For the obtained arrays of layer NWs (Cu / Ni), the dependence of the electrical resistivity on an external magnetic field was investigated. It is shown that if the layers have similar geometric parameters and a thickness of less than 30 nm, then a weak effect of GMR (less than 1%) is observed. The prospects for the use of such structures as sensors are considered.

EMISSION OF ELECTROMAGNETIC RADIATION. Using the so-called "two-bath method", NWs arrays were obtained, consisting of two "layers" of magnetic metals (iron, nickel or cobalt) and including one transition between them. By passing a high-density current through the formed transitions between two magnetic metals, it is possible to detect the generation of electromagnetic radiation. It is shown that radiation occurs in the Terahertz wave region and has a non-thermal nature.

Using the MFM method, it is shown that individual NWs are broken up into domains of 150 nm in size (including several segments of different metals) . These NWs can partially magnetize in an external magnetic field.

Acknowledgements. Synthesis of NWs was supported by RFBR grant No.18-32-01066, SEM measurements- by the State Task of FNIC "Crystallography and Photonics" of RAS.

O1-8: In-void segregated Ag - SnO_2 nano-composite for plasmonic gas sensor

P.I. Gaiduk, S.L.Prokopyev
Department of Physical Electronics and Nanotechnology, Belarusian State University, prosp. Nezavisimosti, 4, 220030, Minsk, Belarus, gaiduk@bsu.by

Tin dioxide is extensively used in many applications e.g. opto-electronic devices, gas sensors and photovoltaic cells. Sensing properties of SnO_2 might be improved by doping with nanoparticles of noble metals which improve chemisorption on the surface and provide a possibility for plasmon-assisted sensing. The idea of this study is to produce SnO_2 -Ag nano-composite for gas sensors by using Kirkendall voids as reservoir for noble atoms.

SnO_2/Ag nano-composite layers were manufactured by magnetron sputtering of 30 nm $Sn_{1-x}Ag_x$ alloy on a fused silica (FS) followed by thermal oxidation in an O_2 ambiance at 450 – 800 ^{O}C for 10 – 30 min. Silver nano-islands and particles were then segregated inside the SnO_2 layer by means of the Kirkendall process followed by segregation (fig.1). Methods and instruments used in the investigation: Rutherford backscattering (2 MeV He^+); PVTEM and TED (200 kV Philips CM20); optical spectroscopy (Perkin Elmer Lambda 1050); RTA system JetFirst-100 with lamp-light illumination.

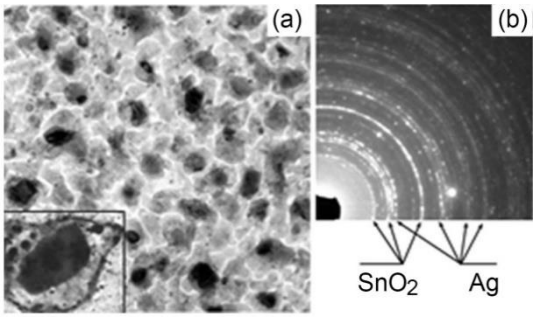

Fig. 1. BFTEM image (a) and SAED pattern (b) obtained from a SnAg alloy layer after deposition and thermal oxidation at 650 ^{O}C for 30 min

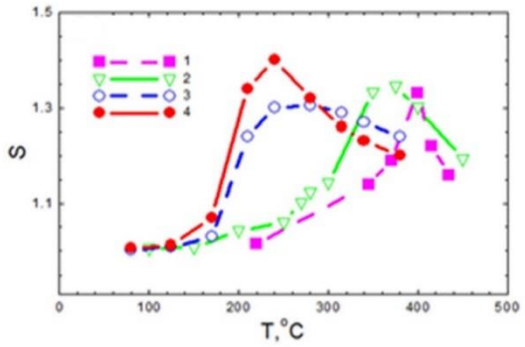

Fig. 2. Sensitivity of SnO_2/Ag sensor as a function of T. 1 and 2 – sensor SnO_2; 3 and 4 - sensor SnO_2/Ag with (4) and without (3) illumination

A plasmonic-based optical sensing effect is demonstrated for selective detection of acetone and alcohol in the temperature range of 200-400 °C. The position of the SPR peak in the transmission spectra depends on the SnO_2+Ag layer quality and gas exposure. A dynamical response of the SnO_2+Ag sensor to methane (CH_4)/air cycles is measured, and the sensitivity of the sensor as a function of the operation temperature and lamp illumination is determined (fig.2). Red- and blue-shifts in the position of the plasmon-resonance peak in optical transmission spectra due to the silver nanoparticles are monitored for different conditions of SnO_2+Ag layer formation and gas exposure. Shorter response time and lower operation temperature of SnO_2/Ag nano-composite sensors are demonstrated.

The concept of plasmonic-based SnO_2 sensors is discussed having in mind two main phenomena: First, the ability of metallic nanoparticles to hold plasmonic resonances which depends on the dielectric properties of surrounding SnO_2 layer and second, the possibility of space-limited heating of nanoparticles and the neighbouring region with light, and in this way to control the chemisorption of oxygen on the sensor's surface.

O2-1: Unsaturated positive magnetoresistance in twisted multilayer graphene

O.V. Kononenko[1] , V.N. Zverev[2] , A.V. Zotov[1] , V.I. Levashov[1] , V.T. Volkov[1] , V.N. Matveev[1]

1. *Institute of Microelectronics Technology and High Purity Materials, Russian Academy of Sciences Chernogolovka, Russia, E-mail address: oleg@iptm.ru 2. Institute of Solid State Physics, Russian Academy of Sciences, Chernogolovka, Russia*

Twisted multilayer graphene grown by CVD technique possess unique characteristics due to high degree of decoupling arising from interlayer twists. Recently, Mogera et al. for the first time demonstrated the possibility of synthesizing twisted multilayer graphene on nickel foil by a modified CVD method. Despite the presence of many layers, twisted graphene demonstrated Raman spectra characteristic of monolayer graphene. In addition, optical absorption bands and other interesting properties were found in the films [1-3].
Multilayer graphene films were grown by the low-pressure chemical vapor deposition (LPCVD) with a single injection of acetylene on an iron film catalyst deposited on oxidized silicon substrate [4]. After treatment of the graphene on the iron film with aqueous solution of iron nitrate the structures consisting of quasi-suspended graphene on reaction products of the iron film with iron nitrate were obtained.
The graphene quality was tested by the SENTERRA Bruker Raman microscope in ambient air and at room temperature. The wavelength of the excitation laser was 532 nm.
The electron transport and magnetotransport properties of the films were investigated. The temperature dependence of the graphene film resistance exhibits the thermally activated (TA) behavior at temperatures above 120° K. At lower temperature the dependence deviates from TA behavior and at temperatures below 40° K becomes close to the variable range hopping conduction. Unusually high positive magnetoresistance (MR) at a room temperature (100% in the magnetic field of 0.5 T) was found in the films. The MR was measured at a temperature 0.5 K in the magnetic fields (up to 16.5 T) normal to the film plane. In low fields up to ~ 0.005 T negative MR was observed, caused by weak localization (WL). In magnetic fields above ~ 0.005 T, the MR increases with increasing magnetic field and becomes positive with quadratic magnetic-field dependence in the fields up to ~ 0.03 T and quasi linear dependence in the fields higher than ~ 0.03 T. No saturation was observed in the fields up to 16.5 T.

1. U. Mogera, R. Dhanya, R. Pujar, C. Narayana and G.U. Kulkarni, “Highly Decoupled Graphene Multilayers: Turbostraticity at its Best” J. Phys. Chem. Lett., **6**, pp.4437–4443, 2015.
2. U. Mogera, N. Kurra, D. Radhakrishnan, C. Narayana, and.U. Kulkarni, “Low cost, rapid synthesis of graphene on Ni: An efficient barrier for corrosion and thermal oxidation” Carbon, **78**, pp. 384-391, 2014.
3. U. Mogera, S. Walia, B. Bannur, M. Gedda, and G.U. Kulkarni, “Intrinsic Nature of Graphene Revealed in Temperature Dependent Transport of Twisted Multilayer Graphene” J. Phys. Chem. C, **121**, pp 13938–13943, 2017
4. O.V. Kononenko, V.N. Matveev, D.P. Field, D.V. Matveev, S.I. Bozhko, D.V. Roshchupkin, E.E. Vdovin, A.N. Baranov, “Investigation of structure and transport properties of graphene grown by low-pressure no flow CVD on polycrystalline Ni films” Nanosystems: Physics, Chemistry, Mathematics, **5**, pp 117–122, 2014

O2-2: Experimental observation of the intermediate phases of the graphite-diamond transition

A.S. Rudy, S.V. Vasil'ev, M.E. Lebedev, A.A. Mironenko, I.S. Fedorov, A.B. Churilov
Valiev Institute of Physics and Technology of Russian Academy of Sciences, Yaroslavl Branch, Yaroslavl, Russia
E-mail: rudy@uniyar.ac.ru

As it is known, a low-energy methods of carbon films deposition, for example, magnetron sputtering, results in the formation of an amorphous ($\alpha-C$) films. The latter are characterized by a graphite-like sp^2-states, since the energy of magnetron deposition is insufficient for the preferential formation of sp^3-bonds. However, due to the low energy of plasma ions, the method of magnetron sputtering allows to obtain intermediate orthorhombic and hexagonal intermediate phases of the graphite-diamond structural transition. These phases are quite difficult to detect, because they are metastable and degrade in the process of measurement, being subjected to ionizing radiation.

The carbon films under analysis have been obtained by magnetron deposition on single crystal silicon (100) with a titanium sublayer with a thickness of 20 and 40 nm at the installation Oratoria 22. The thickness of the films ranged from 80 to 180 nm. The films were studied by scanning electron microscopy (SEM), Raman spectroscopy (RS) and X-ray diffraction methods. According to the SEM the films have a crystalline structure with lateral crystallite sizes varying from 10 to 20 nm. The crystallites are elongated in the direction perpendicular to the surface, what in turn leads to the appearance of peaks of significantly different widths at X-ray diffraction patterns.

To increase the efficiency of Raman scattering, carbon films were coated with a silver layer 5 nm thick. Alongside with stripes, characteristic for diamond-like films, a peak at 518 cm^{-1}, belonging to a silicon substrate, is observed in all spectra. The band in the region of 730-740 cm^{-1} refers to the diamond-like carbon phase, in which quadruple valence bonds prevail over triple and double bonds [3]. According to [4], this is a very wide band with a half-width varying from 400 to 800 cm^{-1}. It is usually observed in the SERS spectra (surface-enhanced Raman spectroscopy) of CVD-diamond films (diamonds grown by chemical vapor deposition) deposited on Ag substrates and at the early stages of growth. D- and G-peaks' form corresponds to the α-C phase. The position of the peaks, determined as the result of their separation and approximation by the Voigt function, shows that the deposition of silver film shifts all carbon peaks into the short-wave region.

X-ray phase analysis of carbon films was performed on a powder diffractometer ARL X'tra, while diffractograms (fig. 1) were identified on the basis of the ICDD PDF-2 database. According to these data a peak with an interplanar distance of 2.715 Å relates to a silicon substrate, to the atomic plane (200). For pure silicon, this peak is forbidden, but in the case of doped silicon the degeneracy is removed due to small distortions of the crystal lattice by impurity atoms. The intensity of this peak is somewhat different from measurement to measurement, what is explained by slight changes in the orientation of the silicon wafers.

In accordance with the ICDD PDF-2 database, peaks with an interplanar distance of 2.773 Å and 2.76 Å were assigned to a transitional phase with an orthorhombic structure (card 01-089-8492) and the symmetry group Cmma (67). These peaks indicate that the film has two characteristic sizes - 10 and 40 nm, what is confirmed by the SEM image, which shows that the crystallites are elongated in the vertical direction. Peaks with an interplanar spacing of 2.65 Å and 2.63 Å were assigned to a transition phase with an orthorhombic structure of the Pban (50) symmetry group (card number 01-089-8494). The size of these crystallites is about 10 nm.

According to the ICDD PDF-2 database, these peaks belong to the hypothetical orthorhombic phases formed during the graphite-diamond transition . The existence of these phases was predicted in [5] in the framework of the model of a continuous structural phase transition from graphite to diamond. The transition consists of several stages of successive compression of the graphite's structure in different directions. As a result of compression, some stable theoretical carbon structures arise, including the diam_cr43_ch and diam_cr44_bo mentioned above (denotations of paper [5]). The first structure is characterized by the presence of both tetrahedral (sp^3) and flat (sp^2) configurations of carbon atoms. The second structure has only tetrahedral sp^3 bonds.

At X-ray diffraction patterns of carbon films deposited at the maximum magnetron power, there is a broad intense peak corresponding to an interplanar distance of 2.74 Å. In accordance with the ICDD PDF-2 database, this peak was assigned to a transition phase of a hexagonal structure (Diamond-8H in the Ramsdell notation, a sequence of diatomic layers AaBbCcBbAaCcBbCc, card 01-079-1471) and the P63/mmc (194) symmetry group. This phase is related to lonsdaleite (Diamond-2H, a sequence of diatomic layers of AaBb) and has a structure similar to it. Thus, the structure of some allotropic carbon modifications can be represented as periodic sequences of folded diatomic layers, differing only in the folding method and the number of layers in the unit cell. The structure of lonsdaleite is thus described as a periodic sequence of carbon layers of 4-atom's "height", while Diamond-8H is a sequence of layers of 16-atom's "high" [6]. The peculiarity of all these phases is that they are metastable and after several X-ray irradiation cycles their peaks disappear completely.

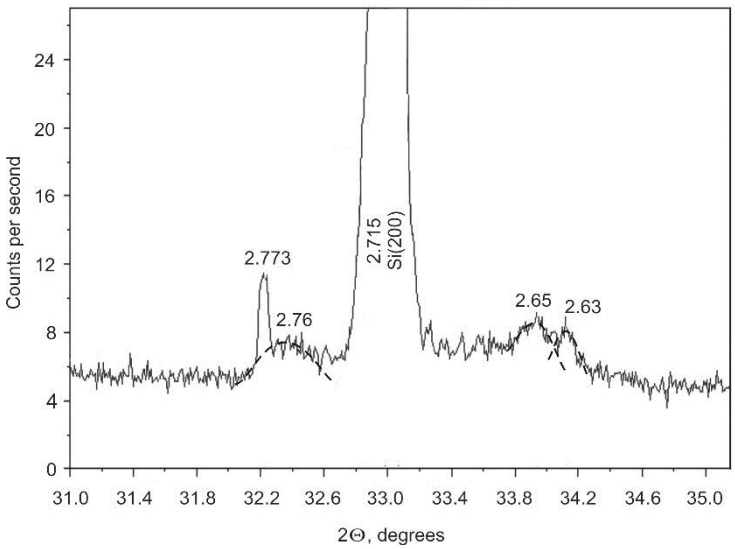

Fig. 1 - X-ray diffraction pattern of the sample, obtained on an ARL X'tra powder diffractometer. The step is 0.01°, the counting time in a point is 40 s. The corresponding interplanar distances are indicated above the peaks. Carbon phases were identified in accordance with ICDD PDF-2 database

Based on the above experimental data, it can be concluded that the peaks observed in the Raman spectra in the region of 740 cm^{-1}, and X-ray peaks corresponding to interplanar distances of 2.773Å, 2.76Å, 2.74 Å, 2.65Å, 2.63Å, belong to transitional structural phases of nanodiamond. It should be noted that these phases are formed only when carbon is deposited on a silicon substrate. Carbon films deposited under the same conditions on the titanium foil and the steel substrate dont found these peakst neither on X-ray diffraction patterns nor in the Raman spectra. It can be assumed that the formation of transitional phases of nanodiamond is affected by the crystal structure of silicon. At the same time, the presence of an adhesive layer of titanium on silicon as well as its thickness do not affect the intensity of these peaks in the Raman and X-ray defraction spectra.

The work was performed as part of the state task of the Ministry of Science and Higher Education of the Russian Federation with the financial support of the Government of the Yaroslavl Region (Grant Agreement No. 38 / 04-2017 of December 29, 2017).
The work was performed on the equipment of the facilities sharing center "Diagnostics of micro- and nanostructures".

1. Ferrari A.C., Robertson J. // Phil. Trans. R. Soc. A., 362 (1824), pp. 2477-2512, 2004. DOI: 10.1098/rsta.2004.1452
2. Robertson J. // Mat. Sci. Eng. R., 37. pp. 129-281, 2002. DOI: 10.1016/S0927-796X(02)00005-0
3. Lopez-Rios T. // Diamond and Related Materials, 5. pp. 608-612, 1996. DOI: 10.1016/0925-9635(95)00457-2
4. Zaitsev A.M. Optical Properties of Diamond. A Data Handbook. Springer-Verlag Berlin Heidelberg GmbH, 2001. 502 p. DOI: 10.1007/978-3-662-04548-0
5. Fayos .J. // J. Solid State Chem.,. V.148. pp. 278-285, 1999. DOI: 10.1006/jssc.1999.8448
6. Ownby, P.D., Yang, X. / J. Am. Ceram. Soc., 75, pp. 1876, 1992. DOI: 10.1111/j.1151-2916.1992.tb07211.x

O2-3: Unusual properties of polytetrafluoroethylene films filled with graphite nanoplatelets

Y.M. Shulga[1,2], A.V. Melezhik[3], E.N. Kabachkov[1], N.N. Dremova[1], N.V. Lyskov[1], V.N. Vasilets[4], A. G. Tkachev[3]

1 Institute of Problems of Chemical Physics RAS
142432, Chernogolovka, prosp. Academician Semenov, 1
2 National Research Technological University "MISiS",
119049, Moscow, Leninsky Prospect 4
3 Tambov State Technical University
392000, Tambov, ul. Leningradskaya, 1
4 Branch of the Institute of Energy Problems of Chemical Physics. V.L. Talrose RAS
142432, Chernogolovka, prosp. Academician Semenov, 1
Email: yshulga@gmail.com

In [1], using a 3D printer, a current collector for a supercapacitor was manufactured from a commercially available polylactone filament filled with carbon-based nanomaterials. Current collectors showed, in principle, good conductivity and stability in an acidic environment, but they lost their flexibility at a thickness of more than 200 μm.

In the present work, nine flexible polytetrafluoroethylene (PTFE) composite films with graphite nanoplatelets (GNPs) were obtained. The content of GNPs in films varied from 2 to 20 mass. %. The films were characterized by various physico-chemical methods. The purpose of this report is to describe the unusual results obtained in the study of the films.

As a source of PTFE were chosen water suspension F-4D (Kirovo-Chepetsk Chemical Company (URALCHEM Group), TU 6-05-1246-81). The suspension contained PTFE, surface-active compound (SAC) as a stabilizer and water in the proportion 6:1:3. GNP was obtained from OOO NanoTechCenter as a paste with the content of 15 mass. % of GNP. Other ingredients of the paste were SAC and water. According to the producer specification, GNPs in the paste consisted of sheets of graphene with an overall thickness of 3-10 graphene layers and a diameter of 2-10 μm (aspect ratio was not less than 570). Methods of GNPs production are described elsewhere [2].

Indeed, the bulk conductivity of the studied samples (σ) increases by almost 4 orders of magnitude from the value of 9.5×10^{-4} S/cm for a sample with an GNPs content of 2 mass. % to a value of 20.4 S/cm for a sample with an GNPs content of 20 mass. %. The percolation threshold for GNPs in the PTFE matrix is in the region of 2 mass. %.

It was unexpectedly found that the surface of the composite film becomes superhydrophobic (the contact wetting angle exceeds 150 °) with a GNPs component content of 15 mass. %. The surface of such a film consists of randomly folded sheets of polymer and graphite plates decorated with polymer. The height of local maxima reaches 500 nm. The ratio [C/F] at on the surface (1.48) substantially exceeds that in the volume (0.87). The film volume consists of 1) sheets (tapes) of the polymer, 2) decorated with polymer graphite plates and 3) long polymer filaments. From the XPS spectra, it follows that with the described procedure for obtaining films (annealing at 370 °C) chemical bonds are formed between GNPs and polymer chains.

Note also that small additions of GNPs (2-6 mass. %) lead to an increase in the melting point, the enthalpy of melting and the degree of crystallinity of PTFE. This effect is attributed to the fact that GNPs serve as centers of additional crystallization of PTFE from the melt.

1. S.A. Baskakov, Y.V. Baskakova, N.V. Lyskov, N.N. Dremova, A.V. Irzhak, Y. Kumar, A. Michtchenko, Y.M. Shulga, Electrochimica Acta, **260**, 557 (2018).
2. Melezhik AV, Pershin VF, Memetov NR, Tkachev AG. Nanotechnologies in Russia, **11**, 421 (2016)

O2-4: Compisition materials on the base of nano- and microcarbon materials and biocompatible calcium phosphates

N. Zakharov[1], E. Shelechov[2], A. Aliev[3], V. Matveev[3], E. Koval[1], T. Zakharova[1]

1. *Kurnakov Institute of General and Inorganic Chemistry of Russian Academy of Sciences, Moscow, Russia, E-mail: zakharov@igic.ras.ru, 31, Leninskiy prisp., Moscow, 119991, GSP-1. 2. NITU, MISiS, 4, Leninskiy prisp., Moscow, 119049. 3. Frumkin Institute of Physical Chemistry of Russian Academy of Sciences, Moscow, Russia, E-mail: zakharov@igic.ras.ru, 31, Leninskiy prisp., Moscow, 119991, GSP-1.*

Several examples are given of development of streamlined synthesis and analysis of fundamental composition – synthesis conditions – structure – dispersity – properties interactions of composition materials (CM) on the base of nano- and microcarbon materials (NMCM) (carbon nanotubes, graphene oxide, fullerene containing materials, carbon fibers) and biocompatible nanosized calcium hydroxyapatite $Ca_{10}(PO_4)_6(OH)_2$ (HA) (NCHA) in compositions of CM HA/NMCM.

The actuality of this investigation defined of goal of effective materials creating for medical applications, that posses of improve biocompatibility, physical, chemical, medical and biological properties. Percpectives of NMCM use for preparing CM for medical use and grow application, that materials in industry make make actual the problem definition of singularities of NMCM and native tissues interactions, in particular, interaction with bone. Stoichiometrical HA is a crystallochemical analog of bone inorganic component. The creating of CM on the base of HA and NMCM is a perspective way for improvement mechanical characteristics of materials on the base of HA and estimation of possible influence of NMCM materials on the mineralized native tissues.

The results of this work include of creating of synthesis methods of CM HA/NMCM for application in medical practice, estimation composition influence, synthesis conditions, NMCM type on the morphology, physical, chemical, medical and biological properties of NMCM in CM composition, estimation perspectives of new materials application in medicine.

This work was made within the scop of state task KIGIC RAS in the area of fundamental scientific investigations.

O2-5: Techniques of synthesis of reduced graphene oxide-$LiNi_{0,33}Mn_{0,33}Co_{0,33}O_2$ composites as cathode materials for lithium-ion rechargeable battery

D. Kornilov

Limited Liability Company «AkKo Lab», Moscow, Russia, e-mail:kornilovdenis@rambler.ru

Nanomaterials of various composition and morphology are widely used in research works on creation of innovative electrodes for LIB [1]. Despite of large number of commercially available LIBs types they do not meet the requirements of various consumers, both military and civil. There is a need of increase of capacity, rate of the charge/discharge, cycle-life, decrease in cost value of LIB, reduction of toxicity and fire danger. This initiates a search of new materials [2, 3] and batteries manufacturing technology that would allow producing light, compact and more capacitive devices of energy storage.

One way of solving these problems is use of a graphene as a part of the electrode material [4]. Graphene has a high conductivity, a high surface area (2640 $m^2 \cdot g^{-1}$) and capabilities of withstanding the enormous current density (more than 10^7 $A \cdot cm^{-2}$). Maximum of charge carrier mobility in single-layer graphene at room temperature is200,000 $cm^2 \cdot V^{-1} \cdot s^{-1}$. Graphene is the most durable material (Young's modulus 1TPa) and it can be subjected to considerable deformation without breaking the crystal lattice. The next advantage in favor of the use of graphene in the LIB is the use of its derivatives, such as graphene oxide. At this time the graphene and graphene oxide are made by a row of companies and these materials are quite available.

This work shows results of research which focused on a modification of lithium-ion rechargeable battery cathode material $LiNi_{0.33}Mn_{0.33}Co_{0.33}O_2$ by reduced graphene oxide coating. The techniques of coating is ultrasonic dispergation of graphene oxide alcoholic solution with cathode material powder. Investigated cathode materials powders as completely (fig. 1a) covered dense of reduced graphene oxide layers as and not in full coated (fig. 1b). The physical property and electrochemical performance of the cathode materials were characterized by X-ray diffraction, Raman spectroscopy, scanning electron microscopy, cyclic voltammetry, charge/discharge testing. The promising results demonstrated synergetic effect from modification of cathode material by reduced graphene oxide coating which showed buildup of power density from 0,1C to 1C with not big decaying of energy density from 154 mAh/g to 178 mAh/g. Research work results can be used for batteries making.

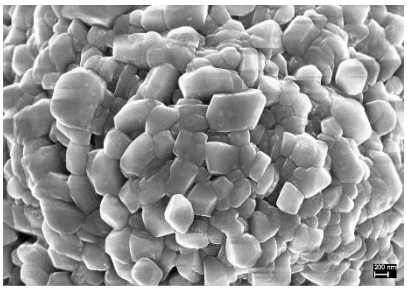

a

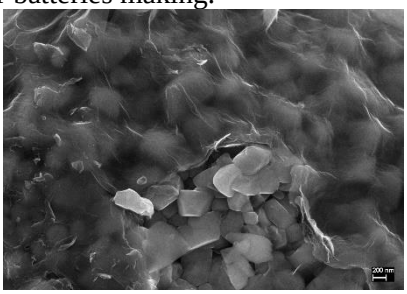

b

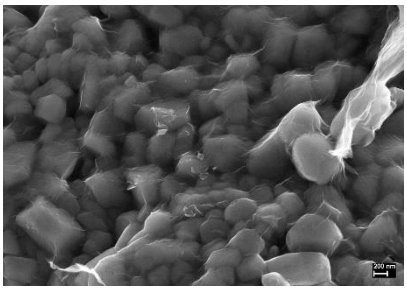

c

1. Yaroslavtsev A. B., Kulova T. L., Skundin A. M. Electrode nanomaterials for lithium-ion rechargeable battery // Russ. Chem. Rev. 2015. 84. P. 826-852

2. Wu Y. Lithium-ion Batteries Fundamentals and Applications / NW. Taylor & Francis Group. 2015. 568.

3. Goodenough J., Park K. The Li-Ion Rechargeable Battery: A Perspective // J. Am. Chem. Soc. 2013. 135. P. 1167−1176

4. Ferrari A. Science and technology roadmap for graphene, related two-dimensional crystals, and hybrid systems // Nanoscale. 2014. DOI: 10.1039/C4NR01600A

O2-6: Heat transfer enhancement by graphene nanofluids

N. Savinski[1], D. Puhov[1], M.Lebedev[1], S.Vasilev[1],
R.Gorshkov[2], A. Zharov[2], L.Mazaletski[3]

1 Valiev Institute of Physics & Technology of Russian Academy of Sciences, Savinski1@yandex.ru
2 Yaroslavl State Technical Universities, Russia
3 P G. Demidov Yaroslavl State University. Russia

The electronics industry has tended to deal with overheating more at the system level using cooling fans, for instance, to regulate rising temperatures inside computers. The higher circuit densities and faster clock speeds are making chips run so hot that manufacturers can no longer ignore the problem. According to the International Technology Roadmap for Semiconductors (ITRS), which reflects a consensus of chip manufacturers worldwide, managing heat generation within ICs will be a crucial issue in developing the next generation of electronics. Growing concern has in turn sparked new research into chip designs and novel materials that would allow electronics to run much cooler, thereby improving their performance and extending their life span. Innovative heat transfer fluids consisting of suspended nanometer-sized solid particles are called "nanofluids." Nanofluids can be considered to be the next-generation heat transfer fluids as they offer exciting new possibilities to enhance heat transfer performance compared to pure liquids. The enhancement of the thermal conductivity is the key idea to improve the heat transfer characteristics of conventional fluids. Dispersion of nano-sized particles of different materials (metals, metal oxides, etc.) in a carrier fluid known as nanofluids has been a subject of intensive investigations over decades due to their potential applications in heat transfer and electronic cooling [1–4]. Multi Layer Graphene (MLG) obtained by electrochemical exfoliation of commercial graphite foil "Graflex" production of the Russian Federation. The essence of the electrochemical exfoliation method is the diffusion of ions from the solution into the interlayer space of graphite layers under the action of an electric field, in the presence of DMSO radical traps. The surfactant PolyVinylPyrrolidone (PVP) is first added to the base fluid and then after stirring, the MLG is added. The mixture is sonicated for 48 hours using an ultrasonic vibrator to break down agglomeration of the nanoparticles. The MLG – water nanofluid is prepared for different volume concentrations of 0.2- 0.75% by suspending the required amount of MLG and PolyVinylPyrrolidone (PVP). The MLG is characterized by a scanning electron microscope, to study the shape, size and phase distribution. The transient hot wire method is used for measuring the thermal conductivity of liquids. In this method, the rate of rise in temperature of the micro wire for an applied voltage with time is used to determine the thermal conductivity of the fluid. Heat flux generated in the micro wire due to the supply of voltage is transferred to the static fluid around it. The higher the thermal conductivity of the fluid, the lower the temperature rise of the wire will be. The thermal conductivities of graphene–water nanofluid with 0.2-0.75% volume concentrations and temperatures from 25 to 60 °C are experimentally studied. Enhancements in the thermal conductivity ratio of up 20 to 60 % have been observed for 0.2% volume concentration at 25 °C and 0.75% at 60 °C respectively. The work has been done under State Programs #0066-2019-0003 of the Ministry of Science and Higher Education of Russia.

1Novoselov, K. S.; Geim, A. K.; Morozov, S. V.; Jiang, D.; Zhang, Y.; Dubonos, S. V.; Grigorieva, I. V.; Firsov, A. A. "Electric Field Effect in Atomically Thin Carbon Films." Science, v. 306,pp.666, 2004.

2 W. Miao, G. Shim, S. Lee, Yu-K. Oh "Structure-dependent photothermal anticancer effects of carbon-based photoresponsive nanomaterials" Biomaterials 35, pp.4058-4065,2014

3 Zhiping Xu "Heat transport in low-dimensional materials: A review and perspective"/ Theoretical and Applied Mechanics Letters 6, pp.113–121, 2016

4 T.T.Baby, S Ramaprabhu "Investigation of thermal and electrical conductivity of graphene based nanofluids"/ J. Appl. Phys. v108, 124308, 2010

O2-7: Influence of surface ordering of smectic films on their stability and layer-by-layer phase transitions

P.V. Dolganov[1] , N.S. Shuravin[1] , V.K. Dolganov[1]

1. *Institute of Solid State Physics, Russian Academy of Sciences, Chernogolovka, Moscow Region, Russia, pauldol@issp.ac.ru*

Smectic liquid crystals are composed by elongated molecules and have layered structure. They can form free-standing (substrate-free) films with thickness only several molecular layers and macroscopic lateral size. In such films surface ordering plays an important and even crucial role. Due to surface ordering thin films can exist in the translationally ordered state above the temperature at which the bulk sample melts. Different unusual effects have been observed in the films. For example, layer thinning transitions occur in the films above the melting temperature of the bulk sample. We report our investigations of free-standing films of polar smectic liquid crystals**.** In polar liquid crystals the long molecular axes in the layers are tilted with respect to the layer normal. Different phenomena related to stability of the layer structure of the films and phase transitions in the films were studied.

We describe the instability of in-plane orientational field found in polar films [1]. The instability is observed near temperatures of thinning transitions. A modulated structure of linear orientational defects is formed in the film. The defects are characterized by continuous rotation of molecular orientation in the plane of the film. Dependence of the defect structure on temperature and film thickness is analyzed. We put forward a model that qualitatively and quantitatively explains the experimental results. Energetical stability of the modulated phase is attributed to linear elasticity of the liquid crystal due to breaking of mirror symmetry.

We investigated structures and phase transition in superthin free-standing films of a liquid crystal compound with sequence of polar phases including ferroelectric, ferrielectric, and antiferroelectric structures [2]. Films with thickness several molecular layers were investigated. The thickness of the films was comparable or even smaller then the periodicity of antiferroelectric and ferrielectric phases existing in the bulk sample. Transitions between states can be observed with the aid of polarized microscopy. The number of different states increases with increasing the film thickness. In six-layer films the number of observed states exceeds the number of polar phases in the bulk sample. We calculated the structures in the bulk samples and in thin films in the framework of Landau theory of phase transitions. The calculations well reproduce the phase sequences and the thickness dependence of transition temperatures observed in experiment. The results of our investigations demonstrate how confined geometry and interlayer interactions can induce formation of different structures.

We investigate the effect of edge dislocations on the orientation of molecules in the film plane [3]. Substantial difference of the orientational effect in ferroelectric and antiferroelectric films was observed. We found that in films of antiferroelectric liquid crystal the orientational action of the dislocation depends on the dislocation's Burgers vector. More precisely, the relative orientation of molecules on the two sides of the dislocation depends on the parity of the number of layers in the dislocation. We propose an explanation of the observed effect.

This work was supported by the Russian Science Foundation under grant 18-12-00108.

1. P.V. Dolganov, E.I. Kats, V.K. Dolganov, and P. Cluzeau, "Linear defects forming the ground state of polar free standing smectic-C* films", Soft Matter, **14**, pp.7174-7179, 2018
2. N.S. Shuravin, P.V. Dolganov, and V.K. Dolganov, "Phase transitions in nanofilms of polar smectic liquid crystals with multilayer periodicity", Phys. Rev. E, **98**, pp.052705-1-052705-10, 2018
3. P.V. Dolganov, N.S. Shuravin, V.K. Dolganov, and A. Fukuda, "Orientational action of edge dislocations on the director field in antiferroelectric smectic-C*$_A$ films", Phys. Rev. E, 95, pp.012711-1-012711-9, 2017

O2-8: Point topological defects in two-dimensional smectic nanofilms

P.V. Dolganov[1] , N.S. Shuravin[1] , V.K. Dolganov[1]

1. *Institute of Solid State Physics, Russian Academy of Sciences, 2 Academician Ossipyan street, Chernogolovka, Moscow Region, 142432 Russia, pauldol@issp.ac.ru*

Smectic liquid crystal nanofilms are classical objects for investigations of structure, dynamics, and phase transitions in two-dimensional systems. Absence of substrate (two free surfaces of the film border with air) allows investigating the effects of two dimensions in pure form. In smectic phases in which the long molecular axes are tilted towards the plane of smectic layers the orientation of molecules forms the two-dimensional field of molecular ordering described by a polar vector, so-called **c**-director. In the field of molecular ordering usual defects can form, which deform but do not destroy the field of molecular ordering, as well as point topological defects with a singularity in the defect center. In vector field of molecular ordering the defects can have only integer topological charges, positive or negative [1]. Defects with fractional charge are observed at the boundaries. Several topological defects with integer charge can also exist at the boundary [2]. Topological defects have substantial influence of physical, in particular optical properties of the films. The defects play a key role in self-organization of inclusions in smectic films [3].

The talk presents the results of investigations of structure and dynamics of point topological defects in smectic nanofilms. Special attention is paid to appearance and behavior of topological defects in confined geometry, in particular in smectic islands (regions with thickness larger than the film in which they are located). Rigid conditions for the orientation of the **c**-director at the boundary impose restrictions on the total value of the topological charge inside the islands. We investigated topological defects for different boundary conditions on the border of islands. Besides simplest situations when in confined geometry one defect with topological charge S=+1 or two defects with charges S=+1/2 exist, more complex topology of the **c**-director field in the islands was investigated. In can appear when films are created or during coalescence of islands in the films. Formation of topological defects with positive and negative topological charge during island coalescence is studied. We investigated the stability of topological defects and their annihilation with conservation of the total topological charge of the system. We observed topological defects with large topological charge, up to 5, and their decomposition into defects with a smaller value of the topological charge. Using the electromagnetic analogy, the distribution of the orientational field was calculated for different combinations of positive and negative topological charges observed in experiment.

This work was supported by the Russian Science Foundation under grant 18-12-00108.

1. M. Kleman and O.D. Lavrentovich, Soft Matter Physics: An Introduction. Springer, New York, 2003
2. P.V. Dolganov, N.S. Shuravin, V.K. Dolganov, E.I. Kats, and A. Fukuda, “Topological defects in smectic islands in antiferroelectric freestanding nanofilms”, Surface Innovations, **7**, pp.168-173, 2019
3. P.V. Dolganov, P. Cluzeau, and V.K. Dolganov, “Interaction and self-organization of inclusions in two-dimensional free-standing smectic films”, Liquid Crystals Reviews, **7**, pp. 1-29, 2019

O2-9: Studies on the formation conditions of surface gaseous nano- and microstructures and their effect on the wetting properties of the surface

A. Karacharov[1], M. Likhatski[1], Yu. Mikhlin[1]
1. Institute of Chemistry and Chemical Technology of the Siberian Branch of the Russian Academy , Russian Academy of Sciences, Krasnoyarsk, Russia, e-mail: karacharov@icct.ru

Hydrophobic and superhydrophobic surfaces are of pivotal importance in many fields of technological and natural processes, including, in particular, corrosion and icing of structural materials. In recent years, it becomes clear that surface submicrometer gas structures ("nanobubbles") are widespread exist at hydrophobic surfaces. The surface gas entities are expected to play a key role in the attachment of hydrophobic particles to air bubbles in the air-saturated mineral pulps. Assumption about the existence of surface gas bubbles on hydrophobic surfaces as a reason for long-range hydrophobic attraction forces was first suggested in the mid-1990s In 2000, the AFM image of nanobubbles was first published. The existence of gas nanostructures has been confirmed with various methods; their fundamental importance for interphase processes is undoubtedly (see special issue of Langmuir 2016, V.32, No.43). However, the mechanism of their stabilization is not clear up to now, and there are serious methodological problems with reproducible acquisition and research. Recently An et al. [1] proposed a "one-stage" generation of nanobubbles using a contact of cold water and a "hot" HOPG substrate without additional reagents. The temperature difference seems to be an extremely promising method for obtaining nanobubbles for their study under controlled conditions and it is seems to be the cause of their occurrence in real systems.

The aim of this work was to study on the formation conditions and evolution of surface gas structures (nano- and (sub) micronbubbles) obtained by the temperature difference method on surfaces of several substrates (highly oriented pyrolytic graphite (HOPG), SiO_2, stainless steel, Ti, TiO_2).

We reproduced the technique for generation of nanobubbles by the method of temperature difference between substrates and water. The formation of nanobubbles on substrate (HOPG, silicon dioxide, stainless steel, Ti, TiO_2) surfaces was observed by the AFM method at a temperature difference between substrates and water of +45 and $+5^0$C, respectively. It was found that the difference can be made minimal if the surface is treated with hydrophobizing reagents such as dixanthogen. Over time, the bubbles become larger; after a certain period of time they become discernible in the optical microscope. It has been established that the formation of nanobubbles and their growth is accelerated by the action of surfactants, especially dixanthogen.

Contact angle measurements by sessile drop technique showed that the treatment of initial substrate surfaces with potassium buthylxanthate aqueous solution or with dibuthyldixanthogen emulsion render them more hydrophobic.

Using in situ atomic force spectroscopy, the sorption of surface active substances was shown to give rise to an increase in both adhesive force magnitude and the range within it acts at the approach of cantilever tip to the surface of both hydrophobic and hydrophilic samples. The maximum of both adhesive force and their range, up to 150 nm, took place in case of retract of cantilever tip from sample surface. Force curves are steeper, which related with the formation of nanobubbles on the surfaces of samples under study arising the long-range hydrophobic force of capillary origin.

1. H. An, B.H. Tan, Q. Zeng, C.-D. Ohl *Stability of Nanobubbles Formed at the Interface between Cold Water and Hot Highly Oriented Pyrolytic Graphite*. Langmuir, 43, pp. 11212−11220, 2016.

This study was supported by RFBR, project 18-33-00302 мол_а

O2-10: Formation onto the track-etched membrane surface of a polymer double-layer coating with superhydrophobic properties

L.I. Kravets[1], M.A. Yarmolenko[2], A.A. Rogachev[2], R.V. Gainutdinov[3], N.E. Lizunov[1]
1. Joint Institute for Nuclear Research, Flerov Laboratory of Nuclear Reactions, Dubna, Russia. 2. Francisk Skorina Gomel State University, Gomel, Belarus. 3. Shubnikov Institute of Crystallography of FSRC "Crystallography and Photonics" RAS, Moscow, Russia.
E-mail: kravets@jinr.ru

The present paper describes the possibility of formation of a double-layer superhydrophobic coating onto a porous substrate from an active gas phase formed via electron-beam dispersion (EBD) of polymers in vacuum. As a porous substrate was served a poly(ethylene terephthalate) track-etched membrane (PET TM) with an effective pore diameter of 250 nm, obtained on the basis of a PET-film (Lavsan, Russia) with a nominal thickness of 10.0 μm. To prepare the membrane, the virgin film was irradiated with cyclotron-accelerated positively charged 3-MeV krypton ions at a fluence of 2×10^8 cm^{-2}. Chemical etching of the irradiated PET-film was carried out at a temperature of 75°C in a 3 mol/L sodium hydroxide aqueous solution according to the procedure described in [1]. Prior to etching, the irradiated film was exposed to UV radiation with a maximum emission wavelength of 310-320 nm to increase the selectivity of the etching process. The powders from ultra-high molecular weight polyethylene (UHMW-PE) with molecular weight of 5×10^6 g/mol and a density of 0.93 g/cm^3 (Foresight Global FZE) and polytetrafluoroethylene (PTFE) with a density of 2.15 g/cm^3 (Aldrich Co.) without additional drying before application were used as the target materials to form coatings on the PET track-etched membrane surface. Polymer coatings were deposited from the active gas phase generated via exposure of the target materials to low-energy electron-beam (800-1600 eV) acceleration voltage with current density of 0.01-0.03 A/cm^2. The initial pressure of the residual gas in the vacuum chamber was 4×10^{-3} Pa, the temperature of the substrate surface was ~ 300 K. UHMW-PE was used as a target to form the first layer on the membrane surface and PTFE was used as a target to form the second layer. The double-layer coatings were formed in a single process cycle without depressurization of the vacuum chamber. The targets were automatically moved into the zone of influence of electron flow. The scheme of the deposition process and the treatment technique are detailed in [2].

It is shown that the formation of a UHMW-PE coating onto the PET track-etched membrane surface by the EBD of virgin polymer in vacuum results in the composite membranes having the hydrophilic and hydrophobic layers. One of the layers is the original PET matrix characterized by a medium level of hydrophilicity. The water contact angle for this layer is equal to 65°. Another layer applied by means of UHMW-PE electron-beam deposition onto the membrane surface is hydrophobic in nature. The water contact angle of this layer, depending on its thickness, varies from 92° to 125°. This change in the wettability is due to the development of roughness of the deposited layer having hydrophobic properties with increase in its thickness [3]. It is found that the deposition of a second layer with a thickness of 100 nm obtained by electron-beam dispersion of the PTFE onto the composite membrane surface leads to the formation of superhydrophobic coating. The values of water contact angle for this type of membranes, depending on the total thickness of the double-layer coating, vary from 150° to 160°. A significant increase in the value of contact angle is due to the lower free surface energy and more considerable development of the roughness of the fluoropolymer comparison to the UHMW-PE coating. In addition, in this case we observed the formation of polymer coating having a hierarchical structure.

This work was supported by the grant (№ 17-08-00812) from Russian Foundation for Basic Research.

1. P.Yu. Apel and S.N. Dmitriev, "Micro- and Nanoporous Materials Produced Using Accelerated Heavy Ion Beams", Adv. Nat. Sci. Nanosci. Nanotechnol., **2**, no. 013002, 2011.
2. J. Xiao, A.V. Rogachev, V.A. Yarmolenko, A.A. Rogachev, Y. Liu, X. Jiang and M.A. Yarmolenko, "Formation Features, Structure and Properties of Bioactive Coatings Based on Phosphate-Calcium Layers, Deposited by a Low Energy Electron Beam", Surf. Coat. Technol., **359**, pp. 6-15, 2019.
3. D. Quere, "Wetting and Roughness", Annu. Rev. Mater. Res., **38**, pp. 71-99, 2008.

O2-11: On the effect of gas nanostructures and surface topography on the wettability of materials

M. Likhatski[1] , A. Karacharov[1] , Yu. Mikhlin[1]
1. Institute of Chemistry and Chemical Technology of the Siberian Branch of the Russian Academy , Russian Academy of Sciences, Krasnoyarsk, Russia, e-mail: lixmax@icct.ru

Surface wettability of materials is of significant technological interest for several decades, including froth flotation processes, manufacture of self-cleaning surfaces, anti-icing surface fabrication etc. In recent years, it becomes clear that surface nanoscale gas structures ("nanobubbles") along with intrinsic nanoscale topographical features of solid surfaces are widespread and play pivotal role in very different areas. There are a lot of publications considering the effect of nanoscale surface features, including intrinsic ones, adsorbed collectors and surface gas nanostructures, on the "static" hydrophobicity of materials, which one can draw in terms of static contact angles. It is worth to note that drop freezing time on the untreated surfaces should be affected by a complicated interplay of many factors such as solid-liquid contact area, oxide layer thickness, intrinsic hydrophobicity, formation of nanobubbles (nanopancakes) etc. However, the influence and interplay of the abovementioned factors on the "dynamical" hydrophobicity of materials (characterized, for example, by water drop freezing rate) is not enough investigated yet. Hence, our study is aimed at dynamical aspects of water freezing process on the surfaces of different supports, and possible interplay between both the wetting contact angles and freezing (unfreezing) rates, on the one hand, and nanoscale surface features, on the other hand.

In a series of experiments, dynamics of deionized water drop freezing on various supports was investigated, with the support identity (highly oriented pyrolytic graphite – HOPG, stainless steel, Ti, TiO_2 and SiO_2) and sort of surface treatment (sorption xanthate ions from 10 mM aqueous potassium buthylxanthate, conditioning the sample in dibuthyldixanthogen emulsion) was varying. The wetting contact angles and freezing rates were measured using OCA 15EC Instrument equipped with temperature unit TPC160 (Dataphysics Instruments GmbH, Germany). In a typical procedure, 5 μl deionized water drop was put onto the support surface, then it was thermostated for 15 minutes at +5 °C, and, after the measuring the static contact angle, the freezing to -20 °C was performed. Along with the contact angles in three different time points (before freezing, during time of existence of an ice bit, and after the unfreezing), the freezing rates were logged and analyzed. Atomic force microscopy (Solver P-47, NT-MDT, Russia) was applied to characterize selected samples.

For example, the water drop freezing time on the surface of stainless steel support was ~117 s, with the static wetting contact angle was being of ~69°. On the other hand, those time for a SiO_2 support is of 128 s (at the contact angle of 60°), which is not extremely different of the stainless steel, with the thermoconductivity of last one being considerably greater. Interestingly, treatment of all the supports under investigation with potassium buthylxanthate aqueous solution or with dixanthogen emulsion is shown to give rise to increase in freezing rate, which implies its ambiguous relation with contact angles. When nanobubbles were generated using the thermal gradient between the water drop (which was at ~0 °C) and the HOPG support (+45 °C), we observed significant, up to 2 orders of magnitude, increase in water drop freezing time. Interestingly, the application of this technique to TiO_2 did not give rise to remarkable change in the freezing time. We suggest that the possibility of overcooled water drop persistence can be provided by the conditions, when topographic inhomogeneities, which can operate as ice nucleation centers, are less in size than air (macro)nanobubbles generated through the change in air solubility at elevated temperature. Also, a contribution from 'chemical' identity of support cannot be excluded. Hence, at least for the TiO_2, the facilitated orientation of water molecules near the surface and the formation of Ti-O···H-OH hydrogen bonds should be taken into account.

This study was supported by RFBR, project 18-33-00302 мол_а

O2-12: Application of spectroscopic ellipsometry to study the initial stages of ALD

A. Miakonkikh[1, 2], I. Clemente[1, 2]
1. Valiev Institute of Physics and Technology, Russian Academy of Sciences, Moscow, Russia.
2. Moscow Institute of Physics and Technology, Dolgoprudny, Russia.

Understanding of the processes occurring on the surface of substrate during atomic layer deposition is necessary to optimize existing and develop new ALD processes. The initial stages of film growth, nucleation delay and control are of interest in the task of developing area selective atomic layer deposition processes.
Spectroscopic ellipsometry (SE) [1] was applied as nondestructive optical technique capable of *in situ* measurements. The sample does not require special preparation for SE measurement. High sensitivities of SE to film thickness and optical properties of material allows to measure thickness with monolayer precision and to distinguish films of different materials [2, 3]. So that, ellipsometry makes it possible to observe in situ the film growth and precursor desorption kinetics during ALD process which could be crucial for deposition of films on the sidewalls of high aspect trenches.
In present work initial stage of La_2O_3 and TiN deposition processes were studied in plasma enhanced and thermal ALD process. These layers are perspective for the development of memristive devices, and controlled properties of ultrathin layers of these compounds are desirable. As metalloorganic precursors for La_2O_3 growth we used Tris(2,2,6,6-tetramethyl-3,5-heptanedionato)lanthanum (III), 99% ($La(TMHD)_3$) and for TiN - Tetrakis(ethylmethylamino)titanium dosed to the reactor chamber by fast valves from heated vessels.
Films were deposited in FlexAl ALD tool (Oxford instruments plasma technology, UK). SE measurements were carried out in 245 – 998 nm wavelength range at angle of incidence of 71° by M2000X spectral ellipsometer (Woollam Co) with temporal resolution of 1 s. Although optical constants of monolayer could not be derived in the same measurements, the optical parameters of underlying layer were used, giving "apparent thickness" of monolayer of adsorbed precursor. Using the temperature dependence of Silicon optical constants the temperature of sample could be estimated.
Temperature dependence of growth rate for both materials will be presented as well as measurements of thickness uniformity across the wafer depending on the process parameters.

The reported study was carried out under Program of FASO of Russia and was partially supported by RFBR, research project # 18-37-00354.

1. H. Fujiwara, Spectroscopic Ellipsometry: Principles and Applications. John Wiley & Sons, Chichester, England; Hoboken, NJ, 2007.
2. Clemente I.E., Miakonkikh A.V., "Application of spectral ellipsometry to in situ diagnostics of atomic layer deposition of dielectrics on Silicon and AlGaN", Proc. of SPIE, 10224, pp. 1022425-1-7 , 2016
3. Langereis, E. et al. In situ spectroscopic ellipsometry as a versatile tool for studying atomic layer deposition. Journal of Physics D: Applied Physics 42, 73001 (2009).

O2-13: Measurement of optical coefficients of ultrathin copper films in the microwave range

V. Andreev[1], V. Vdovin[2], P. Glazunov[1], Yu. Pinaev[2], I. Khorin[3]
1. M.V. Lomonosov Moscow State University, Moscow, 119991 Russia,
2. Kotel'nikov Institute of Radio Engineering and Electronics of RAS, Moscow, 125009 Russia,
3. Institute of Physics and Technology of RAS (IPT RAS), Moscow, Russia,

Nanometer-thick metal films possess anomalously high (up to 50%) absorption of electromagnetic radiation in the microwave and terahertz range. The film thickness at which the absorption maximum is observed is several nanometers, and it is significantly less than the skin depth. The uniqueness of ultrathin films consists in the absence of the frequency dependence of their absorbing properties in a wide range of wavelengths and in a weak dependence on the type of metal. The aim of this work was to study the optical coefficients of copper films produced by magnetron sputtering in the thickness range from 1 to 30 nm.
Calculation of the optical coefficients of copper films on a quartz substrate 2 mm thick was carried out for the TE_{10} wave in a 3-cm waveguide. The amplitudes and phases of the reflected and transmitted waves were calculated numerically, taking into account the boundary conditions and the wave reflections inside the layers. The wave number in the copper film was calculated using the model dependence of conductivity on thickness [1]. The amplitude and phase of the optical coefficients in the 9–11 GHz range were measured in a 3-cm waveguide using the ZVA 24 vector network analyzer.

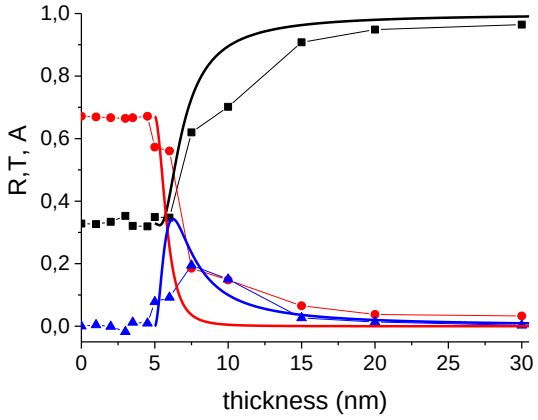

Fig.1. Comparison of optical coefficients measured in a waveguide at a frequency of 10 GHz (symbols) with those calculated for the conductivity of bulk copper $\sigma_0 = 5.9 \cdot 10^7$ Sm/m (solid lines). The calculated curves are shifted by 5 nm — the thickness of the copper film at which a continuous conducting layer begins to form.

The results of measurements of the reflection and transmission coefficients demonstrated that copper films with a thickness not exceeding 5 nm are almost transparent for electromagnetic waves (Fig.1). Nanometer-thick copper films exposed to air oxidize very quickly, resulting in formation of an oxide layer with a complex structure. The formation of the oxide layer occurs in several stages and substantially depends on the technological process of magnetron sputtering. The films whose thickness exceeds 5 nm exhibit metallic properties. A conductive layer, reflected electromagnetic waves is forming inside the films. The thickness of this layer d can be estimated as $d = d_f$ - 5 nm, where d_f is the thickness of the deposited film. The non-uniform structure of the conductive layer results in the discrepancy between the experimental and calculated values of the optical coefficients. The layer consists of grains of a few nanometers in size contacted each other. Percolation transition to a continuous film occurs at a thickness exceeding 10 - 12 nm. Films whose thickness exceeds the specified threshold exhibit purely metallic properties, while the conductivity of films with a smaller thickness is defined mostly by the morphology of the films.
The work is supported by RFBR grants 16-29-09581, 18-29-02094.

1. Kaplan A. E. "Metallic nanolayers: a sub-visible wonderland of optical properties [Invited]", J. Opt. Soc. Am. B., 35, pp. 1328-1340, 2018

O2-14: Conductivity of ultrathin silver films

K. Tsysar[1] , V. Andreev[1] , V. Vdovin[2] , E. Smelova[1] , V.Zelensky[1]

1. *M.V. Lomonosov Moscow State University, Moscow, Russia, 119991; 2. Kotel'nikov Institute of Radio Engineering and Electronics of RAS, Moscow, Russia 125009, E-mail smelova_k_m@mail.ru.*

In recent years the quantum and electronic properties of low-dimensional structures is of special interest. The most interesting part is the study of electronic properties of thin metal films [1-3]. One more significant problem is the appearance of quantum size effects (QSE) - the dependence of properties of a nanostructure on its size due to the quantum confinement or surface effects [4,5]. When the thickness of a metal film is comparable with the electron Fermi wavelength, quantum effects become more significant and influence more extensively on physical properties of studied systems [2]. The present work is focused on the study of conductivity of ultrathin silver films and its thickness dependence.

All calculations were performed using the program Vienna Ab-initio Simulation Package (VASP), which is based on the density functional theory (DFT) [6]. We calculate the frequency-dependent conductivity of silver nanofilms by Kubo-Greenwood formalism realized in the VASP code [6].

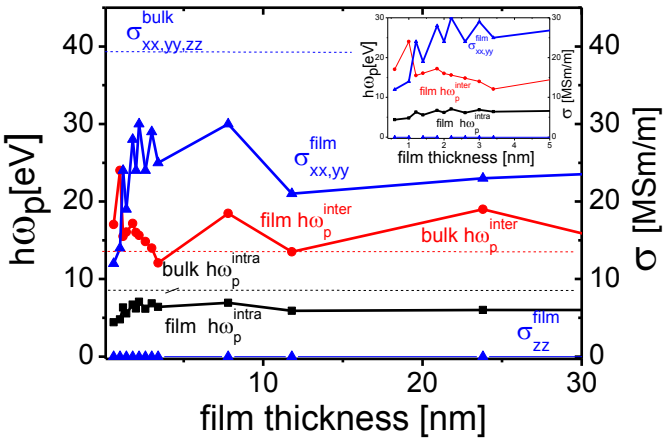

Figure 1. The conductivity (σ) (blue) and plasma frequency (interband (red) and intraband (black)) as a function of the film thickness.

The conductivity (σ) dependence of silver thin film on its thickness has been studied theoretically. The emergence of QSE was found in the conductive properties of Ag nanofilms (Fig.1). The quantum oscillation of σ was found in ultrathin Ag nanofilms thinner than 5 nm (inset, Fig.1). We found the appearance of dielectric properties in ultrathin silver nanofilms. It is expressed by a significant suppression of out-of-plain component of conductivity tensor (σ_{zz}). The mechanism of nanofilm conductivity has been proposed due to strong changes of film band structure in compare to silver bulk. The emergence of two hybridized band in electronic structure of silver nanofilm is found: in-plain band (conductive band) and out-of-plain (nonconductive band). It leads to appearance of anisotropy in to electronic structure and as a consequence in conductive properties of ultrathin Ag nanofilms. Our study predicts a strong dependence of conductive properties of ultrathin metal films on their thickness due to strong changes of their electronic structure.

Work is supported by RFBR grants 17-07-00745, 16-29-09581. This work was carried out using high-performance computing resources of NRC "Kurchatov Institute", HPC of Lomonosov MSU and JSCC of the RAS.

1. Gong, J., *Scientific Reports* 5, 9279, 2015.
2. Hong H, Wei C-M, Chou M Y, et al., *Phys. Rev. Lett.* 90, 076104, 2003
3. Tsysar K., Andreev V., *Proc. of SPIE,* 10224, 1022408-1-1022408-6, 2016
4. Dryzek, J. and Czapla, A., *Phys. Rev. Lett*. 58, 721, 1987
5. Laref, S., Cao, J., Asaduzzaman, A., Runge, K., Deymier, P., et al., *Opt. Express* 21, 11827, 2013
6. Hafner J., Kresse, Vasp workshop, http://cms.mpi.univie.ac.at/vasp-workshop/slides/documentation.htm

O2-15: Investigation of the quasiresonance effect in the amorphous silicon nanowire polarizer

I.M. Akhmedzhanov[1] , D.Kh.Nurligareev[2] , B.A. Usievich[1]
1. Prokhorov General Physics Institute of the Russian Academy of Sciences, Moscow, Russia, eldar@kapella.gpi.ru
2. MIREA - Russian Technological University, Moscow, Russia, jam-nurligareev@yandex.ru

Wire grid polarizers (WGP) are a real alternative to conventional optical polarizers in various applications due to their inherent compact planar structure and relatively high optical characteristics. The undoubted advantage of WGP polarizers is their compatibility with modern thin-film technologies that are used in electronic and optical integrated circuits. Today, this kind of polarizers already finds its application in the perspective optical devices [1].

In [2], we studied the behavior of the extinction ratio of the amorphous silicon nanowire polarizer (Fig. 1) for various structure parameters and have revealed for the first time an interesting peculiarity in the form of a sharp, narrowband extinction ratio increase up to values ~ 10^6 in the vicinity of the wavelength ~ 378nm for the structure with the following parameters h = 80nm, Λ =120 nm, filling factor f = 0.5 (Fig. 2). The effect was called quasi-resonance and was interpreted in the framework of the waveguide-mode model [3] as a dissipative-interference one.

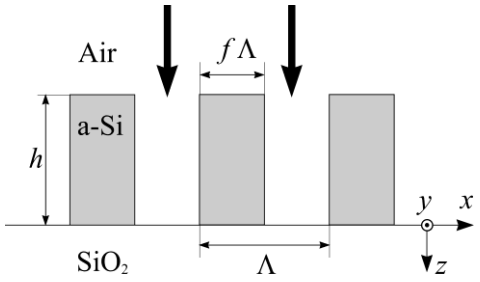

Fig.1 Nanowire polarizer structure

In the current work we have proved that the effect arises due to the destructive interference of exactly two modes propagating in the polarizer structure, one of them mainly residing in the air gaps (Fig.3 dashed line) while the other in the a-Si ridges (solid line). The understanding of the effect background provides the possibility to optimize the polarizer structure to get the high extinction ratio at the desired wavelength by adjusting the geometrical parameters of the structure.

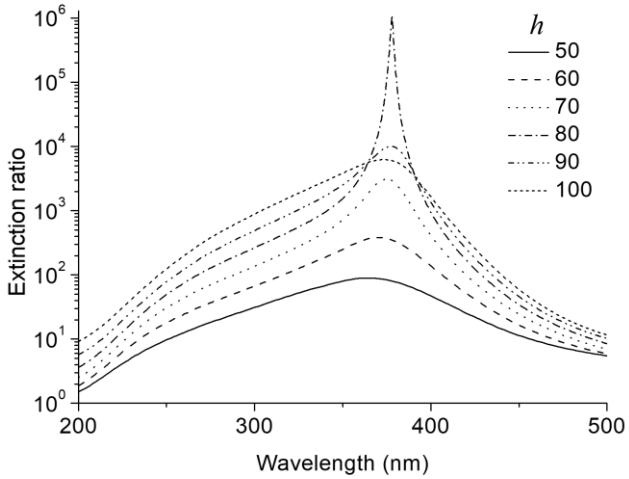

Fig.2 Extinction ratio as a function of wavelength for the different thicknesses h.

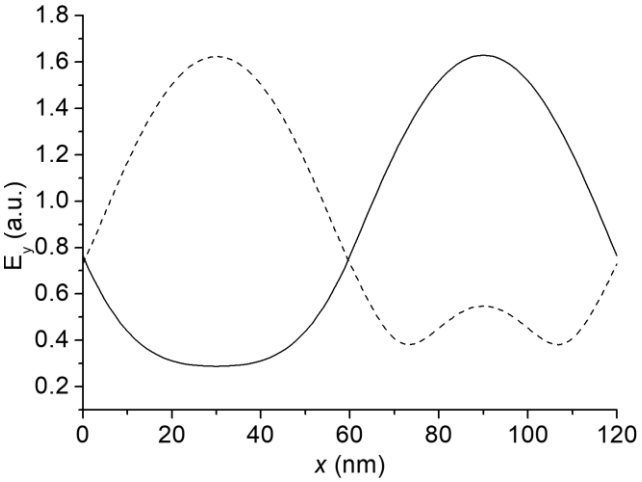

Fig.3 Field distribution for the main TE modes propagating in the structure

1. Thomas Siefke, Martin Heusinger, Carol B. Rojas Hurtado, Johannes Dickmann, Uwe Zeitner, Andreas Tünnermann and Stefanie Kroker, "Line-edge roughness as a challenge for high-performance wire grid polarizers in the far ultraviolet and beyond", Optics Express., **26** (15), 19534, 2018
2. I.M. Akhmedzhanov, D.Kh. Nurligareev, and B.A.Usievich, "Quasi-Resonant Enhancement of the Extinction Ratio in the Amorphous Silicon Nanowire Grid Polarizer", Phys. Wave Phenom., **26** (2), pp.109-115, 2018
3. A.V.Tishchenko, "Phenomenological representation of deep and high contrast lamellar gratings by means of the modal method", Optical and Quantum Electronics, **37** (1-3), pp.309–330, 2005

O2-16: Оптические свойства тонких пленок сплавов кремния

Б.А. Наджафов[1], Х.Ш. Абдуллаев[2], Ф.П. Абасов[1]
[1]*Институт Радиационных Проблем НАН Азербайджана,*
[2]*Бакинский Государственный Университет.*

Исследуются спектры ИК поглощения пленок сплавов *a*-nk-Si:H (*a*-аморфные, nk-нанокристаллические) в диапазоне энергии 0,03 ÷ 3,0 эВ. Определены оптические коэффициенты поглощения (α) пленок для слабо и сильно поглощающих областей спектра, а также определены коэффициенты преломления (*n*) и коэффициенты ослабления (k_0) для различных прозрачных и не прозрачных подложек.

При определении оптических констант, коэффициентов поглощения (**α**) и преломления (**n**), ослабления (κ_0) измеряется величина пропускания **T**, отражения **R** [1,2]. Используя условие сохранения энергии можно найти коэффициент поглощения α:

$$\alpha + R + T = 1.$$

Из-за многократных отражений в подложке и пленке, задача установления связи между ***R*** и ***T*** и оптическими константами не тривиальна. Обычно делается несколько упрощающих предположений для получения связи измеряемых величин ***R, T, α, n*** и $\boldsymbol{k_0}$. При прохождении светом границы раздела двух сред, падающий луч разбивается на отраженный и преломленный. Направления этих лучей определяется законами геометрической оптики – законами отражения и преломления. Воспользуемся известными соотношениями [1,2] определяем вышеуказанных величин следующим образом:

1) n=1 и n_1=1, тогда: $R_1 = R_2 = R = \dfrac{k_0^2}{4 + k_0^2}$:

$$T = \frac{(\frac{4}{4 + k_0^2})^2 \exp(-\alpha d)}{1 - (\frac{k_0^2}{4 + k_0^2})^2 \exp(-2\alpha d)} \qquad (1)$$

$$T = \frac{16 \exp(-\alpha d)}{(4 + k_0^2)^2 k_0^4 \exp(-2\alpha d)} \qquad (2)$$

$$(4 + k_0^2)^2 - k_0^4 y^2 = \frac{16}{T} y;$$

$$k_0^4 y^2 + \frac{16}{T} y - (4 + k_0^2)^2 = 0,$$

Здесь: n_1- коэффициент преломления подложки, и *d*-толщина пленки.

Тогда:

$$D = 64 - (4 + k_0^2)^2 T^2 \qquad (3)$$

$$\alpha = \frac{1}{d} \ln \frac{T k_0^4}{8 \pm \sqrt{D}} \qquad (4)$$

Значит коэффициенты поглощения (α) можно определить с помощью уравнения (4).

[1]. Determining the amount of hydrogen in thin films well $Si_{1-x}g_{ex}$:H (x=0÷1) for electronic devices.//Journal of materials sciences and engineering2017. v.5, issue 6, p.

[2**].** Оптоэлектронные свойства тонких пленок α-$Si_{1-x}Ge_x$:H (x=0÷1).//Успехи прикладной физики. 2018, том 6,№3, с.242-251.

I3-1: Ion beam lithography: from “forgotten” technology to sub-10nm stereolithography

S.I. Zaitsev, Ya. L. Shabelnikov,
Institute of Problems of Microelectronics Technology and High-Purity Materials RAS, Chernogolovka, Russia
e-mail: zaitsev@iptm.ru

For the past 30 years, the methods of electron, ion, photo-, and X-ray lithography have evolved with varying success independently of each other. At present, the characteristic dimensions of the elements of microcircuits have significantly decreased, there is a question of overcoming the sub-ten-nanometer boundary, and only electron-beam (EBL) and ion lithography methods have the potential to demonstrate an appropriate resolution.

Ion-beam lithography (Ion Beam Lithography, IBL) for a number of reasons (and the reasons for “oblivion” will be discussed) occupies an insignificant position compared to electron-beam lithography (EBL), despite the fact that it has obvious advantages. Indeed, being heavy particles, ions with the same energy have several orders of magnitude lower velocities than electrons, and therefore move along more direct and shorter trajectories, and secondary particles displaced by ions (mainly atoms) also have smaller paths than secondary electrons in EBL.

The report discusses the advantages of IBL compared to other technologies using Focused Ion Beam (FIP), local sputtering, ion-stimulated deposition / decomposition .... In addition, ion lithography has the potential to become a tool of three-dimensional nanostructuring, since all the energy of a beam of heavy ions is deposited in compact area that allows you to selectively irradiate the negative resist layer by layer, followed by simultaneous manifestation.The latest results of wide modeling (Fig. 1) will be presented, showing small (sub-10nm) sizes of the resist modification zone.

The results of an experimental study of sensitivity and contrast (for the first time) of PMMA will be presented. A comparison (Fig.2) of the experimental results and the results of the simulation established (for the first time) the relationship of the absorbed energy and the dissolution rate of the resist. From comparative experiments it is clear that IBL is more than a thousand times more efficient technology compared to EBL.

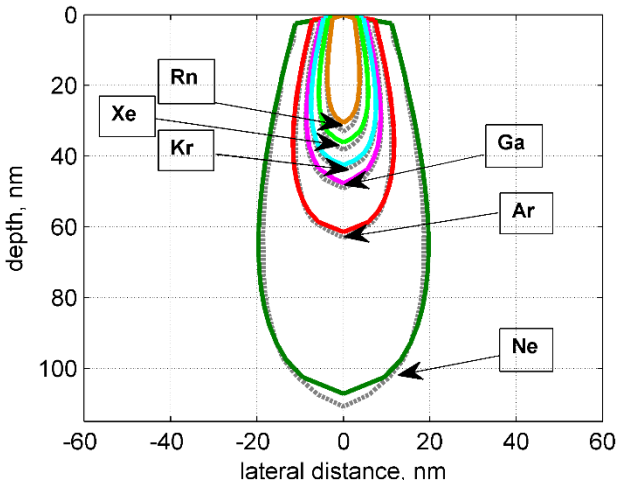

Fig. 1. Section of the absorbed energy isosurfaces. The dashed curves correspond to the Eemp (r, z) isosurfaces given by the empirical expression (1), the solid ones to model calculations based on TRIM data

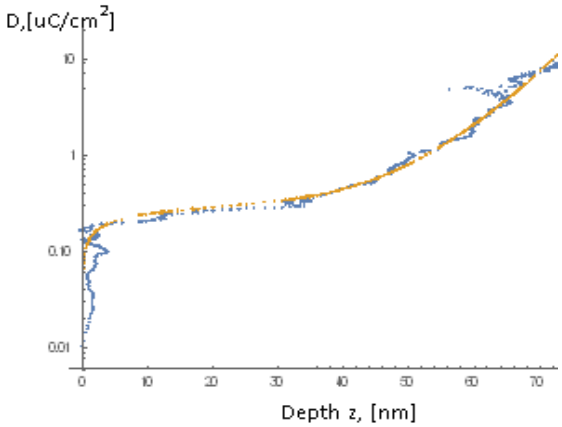

Fig. 2. Comparison of experimental (blue dots) and model (yellow dots) dose-dependence curves of etching depth to extract contrast. The model curve is calculated for Lenergy. = 43nm, $\gamma = 3.1$.

O3-1: X-ray topographic and diffraction studies of Al and Ga termomigrated Si layers

A. Lomov[1], B. Seredin[2], S. Martyushov[3], A. Zaichenko[2], S. Simakin[4], I. Shul'pina[5]

1. Valiev Institute of Physics and Technology of Russian Academy of Sciences, Moscow, lomov@ftian.ru.
2. Platov South-Russian State Polytechnic University, Russia, Novocherkassk, seredinboris@gmail.com.
3. Technological Institute for Superhard and Novel Carbon Materials, Russia, Troitsk, stemart@yandex.ru. 4. Valiev Institute of Physics and Technology of Russian Academy of Sciences, Yaroslavl Branch, simser@mail.ru. 5. Ioffe Physical-Technical Institute of the Russian Academy of Sciences, St. Petersburg, iren.shulpina@yandex.ru

An advantage of the Al/Si and Ga/Si thermomigration (TM) doping technique (temperature gradient zone melting) is in its high rate which exceeds by two or three orders the rate of the conventional diffusion based doping techniques. The interest in the thermomigration (as compared with thermal diffusion) is associated with the principal possibility of obtaining p-layers and p-n junctions with sharp boundaries. By TM features one can grows high perfect structure films and layers. It is one of the promising approaches capable to increase the efficiency of power high-voltage devices. Today TM can be applied for diverse applications. By means of Al/Si thermomigration one can fabricate a micro silicon matrix composed of connected photocells with p-n junction channels on faces normal to the working surface of conventional Si wafers [1]. For metrological control of growth defects of the TM layers (dislocation, Al_xO_y, Ga_xO_y precipitates and so on) and dopant concentration X-ray topographic and double crystal experiments can be applied (Fig.1,2). In the present work both TM epitaxial films and channels were examined. The results of recent studies on the optimization of the TM technique in order to expand the range of silicon substrates doping with an acceptor impurity, in which the impurity concentration is usually limited to the solidus position, are presented. Ternary Al-Ga-Si and Al-Sn-Si melts were used as ligatures. The liquid zones migration rate dependences on the temperature and composition for the Al-Ga and Al-Sn solvent metal are obtained. The threshold temperature of the thermomigration process start and the liquid zone critical thickness were experimentally determined. The possibility of acceptor concentrations changing in the range from $7\cdot10^{17}$ cm^{-3} to $6\cdot10^{19}$ cm^{-3} is shown.

On the X-ray topographic image (Fig.1) of the layer, both growth defects misfit dislocations are not observed, which confirms the perfection of the layer and the phase boundary. The rocking curves from the Si (Al) layer with a thickness of 25 μm show a structural perfection of the layers, comparable with the original substrate. The magnitude of the deformation in the layer with respect to the silicon substrate is $\Delta d/d=2.3\cdot10^{-5}$. The estimation of the Al concentration on the basis of the diffraction data in the substitution model is $(1–2)\cdot10^{19}$ $см^{-3}$, which is in good agreement with the results of the SIMS study.

.

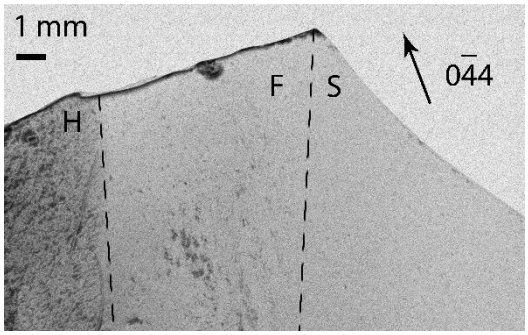

Fig.1. Part of the projection Lang topograph of Al TM-doped Si(111) n-type wafer under a temperature 1450°K for 10 min.

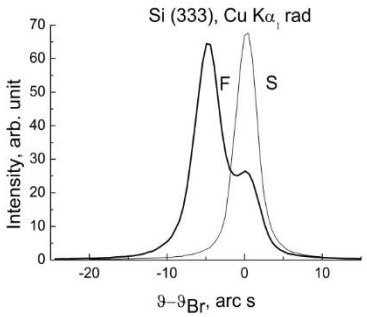

Fig. 2. DCD rocking curves from origin Si(111) part (S) and TM Si(Al)/Si(111) structure (F) with 333 refl., $CuK\alpha_1$ rad.

The studies was supported by Prog. № 0066-2019-0004 of the Ministry of Science and Higher Education of Russia for Valiev Institute of Physics and Technology of RAS and partially supported by RFBR, grant no. 19-07-00306.

1. V. N. Lozovskii, A. A. Lomov, L. S. Lunin, B. M. Seredin and Yu. M. Chesnokov. Semiconductors, 51 (3), pp. 285-289, 2017

O3-2: Processes of the platinum silicides formation at low-temperature annealing on the surface of poly-Si

K. V. Chizh[1], L. V. Arapkina[1], V. P. Dubkov[1], S. A. Mironov[1], D. B. Stavrovskii[1,3], P. I. Gaiduk[2], V. M. Senkov[3], I. V. Pirshin[3], V. A. Yuryev[1]

1. A.M. Prokhorov General Physics Institute of RAS, Moscow, Russia, E-mail: chizh@kapella.gpi.ru.

2. Belorussian State University, Minsk, Belarus, E-mail: gaiduk@phys.au.dk.

3. P.N. Lebedev Physical Institute of RAS, E-mail: senkov42@yandex.ru.

Platinum silicides are widely used in microelectronics and microphotonics for the production of Schottky diodes, e.g., in IR detector arrays, as tracks in microcircuits, in the manufacture of atomic force microscope probes, etc. [1,2]. This research is aimed at a detailed study of the formation of Pt silicide films on the surface of poly-Si at low-temperature annealing up to 550°C.

The Pt silicides formation was carried out by the method of equilibrium heat treatment in an Ar atmosphere. Pt films with a thickness of (20–22) nm were deposited by a magnetron sputtering on substrates of the c-Si/SiO_2/Si_3N_4/poly-Si under standard technological conditions. Further heat treatment varied from 30 min up to 8 h was carried out at a stable Ar flow of 60±10 l/min at temperatures from 120 to 550°C in a reactor with the temperature stabilization not worse than ± 1%.

The samples were studied by Fourier transform infrared spectroscopy, X-ray photoelectron spectroscopy and X-ray phase analysis. It was found that as a result of annealing at temperatures up to 300°C for 30 min of Pt film deposited on poly-Si, platinum silicides were not detected by X-ray phase analysis. However, a mixture of different silicides (Pt_3Si, Pt_2Si and PtSi) was detected by X-ray photoelectron spectroscopy in these samples. As a result of annealing at temperatures in the range from 320 to 480°C for 30 min, mainly PtSi formed. All the deposited platinum transformed to Pt_2Si due to annealing at 230°C for ~ 8 h, while a part of Pt transformed to Pt_2Si and some remained unreacted after the treatment at 185°C for ~ 8 h. After the removal of metallic platinum from the samples annealed at 185°C for ~ 8 h, the Pt_3Si reflex was observed in the X-ray diffraction patterns, which is consistent with the data previously obtained using X-ray photoelectron spectroscopy [3, 4].

The research was funded by the Russian Foundation for Basic Research, grant number 18-52-00033, and the Belarusian Republican Foundation for Fundamental Research, grant number T18P-190.

1. V. A. Yuryev, K. V. Chizh, V. A. Chapnin, S. A. Mironov, V. P. Dubkov, O. V. Uvarov, V. P. Kalinushkin, V. M. Senkov, O. Y. Nalivaiko, A. G. Novikau, P. I. Gaiduk, "Pt silicide/poly-Si Schottky diodes as temperature sensors for bolometers," J. Appl. Phys., 117, 204502, 2015.
2. V. A. Yuryev, K. V. Chizh, V. A. Chapnin, V. P. Kalinushkin, "Metal silicide/Si thin-film Schottky-diode bolometers," Proc. SPIE, 9519, 95190K, 2015.
3. S. A. Mironov, V. P. Dubkov, K. V. Chizh, V. A. Yuryev, "Room-temperature formation of Pt_3Si/Pt_2Si films on poly-Si substrates," J. Phys.: Conf. Ser., 816, 012011, 2017.
4. M. S. Storozhevykh, V. P. Dubkov, L. V. Arapkina, K. V. Chizh, S. A. Mironov, V. A. Chapnin, V. A. Yuryev, "Silicon-germanium and platinum silicide nanostructures for silicon based photonics," Proc. SPIE, 10248, 102480O, 2017.

O3-3: Influence of deposition time on the synthesis of indium catalyzed silicon oxide nanowires

A. Zamchiy[1,3], I. Merkulova[1,3], E. Maximovskiy[2,3], E. Baranov[1]
1. *Kutateladze Institute of Thermophysics SB RAS, Novosibirsk, Russia*
2. *Nikolaev Institute of Inorganic Chemistry SB RAS, Novosibirsk, Russia*
3. *Novosibirsk State University, Novosibirsk, Russia*
zamchiy@gmail.com

In recent years, low-dimensional structures have attracted a scientific and technological interest because of their unique physical and chemical properties. One of them, the silicon oxide nanowires having a high intense and stable blue light emission at a room temperature [1], a low refractive and absorption indices, good chemical stability and biocompatibility [2] can be applied as building blocks in optoelectronic devices.
A synthesis of one-dimensional nanostructures (in particular nanowires) in a controlled manner (with a given morphology, aspect ratio, direction, etc.) is an urgent task, the solution of which can significantly expand their potential applications. Also an important aspect is the study of the effect of abovementioned parameters on the physicochemical and functional properties of the synthesized structures.
In this work, silicon oxide nanowires (SiO_xNWs) were synthesized by the gas-jet electron beam plasma chemical vapor deposition method according to the vapor-liquid-solid mechanism at different synthesis times (0.5-10 min) using indium nanoparticles as a catalyst. The synthesis temperature was maintained at 300°C in order to obtain aligned microropes (bundles) of the SiO_xNWs [3]. The morphology of the structures synthesized at different deposition times was investigated by means of TEM and SEM. FTIR spectroscopy was used for investigation of the composition and the bonding network of the SiO_xNWs. The photoluminescence of the nanostructures was investigated at the room temperature using a 10 mW He–Cd laser at 325 nm as the exciting source.

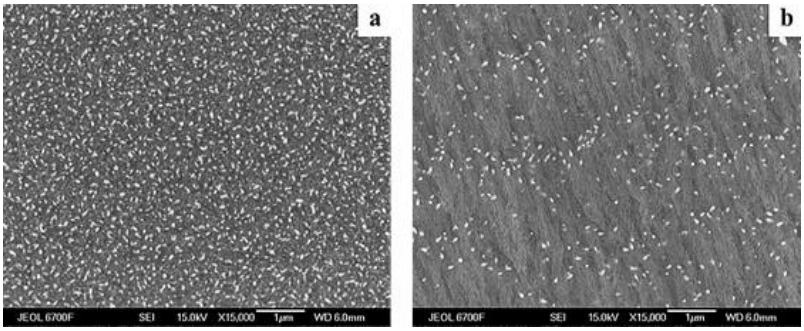

Fig. 1. SEM image of SiO_xNWs synthesized at different deposition times: (a) 1 min and (b) 10 min.

The length of the structures increases systematically with the synthesis time increase that indicates their constant growth rate (Fig.1). FTIR spectroscopy shows that the nanowires synthesized at different times have the bonding network of SiO_x and are very similar in chemical composition ($x \approx 2$). The structures exhibit the intense photoluminescence at the room temperature with a maximum in a range of the energies from 2 to 3 eV.
This study was financially supported by the grant of the President of the Russian Federation, the project MK 638.2019.8.

1. D.P. Yu, Q.L. Hang, Y. Ding, H.Z. Zhang, Z.G. Bai, J.J. Wang, Y.H. Zou, W. Qian, G.C. Xiong and S.Q. Feng, "Amorphous silica nanowires: Intensive blue light emitters", Applied Physics Letters, 73, pp.3076-3078, 1998.
2. R.G. Elliman, A.R. Wilkinson, T.H. Kim, P.K. Sekhar and S. Bhansali, "Optical emission from erbium-doped silica nanowires", Journal of Applied Physics, 103, p.104304, 2008.
3. S. Khmel, E. Baranov, A. Barsukov, A. Zamchiy, A. Zaikovskii, E. Maximovskiy, D. Gulyaev and K. Zhuravlev, "Indium-Assisted Plasma-Enhanced Low-Temperature Growth of Silicon Oxide Nanowires", Physica Status Solidi (a), 215(12), p.1700749, 2018.

O3-4: Electrical characterization of Si thin films near heterointerfaces

E. Zaytseva, O. Naumova, B. Fomin
Rzhanov Institute of Semiconductor Physics, Siberian Branch of Russian Academy of Sciences, Novosibirsk, Russia,
E-mail ifp@isp.nsc.ru

For large class of advanced devices based on thin films, in particular, silicon-on-insulator (SOI) films (waveguides and optical modulators, thin-film transistors, chemical and biological sensors, etc.), the properties of the internal interface between film and the buried insulator, as well as the properties of the interface between film and the top dielectric layer, are equally significant [1]. It is known that the structural quality of the film near the heterointerfaces and their roughness have a significant impact both the light scattering and the scattering of free charge carriers.

Methods of electrical characterization are the most common and simple methods of interface characterization. However, in the thin films, the electrical potentials at the opposite interfaces of the films are interconnected ones, exhibiting the so-called coupling effect [2]. This effect does not allow one to independently determine the parameters for different interfaces of the film. Therefore, one of the key issues for thin films and devices based on them is the development of methods for the independent determination/control of interface properties.

The carrier mobility μ_{eff} is an excellent parameter for monitoring the quality of the interfaces. However, it is well known that μ_{eff} involves several components. In bulk of the material, μ_{eff} are determined by scattering on ionized impurities (μ_{b_C}) and on phonons (μ_{b_ph}). Near the heterointerfaces the carrier mobility limited by scattering on charges of the surface states (μ_{s_C}), surface phonons (μ_{s_ph}), and interface roughness (μ_{sr}) [3]. For characterization of the semiconductor/dielectric system properties, the most important components are μ_{s_ph} and μ_{sr}, whose values are defined by the structural quality of the films near the heterointerface.

The aim of this study was to develop a new approach for independent determination and profiling of the mobility components μ_{s_ph} and μ_{sr} near the interfaces in thin-film structures. For this aim we propose (i) using the coupling effect for controlled localization of free-carriers relative to the interface under study; (ii) determination of the components of μ_{eff} using the different temperature behavior of those components. This method was applied for characterization of the internal interface of Si film with buried oxide in SOI structures. The results of electrical characterization on the basis of the profiling of mobility components μ_{s_ph} and μ_{sr} were confirmed by HREM and Raman spectroscopy data. In this study, we also discuss the conditions of applicability of the proposed method for comparing components in structures with different design parameters (different film thicknesses, different dielectrics surrounding the film thickness).

The work was supported by a research project RFMEFI58117X0026. The results were obtained using the equipment of CKP “Nanostructures” (ISP SB RAS, Novosibirsk) and CKP “High-resolution spectroscopy of gases and condensed matter” (IA&E SB RAS, Novosibirsk).

1. Naumova O. V., Zaytseva E. G., Fomin B. I., Ilnitsky M.A.,Popov V. P., “Density dependence of electron mobility in the accumulation mode for fully depleted SOI films” Semiconductors, 49, pp.1316-1322 (2015)
2. Rudenko T., Nazarov A., Kilchytska V., Flandre D., “A review of special gate coupling effects in long-channel SOI MOSFETs with lightly doped ultra-thin bodies and their compact analytical modeling”, Solid-State Electronics, 117, pp. 66-76 (2016)
3. Zaytseva E. G., Naumova O. V., Fomin B. I., “Electron mobility in the inversion layers of fully depleted SOI films” Semiconductors, 51, pp.423-429 (2017)

O3-5: Diffusion of hydrogen atoms in Si films grown by molecular beam deposition on Si_3N_4 and SiO_2 substrates

K. V. Chizh[1], L. V. Arapkina[1], D. B. Stavrovsky[1,2], O. V. Uvarov[1], P. I. Gaiduk[3], V. A. Yuryev[1]

1. Prokhorov General Physics Institute of the Russian Academy of Sciences, Moscow, Russia, arapkina@kapella.gpi.ru
2. Lebedev Physical Institute of the Russian Academy of Sciences, Moscow, Russia
3. Department of Physical Electronics and Nanotechnology, Belarusian State University, Minsk, Belarus

A diffusion process of hydrogen atoms in thin amorphous and polycrystalline Si layers deposited from molecular beams has been investigated using FTIR spectroscopy [1]. Structure of the Si layers has been studied by HRTEM. The Si films were deposited on dielectric Si_3N_4 or SiO_2 layers or a Si(100) substrate. The Si_3N_4 layers were produced by CVD at the temperature higher than that of all subsequent processes (i.e. annealing and growth in an MBE chamber). The SiO_2 layers were obtained by thermal oxidation of a silicon wafer also at high temperatures. Non-hydrogenated amorphous or polycrystalline Si films were deposited at the temperatures ranged from 30 to 650°C. With the temperature increase, Si layer structure changed from amorphous to polycrystalline [2]. It has been found that the intensities of FTIR spectral bands assigned to the vibrations of the N–H bond reduces while those related to the Si–N bond increases due to Si deposition on Si_3N_4 layers at all temperatures. At the temperatures below 160°C, the band assigned to the vibrations of the Si–H bond appears that is absent in the spectra of the substrates before Si deposition. During Si deposition on the SiO_2 surface at 30°C, this band is also observed, yet it is absent in the samples grown on a Si(100) substrate. The reduction of the IR absorption at the bands related to the N–H bonds vibrations and the increase of the IR absorption at the bands relating to the Si–N bonds vibrations in IR spectra demonstrate that hydrogen atoms leave Si_3N_4 layer during Si deposition. The absorption band assigned to the vibrations of the Si–H bond emerging in IR spectra obtained at samples deposited both on Si_3N_4 and SiO_2 layers indicates the accumulation of hydrogen atoms in Si films. The difference in chemical potentials of hydrogen atoms in the dielectric layer and the Si film explains the transfer of hydrogen atoms from the Si_3N_4 or SiO_2 layer into the growing Si film [3,4].

The research was funded by the Russian Foundation for Basic Research (grant number 18-52-00033) and the Belarusian Republican Foundation for Fundamental Research (grant number T18P-190).

1. K. V. Chizh, L. V. Arapkina, D. B. Stavrovsky, P. I. Gaiduk, V. A. Yuryev, “Diffusion of hydrogen atoms in silicon layers deposited from molecular beams on dielectric substrates,” Mater. Sci. Semicond. Proc., 2019; arXiv:1901.10748.
2. M. S. Storozhevykh, V. P. Dubkov, L. V. Arapkina, K. V. Chizh, S. A. Mironov, V. A. Chapnin, V. A. Yuryev, “Silicon-germanium and platinum silicide nanostructures for silicon based photonics,” Proc. SPIE, 10248, p.102480O, 2017.
3. R. A. Street, “Hydrogen chemical potential and structure of a-Si:H,” Phys. Rev. B, 43 (3), pp. 2454–2457, 1991.
4. W. Beyer, “Hydrogen incorporation, stability, and release effects in thin film silicon,” Phys. Stat. Sol. (a), 213 (7), pp. 1661–1674, 2016.

O3-6: Nanoscale patterning Si, SiO_2 surface using edge lithography method

I.I. Amirov, V.V. Naumov, M.O. Izyumov, L. Mazaletsky

Valiev Intitute of Physica and Technology of RAS, Yaroslavl Branch, Yaroslavl, Russia

The method of edge lithography (EL) of forming nanostructures on a Si surface is one of the simplest and most effective methods for surface nanostructuring using the optical lithography [1, 2]. It is based on the use of a nanometer thickness of the material deposited on the walls of the initially formed microstructures. The result is a perimeter pattern of the original mask pattern. This method can be called the method of forming the contour of the image. There are several options of this method depending on the method of applying a layer of material on the mask walls. In this paper the EL method is presented for forming nanostructures in the form of metal (Co, Cr, Pt) nanowire and ring nanostructures on a Si, SiO_2 surface with using the effect of redeposition during ion-plasma sputtering.

Methods of forming metallic nanostructures on the surface of Si and SiO_2 can be different. The simplest EL method consists of four stages. At the first stage desired mask pattern formed in the photoresist layer using optical lithography. Further, by anisotropic etching in fluorine-containing plasma, the mask pattern is transferred to the underlying layer. Then the resist is removed and a layer of metal 20-50 nm thick is applied on a structured surface (Si, SiO2) by magnetron sputtering. At the next stage, a controlled ion-plasma sputtering of the metal film is carried out, as a result of which a layer of metal of nanometer thickness is deposited on the side wall. Figure 1 shows an array of nanowires obtained in this way. The dimensions of the formed nanostructures (width and height of nanowires) are determined by the height, slope of the wall, the initial thickness of the applied metal film, the sticking coefficient Me-Si, Me-Me. The experiments were carried out in a dense plasma reactor described in detail in [3]. Films of metals were applied by the magnetron method.

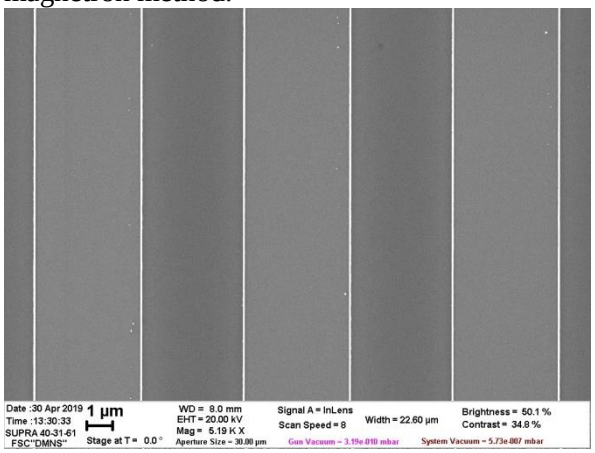

Fig 1. SEM image of the Co nanowire on the Si.

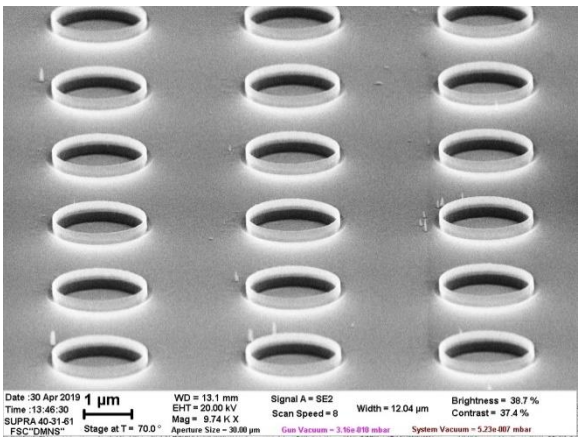

Fig 2. SEM image of the cylindrical SiO_2 microstructures

The resulting metal nanostructures can be used as a mask for the formation of 3D microstructures with nanometer wall thickness by plasma-chemical anisotropic etching. In Fig.2 cylindrical SiO_2 microstructures obtained as a result of anisotropic SiO_2 etching in a C_4F_8 / Ar plasma using a Co mask in the form of rings of a nanometer width are shown. It can be assumed that the development of this method opens up new opportunities for biosensing, nanofluidics, nanophotonics, and nanoelectronics.

The work has been done under State Programs #0066-2019-0002 of the Ministry of Science and Higher Education of Russia.on the equipment of the center for collective use of the scientific equipment «Diagnostics of micro- and nanostructures»

11. Y. Zhao, E.Berenschot, H. Jansen, N.Tas, J. Huskens, M. Elwenspoek. "Multi-silicon ridge nanofabrication by repeated edge lithography". Nanotechnology., **20**, pp. 315305, 2009

2. H. Mao, W. Wu, Y. Zhang, G. Zhai, J. Xu. "Fabrication of high-compact nanowires using alternating photoresist ashing and spacer technology". J. Micromech. Microeng., **20**, pp. 085029, 2010

3. I. Amirov, M. Izyumov, V. Naumov. "Low energy selective etching of metal films in oxygen-containing high-density argon plasma". Journal of Surface Investigation: X-ray, Synchrotron and Neutron Techniques, **10**, pp. 855–859, 2016

I3-2: Principle opportunity of the waveguide-resonance phenomenon assistance to cold nuclear fusion process

V. Egorov[1] , E. Egorov[1,2,3]

1. *Institute of Microelectronics Technology, Russian Academy of Sciences, Chernogolovka, Russia, E-mail egorov@ipttm.ru. 2. Institute of Radioengineering and Electronics, Russian Academy of Science, Fryazino, Russia. 3. Financial university under the government of the Russian federation, Moscow, Russia*

The phenomenon of low energy nuclear reaction process is the experimental proving fact today [1]. But the useful effect of this phenomenon is very small. The cold nuclear fusion is registered in different chemical and biological [2] conditions, but the process mechanism is not clear. It is connected with great variety of conditions admitting the cold fusion and low repeatability of experimental results. We assume that our investigations data connected with consequences of radiation fluxes waveguide-resonance propagation study [3] can form the basis for self-consistent mechanism elaboration of the cold nuclear fusion process.

The phenomenon of radiation fluxes waveguide-resonance propagation was discovered in result of our systematic investigations the peculiarities set of X-ray quasimonochromatic (characteristic) fluxes transportation by the planar extended slit clearance formed by polished quartz reflectors. These investigations showed that the wide slit clearance transports X-ray fluxes according to the multiple total external reflection mechanism.. At the same time,, the radiation propagation mechanism changed when the slit clearance width was smaller as half of the radiation coherence length [4]. New mechanism is the result of waveguide-resonance phenomenon manifestation for X-ray beam propagation, and devices functioned in frame of the phenomenon were called as planar X-ray waveguide-resonator (PXWR). These devices are very useful for X-ray nanophotonics because its form X-ray beams with nanosize width and enhanced radiation density. The phenomenon of X-ray fluxes waveguide-resonance propagation is connected with the uniform interference field radiation standing wave appearing in all space of PXWR slit clearance. Our investigations of waveguide-resonance devices properties and peculiarities showed that the independent radiation fluxes can interact in specific conditions through mutual influence of radiation standing waves uniform interference fields activated these fluxes. The interaction effect has the resonance character. The principle of wave-corpuscle dualism gives grounds to expect that the uniform interference fields of radiation standing waves can be excited by particles fluxes characterized by non zero rest mass. This expectation supports by investigations with thermal neutron fluxes use [5]. Atomic and molecular deuterium fluxes can form analogical interference fields, too. The mirror principle allows to assume that conditions exist for these fields mutual influence. In the result, we can expect the cold nuclear fusion realization according to one of d-d nuclear reactions. It is apparent that the mechanism of cold nuclear fusion through the mutual influence of uniform interference fields of deuterium standing waves does not contradict to fundamental physical principles but the effect experimental realization by offering manner is not simple.

1. E. Storm. *The science of low energy nuclear reaction*. World scientific, New Jersey, 2007.
2. V.I. Vysotski, A.A. Kornilova. *Nuclear fusion and transmutation of isotopes in biological system*. Mir, Moscow, 2003.
3. V. Egorov, E. Egorov. *Planar X-ray waveguide-resonators. Realization and perspectives*. Lambert Acad. Publ., Saarbrucken, 2017.
4. V. Egorov, E. Egorov, “Waveguide-resonance mechanism for X-ray propagation physics and experimental background”, J. Advances in X-ray Analysis, 46, pp. 307-313, 2003.
5. V.L. Aksenov, V.K. Ignatov, Yu. V. Nikitenko, “Neutron standing waves in layered systems”, J. Crystallllography Rep., 51, pp. 734-753, 2006.

O3-7: Features of low-energy high dose ion implantation of semiconductors.

Yu. Kudriavtsev, C.Salinas, A.Hernandez, R.Asomoza
Departamento Ingenieria Electrica – SEES, Cinvestav-IPN, Mexico DF, 07360 Mexico
E-mail:yuriyk@cinvestav.mx

The report discusses the results of a study of the implantation of various semiconductors (Si, Ge, GaAs, GaSb, GaN) with different ions (O_2^+, Al^+, Si^+, Ge^+, In^+) with ion energy from 500 eV to 30 keV. The optical, elemental, and structural properties of implanted samples were studied using SIMS, Raman, PL, SEM, and AFM methods. Special attention was paid to additional physical effects accompanying implantation: for the selected ion energy, the effect of ion sputtering of the surface during the implantation process is very strong. We show in the report the effect of ion sputtering on the composition of the implanted layer, as well as on the structure of the sample surface. The existence of the maximum concentration of an implanted element was experimentally and theoretically shown.

The implantation of low-energy ions in semiconductors, among other things, leads to the formation of pores in the near surface region. The formation of porous layers was detected for all investigated semiconductors. The pore size depends on the implanted dose and the temperature of post-implantation annealing and can reach one micron (in the plane parallel to the surface). Implantation of indium ions with a dose of 10^{16} ions/cm^2 into a GaSb led to the formation of a sponge-like surface. The report discusses the physical mechanisms of pores and sponge-like surface formations, as well as the formation of surface relief in the form of nano-sized holes and pits in the process of ion etching of semiconductors by low-energy ions.

The excitation of the semiconductor samples with porous layers by a blue laser leads to luminescence in the visible part of the spectrum. The luminescence spectrum differs a little depending on the target material and implanted ion, as well as the implantation mode. In this case, for all samples studied, the spectrum of the emitted light is close to white light. In the case of the sponge-like surface (GaSb), a narrow luminescence peak is observed near 1434 nm.

O3-8: Low-temperature plasma modification of polymers: surface charging, changing of wettability and nanostructuring

M. Yablokov[1], R. Gainutdinov[2], A. Tolstikhina[2], D. Temnov[3,4], S. Kulemina[3,4], A. Kuznetsov[1]

1.Enikolopov Institute of Synthetic Polymer Materials, Russian Academy of Sciences, Moscow, Russia. 2. Shubnikov Institute of Crystallography of FSRC "Crystallography and Photonics"Russian Academy of Sciences, Moscow, Russia. 3. Herzen State Pedagogical University of Russia, St. Petersburg, Russia. 4. Saint Petersburg National Research University of Information Technologies, Mechanics and Optics,, St. Petersburg, Russia. E-mail: yabl1@yandex.ru

Low-temperature plasma - induced modification of polymers is as a very effective method for enhancement of the films wettability and adhesive strength [1]. The thickness of plasma-modified layer of polymers is not exceeding 50 nm [2]. Direct current (DC) glow discharge treatment of fluorine-containing polymers leads to significant hydropilization and also to the appearance of stable surface charges [3].

Stability of properties of plasma-modified polymer films is very important for their practical usage. One of the most significant problems is the stability of wettability. Hydrophobic polymer surfaces after plasma treatment become hydrophilic, and this hydrophilicity is lost with time. This process is called "hydrophobic recovery", and the nature of this process is not yet well established.

This work is devoted to investigations of nanostructuring, hydrophilization and electric charging of plasma-modified polymer films. Important question is the evolution of surface morphology and distribution of surface charges of polymer film after plasma treatment. Kelvin probe force microscopy [4] gives the possibility to measure the distribution of surface potential and surface charges. AFM and Kelvin probe force microscopy was used in this work for surface characterization of glow-discharge treated polymer films.

Heating of polymer films to the temperature of full relaxation of electret charges, determined from thermostimulated depolarization (TSD) currents measurements, leads to complete loss of hydrophilicity of plasma-treated films and hydrophobic recovery. Contact angles of plasma treated and heated films return to the value of contact angles, relevant to pristine samples. For TSD curves maximums of currents with different polarity were observed. Major high-temperature peaks on the curves obviously belong to relaxation of homocharges, which are injected into the polymer surface during DC discharge treatment. Low-temperature minor peaks may be attributed to heterocharge, connected with orientation of polar groups during plasma treatment of polymer film. These polar groups are formed during oxidation reactions and oriented in electric field in the surface layer during polymer plasma modification.

Direct current glow discharge treatment leads to dramatic changes in polymer film morphology. The characteristic dimensions of the morphological features of the PTFE film treated at the anode and cathode differ significantly. For the film processed at the anode a relatively flat relief is characteristic with pronounced nanosized cracks forming many-sided, relatively flat fragments with a characteristic size of 15-20 nm. For the film treated at the cathode, the characteristic elements of the relief are cylindrical elongated formations with a diameter of about 30 nm and a length of up to 100 nm, oriented coaxially.

The serious problem in the study of the surface of dielectrics by the method of AFM is the effect of surface charge on the mapping of the surface topography - will be reported and discussed.

1. U. Cvelbar, J. Walsh, M. Černák et al., "White paper on the future of plasma science and technology in plastics and textiles", Plasma Process Polym., e1700228, 2018
2. M. Yablokov, I. Sokolov, O. Malinovskaya, A. Gilman, A. Kuznetsov, "Determination of modified-layer thickness of glow-discharge-treated polytetrafluoroethylene film", High Energy Chemistry, 47, pp. 32-33, 2013
3. A. Rychkov, M.Yablokov, A. Kuznetsov, A. Gilman, A. Kuznetsov, "The electret properties of tetrafluoroethylene–hexafluoropropylene copolymer films modified in glow discharge", High Energy Chemistry., 44, pp. 346-349, 2010
4. K. Sorokina, A. Tolstikhina, "Atomic force microscopy modified for studying electric properties of thin films and crystals. Review" Crystallography Reports, 49, pp.476-499, 2004

O3-9: Ion-plasma treatment of textured Pt films

R.V. Selyukov[1], V.V. Naumov[1], M.O. Izyumov[1], L.A. Mazaletskiy[2]

1. Valiev IPT RAS, Yaroslavl Branch, Yaroslavl, Russia, rvselyukov@mail.ru. 2. P.G. Demidov Yaroslavl State University, Yaroslavl, Russia.

Textured Pt films are used as bottom electrodes in ferroelectric film devices. The device performance depends on the parameters of Pt crystalline texture, thus the methods of Pt texture modification is the object of interest. Little is known about the influence of post-deposition ion-plasma treatment (IPT) on the fraction of crystalline phase δ and on the film texture parameters: type, axis directions and sharpness (which characterized quantitatively by the full width at half maximum $\Delta\omega$ of rocking curve). The investigation of the influence of IPT on the crystalline structure is complicated due to the film thinning during IPT. The most of film structure parameters have non-uniform depth distribution, thus the measured values $\Delta\omega$ and δ are changed during IPT due to ion bombardment and to film thinning. In this work we propose the method allowing to separate these two contributions. This method is based on the assumption of the immobility of grain boundaries during film deposition. This assumption is valid for room-temperature Pt deposition. If the films with various thicknesses $h_1 < h_2 <...< h_n$ are deposited at the same conditions providing the immobility of grain boundaries, the value of δ and the texture parameters for film h_i will be the same as for the bottom layer h_i of film with $h_j > h_i$. Thus it's possible to determine the IPT influence on $\Delta\omega$ and δ comparing the $\Delta\omega(h)$ and $\delta(h)$ obtained for as-deposited films and for film h_n after IPT.

20-80 nm Pt films were deposited by magnetron sputtering on oxidized Si(100) at room temperature and at Ar pressure 0.2 Pa. 80 nm film was subjected to the series of four IPTs in Ar plasma. The Ar ion energy was 75 eV, the ion current density was 3.6 mA/cm^2 and the film temperature was ~45°C. 10-20 nm layers were removed during every IPT. The h was measured using EDS, $\Delta\omega$ and δ were determined using Pt(111) rocking curve analysis before and after every IPT. The same measurements were also performed for as-deposited films. As-deposited and treated films have fiber (111) texture and the texture type doesn't change during IPT. The dependencies $\Delta\omega(h)$ and $\delta(h)$ for as-deposited films and for 80 nm film after IPT are shown on fig.1. It is shown that $\Delta\omega(h)$ and $\delta(h)$ are close for as-deposited and treated films in the range h=30-80 nm. This indicates that IPT doesn't change the $\Delta\omega$ and δ for $h > 30$ nm. However the treated film has the sharper texture and larger δ for $h < 30$ nm and this difference can be interpreted as crystalline structure improvement during IPT. Similar improvement is often observed for ion-assisted film deposition and can be explained by the increasing of atom mobility caused by ion bombardment. It's assumed that the same process occurs during IPT. The fact that the structure improvement is observed for $h < 30$ nm can be explained by the inhomogeneity of film microstructure. Grains are smaller in the bottom layers, thus the amount of material in grain boundaries is larger than in the layers near the surface. The binding energy is less in the grain boundaries, consequently for smaller h the atom mobility is higher during IPT.

The investigation was supported by Program no. 0066-2019-0002 of the Ministry of Science and Higher Education of Russia for Valiev Institute of Physics and Technology of RAS.

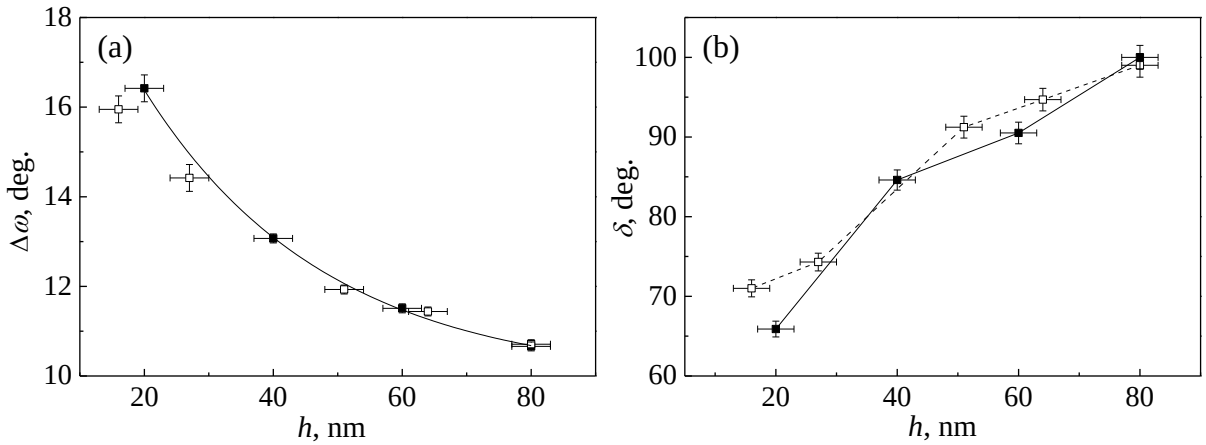

Fig.1. (a) - $\Delta\omega(h)$ for as-deposited Pt (black squares, line) and for 80 nm film after IPT (white squares). (b) - $\delta(h)$ for as-deposited Pt (black squares, solid line) and for 80 nm film after IPT (white squares, dashed line).

O3-10: Evolution of profile silicon nanostructures during sputtering in argon plasma

A. Shumilov, Amirov I.I.

Valiev Intitute of Physica and Technology of RAS, Yaroslavl Branch, Yaroslavl, Russia

The control of feature profiles in directional plasma etching processes is crucial as critical a formation of nanostructures, line-edge roughening, dimension and other artifacts affect device performance and process yields. The molecular dynamics (MD) calculations [1, 2] explore the atomic scale mechanisms of nucleation of nanostructures, provide pertinent information and physical insights. However, in the framework of that methods is impossible to simulate the processes of formation of high aspect ratio nanostructures in real time intervals. That's why the predictable modeling of this process is necessary to understand the surface processes responsible for changes in profile morphology. In our work [3], a method was developed for simulating the sputtering of Si nanostructures taking into account the processes of ion reflection and redeposition of sputtered Si atoms. The method was incorporated into the 2-DimensionaI Monte Carlo profile simulator EDPS with a cell-based representation. Model was tested for accuracy using pyramidal-like Si grooves sputtered in Ar plasma. In this work, using experimental data on the sputtering of high aspect comb nanostructures by low energy Ar^+ (E_i =100 eV) (Fig.1a, b) the evolution of their profile during the sputtering process was simulated. At 100eV the sputtering rate on flat surface was about 0.06 atoms/ion and E_{th} = 46eV. An analytical formula of angular dependence of sputtering yields with the peak in ~60° was used. Under the ~60-65° of ion's incident angle we increased the sputtering probability to ~6.5 times relatively the flat surface. This values correlates with [1]. It was found that the angular distribution of sputtered particles by low-energy ions is very different from the well-known distribution of cosines of Sigmund and is close to the distribution of ~ cos0,1x. Experiments show that the sputtered atoms fly out at the semi-specula direction of reflected ions at off-normal ion angles and along the surface at direct strikes and stick with a probability that was close to unity [2, 3]. The simulation results agree well with the experimental data (Fig 1c). In accordance with the experiment, sharpening of comb structures is observed. With prolonged sputtering, the surface with comb structures becomes smooth.

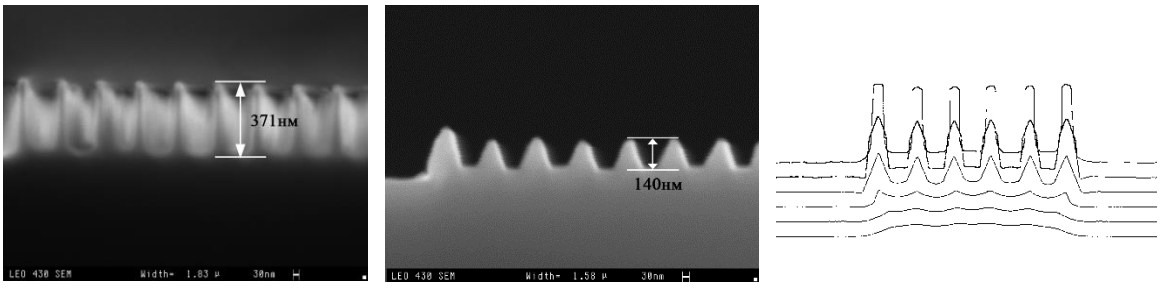

a) b) c)

Fig. 1. Sputtering of comb Si nanostructures on silicon with width 150 nm and height 370nm, AR = 2.5. Initial profile (a), sputtering with time 80c (b), comparing with modeling results with profile lines time 40c (c).

1. A.P. Palov, G.G. Balint-Kurti, E.N. Voronina, T.V. Rakhimova. Sputtering of Si by Ar: A binary collision approach based on quantum-mechanical cross sections. J. Vac. Sci. Technol. A 36(4), pp. 041303, 2018

2. X.-Y. Liu, M.S. Daw , J.D. Kress , D.E. Hanson , V. Arunachalam , D.G. Coronell , C.-L. Liu , A.F. Voter. Ion solid surface interactions in ionized copper physical vapor deposition. Thin Solid Films 422, pp.141–149, 2002

3. A.S. Shumilov, I.I. Amirov. Morphology simulation of the surface subjected to low-energy ion sputtering. Technical Physics. V.60, pp 1056-1062, 2015.

I3-3: Influence of the dispersion forces on elements of MEMS

V. B. Svetovoy[1,2], G. Palasantzas[2]

1. *A.N. Frumkin Institute of Physical Chemistry and Electrochemistry RAS, Leninsky pr. 31, 199071 Moscow, Russia*
2. *Zernike Institute for Advanced Materials, University of Groningen, The Netherlands, v.b.svetovoy@rug.nl*

The dispersion forces in vacuum (or gas) start to play an important role when the interacting bodies are separated by distances smaller than 100 nm. Such small gaps characterize modern micro and nano-electro-mechanical systems (MEMS/NEMS). Although the forces were reliably measured and compared with the theory in the range of 30-100 nm [1], severe problems appear at the distances shorter than 30 nm. Information on the forces in this short-distance range is very important for understanding and control the adhesion between naturally rough bodies. It is difficult to explore the short-distance range experimentally due to jump-to-contact instability. Theoretically it is difficult to predict the forces when the surface roughness becomes comparable with the distance between the bodies. We propose a new method to measure the forces at short separations close to contact. The method is based on the shape of an adhered cantilever. Such a cantilever does not suffer from the jump-to-contact instability and its shape carries information on both the adhesion energy and the force acting nearby the adhered area [2]. The challenges to perform this kind of experiment are described. The aim is to measure the forces between different materials with different roughness statistics in the distance range 5-20 nm with 5% precision. The results will have both fundamental and technological importance since they provide understanding of the adhesion between naturally rough surfaces and clarify the role of the dispersion forces in this adhesion.

1. A. W. Rodriguez, F. Capasso, and S. G. Johnson, Nature Photonics 5, (2011) 211
2. V. B. Svetovoy, A. E. Melenev, M. V. Lokhanin, and G. Palasantzas, Appl. Phys. Lett. 111, (2017) 011603

O3-11: Design of a MEMS switch for improved lifetime and contact resistance

N.V. Marukhin, I.V. Uvarov
Valiev Institute of Physics and Technology of Russian Academy of Sciences, Yaroslavl Branch, Yaroslavl, Russia, i.v.uvarov@bk.ru

MEMS switches combine the advantages of electromechanical relays and solid state switches. They provide superior RF characteristics, small size, low power consumption, and high integration capability [1]. The weak point of ohmic MEMS switches is the contact of a beam with a drain electrode. The contact degrades during operation, which increases the resistance and leads to the switch failure. The reliability can be improved by proper selection of the contact material or choosing the optimal operation conditions. Another approach is to change the switch design. In this work we investigate the influence of two design solutions on the switch performance. The first one is to equip the beam with several contact bumps, and the second way is to use several beams.

The basic switch with a single beam is shown in Fig. 1a. It includes an aluminum beam, platinum gate and drain electrodes and one platinum bump per arm, while the modified switch has two bumps per arm. Fig. 1b illustrates the device with four beams connected to each other. The beams have the same geometry as in the basic design. They are actuated by a common gate electrode and, therefore, operate simultaneously. Both 1-beam and 4-beam switches are fabricated in 1-bump and 2-bump versions. Thus, the devices of four different layouts are fabricated and tested.

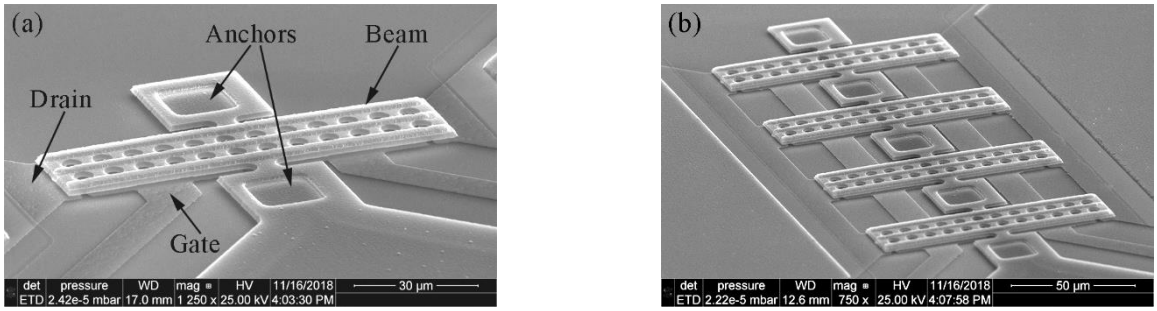

Figure 1. SEM images of the MEMS switch: (a) the basic design with one beam, the main structural parts are shown by the arrows; (b) the switch with four beams.

The switches are tested in a standard laboratory environment, unpackaged. Rectangular voltage pulses are periodically applied to the both gates in such a way that the channels are actuated alternately with the frequency of 3 Hz. The switches operate in a cold mode. Contact resistance R_c randomly changes from several tens to several thousand ohms during the test. To all appearance, the instability is caused by contamination of the platinum contacts. Using two bumps instead of one reduces R_c by about 20%. This indicates that both bumps touch the drain, thereby expanding the contact area. However, increasing the number of beams does not reduce R_c significantly. Probably, the current is distributed unevenly between the beams, and the main part of the current flows only through one beam. After a certain number of cycles the contact resistance increases dramatically up to 100 MΩ, which is considered as a failure of the switch. The device with one bump and one beam has the shortest lifetime of 2.3×10^4 cycles. Increasing the number of bumps prolongs the lifecycle approximately two times, which can be explained by the distribution of the transmitted power between the bumps. Using four beams instead of one gives an almost triple improvement. If one beam fails, the others continue operation, thereby increasing the lifecycle. As a result, the two-bump four-beam switch demonstrates the longest lifetime of 12.1×10^4 cycles.

This work is supported by Program no. 0066-2019-0002 of the Ministry of Science and Higher Education of Russia for Valiev Institute of Physics and Technology of RAS and performed using the equipment of Facilities Sharing Centre “Diagnostics of Micro- and Nanostructures”.

1. G.M. Rebeiz. *RF MEMS: Theory, Design, and Technology.* John Wiley and Sons, Hoboken, 2003
2. I.V. Uvarov, N.V. Marukhin, V.V Naumov, “Contact resistance and lifecycle of a single- and multiple-contact MEMS switch”, Microsyst. Technol., 2019, DOI: 10.1007/s00542-018-4279-2

O3-12: Choosing an optimal electrode shape for the fast electrochemical actuator

P.S. Shlepakov[1], I.V. Uvarov[1], V.V. Naumov[1], A.E. Melenev[1], V.B. Svetovoy[2,3]

1. Valiev Institute of Physics and Technology RAS, Yaroslavl Branch, Yaroslavl, Russia. 2. Zernike Institute for Advanced Materials, University of Groningen, Groningen, The Netherlands 3. A.N. Frumkin Institute of Physical Chemistry and Electrochemistry RAS, Moscow, Russia

Electrochemical actuators are widely used in various microfluidic systems such as drug delivery devices and laboratories on a chip [1]. Voltage applied to the electrodes induces water electrolysis. Hydrogen and oxygen bubbles generated in the chamber push the flexible membrane up. Using a series of microsecond AP voltage pulses instead of one single-polarity pulse can increase the operation frequency of the actuator by several orders of magnitude [2]. However, the electrodes are quickly destroyed in the AP electrolysis. Most metals cannot withstand a high current density ~100 A/cm^2. Titanium electrodes are the most durable, but they oxidize during operation. As a result, less gas is produced, and the performance of the actuator is reduced. The performance can be enhanced by optimizing the electrode layout. The design of electrodes determines the distribution of the current density and, therefore, the preferred location and rate of degradation. In this work, we test several layouts of the electrodes (figure 1) in the AP process and choose the shape that ensures the highest gas generation efficiency and the lowest wear of electrodes.

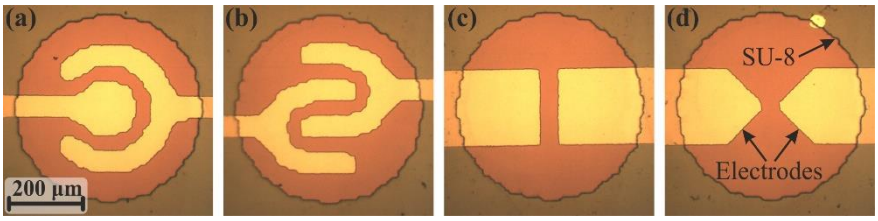

Figure 1 (a,b,c,d). Optical images of the electrodes with different shape: (a) Circular; (b) Interdigitated; (c) Rectangular; (d) Triangular.

The sample is placed in a Petri dish filled with the electrolyte, which is a molar solution of Na_2SO_4 in distilled water. Square voltage pulses of a positive and negative polarity are applied to the working electrode while the other one is grounded. The samples are tested in two modes. In the first mode, the pulses are applied continuously during 180 s. The frequency of pulses f = 200 kHz and the amplitude U = 6 V are fixed. The amplitude is not large enough to cause explosions of the microbubbles [2]. Current flowing through the cell is recorded and the average absolute value I_{av} is calculated. In the second mode, a series of $N = 10^5$ pulses is applied to the sample every 2 s. The amplitude is adjusted to the threshold level U_{th}, at which the concentration of nanobubbles in the electrolyte reaches a critical value. They merge into a microbubble that explodes. The experiment lasts till the U_{th} reaches 19 V that is the upper limit of the amplifier. In the continuous mode the average current decreases with time due to oxidation of titanium. At the beginning of the process the circular and interdigitated electrodes demonstrate the highest I_{av} of 38-40 mA, while the other layouts carry a current of 16-22 mA. In the explosive mode the circular and interdigitated electrodes have the lowest initial value of U_{th} = 10 V. But the interdigitated design reaches the limit very fast (3 min). Triangular layout shows the largest starting voltage U_{th} = 13 V. Rectangular electrodes begin to generate explosions at U_{th} = 12 V. The limit voltage is reached in 22 min. Degradation of the electrodes manifests itself as darkening and partial removal from the substrate. Rectangular electrodes show the highest wear. Taking into account the results described above, rectangular shape is the most suitable for the long-time production of nanobubbles and explosive microbubbles in an open system. Further, we plan to test the selected layouts in a closed chamber of an actuator and to choose the design that provides the best performance of the device.

This work is supported by the Russian Science Foundation, Grant No. 18-79-10038.

1. A. Cobo, R. Sheybani, E. Meng, “MEMS: Enabled Drug Delivery Systems”, Adv. Healthcare Mater., **4**, pp.969-982, 2015

2. I. Uvarov, M. Lokhanin, A. Postnikov, A. Melenev, V. Svetovoy, “Electrochemical membrane microactuator with a millisecond response time”, Sensor Actuat. B: Chem., **260**, pp.12-20, 2018

O3-13: Mechanism of influence of ion bombardment in Ar plasma on residual stress in thin Cr films

A. Babushkin,
Valiev Institute of Physics and Technology of Russian Academy of Science, Yaroslavl Branch, Yaroslavl, Russia,
artem.yf-ftian@mail.ru

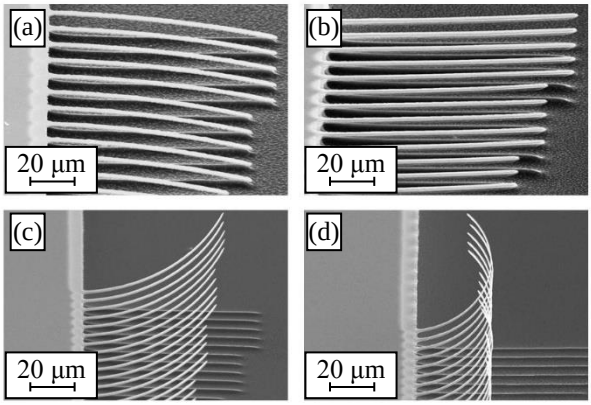

Fig.1. Microcantilevers initially bending down fabricated from as-deposited film (a) and after IPT (b) ε_i = 30eV, t = 45 min, microcantilevers initially bending up fabricated from as-deposited film (c) and after IPT (d) ε_i = 25eV, t = 60 min.

The regulation of mechanical stress in thin metal films is an actual task that has many applications in MEMS and other areas related to coatings. One of the methods to modify the stress in films after their deposition is the bombardment with inert gas ions. Most of the recent work is devoted to the study of the ion energy more than 1 keV [1]. However, bombardment with that ion energy results in the sputtering of the film material. This can be avoided by using ion energy below the sputtering threshold.

In our previous works, it was shown that ion-plasma treatment (IPT) with ion energy below the sputtering threshold (ε_i = 15-30 eV) can have a significant effect on residual stress in Cr films and bending structures made of them (Fig.1) [2, 3]. Depending on the treatment conditions and the initial stress state of Cr films, IPT can both reduce average stress and stress gradient (beams become straight), and increase them (bending of beams increases), that allows to use IPT as a non-destructive tool for stress regulation. However, this requires an understanding of the mechanism of influence and the ability to theoretically predict the effect of IPT.

The most comprehensive study of the effects of ion bombardment on stress in films is presented in the works of Chen et al. [1]. They report that when the ion energy is below several keV, the only possible mechanism responsible for the change in stress is the generation and redistribution of point defects in the near-surface region of the film. The introduction of atoms leads to an increase in compressive stress in the film, and the introduction of vacancies to their decrease. But this model is not applicable to our results. First at an energy of 30 eV the ions are not able to penetrate even into one atomic layer, the generation of defects in our case occurs only on the surface of the film (Fig.2). Secondly, this model considers the movement of defects due to diffusion inside the grains. However, the depth of stress changes comparable to film thickness [3] can be caused only by movement along grain boundaries. Thus, the kinetics of defects determines the change in stress in the film. The report presents the solution of the system of kinetic equations that include the generation, diffusion and drift of defects along the grain boundary due stress gradient. Reported study was carried out under State Programs №0066-2019-0002 of the Ministry of Science and Higher Education of Russia.

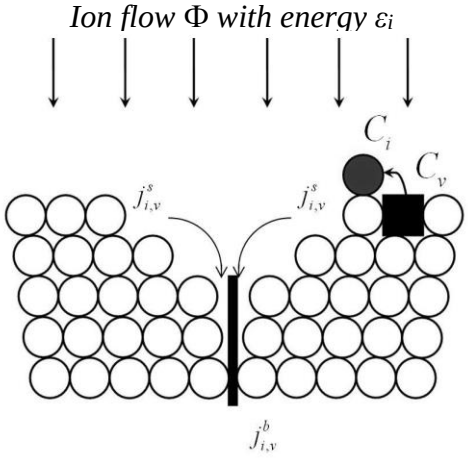

Fig.2. The scheme of the junction of the grains surfaces and the grain boundary.

1. W.L. Chan, E. Chason, “Stress evolution and defect diffusion in Cu during low energy ion irradiation: Experiments and modeling”, J. Vac. Sci. Technol. A, 26, p.44, 2008
2. A.S. Babushkin, I.V. Uvarov and I.I. Amirov, “Influence of ion-plasma treatment on residual stress in the microcantilever”, J. Phys.: Conf. Ser., 741, p.012208, 2016
3. A.S. Babushkin, I.V. Uvarov and I.I. Amirov, “Effect of low-energy ion-plasma treatment on residual stresses in thin chromium films”, Technical Physics, 63. pp.1800–1807, 2018

P2-1: Study of memristor effect in nanocrystalline hafnium oxide thin films for neuromorphic systems application

V. Smirnov[1], R. Tominov[1], V. Avilov[1], D. Dukhan[1], A. Fedotov[1], O. Ageev[1]
1. Southern federal university, Institute of Nanotechnologies, Electronics and Equipment Engineering, Taganrog, Russia, E-mail: vasmirnov@sfedu.ru

Today «bottleneck problem» is the one of the main problems in computer systems, which restricts bandwidth between processor and memory. Overcoming such problem is integration of processor and memory into single device [1]. It allows getting advantage over traditional computers in pattern recognition, as well as in adaptive self-learning systems. Such computer system architecture is called neuromorphic system and is like human brain, which is a set of low-power memory elements - neurons, interconnected via special channels - synapses. One of the most suitable methods of neuromorphic system manufacturing is crossbar based on non-volatile resistive memory (ReRAM) fabrication. Working principle of ReRAM is a memristor effect - resistance change between low resistance state (LRS) and high resistance state (HRS) under the influence of an external electric field. One of the promising materials for this purpose is nanocrystalline hafnium oxide (HfO_2) formed by pulsed laser deposition, which has low power consumption, good endurance and high data retention. To manufacture based on nanocrystalline HfO_2 neuromorphic systems it is needed to study the memristor effect. So, the aim of this work is a study of memristor effect in nanocrystalline HfO_2 films for neuromorphic systems.

Hafnium oxide thin film was grown using pulsed laser deposition technique. Al_2O_3/TiN as a wafer was used. Deposition performed under the following conditions: wafer temperature: 400°C, target–wafer distance: 50 mm, O_2 pressure: 1 mTorr, pulse energy: 300 mJ. Electric measurements were carried out using semiconductor characterization system Keithley 4200-SCS (Keithley, USA) with W probes. During experiment TiN layer was grounded. Current-voltage curves (CVC) were obtained at –1 to +1 voltage sweep. Using the results obtained, resistance of HfO_2 dependence on number of cycle number (endurance test) was built. Curves analyzing was implemented using Origin 8.1 software. Figure 1 shows electric measurements of TiN/HfO_2/W structure. Resistive switching from HRS to LRS (SET) was occurred at 0.48±0.11 V, and from LRS to HRS (RESET) at -0.51±0.18 V (Figure 1a). Endurance test shown that HRS was 353.13±75.42 kΩ, LRS was 0.37±0.08 kΩ (Figure 1b). It was shown, that HRS/LRS ratio was about 954.4 at read voltage 0.3 V.

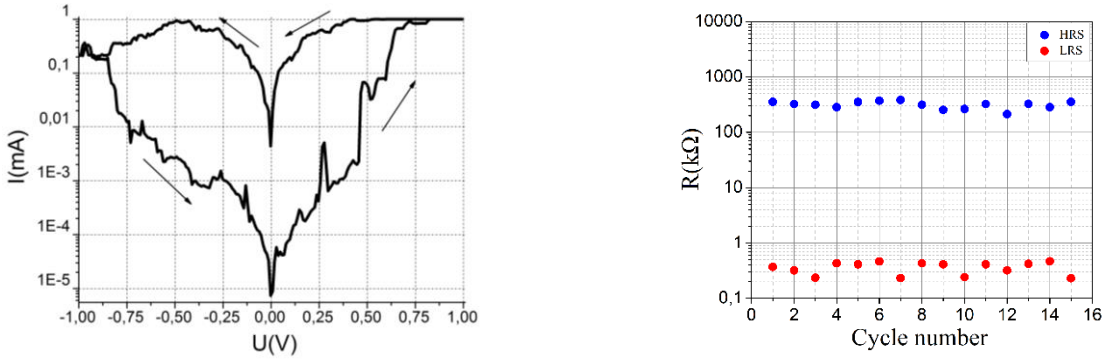

a) b)

Figure 1. Study of resistive switching in nanocrystalline HfO_2: a) – CVC; b) – endurance test

The obtained results can be used for development of technological processes of nanocrystalline HfO_2 film based neuromorphic systems. This work was supported by Grant of the President of the Russian Federation № MK-2721.2018.8 and RFBR (№ 18-37-00299 mol_a project). The results were obtained using the equipment of the Research and Education Center and Center for Collective Use "Nanotechnologies" of Southern Federal University.

1. V. Klimin, R. Tominov, V. Avilov, D. Dukhan, A. Rezvan, E. Zamburg, O. Ageev “Nanoscale profiling and memristor effect of ZnO thin films for RRAM and neuromorphic devices application”, SPIE – The International Society for Optical Engineering, 11022, pp. 110220E, 2018

P2-2: Influence of electrodes material on electroforming and functioning of the open metal-SiO_2-metal sandwich structure

S. E. Kudryavtsev, V. M. Mordvintsev, V. V. Naumov
Yaroslavl Branch of the Valiev Institute of Physics and Technology, Russian Academy of Sciences, Yaroslavl, Russia, E-mail: SergeyKudrjavtsev@yandex.ru

Memory at the electroformed open metal-insulator-metal (MIM) sandwich structures is one of kinds of memristor memory which is actively investigated in recent years. Open MIM sandwich structure is made from the normal MIM sandwich structures by local etching of two upper layers that leads to formation of the butt-end of the dielectric film discovered in a gas phase and performing the function of the isolating slit between two metal electrodes. The electroforming is carry out by a supply of voltage to the metal electrodes with a certain algorithm. Then the structure takes properties of non-volatile electrically reprogrammable memory element.

It was usually used TiN-SiO_2-W open sandwich structure, where the titanium nitride film played role of lower electrode. Thickness of a SiO_2 layer is of great importance for reliability of memory element functioning. In was showed that the optimal value of thickness is about 25 nanometers [1]. The principle role was played by thickness (1 – 3 nanometer) of the "natural", but controlled, TiO_2 layer which is formed on a surface TiN [2], and so actually it is necessary to talk about structure TiN-TiO_2-SiO_2-W. The memory cell contained also bipolar n-p-n-transistor which provided an electric decoupling of elements in a memory matrix. So it was possible to supply on the structure a voltage with only one polarity ("minus" on upper W electrode). Manufacture of memory cells without transistor structure allowed to carry out experiments for both polarity of voltage. It turned out that electroforming process at "plus" on upper W electrode occurs more stably, and N-type current-voltage characteristics (I-U) of electroformed structure under action of cyclically and slowly varying voltage (about 1 V/c) in the region from 0 to 10 V (maximum current was about 3 V) can repeated many times without breakdowns and uncontrollable switching what earlier (at "minus" on W) it was not observed.

Such influence of voltage polarity, in principle, could be connected with one of the following factors. First, it may depend on a certain material of one of electrodes (the cathode, or the anode). Second, it could be connected with the geometrical position of critical material electrode (upper or lower). At the same time the form of the isolating slit is changed (an upper electrode – sharp, lower – flat, and the surface of the isolating slit has a positive slope). Third, it could be connected with existence of a TiO_2 layer on TiN surface. Oxides on W are conducting therefore their existence is not so critical.

For the purpose of examination what of these factors plays the main role in the features of electroforming process and I-U-curves, samples without transistor and with different open sandwich structures were made: normal TiN-TiO_2-SiO_2-W, W-SiO_2-TiN (W - lower electrode, TiN - upper electrode), W-SiO_2-TiO_2-TiN (~2 nanometer Ti layer was deposited on SiO_2 and then oxidized in the oxygen plasma), W-SiO_2-W, TiN-SiO_2-TiN, TiN-SiO_2-TiO_2-TiN. Manufacturing techniques for different structures were similar, but had the more or less significant details.

The research of electroforming processes in different structures and I-U-curves at both polarity of voltage allowed unambiguously reveal the main factor, responsible for existence of stable electroforming and lack of breakdowns and uncontrollable switching at measuring of quasi-stationary I-U-curves. This factor is the manufacturing of the anode of structure from tungsten at any (top or lower) position of this electrode. It was proposed some version explaining such influence of tungsten on structures electrical property. The received result allowed optimizing a memory element design.

1. V. M. Mordvintsev, S. E. Kudryavtsev, V. L. Levin *"*Influence of the Silicon Dioxide Layer Thickness on Electroforming in Open TiN–SiO_2–W Sandwiches", Technical Physics, Vol. 63, No. 11, pp. 1629–1635, 2018.
2. V. M. Mordvintsev, S. E. Kudryavtsev "Effect of Constructional Features of the Insulating Gap of Open TiN–SiO_2–W and Si–SiO_2–W "Sandwich" Structures on the Process of Their Electroforming", Russian Microelectronics, Vol. 46, No. 4, pp. 243–251, 2017.

P2-3: Schottky diode effect in MDP memristors in the conducting state

Popov A.A., Berdnikov A.E.
Valiev Institute of Physics and Technology of Russian Academy of Sciences, Yaroslavl Branch, Yaroslavl, 150007 Russia.

Memristors are promising devices that allow you to create non-volatile memory devices, programmable logic arrays, neural networks, etc. Therefore, the study of the mechanisms of the processes occurring in them is relevant. This paper describes the features of MIS memristors in the conducting state.
The memristor design is as follows. Silicon dioxide 30-40 nm thick by plasma chemistry in a low-frequency discharge is deposited on a p-type silicon wafer with a backside ohmic metallic contact. Metal is applied on this dielectric. This structure has the effect of conduction switching. The I-V plot in the open state is asymmetric at low voltages. Namely rectifying effect is observed, see fig.1.

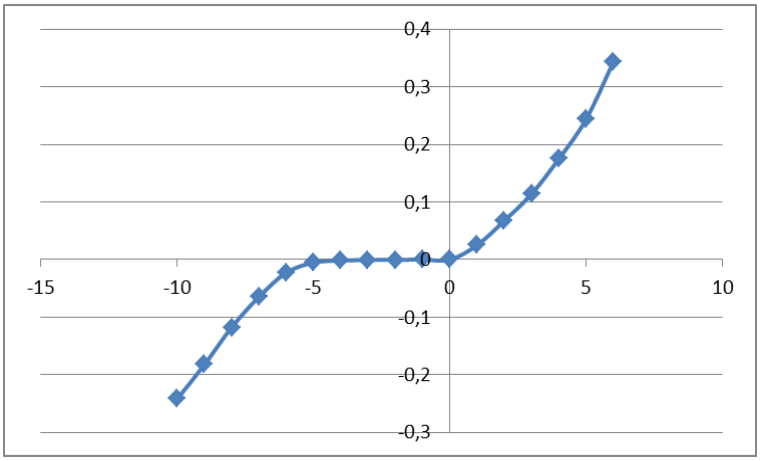

Fig.1. I-V plot of memristor in conductive state. Voltage in V, current in mA.

The purpose of this study is to find out how the parameters of the metal affect the rectifying effect, and determines the occurrence of a Schottky diode. For this purpose, samples were made with different types of metals, namely, Al, Ga, Ni, Ti, Ti-W (90% W), V, Pt. In this case, the work function of electrons from a metal was both less than the work function of silicon and more. In the first case there must be a Schottky diode, in the second there should be an ohmic contact [1]. Experimental data showed that there is no difference in the I-V plot. Thus, regardless of the work function of the metal, there is a Schottky diode, and there is no ohmic contact. It is known that conduction channels of nanometer diameters arise in the open state in a dielectric. They ensure the flow of charge carriers between the metal and the semiconductor. Since the diameter of the conduction channel is extremely small, of the order of a nanometer, and their number is limited and most likely equal to one channel, the contact area between the metal and the semiconductor is very small. Consequently, the diffusion flux of electrons between silicon and metal is extremely small. Because it, the excess of carriers in the near-surface silicon layer, which is necessary for an ohmic contact, disappears when current passes under the action of an applied voltage. The difference in the properties of different structures can be probably seen only at the initial moment of time when a voltage of reverse polarity is turn on. But unfortunately we did not notice any difference in this case.
With a further increase in the reverse voltage, electric field intensity arises in silicon, sufficient to generate electron-hole pairs. As a result, the current rises sharply. The work has been done under State Programs #0066-2019-0003 of the Ministry of Science and Higher Education of Russia.on the equipment of the center for collective use of the scientific equipment «Diagnostics of micro- and nanostructures»

1. К. Шимони Физическая электроника. "Энергия", Москва, 1977г.

P2-4: Effect of ion implantation and annealing on characteristics of memristive structures based on silicon dioxide

Shuyski R.A.[1], Okulich E.V.[1], Okulich V.I.[2], Mikhaylov A.N.[1], Belov A.I.[1]

1. Lobachevsky State University, Nizhniy Novgorod, Russia, ryslan.shuyski@mail.ru. 2. Nizhniy Novgorod branch of the Russian Presidential Academy of National Economy and Public Administration, Nizhniy Novgorod, Russia, victorokulich@mail.ru.

Memristive structures based on oxide materials have been intensively studied in the last decade as the most likely candidates for the creation of computer memory of a new type and as components of artificial neural networks. An important incentive to create them with the use of silicon dioxide is the greatest compatibility of such structures with silicon technology.

Until now, the main obstacle to the use of memristive structures was the uncontrolled reproducibility of their parameters, which was largely due to the stochastic nature of the formation and evolution of conductive pathways – filaments.

The literature suggests that in silicon dioxide-based memristive structures, resistive switching is provided by filaments containing silicon nanoclusters [1]. Since the technology of ion implantation and subsequent annealing will allow tailoring the introduction of silicon nanoclusters in amorphous SiO_2 films in a sufficiently controlled way, it can be assumed that their artificial introduction into such films can be used to control the parameters of memristors. The paper presents the results of such an investigation for $Au/SiO_2/TiN$ structures with a SiO_2 thickness of 40 nm.

SiO_2 films were irradiated with silicon ions with an energy of 20 keV and a dose of $2 \cdot 10^{15}$ cm^{-2}, followed by annealing in vacuum (at 600, 800 and 1000°C) and deposition of gold contacts.

It turned out that only annealing at 600°C led to a noticeable improvement in the parameters of memristors. This is manifested in greater endurance to multiple resistive switching operations compared to reference structures. The study of the surface morphology of the SiO_2 film by the AFM method showed that annealing at temperatures of 800 and 1000°C leads to a noticeable increase in the roughness of the film surface.

This work was supported by the Russian Foundation for Basic Research (Scientific Project No. 18-37-00456).

1. E. Manolov. *Investigation of resistive switching in SiO_2 layers with Si nanocrystals.* IOP Conf. Series: Journal of Physics: Conf. Series, 1186, pp.012022-1-6, 2019

P2-5: Effect of ion irradiation and annealing on quantitative composition of SiO_2-based memristive structures

Okulich E.V.[1], Vorobyov V.L.[2], Bayankin V.Ya.[2], Chigirinsky Yu.I.[1], Dudin Yu.A.[1], Tetelbaum D.I.[1]

1. Lobachevsky University, Nizhniy Novgorod, Russia, jenuha@ya.ru. 2. Udmurt Federal Research Center, Ural Branch of the Russian Academy of Sciences, Izhevsk, Russia, vasily_l.84@mail.ru

The control of parameters of memristive structures based on oxide dielectrics is possible by the method of ion implantation [1]. In particular, it is possible to create a chain of silicon nanoclusters in a film of amorphous silicon dioxide by introducing Si^+ ions into it. In this case, the necessary stage is high-temperature post-implantation annealing. The paper presents the results of the influence of temperature annealing at 600°C (t = 30 min) and irradiation of the Si^+ ion (energy 20 keV, dose $2 \cdot 10^{15}$ cm^{-2}) on the quantitative composition and chemical state of the elements of films SiO_2(40 nm)/TiN(25 nm)/Ti(25 nm)/ SiO_2(0.97 μm)/Si(substrate) at various stages of their manufacture. Measurements were performed by XPS on a SPECS spectrometer using Mg K_α-radiation (E = 1253.6 eV) in combination with layer-by-layer etching with argon ions (etching rate was 1 nm/min).

In the framework of this study, the following results were obtained. The TiN film (before SiO_2 deposition) consists mainly of titanium nitride TiN. However, in addition to titanium and nitrogen, it contains oxygen and carbon in the form of titanium oxides TiO_2 and TiO_x and titanium carbide TiC. In a sample with a silicon dioxide film deposited by magnetron sputtering (at 300°C), before annealing and irradiation to a thickness of about 25 nm, a composition corresponding to the stoichiometric formula SiO_2 was observed, and titanium oxides TiO_2, TiO_x and titanium nitride TiN were observed in a 15 nm thick layer. After annealing of the deposited sample, both before and after silicon implantation, there is a blurring of the distribution profiles of the elements especially in the transition layer, accompanied by an increase in the oxygen concentration with the predominant formation of titanium oxide TiO_2 and the absence of nitrogen in the analyzed layer. In addition, in the transition layer of these samples, silicon Si^0 was observed in a metallic, chemically unbound state.

The results obtained indicate that the elements of various films are strongly mixed, which is explained by their sufficient looseness, and lead to the necessity of reducing the temperature of post-implantation annealing as much as possible.

We gratefully acknowledge the support of the Government of the Russian Federation (contract No. 074-02-2018-330 (2)).

1. A. D. Pogrebnjak (Editor). *Ion Implantation: Synthesis, Applications and Technology.* Chapter 1, Nova, NY, USA, 2018

P2-6: Computer simulation of structural rearrangement of amorphous silicon dioxide under strong supersaturation with oxygen vacancies

Okulich V.I.[1], Okulich E.V.[2], Tetelbaum D.I.[2]

1. Nizhniy Novgorod branch of the Russian Presidential Academy of National Economy and Public Administration, Nizhniy Novgorod, Russia, victorokulich@mail.ru. 2. Lobachevsky State University, Nizhniy Novgorod, Russia, jenuha@ya.ru.

In order to estimate the structural rearrangement of amorphous silicon dioxide in the region with local supersaturation of oxygen vacancies, computer simulation was performed using the molecular dynamics method (LAMMPS code). The behavior of amorphous SiO_2 cluster was simulated when it was saturated with oxygen vacancies with their concentration corresponding to the average stoichiometric $SiO_{1.7}$ formula. In this case, two types of interatomic interaction potentials were used for SiO_2 - Tersoff and ReaxFF. Simulation was carried out for temperatures in the range of 300-1500 K. The time was reached ~ 9 ps. The calculations were carried out on a supercomputer of Lobachevsky State University.

Analysis of the nodal coordinates of Si atoms and the radial functions of the atomic distribution constructed for them showed the appearance of two-three-node clusters of these atoms in the region of the maximum concentration of vacancies at temperatures > 1000K.

In the literature, there are two models of the formation and operation of conduction paths (filaments) in memristic structures based on amorphous silicon dioxide: with the participation of O-vacancies [1] and Si-nanoclusters [2]. The results obtained can be considered as an argument in favor of the 2nd (cluster) model or, at least, in favor of their symbiosis.

We gratefully acknowledge the support of the Government of the Russian Federation (contract No. 074-02-2018-330 (2)).

1. A. Mehonic. *Silicon Oxide (SiO_x): A Promising Material for Resistance Switching?.* Adv. Mater. 1801187, pp.1-21, 2018

2. E. Manolov. *Investigation of resistive switching in SiO_2 layers with Si nanocrystals.* IOP Conf. Series: Journal of Physics: Conf. Series, 1186, pp.012022-1-6, 2019

P2-7: The change of the forming voltage of $Al_2O_3/HfO_2/Al_2O_3$ memristor structure after implantation and annealing

O. Permyakova[1,2], A. Miakonkikh[1], K. Rudenko[1], A. Rogozhin[1]

1. *Valiev Institute of Physics and Technology, Russian Academy of Sciences, Moscow, Russia, rogozhin@ftian.ru*
2. *Moscow Institute of Physics and Technology (State University), Dolgoprudny, Russia, o.permyakova@phystech.edu*

One of the most prominent types of the next-generation non-volatile memory is resistive switching memory (ReRAM). It has the following advantages: high-speed operation, low power consumption, comparatively simple structure and amazing scalability. Typically, ReRAM cell has metal-insulator-metal (MIM) structure, different materials from metal oxides to various organic compounds can act as insulators [1, 2]. It was shown that the $Al_2O_3/HfO_2/Al_2O_3$ stack-based structure demonstrates the properties required in ReRAM [3].
Several ways to improve the ReRAM structure characteristics by incorporation of defects were proposed. For instance, annealing in different media (vacuum, oxygen, inert gases) [4] and temperature [5] or focused ion beam processing [6] were suggested. In this paper we present the investigation of the effect of post-metal annealing and He^+ ion implantation on the forming voltage for the $Al_2O_3/HfO_2/Al_2O_3$ structure.
The Al_2O_3(6nm)/HfO_2(10nm)/Al_2O_3(3nm) structures were formed by PEALD on the Si wafers covered by sputtered TiN. After that structures were coated Pt and Ni. Then some of the structures were annealed in the nitrogen atmosphere at 450°C for 300 s. For other samples plasma immersion ion implantation of He^+ was used to incorporate defects in the dielectric stack structure. The energy of He ions was 2keV. The dose values varied in the range of 10^{14}-10^{16} cm^{-2}. After implantation some structures were annealed. Current-voltage characteristics were measured using semiconductor characterization system Keithley 4200-SCS.
Voltage characteristic of the obtained structures are presented in the Table 1.

Table 1. Voltage characteristics and yield.

	Forming voltage, V	SET voltage, V	RESET voltage, V	Yield*, %
Initial structure	13.1 ± 0.8	-2.3 ± 0.3	1.7 ± 0.2	88
Annealing in N_2 atmosphere	10.9 ± 0.6	-3.2 ± 0.4	2.6 ± 0.5	72
Implantation dose 10^{14} cm^{-2}	9.5 ± 0.7	-5 ± 2	2.7 ± 0.6	33
Implantation dose 10^{15} cm^{-2}	8.8 ± 0.3	-4.5 ± 1.2	2.3 ± 0.6	62
Implantation dose 10^{16} cm^{-2}	10.6 ± 0.2	-4.9 ± 1.4	1.6 ± 0.6	74

* For each structure up to 20 cells were measured

The reported study was funded by RFBR according to the research project № 18-37-20076.

[1] Ielmini D, Waser R, *Resistive Switching*, Wiley-VCH, Weinheim, 2016
[2] Mario Lanza et al., "Recommended methods to study resistive switching devices", Advanced Electronic Materials, **5**, 1800143, 2019
[3] Lai-Guo Wang et al., "Excellent resistive switching properties of atomic layer-deposited $Al_2O_3/HfO_2/Al_2O_3$ trilayer structures for non-volatile memory applications", Nanoscale Research Letters, **10**:135, 2015
[4] Tsung-Ling Tsai et al., "Impact of Post-Oxide Deposition Annealing on Resistive Switching in HfO_2-Based Oxide RRAM and Conductive-Bridge RAM Devices", IEEE Electron Device Letters, **36**, pp.1146-1148, 2015
[5] Yu-Ting Su et al., "A Method to Reduce Forming Voltage Without Degrading Device Performance in Hafnium Oxide-Based 1T1R Resistive Random Access Memory", IEEE Journal of the Electron Devices Society, **6**, pp.341-345, 2018
[6] Avilov V. et al., "Investigation of memristor effect on the titanium nanowires fabricated by focused ion beam", Proc. of SPIE, vol. 10224, Moscow: Max press, Zvenigorod, 2016

P2-8: Application of laser reflectomery for study of adsorption of gases on porous low-k dielectrics during cryo etching

R. Gaydukasov[2], A. Miakonkikh[1]

1. Valiev Institute of Physics and Technology of Russian Academy of Sciences, miakonkikh@ftian.ru. 2. Moscow Institute of Physics and Technology (State university) (MIPT), Dolgoprudny, Moscow Region, Russia.

Low damage (LD) plasma etching is one of the key challenges for successful integration of porous low-k dielectrics in advanced interconnects. This problem is becoming even more important during the implementation of highly porous dielectrics with k < 2.5. Plasma etching degrades k-value because of impact of chemically active radicals, ions and VUV photons. Increase of the k-value is caused by surface densification, changes in the chemical composition and bonds configuration. Results [1] comparing CF_4 and CF_3Br at low temperature show that the polymer layer, which is deposited on the dielectric surface in CF_4 plasma, protects the low-k film against the fluorine atoms penetration, but in the plasma of the CF_3Br, gas condensation in the pores is poor and the damage is great, moreover, the film becomes hydrophilic after treatment in such plasma and the hydrophilic properties do not disappear during annealing. It is expected that $C_2F_4Br_2$ gas is able to condense in the pores at -80 to -120 °C at the typical pressures for plasma etching and could prevent damage.

In this paper, the process of gas adsorption in a porous dielectric is investigated. $C_2F_4Br_2$ is used as the working gas; the sample temperature ranges from -110°C to -100°C. The processes were carried out in the ICP etching tool (Plasmalab 100, OIPT) at a pressure of 0 to 90 mTorr. As a sample we used OSG films (30% open porosity and k=2.3) with 200 thickness on Silicon substrate. Initial refractory index was 1.3 according to spectral ellipsometry. When gas is condensed in pores the refractive index is increased. Fig. 1a shows change in reflection coefficient for laser light (632.8 nm) depending on film refractive index.

In order to measure the change in the light reflection coefficient of the film in the adsorption process, was we apply *in situ* laser based reflectometer. The radiation source is a helium-neon laser with a wavelength of 632.8 nm. The sample was preliminary annealed in the room atmosphere at 300°C for 30 min. The table temperature was controlled by thermocouple and maintained by flow of liquid nitrogen. The sample temperature was maintained by helium flow under the substrate. The change if reflection coefficient with pressure of $C_2F_4Br_2$ was observed (Fig. 1b). The dependence of pressure when gas is condensed in the film on the sample temperature will be presented. This data is crucial for development of low-damage processes of cryo etching of low-k films.

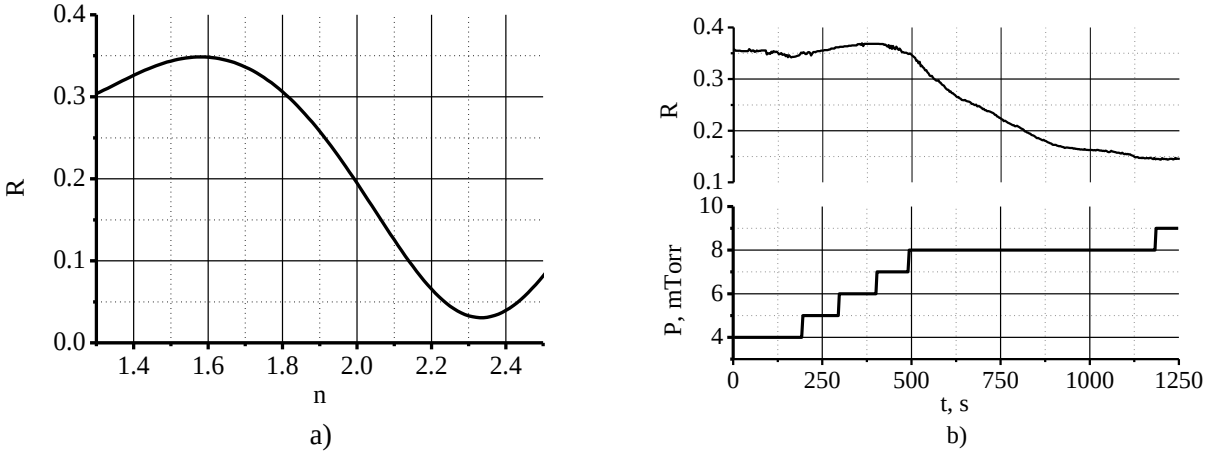

Fig 1. a) Calculated dependency of reflection coefficient on film refractive index; b) Pressure мы time graph (top) and reflection coefficient during pores filling during increase of pressure of $C_2F_4Br_2$ at constant temperature T=-105°C

This work was partially supported by the RFBR grant No. 18-29-27025.

1. A. Rezvanov, A. V. Miakonkikh, A. S. Vishnevskiy, K. V. Rudenko, M. R. Baklanov, J. Vac. Sci. Technol. B **35**, 021204 (2017)

P2-9: Approaches to atomic layer etching of dielectrics in conventional plasma etching tool

V. Kuzmenko[1,2] , A. Miakonkikh[1,2], K. Rudenko[1,2]

1. *Valiev Institute of Physics and Technology of Russian Academy of Sciences, Moscow, Russia,* kuzmenko.vo@phystech.edu
2. *Moscow Institute of Physics and Technology, Dolgoprudny, Russia*

At present work different approaches to atomic layer etching (ALE) of dielectrics are studied. Materials which are used in FEOL are reviewed: high-k dielectrics (HfO_2, Al_2O_3) and SiO_2. With scaling modern devices gate dielectric becomes thin and multi-layered [1], as high-k provide to scale electric field in transistor and SiO_2 provides quality interface with Si. That is why development commercial technology of atomic layer etching will be valuable for these materials. The efforts of the scientific community are mainly focused on the use of equipment with accelerated ion or neutral beams, which is reflected in publications [2], which cannot be applied in microelectronic industry. Development of the ALE process on a commercial tool is vital for the application.

In this cyclic process on the surface thin modified layer is formed and then reaction between this layer and surface is activated. Volatile products remove from surface. In ideal routine atomic precision provided by process condition in which both step are self-limiting. In fact etching occurs only because of stimulated chemical surface reaction.

There are two attempts of realizing of atomic layer etching presented in this work. The first applies chlorine-containing gas, the second – fluorine-containing.

First, BCl_3 is used for etching of ALD HfO_2 and ALD Al_2O_3. In this process modified layer is formed by adsorption from gas phase. For reaction activation we use Ar CCP with 60-100V DC bias. As desorption rate grows with increase of sample temperature, sample was cold to -20°C. Dependence of etch rate per cycle from BCl_3 dose was measured. Duration of activation was 10 s. When activation performed at 75 V DC bias process shows both saturation and moderate sputtering. Etch rate for HfO_2 was about 0.025 nm/cycle and for Al_2O_3 - 0.020 nm/cycle. This is slow enough to be considered as ALE, comparing with [3], which could be better referred as pulsing etching.

Another task was to etch SiO_2. Experiment was carried out on amorphous SiO_2 deposited by CVD. In this process polymer film from C_4F_8 plasma was used as modification layer. Deposition step was studied in details and appropriate regime was chosen. In cyclic process surface etching reaction was activated by O_2 ICP with about 22 V DC bias. Etch rate was measured with changing time of deposition step. Duration of activation step remains constant 12 s. It was observed that saturation of etch rate takes place at the value of 0.22 nm/cycle. That is close to interatomic distance in amorphous SiO_2 (0.23 nm), and proves single atomic etching regime.

Overall, this work shows opportunities of realization atomic layer etching in conventional tool. Slow etching rate confirm that achieved process are close to atomic regime. For SiO_2 it was managed to reach quite good accordance etch rate with interatomic distance. The main parameters determining the etching rate and reproducibility of the process are the substrate bias voltage, its temperature, and the duration of the two stages of the process. At the same time, the observed process window often has blurred boundaries. Further improvement of the results is possible by optimizing the dosing of gases into the reactor and the matching box, allowing more accurately setting of the bias voltage during the process at low values of RF power.

1. K. Hui Jing et al., “Gate Dielectric Scaling in MOSFETs Device”, AIP Conference Proceedings, 1733, pp. 020073-1-020073-6, 2016

2. K.S. Min et al., “Atomic layer etching of Al_2O_3 using BCl_3/Ar for the interface passivation layer of III–V MOS devices”, Microelectron. Eng., 110, pp.457-460, 2013

3. T. Tsutsumi et al., “Atomic layer etching of SiO_2 by alternating an O_2 plasma with fluorocarbon film deposition”, J. Vac. Sci. Technol. A, 35, pp. 01A103-1-01A103-4, 2017

P2-10: GeSn/Ge/Si(100) heterostructures grown by hot wire CVD

S. Denisov, A. Zaitsev, V. Chalkov, V. Shengurov, M. Ved', A. Zdoroveyshchev, D. Filatov, A.Nezhdanov, D.Pavlov, A.Syshkov

Lobachevskii State University of Nizhnii Novgorod, Nizhnii Novgorod, Russia, denisov@nifti.unn.ru

The epitaxial layers of GeSn alloy are considered as a promising material for the photodetectors for the communication wavelength band 1.3 – 1.6 mkm as well as for the light emitting diodes capable for the monolithic integration into the silicon integrated circuits. In recent years, various methods of low-temperature epitaxy have been applied for growing the GeSn layers extensively.

In the present work, we report on the results of investigations of the GeSn layers grown on the Si(100) substrates with Ge buffer layers by chemical vapor deposition utilizing the decomposition of monogermane on a hot wire. The Sn flow was generated by its evaporation form an effusion cell. the properties of the GeSn/Ge/Si(100) layers were compared to the ones of similar layers of the GeSn alloys grow directly on the Si(100) substrates.

The GeSn layers were grown at low temperatures (250 – 325°C). The crystal quality of the epitaxial layers was evaluated by X-Ray Diffraction (XRD) and by Cross sectional Transmission Electron Microscopy (X-TEM). According to the XRD data, the crystal quality of the GeSn layers increased with increasing growth rate (i.e. with increasing temperature of hot wire, where the decomposition of monogermane takes place): the full width at half maximum (FWHM) of the GeSn (004) rocking curves decreased from 14 angular min. down to 7.5 angular min. However, the crystal quality of the GeSn layers worsened wit increasing the atomic fraction of Sn in the alloy up to 9.8% at.

The X-TEM investigations of the heterostructures revealed no interface defects to nucleate in thin ($\leq$ 250 nm) GeSn layers. In thicker (700 nm) layers Sn precipitation has been observed. The precipitates were scribed to the segregation of Sn on the growing surface. Raman spectroscopy revealed the Ge–Ge and Ge–Sn vibration modes in the GeSn alloys.

In the photoluminescence spectra (300 K) of the GeSn/Ge/Si(001) epitaxial layers, the peaks in the photon energy range 0.7 – 0.73 eV and 0.63 – 0.65 eV have been observed. These peaks were attributed to the direct and indirect interband radiative optical transitions in GeSn, respectively.

P2-11: Surface mobility of electrons near SiO_2 – Si interfaces of electrons SOI double gates MOS transistors with weakly doped built – in channel

A.Leonov, V.Mordkovich

Institute of Microelectronics Technology and High Purity Materials, Russian Academy of Sciences (IMT RAS), Russia, Chernogolovka, alex25.08@mail.ru

Electrons surface mobility near SiO_2 – Si interfaces in TFY SOI double gates MOS transistors with weakly doped ($5 \cdot 10^{14}$ sm^{-3}) built – in channel was investigated. The lateral surface sides of channel contained an additional n^+ contacts used for measurement of mobility using the Hall effect. Such magnetosensitive junction less transistor (MILT) is able to function in the accumulation mode near Si surfaces (positive potentials on MOS gates) or in the depletion mode near Si surfaces (negative potentials on MOS gates). Electrons concentration near Si surfaces in accumulation mode was $10^{17} – 10^{18}$ sm^{-3} depends on the values of gates potentials. In this case the channel thickness was about 20 -30 nm.

It is established that in the conditions of deep cooling (2 – 20K) are absent MILT in accumulation mode continues to function due to the flow of electrons coming from the power source and moving directly along the SiO_2 – Si interfaces.

Herewith the value of the channel current depends on the density of states N_{ss} at the interface N_{ss} depends from the technology of forming the buried dielectric of SOI structure and a front oxide of MOS structure. It was shown that in the case of formation of hidden layer of SiO_2 in Si by implantation of oxygen ions and postimplantation annealing (SIMOX process – Separation by Implanted Oxygen) N_{ss} is at least an order of magnitude grater that in the case of thermal SiO_2 in smart - cut SOI process. It has been shown that a significant role in the increase of N_{ss} in SIMOX interface play the Si clusters creation inside SIMOX SiO_2 as result of postimplantation annealing of Si implanted region representing a region of solid solution supersaturated with radiation defects and oxygen atoms.

It was also shown that in the depletion mode of operation MILT has significantly higher resistance to ionizing radiation than in the accumulation mode (in particular due to the capture of electrons on N_{ss}, which decreased the scattering).

In additional it was shown that the effect of surface mobility on the magnetic sensitivity reduced due to effect of charge coupling between dielectrics layers of two MOS sistems.

P2-12: Modeling of plasmonic interaction in periodic silicon-based multilayer structures

A. Mukhammad[1], M. Lobanok[1] K. Chizh[2], V. Yuryev[2], P. Gaiduk[1]
1. Belarusian State University, Nezavisimosti av. 4, 220030 Minsk, Belarus, rct.muhammad@bsu.by
2. A. M. Prokhorov General Physics Institute of RAS, Moscow, Russia

Light absorption due to excitation of plasmon resonances in metallic particles can be used for sensibilization of photodetectors in a visible region of optical spectrum. This approach is potentially interesting and relevant for development of devices in the infrared region [1]. However, the metallic-associated plasmon resonance manifests itself for the red to blue photons, thus there is a necessity in the search of alternative plasmonic materials. It has been recently proposed [2], that highly-doped semiconducting islands might be an alternative class of plasmonically active materials which are efficient in the mid and far infrared region. The present investigation deals with comparative modelling of light absorption in highly doped periodic silicon-based multilayer structures.

Si-SiO_2-Si stack of layers is used as a model structure. The surface layer consists of 2D array of Si islands periodically positioned along x and y directions. 8 μm periodicity and a fill factor of 0.5 are used for surface distribution of islands. The thickness of the surface Si layer is selected to be 1.2 um. Top and bottom silicon layers were doped to concentration of 10^{19} cm^{-3} and optical constants for the doped silicon layers are taken from [3]. The thickness of intermediate SiO_2 layer is varied from 0.4 to 2.2 μm. Simulation of light absorption due to plasmonic excitations is carried out by the FDTD method. The effect of the thickness of the silicon dioxide layer on absorption spectra is investigated.

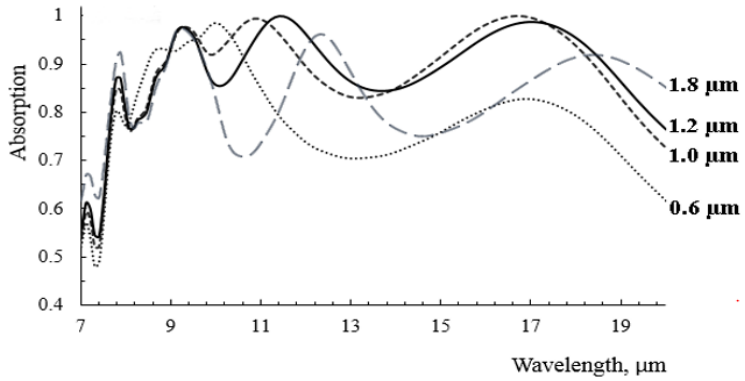

Figure 1. Effect of SiO_2 thickness on absorption spectra of Si-SiO_2-Si structures

It is found from the FDTD simulations that the light absorption spectra have plasmon resonance related absorption peaks at wavelengths of 8 μm, 9.5 μm and 17 μm and they depend strongly on the thickness of intermediate SiO_2 layer (fig.1). The position of the peak at 8 μm is the same for all structures, as this range is dominated by absorption on Si islands. The molecular resonance of SiO_2 appears at 9.5 μm and the absorption intensity in this range is also similar for all structures. Wide absorption band at 17 μm is due to interaction of localized and surface plasmons of different layers in the stack. The thickness of SiO_2 layer impacts on this interaction non-monotonically: optimal range is registered around 0.8 – 1.2 μm, where the absorption level is as high as 0.9 – 0.95. The layered structures of Si-SiO_2-Si simulated in this research can be manufactured using standard optical lithography, which makes it cost-effective for production.

This research was supported by BRFFR, grant # T18P-190 and by RFBR, grant #18-52-00033.

1. K. Gorgulu and M. Yilmaz, “All-Silicon Ultra-Broadband Infrared Light Absorbers”, Scientific reports., 6, pp.38589, 2016
2. А.И. Мухаммад, М.В. Лобанок, К.В. Чиж и др. “Моделирование локализованных плазмонов в периодических многослойных структурах на основе кремния”, материалы VIII международной научной конференции “Материалы и структуры современной электроники”, Минск 10-12 октября 2018 г., с 318-322
3. E. D. Palik, *Handbook of optical constants of solids*. Academic Press, 1985

P2-13: Effect of laser annealing on diode heterostructures with a ferromagnetic GaMnAs layer

O. Vikhrova, Yu. Danilov, M. Dorokhin, B. Zvonkov, A. Zdoroveyshchev, I. Kalentyeva, A. Kudrin, E. Larionova

N.I. Lobachevsky State University, Nizhny Novgorod, Russia, E-mail address:vikhrova@nifti.unn.ru

This paper presents the results of an experimental study of *p*-(Ga,Mn)As/*n*-InGaAs/n^+-GaAs diode heterostructures in the initial state and after pulsed excimer laser annealing (wavelength 248 nm, pulse duration 30 ns, energy density 270 mJ/cm^2) on a *p*-(Ga,Mn)As layer. Samples were obtained by a combination of MOC-hydride epitaxy (MOCVD) and pulsed laser deposition (PLD). The *n*-$In_xGa_{1-x}As$ (x ~0.1) buffer layer ~ 1.8 μm thick doped with Si atoms (n ~8×10^{16} cm^{-3}) was grown on n^+-GaAs(001) substrates using the MOCVD method at a temperature of 650°C. Then, at 330°C, a *p*-type (Ga,Mn)As layer (ratio of Mn and GaAs target sputtering times t_{Mn}/t_{GaAs} = 0.15) with a thickness of 30 nm and a GaAs coating layer (9 nm) was formed using the PLD method. It was previously shown that such GaMnAs layers have ferromagnetic properties [1]. An ohmic contact based on Au was deposited on top of the (Ga,Mn)As layer by electron beam evaporation, and mesa structures of ~ 600 μm in diameter were made using photolithography and chemical etching. An ohmic contact to the n^+-GaAs substrate was formed by the electric-spark firing of the Sn foil. Current-voltage characteristics and magnetic field dependences of diode resistance were studied using a Keithley 2400 measuring source and a Janis CCS-300S/202 closed-cycle helium cryostat at temperatures from 10 to 300 K. A magnetic field (± 3600 Oe) was applied perpendicular to the surface of the structures using electromagnet.

The influence of an external magnetic field on the current-voltage characteristic and the resistance of as-grown and pulsed laser annealed diodes were found. When a magnetic field was applied, an increase in the current through the *p*-*n* junction was observed at forward bias, due to the negative magnetoresistance (NMR) effect of the (Ga,Mn)As layer. The presence of the NMR is confirmed by the corresponding magnetic field dependences of the resistance of the diodes - *MR* (*H*), obtained in the forward bias (*U*) mode (Fig. 1). The value of the NMR effect is non-monotonically (maximum near U = 1 V) depends on the magnitude of the forward bias on as-grown and laser-annealed samples of the diodes. A significant increase in maximum temperature of observation of the NMR effect was registered (from 70–80 K for the initial sample to 120–140 K for the annealed sample), that may indicate an increase in the Curie temperature of the (Ga,Mn)As layer due to pulsed laser annealing. The *MR*(*H*) dependences of as-grown diode have a hysteresis appearance (Fig. 1), due to the presence of a component of the magnetization vector perpendicular to the surface of the structures. The use of laser annealing leads to a significant increase in the coercive field. The obtained results make the p-(Ga,Mn)As/n-InGaAs/n^+-GaAs diode heterostructures promising for use in spin electronics.

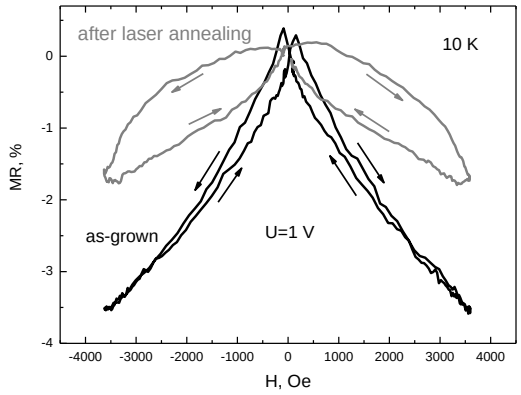

Fig. 1. The magnetoresistance dependence on the magnetic field for as-grown and laser-annealed samples of the *p*-(Ga,Mn)As/*n*-InGaAs/n^+-GaAs diode heterostructure.

This study was supported by Russian Science Foundation (grant 19-19-00545).

1. B.N. Zvonkov, O.V. Vikhrova, Yu.A. Danilov, Yu.N. Drozdov, A.V. Kudrin, and M.V. Sapozhnikov, "Effect of Compressive and Tensile Stresses in GaMnAs Layers on Their Magnetic Properties", Physics of the Solid State, 52, pp. 2267–2270, 2010.

P2-14: Micromagnetic and magneto-optical properties of CoPt (CoPd) films grown by electron-beam evaporation

A. Zdoroveishchev[1], O. Vikhrova[1], P. Demina[1], M. Dorokhin[1], A. Kudrin[1], A. Temiryazev[2], M. Temiryazeva[2], I. Khodos[3]

1. *Physico-Technical Research Institute, N.I. Lobachevsky State University, Nizhny Novgorod, Russia, E-mail address: zdorovei@nifti.unn.ru.*
2. *Kotelnikov Institute of Radioengineering and Electronics, Russian Academy of Sciences, Fryazino branch, Fryazino, Russia*
3. *The Institute of Microelectronics Technology and High-Purity Materials, Russian Academy of Sciences, Chernogolovka, Russia*

An important task of spintronics is the search, production and study of materials for the creation of thin ferromagnetic films with easy magnetization axis lying perpendicularly to the growth plane. One of such materials is an alloy of ferromagnet and heavy metal. This material has a unique magnetic structure, which causes the vertical anisotropy of the magnetization of very thin (about 8 nm) films [1]. The use of such films in a number of spintronics devices, for example, CoPt layers in the construction of a spin light-emitting diode [1], can significantly reduce the range of operating magnetic fields up to the possibility of operating the device without an external magnetic field due to the use of residual magnetization of the material. In addition, due to the presence of interfacial exchange interaction of Dzyaloshinskii – Moriya [2] between metal atoms, in such films it is possible to have skyrmions that are stable at room temperature [3].

The films under study were formed by the method of electron-beam alternate high-vacuum evaporation of targets from high-purity materials (Co, Pt, or Pd). The composition of the films was varied by varying the ratio of the thicknesses of the Co and Pt (Pd) layers and was measured by X-ray photoelectron spectroscopy [4]. This paper presents a comparative analysis of the magnetization, Kerr and Faraday magneto-optical effects, results of measuring the micromagnetic structure with a magnetic force microscope, and studies of transmission electron microscopy for thin films of CoPt, CoPd alloys with different cobalt contents. It was found that with an increase in the cobalt content in films of both types, a sharp decrease in the average size of the magnetic domain is observed. In the case of a Co thickness of 0.3 nm, the size is about 100 nm. From the study of the magnetic field dependences of magnetization, it was found that for all compositions the axis of easy magnetization is located perpendicularly to the film surface, the magnetization quickly saturates in relatively small magnetic fields. If the field is applied in parallel to the film surface, the magnetization does not reach saturation in the magnetic fields of up to 300 mT available to us. With an increase in the cobalt content in the CoPd and CoPt films, the coercive field decreases from 50–55 mT to 8–10 mT, and the hysteresis loop becomes less “rectangular”. The magnetic field dependence of the Faraday rotation angle in combination with the weak dependence of the transverse Kerr effect on the magnetic field confirms the prevailing orientation of the axis of easy magnetization along the normal to the surface of both types of films. Unlike CoPd, the CoPt films exhibit stronger magneto-optical properties. The Faraday angle in saturation is more than twice as large for the CoPt alloy and reaches 1.5×10^6 deg/cm.

This work was supported by the project part of the state assignment of the Ministry of Science and High Education of Russia (No. 8.1751.2017 / PCh), the Russian Foundation for Basic Research (18-29-19137_mk) and the grant (MD-1708.2019.2) of the President of the Russian Federation.

1. A.V. Zdoroveyshchev, M.V. Dorokhin, O.V. Vikhrova, et al., “Properties of CoPt ferromagnetic layers for application in spin light-emitting diodes”, Physics of the Solid State, 58, pp.2267-2270, 2016
2. A. Samardak, A. Kolesnikov, M. Stebliy, et al. “Enhanced interfacial Dzyaloshinskii-Moriya interaction and isolated skyrmions in the inversion symmetry-broken Ru/Co/W/Ru films”, Appl. Phys. Lett., 112, N.192406, 2018
3. A. Fert, N. Reyren, and V. Cros, “Magnetic skyrmions: advances in physics and potential applications”, Nat. Rev. Mater., 2, N.17031, 2017
4. A.V. Zdoroveyshchev, M.V. Dorokhin, P.B. Demina, et al., “CoPt ferromagnetic injector in light-emitting Schottky diodes based on InGaAs/GaAs heteronanostructures”, Semiconductors, 49, pp.1601-1604, 2015

P2-15: Photoluminescence in IR-range from silicon irradiated with swift heavy ions

Volodin V.A.[1,2], Cherkova S.G.[1], Skuratov V.A.[3]

1. A.V. Rzhanov Institute of Semiconductor Physics, Russian Academy of Sciences, Novosibirsk, Russia, volodin@isp.nsc.ru. 2. Novosibirsk State University, Novosibirsk. 3. Joint Institute for Nuclear Research, Dubna.

The defect engineering in semiconductors has long been widely discussed [1]. In particular, dislocation-related photo- and electroluminescence in IR-range gives chance to establish Si-based optoelectronics. There are a number of techniques for such defects formation. The optical properties of silicon irradiated with swift heavy ions are poorly studied. Although it can be interesting as a way to create defects emitting light at wavelength about 1.5 microns.

Samples of float-zone (2000 Ohm·cm) silicon (111) were irradiated at room temperature with 167 MeV $^{132}Xe^{26+}$ ions to fluences from $3x10^{11}$ to 10^{13} cm^{-2} using the cyclotron at FLNR JINR, Dubna. According to the SRIM calculations (www.srim.org), the projective range of Xe ions was ~ 19.9 μm and the ionization losses at near-surface region reached 12.5 keV/nm. Photoluminescence (PL) spectroscopy was used for characterization of samples with the excitation lines 325 and 488 nm. A cryostat with temperature stability ±0.5K was used for the low-temperature PL measurements.

PL spectra of as-implanted samples are shown in Figure 1. A wide PL band in the region of 1150–1600 nm (1.1–0.77 eV) was observed at cryogenic temperatures at the excitation 325 nm. In addition, a set of narrow peaks is visible, which can be correlated with the known PL-lines - X (1.033 eV), W (1.018 eV), W' (1.0048 eV) related to small interstitial clusters, R (0.901 eV) associated with {311} defects and C (0.79 eV) - usually attributed to C-O complexes. As the irradiation dose increases to 10^{13} cm^{-2}, the PL peak shifts to the long-wavelength region, and the intensity decreases by about an order of magnitude. The position of the observed broad PL is around the position of the known "dislocation" peaks: D1 – D4 (0.81–0.99 eV) [1, 2]. It is known that irradiation with swift heavy ions does not produce extended defects in near-surface regions. PL sources are rather due to dense dislocations net localized along the ions trajectory. The role of ionization losses in defect formation and the contribution of defect complexes to the luminescent properties are discussed. The decrease in PL signal with the Xe dose is probably due to the competition between luminescent defects and non-radiative centers introduced by the irradiation.

The temperature dependence of the PL and the ways to increase its quantum yield are also discussed.

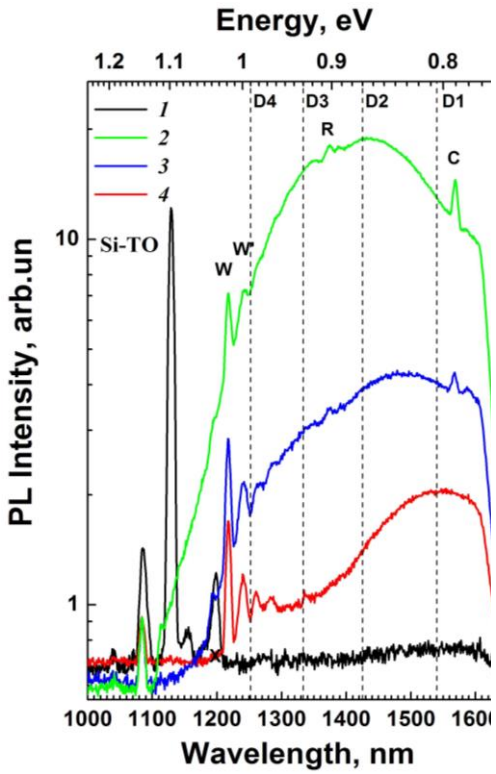

Figure 1. PL spectra (10 K, λ_{ex}=325 nm) of Si implanted with Xe, 167 MeV ions to the fluencies, cm^{-2}: 1- 0; 2- $3x10^{11}$; 3- $2x10^{12}$; 4- 10^{13}.

1. N.A. Sobolev, "Defect engineering in mplantation technology of silicon light-emitting structures with dislocation-related luminescence", Semiconductors, **44**, pp. 3-23, 2010.

2. L.I. Fedina, A.K. Gutakovskii, T.S. Shamirzaev, "On the structure and photoluminescence of dislocations in silicon", J. Appl. Phys., **124**, p. 053106, 2018.

P2-16: Nucleation and growth of the nanocrystals of Si and solid solution SiGe on dielectric substrates

G. Kamaev[1,2], A. Katsyuba[1], P. Kuchinskaya [1], V. Volodin[1,2], and A. Antonenko[2]
[1]*Rzhanov Institute of Semiconductor Physics, Russian Academy of Sciences, Novosibirsk, Russia, E-mail: kamaev@isp.nsc.ru.*
[2]*Novosibirsk State University, Novosibirsk 630090, Russia.*

Interest in dielectric-film-embedded nanocrystals of Si and Ge, and in nanocrystals of the solid solution of these elements, is due to the possibility of using such nanocrystals in multi-functional nanostructured materials intended for fabrication of solid-state devices whose operation is based on quantum-size effects. That is why the fabrication of structures containing arrays of Si nanoparticles on non-orienting substrates or in dielectric surrounding, capable of acting as nuclei for the formation of the nanocrystals of Si, solid solution SiGe, and diluted magnetic semiconductors (such as, for instance, Si nanocrystals with hosted Mn impurities), presently remains an urgent task.

In the present study, we analyze the possibility of forming embedded in SiO2 Si nuclei via the deposition of a-Si:H onto oxidized Si substrates followed by subsequent partial oxidation of the a-Si:H film thus obtained to a certain depth in oxygen plasma. After the deposition of Si onto oxidized silicon substrate, the obtained α-Si:H film of a certain thickness deposited onto the surface of the sample was exposed to inductively excited oxygen plasma [1] to make the continuous α-Si:H layer disintegrated into individual α-Si clusters [2]. Then, heat treatment was given to the sample *in situ*, like in the standard pre-MBE surface cleaning process, accompanied with an additional sputtering of Si. As a result of evaporation of the material, the thickness of the SiO_2 layer decreased in value, and a surface layer with α-Si nanoclusters exposed to ambient medium on the surface of the specimen was obtained. Those nanoclusters could then be used as nuclei for subsequent MBE growth of SiGe nanocrystals of various compositions. Before the growth, some specimens were given an additional chemical etching treatment in plasma.

The properties of the structures obtained at different stages of their formation process were studied using atomic force microscopy (AFM) and Raman spectroscopy. Figure 1 shows AFM images of the investigated structures before (upper image) and after the deposition of Ge held at temperatures 400 and 550^{0}C (central and lower image, respectively). Evidently, the process temperature had a profound influence on the growth of nc-Ge. At 550^{0}C, germanium predominantly grew on large nuclei. From an analysis of Raman data, conditions under which the incorporation of Ge into growing SiGe nanocrystals occurred were identified, and the composition of formed nanocrystals was determined.

This work was supported by the Russian Foundation for Basic Research (Grant No. 18-07-01278).

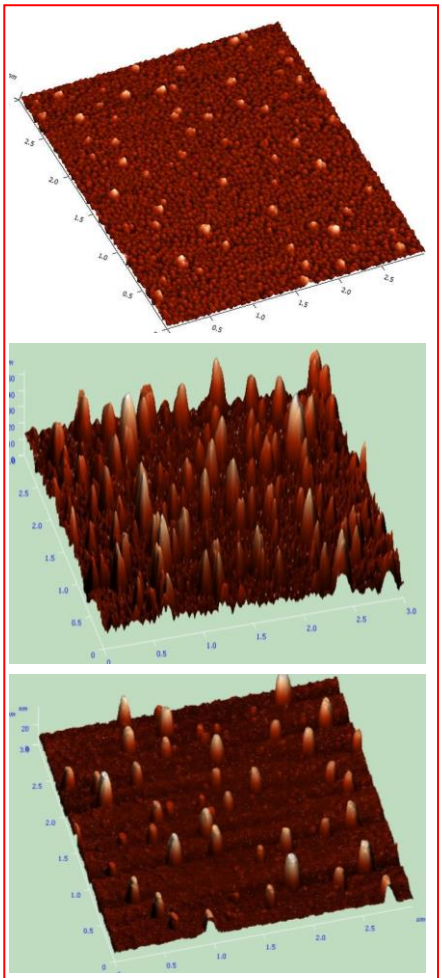

Fig.1. – AFM images of specimens before (upper image) and after deposition of Ge at temperatures 400 and 550^{0}C (central and lower image, respectively).

1. I. G. Neizvestnyi, V. A. Volodin, G. N. Kamaev, S. G. Cherkova, S. V. Usenkov, and N. L. Shwartz, "Formation of Silicon Nanocrystals in Si—SiO_2—α-Si—SiO_2 Heterostructures during High-Temperature Annealing: Experiment and Simulation", Optoelectronics, Instrumentation and Data Processing, **52**, No.5, pp. 486-495, 2016.

2. A. Kh. Antonenko, V. A. Volodin, M.D. Efremov, P. S. Zazulya, G. N. Kamaev, D. V. Marin, "Oxidation Kinetics of a Silicon Surface in a Plasma of Oxygen with Inert Gases", Optoelectronics, Instrumentation and Data Processing, **47**, No. 5, pp. 459–464, 2011.

P2-17: Strain relaxation and intermixing in Ge/Si heterostructures with arrays of low-temperature quantum dots

M. S. Storozhevykh[1], L. V. Arapkina[1], S. M. Novikov[2], O. V. Uvarov[1], V. A. Yuryev[1]
1. Prokhorov General Physics Institute, Russian Academy of Sciences, Moscow, Russia, storozhevykh@kapella.gpi.ru
2. Moscow Institute of Physics and Technology, Dolgoprudny, Russia, novikov.s@mipt.ru

Ge/Si heterostructures with dense arrays of epitaxial self-organized Ge quantum dots (QD) were investigated by Raman spectroscopy and high resolution transmitting electron microscopy (HRTEM). The mechanism of strain relaxation in Ge/Si heterostructures with QDs grown by molecular beam epitaxy at the temperatures of ~ 360ºC and the influence of growth conditions on composition of QDs and adjacent layers of Si were the subject of this study. HRTEM images of structures with QDs were analyzed by the "peak pairs" method [1]. There is a thin domain of 2 to 5 ML thick above a QD layer with the lattice constant larger than that of unstrained Si in the [001] direction and equal to that of unstrained Si in the [110] direction. We suppose that this region has a mixed Si_xGe_{1-x} composition and its lattice is compressed in the [110] direction since the Si lattice has no reason to undergo tensile strain in the [001] direction. We have found (fig. 1) a significant line broadening in the range form 301 to 302 cm^{-1} in Raman spectra obtained for the structures grown at the higher deposition temperature (530ºC) of Si spacers between QD layers. This spectral range corresponds to overlapping lines of Si and Ge and we assign band broadening to a shift of the Ge line due to the compressive strain in the Ge lattice caused by the lattice mismatch between Ge and Si. Two separate bands peaked at 302 and 313 cm^{-1} are observed in the spectra of the structures grown at the lower deposition temperature (360ºC) of Si spacers. This is due to a larger shift of the Ge line and is a reflection of the fact that the Ge lattice is more strained in QD layers of these structures. Besides, the Si–Ge line peaked at 420 cm^{-1} is more apparent in the spectra of the structures grown at the higher temperature of Si spacers that corresponds to the higher degree of Si/Ge intermixing. At the same time, the less shift of the Ge line in the spectra of these structures proves the suggestion that the strain relaxes in the region of the mixed composition. We have also investigated a number of Ge/Si heterostructures with QDs grown at different thickness of Ge layers and Si spacers to clarify the effect of the Ge segregation [3] and the strains in Si layers on QD forming and growing dense chains of vertically correlated QDs [4].

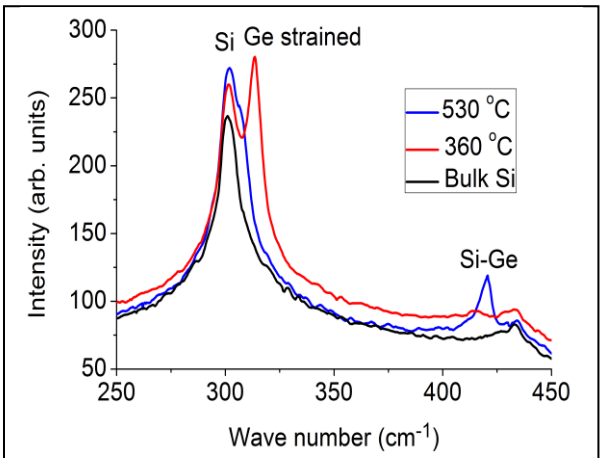

Fig. 1. Raman spectra of Ge/Si heterostructures with Ge QDs grown at different deposition temperatures of Si spacers as compared to bulk Si.

In summary, strains arising at Ge–Si heterojunction relax to a significant extent by compressing the mixed composition region in the [110] direction. QD layers are more strained in the structures with the lower growth temperature of Si spacers that is caused by the less intermixing degree of Si and Ge in the mixed composition layer.

1. P. L. Galindo, S. Kret, A. M. Sanchez et al., "The Peak Pairs algorithm for strain mapping from HRTEM images," Ultramicroscopy, 107, p. 1186, 2007.
2. P. H. Tan, K. Brunner, D. Bougeard, G. Abstreiter, "Raman characterization of strain and composition in small-sized self-assembled Si/Ge dots," Phys. Rev. B, 68, p. 125302, 2003.
3. D. E. Jesson, S. J. Pennycook, "Direct imaging of interfacial ordering in ultrathin $(Si_mGe_n)_p$ superlattices," Rhys. Rev. Lett., 66, pp. 750–753, 1991.
4. V. A. Yuryev, L. V. Arapkina, M. S. Storozhevykh, O. V. Uvarov, V. P. Kalinushkin, "Ge/Si heterostructures with dense chains of stacked quantum dots (Review)," J. Nanoelectron. Optoelectron., 9, pp. 196–218, 2014.

P2-18: Crystallization of Si layer and Ge/Si multi-nanolayers using femtosecond infrared laser annealing

G.K. Krivyakin[1,2], A.A. Popov[3], A.V. Bulgakov[4,5], I. Mirza[5], V.A. Volodin[1,2]

1. *Rzhanov Institute of Semiconductor Physics, Russian Academy of Sciences, Novosibirsk, Russia, E-mail krivyakin@isp.nsc.ru.*
2. *Novosibirsk State University, Pirogova Str. 2, Novosibirsk 630090, Russia.*
3. *Valiev Institute of Physics and Technology of Russian Academy of Sciences, Yaroslavl Branch,, Yaroslavl, 150007 Russia.*
4. *Kutateladze Institute of Thermophysics SB RAS, Ac. Lavrentiev Ave. 1, Novosibirsk 630090, Russia.*
5. *HiLASE Centre, Institute of Physics AS CR, Doln, Beany, Czech Republic.*

Pulsed laser annealing (PLA) is a widely used method of crystallizing amorphous semiconductor films [1]. The main advantages of PLA are the possibility of crystallizing films on not refractory substrates and selectively crystallizing of films with a lateral resolution corresponding to the laser-spot dimensions. The PLA method provides a means for producing both completely crystallized films and two-phase structures consisting of a mixture of amorphous and microcrystalline or nanocrystalline phases. Structures crystallized by PLA can be used in micro- and optoelectronic devices fabricated on relatively low-melt large-format substrates.

For these experiments, a-Si:H layers and an a-Si:H/a-Ge:H multilayer structure on glass substrates were prepared. The latter consisted of 11 silicon (5 nm) and 10 germanium (10 nm) amorphous layers grown alternately by plasma enhanced chemical vapor deposition (PECVD) on a glass substrate. The thickness of the first (buffer) and last (cover) Si layers was 25 nm. The sample was annealed by a femtosecond laser (λ=1030 nm, pulse duration 240 fs) with the pulse energy density (laser fluence) in the range of 70 to 285 mJ/cm^2. The structural analysis of the irradiated samples was performed by Raman spectroscopy using a T64000 spectrometer with micro-Raman setup and an Ar laser (514.5 nm) as an excitation source.

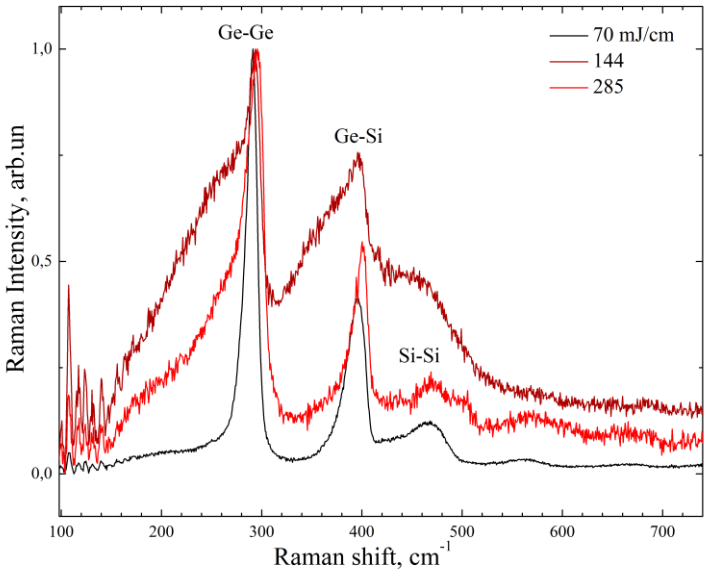

According to Raman data analysis (spectra are not shown here) the as-deposited films were totally amorphous. Figure shows Raman spectra of the Ge/Si multilayers after PLA at different fluences. As seen from the figure, germanium is already fully crystallized (narrow peak at ~300 cm^{-1}) after PLA with the lowest fluence of 70 mJ/cm^2. This is rather unexpected taking into account the very low IR light absorption in a-Si:H and a-Ge:H at 1030 nm. A plausible explanation is in a strong increase of the two-photon absorption probability after some threshold light intensity that leads to a sharp increase of the amount of absorbed energy by material and a-Ge crystallization. The same effect we observed in the Raman spectra of the a-Si:H films after PLA. One can see the appearance of Ge-Si peaks in the Raman spectra, so some intermixing of the Ge and Si layers took place after PLA. Also a peak of a-Ge (~280 cm^{-1}) is clearly seen at fairly high laser fluences. This is likely due to partial ablation of the structure top layers and subsequent redeposition. With fluences higher than 285 mJ/cm^2, the structure was fully ablated.

In summary, the first attempt to crystallize Ge/Si multi-nanolayers using femtosecond infrared laser annealing was demonstrated.

1. F. Falk, G. Andrä. Laser crystallization — a way to produce crystalline silicon films on glass or on polymer substrates. Journal of Crystal Growth. – 2006. – Vol. 287. – № 2. – P. 397-401.

P2-19: Effect of stoichiometric coefficient on solid-phase crystallization of silicon suboxide thin films

A. Zamchiy[1], I. Merkulova[1] , E. Baranov[1], V. Volodin[2]
1. *Kutateladze Institute of Thermophysics SB RAS, Novosibirsk, Russia*
2. *Rzhanov Institute of Semiconductor Physics SB RAS, Novosibirsk, Russia*
zamchiy@gmail.com

Currently, silicon nanocrystals (nc-Si) are widely used in such fields as microelectronics, optoelectronics, photovoltaics, plasmonics and thermoelectrics. The nc-Si electronic structure is very different compared to the case of bulk silicon due to size-related effects, as a consequence of the quantum confinement. As it is known, the nc-Si in a silicon dioxide (SiO_2) matrix (nc-Si/SiO_2) exhibit intensive luminescent properties at a room temperature in the wide spectral range, 500-1000 nm [1]. Moreover, for the photoluminescence of the nc-Si, an important competitive effects have to be taken into account, such as the presence of surface induced defects and different surface passivation effects.

To date, the main method of thin-film nc-Si/SiO_2 systems obtaining is high-temperature annealing of an amorphous non-stoichiometric silicon oxide (a-SiO_x, $0<x<2$) [2]. The formation and the growth of nc-Si in the a-SiO_x matrix are determined by the kinetics of the solid-phase crystallization. The stoichiometry of the initial a-SiO_x films significantly affects the structural and optical properties of the material obtained in the annealing process. Thus, it was shown in [3] that the increase in the stoichiometric coefficient of the a-SiO_x resulted in a decrease in the degree of crystallinity and the size of crystallites in the nc-Si/SiO_2. However, the authors [4] showed that the increase in the co-presence of excess silicon in the a-SiO_x led not only to an increase in the average size of the crystallite, but also to a decrease in the luminescent signal in the spectral range of 560-890 nm.

The a-SiO_x thin films of different stoichiometry (x=0.1-1.5) were obtained by a gas-jet electron beam plasma chemical vapor deposition method [2] by changing the composition of the gas mixture with monosilane (SiH_4) on monocrystalline silicon and fused quartz substrates. The thin films were further annealed at a temperature of 900°C for 4 hours in an argon atmosphere. The structure and composition of initial and annealed films were studied by FTIR. The morphology and thickness of the thin films were investigated by SEM. The size of crystallite and the degree of crystallinity of the annealed material was obtained by the Raman and XRD methods. The optical properties of the thin films were investigated by spectrophotometry. The photoluminescence properties of the nc-Si/SiO_2 were studied by means of a HeCd laser with a wavelength of probing radiation of 325 nm.

In the study, it was shown that the degree of crystallinity and the crystallite average size increased with a decrease in the stoichiometry of the initial a-SiO_x thin films. The annealed a-SiO_x thin films exhibit photoluminescence properties in the spectral range of 400-1000 nm at the room temperature. The values of the average size of crystallite found by the position of the photoluminescence peak are in good agreement with the results obtained by Raman and XRD methods.

This study was financially supported by the state assignment of IT SB RAS (the deposition of a-SiO_x) films and the grant of the President of the Russian Federation, the project MK 638.2019.8 (annealing of a-SiO_x films).

1. I.B. Olenych, L.S. Monastyrskii, Y.V. Boyko, A.P. Luchechko and A.M. Kostruba, “Photoluminescent properties of nc-Si/SiO_x nanosystems”, Appl. Nanosci., pp.1-6, 2018
2. A.O. Zamchiy, E.A. Baranov, I.E. Merkulova, V.A. Volodin, M.R. Sharafutdinov and S.Y. Khmel, “Effect of annealing in oxidizing atmosphere on optical and structural properties of silicon suboxide thin films obtained by gas-jet electron beam plasma chemical vapor deposition method”, Vacuum, 152, pp.319-326, 2018
3. J. Huang, C. Gui, M. Ding, H. Wang, W. Xu, J. Li, M. Gao and H. Guan, “Effects of chemical stoichiometry on the structural properties of Si-rich oxide thin films”, Thin Solid Films, 595, pp.79-83, 2015
4. A. Coyopol, M.A. Cardona, T.D. Becerril, L.L. Jimenez and A.M. Sánchez, “Silicon excess and thermal annealing effects on structural and optical properties of co-sputtered SRO films”, Journal of Luminescence, 176, pp.40-46, 2016

P2-20: Determination of oxygen concentration in amorphous silicon suboxide thin films by FTIR, RBS, and WDS methods

I. Merkulova[1], A. Zamchiy[1], E. Baranov[1]
1. *Kutateladze Institute of Thermophysics SB RAS, Novosibirsk, Russia*
zamchiy@gmail.com

The hydrogenated amorphous silicon suboxide (a-SiO_x:H) thin films are widely used in fields related to the fabrication of silicon-based semiconductor devices. The oxygen concentration in the films plays an important role, since its value has a direct impact on the optoelectronic properties of the material.
In this work, the a-SiO_x:H thin films were deposited by the gas-jet electron beam plasma chemical vapor deposition method [1] on double-side polished monocrystalline silicon wafers using a mixture of monosilane (SiH_4), argon (Ar), and oxygen (O_2) gas reagents. The feature of the synthesis method is that by changing gas flow ratio R = G(Ar)/G(SiH_4) the films of a different oxygen concentration are obtained. The parameter R was varied by changing the Ar flow rate and set equal to 20, 40, 60, 80, and 100. The O_2 was fed directly into the vacuum chamber.
Fourier transformed infrared spectroscopy (FTIR), Rutherford backscattering spectroscopy (RBS), and wavelength dispersive X-ray spectroscopy (WDX) were used to determine the oxygen concentration in the thin films. The bonded hydrogen and oxygen concentrations in the thin films were obtained from the IR spectra using the integrated absorption of the Si-H wagging mode centered at 640 cm^{-1} and the Si-O-Si stretching mode in the range of 900 – 1250 cm^{-1}. The hydrogen concentration in the a-SiO_x:H thin films was about 5 at.%. Fig. 1 shows the stoichiometric coefficient values evaluated as a function of R by FTIR, RBS, and WDS. The oxygen concentration in the a-SiO_x:H thin film decreases from 45 to 13% with an increase of the parameter R. The results obtained by different methods are in good agreement.

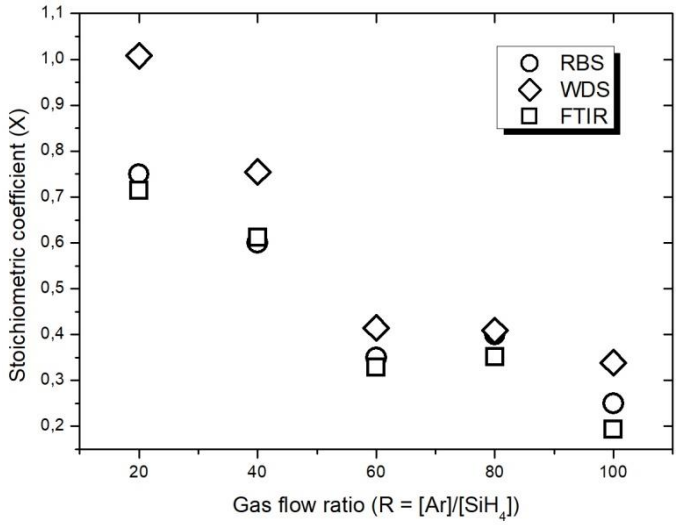

Fig. 1 Stoichiometric coefficient x in the films as a function of the gas flow ratio R evaluated from FTIR, RBS and WDS measurements.

The study was funded by RFBR according to the research project №19-08-00848.

1. Zamchiy A.O., Baranov E.A., Merkulova I.E., Volodin V.A., Sharafutdinov M.R. and Khmel S.Y., "Effect of annealing in oxidizing atmosphere on optical and structural properties of silicon suboxide thin films obtained by gas-jet electron beam plasma chemical vapor deposition method", Vacuum, 152, pp.319 326, 2018

P2-21: On the relation of cross-hatch pattern surface morphology and extended defects in buffer layers of (Ga,Mn)As/(In,Ga)As/GaAs ferromagnetic structures

O.A. Soltanovich[1], V.A. Kovalskiy[1], V.G. Eremenko[1], P.S. Vergeles[1], M.V. Dorokhin[2], Yu.A. Danilov[2]

1. Institute of Microelectronics Technology Russian Academy of Sciences, Chernogolovka, Russia, solt@iptm.ru
2. Research Institute of Physics and Technology, Lobachevsky State University, Nizhni Novgorod, Russia

(Ga,Mn)As/(In,Ga)As/GaAs structures are extensively considered as promising systems for spintronic and ferromagnetic applications. However, in heteroepitaxial systems with a small lattice mismatch, a specific surface morphology known as cross-hatch pattern (CHP) is usually formed [1]. CHP is revealed as a regular sequence of valleys and ridges observed on the surface of the structure. In real structures it may cause the dispersion of optical, magnetic and electrical properties of active layers and could effect on the device performance and stability. On the other hand, understanding of the mechanisms driving the CHP formation could allow to manage the surface morphology and, probably, to develop special artificial templates with controlled strains on the surface.

According to current understanding, the CHP on the surface is correlated with the network of misfit dislocations (MDs) formed at the lattice-mismatched (In,Ga)As/GaAs interface under dislocations' gliding during strain relaxation of the epilayers. In the case of epitaxy on (001) substrates, the characteristic CHP features (valleys and ridges) are aligned along the two orthogonal <110> directions. However, the mechanism of CHP-formation is not understood completely, and several contradicting models are proposed to explain it (see, e.g., [2,3] and references inside). Therefore, the study of the defects formed in InGaAs and GaMnAs layers during growth and lattice relaxation looks to be useful and promising for further understanding of the phenomenon.

In the present work, the combined study of the surface morphology and of the electrically active defects in the buffer layers of (Ga,Mn)As/(In,Ga)As/GaAs structures is reported. Surface morphology was analyzed by AFM technique, while the electrically active defects in the structures were studied by the deep level transient spectroscopy (DLTS), capacitance-voltage (CV) profiling and electron beam induced current (EBIC) techniques. The structures with the various thicknesses of InGaAs and GaMnAs layers were considered.

It is found that the specific electrically active extended defects are observed in the investigated structures not only near the (In,Ga)As/GaAs interface, but in the whole buffer InGaAs layer. According to the results of EBIC studies [4], the orientation of these defects is found to be the same as that of CHP ridges on the surface of the structures. The DLTS study shows the existence in the buffer InGaAs layer of several deep traps with the energy levels in the lower part of the bandgap [5]. It is shown that some of these traps could be identified as extended defects. The origin of the revealed deep level defects, their possible relation to the recombinationally active defects observed by EBIC and to the CHP surface morphology are discussed.

1. K.H. Chang, R. Gibala, D.J. Srolovitz, P.K. Bhattacharya and J.F. Mansfield, "Crosshatched surface morphology in strained III-V semiconductor films", J. Appl. Phys., **67**, pp. 4093-4098, 1990
2. M.A. Lutz, R.M. Feenstra, F.K. LeGoues, P.M. Mooney and J.O. Chu, "Influence of misfit dislocations on the surface morphology of $Si_{1-x}Ge_x$ films", Appl. Phys. Lett., **66**, pp. 724-726, 1995
3. A.M. Andrews, J.S. Speck, A.E. Romanov, M. Bobeth and W. Pompe, "Modeling cross-hatch surface morphology in growing mismatched layers", J. Appl. Phys., **91,** pp. 1933-1943, 2002
4. V.A. Kovalskiy, P.S. Vergeles, V.G. Eremenko, D.A. Fokin, M.V. Dorokhin, Yu.A. Danilov and B.N. Zvonkov, "Dislocation gliding and cross-hatch morphology formation in AIII-BV epitaxial heterostructures", Appl. Phys. Lett., **105,** 231608, 2014
5. O.A. Soltanovich, V.A. Kovalskiy, P.S. Vergeles, M.V. Dorokhin, Yu.A. Danilov, "Study of extended electrically active defects in (Ga,Mn)As/(In,Ga)As based heterostructures by EBIC and DLTS techniques", J. Surf. Invest.: X-Ray, Synchrotron Neutron Tech., **13**, pp. 105-110, 2019

P2-22: Monte Carlo simulation of electron transport in MOSFETs flash memory cells

O. Zhevnyak[1], Ya. Zhevnyak[1]
1. Belarussian State University, Minsk, Belarus, Zhevnyakol@tut.by.

As known modern flash memory cells are based on silicon MOSFETs. Byte is written or erased by mechanism of electron tunneling from MOSFET channel to floating gate [1]. At high gate bias electron tunneling called Fowler-Nordheim tunneling takes place. While gate bias is relatively small the floating gate can be charged by hot electrons overcoming oxide potential barrier that may be considered as a parasitic byte. That is why the kinetic features of electron drift in MOSFETs channel of flash memory cells have to be investigated.

The purpose of present work is to study electron kinetic properties in flash memory cells at various gates and drain biases. Electron mobility, drift velocity, average energy as well as mean free path are calculated by using Monte Carlo simulation of electron transport in MOSFETs channel of flash memory cells. Algorithms of the simulation of electron tunneling in flash memory cells as well as electron transport in MOSFETs are discussed in papers [2-3].As an example of obtained data the simulation results of floating gate current and electron mobility along the MOSFET channel are presented on figure for V_{gate} = 3 V and V_{drain} = 3 V. Simulated MOS-transistor have had following parameters: channel lengths L_{ch} = 0,2 μm, gate oxide thickness L_{gate} = 7 nm, floating gate oxide thickness L_{tun} = 3 nm, shallow drain region x_{drain} = 10 nm.

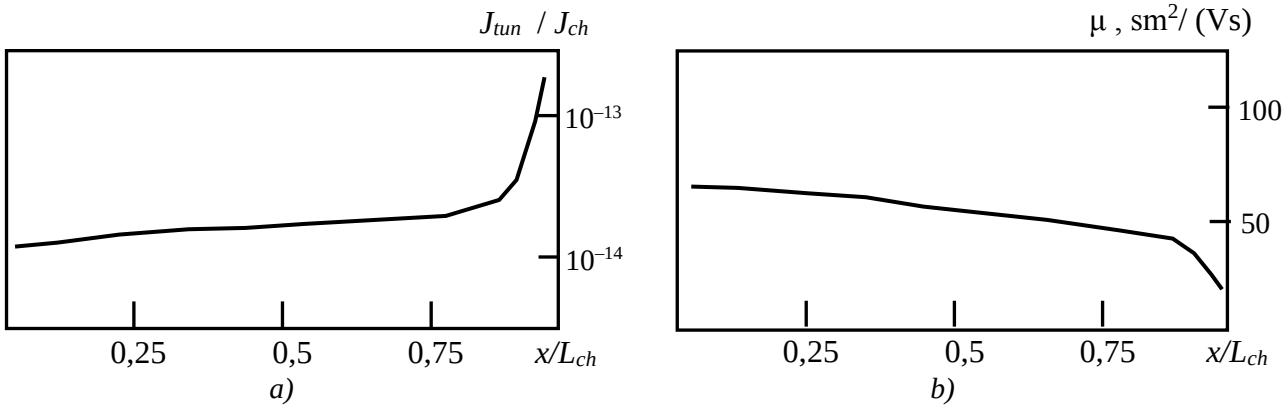

Figure. The relation of floating gate current to drain current (a) and electron mobility (b) along the transistor's channel.

Obtained results have allowed to study the effects of gate and drain voltages on electron transport in silicon MOSFETs with floating gate. Also the effects of channel length and drain region deepness on electron tunneling in simulated transistors have been investigated.

1. J. C. Ranuarez, M. J. Deen, C.-H. Chen, "A review of gate tunneling in MOS devices", Microelectron. Reliability, 46, pp.1939-1956, 2006
2. O. Zhevnyak, "Temperature effect on electron transport in conventional short channel MOSFETs: Monte Carlo simulation", Proc. SPIE, 7025, pp.1M-1-8, 2008
3. O. Zhevnyak, "Simulation of tunneling current in flash memory cells", International Research Journal, 40, pp.46-48, 2015 (in Russian)

P2-23: Features of the effect of the substrate morphology on the nucleation processes of In/GaAs nanostructures during droplet epitaxy

N. Chernenko[1,2], S. Balakirev[3], M. Eremenko[1], O. Ageev[1], M. Solodovnik[1,3]

1. Research and Education Center "Nanotechnologies", Southern Federal University, Taganrog 347922, Russia.

2. Department of Radio Engineering Electronics, Southern Federal University, Taganrog 347922, Russia.

3. Department of Nanotechnologies and Microsystems, Southern Federal University, Taganrog 347922, Russia

Modern semiconductor technology is steadily nearing the threshold of miniaturization and, consequently, an increase in its efficiency. This necessitates a transition to fundamentally new architectures of computing and telecommunication platform. From this point of view, the realization of exactly solid-state schemes for implementing such platforms based on the using of A3B5 nanoheterostructures with self-organized structures looks most promising. But the creation of such heterostructures requires the effective control of self-organization processes. Studying the physics and mechanisms of the processes underlying droplet epitaxy allows significant progress in the implementation of the technology for controlling the epitaxial synthesis and self-organization of A3B5 nanostructures, which ensures effective control of the structure properties and positioning.

The goal of this work is theoretical study of the self-organization processes of nanoscale In droplets on the GaAs growth surfaces with complex morphology, taking into account the main control parameters of the droplet epitaxy technique. For this, we used the previously developed hybrid mathematical model of droplet epitaxy processes [1].

The calculation results showed that on substrates with complex morphology, the probability of island nucleation is distributed non-uniformly and depends on the surface area. On GaAs substrates with rectangular grooves, nucleation can occur on flat areas, the groove bottom or walls, or on the facet junctions. Research shows that in order to achieve the best homogeneity of the nanostructure geometric characteristics, the diameter of rectangular grooves should be reduced, adjusting the height so as to achieve the required effective volume and aspect ratio.

Analysis of the theoretical study results has shown that the using of a shape close to triangular differs in more pronounced positions for nucleation, allowing us to increase the uniformity in size and accuracy of nanostructure positioning (Fig. 1).

Fig. 1 – The morphology of an array of In nanostructures after deposition of 5 ML of In on an As-stabilized GaAs(001) substrate with triangular grooves with a diameter and a depth of 20 nm.

For 100% groove filling by the material and suppression of the formation of undesirable structures outside the modified areas, we must provide sufficient diffusion length of adatoms, taking into account the peculiarities of morphology. The use of patterned surfaces allows regulating the density of nanostructures, providing the possibility of quantum structure obtaining, including laterally coupled ones. The transition to the incomplete condensation mode can further reduce the size of the forming structures while maintaining their density. In addition, the analysis of the results showed that nanostructures can be formed on the patterned surfaces at much lower deposition thicknesses, which is caused by a decrease in the nucleation activation barrier relative to flat areas. It can also serve as an additional parameter controlling the size of droplet nanostructures.

Acknowledgement. This work was supported by the Russian Science Foundation Grant No. 15-19-10006. The results were obtained using the equipment of the Research and Education Center and Center for Collective Use "Nanotechnologies" of Southern Federal University.

1. S. Balakirev, M. Solodovnik and O. Ageev, "Hybrid analytical–Monte Carlo model for In/GaAs(001) droplet epitaxy: Theory and experiment", Phys. Status Solidi, 255, p.1700360, 2018

P2-24: DC-and AC-hopping conductivity in layered gallium monosulfide

S. Asadov[1], S. Mustafaeva[2], V. Lukichev[3]

1. Institute of Catalysis and Inorganic Chemistry, National Academy of Sciences, Baku, Azerbaijan, E-mail: salim7777@gmail.com. 2. Institute of Physics, National Academy of Sciences, Baku, Azerbaijan, E-mail: solmust@gmail.com. 3. Institute of Physics and Technology of Russian Academy of Sciences, Moscow, Russia, E-mail: icic.lab6@yandex.ru

GaS single crystals are layered wide-gap semiconductors with a rather high dc-resistivity. The results of investigation of electrical, photoelectric and optical properties of these crystals were presented in the works [1,2]. GaS-based materials, combining interesting electrical and optical properties, are potential candidates for use in various transducers, light modulators, and information storage units. The investigation of electric properties of semiconductor materials in dc-and ac-electric fields gives information about the nature of charge transport and localization states in forbidden gap. For the establishment of mechanism of charge transport it is necessary to know the temperature dependence of dc-conductivity. The objectives of this work were to study the dc-and ac- electrical properties of GaS single crystals, to gain insight into the mechanism of charge transport in the crystals, and to evaluate the parameters of localized states in their band gap.

The layered GaS single crystals used for our study were grown by the Bridgman method and have hexagonal structure with lattice parameters: a = 3.58 Å, c = 15.47 Å at room temperature. The samples for electrical measurements had the shape of rectangular plates. The thickness of the single-crystal GaS samples was 300–500 μm. Ag paste was used as a contact material to the GaS samples. Dc-electric field from Ohmic region of current-voltage characteristic was applied crosswise to the natural layers of a GaS single crystal. All dc-electrical measurements were carried out in the temperature interval 116–294 K on samples placed into a cryostat with a temperature stabilization system (the stabilization accuracy is 0.02 K). The ac-electric properties of the GaS single crystals were studied by a resonance technique [3] in the frequency range $f = 5\times 10^4$ to 3.5×10^7 Hz. The single crystal GaS samples for ac-electric measurements had the form of planar capacitors normal to the C axis of the crystals, with silver-paste electrodes. All of the ac- measurements were performed at 300 K in electric fields corresponding to Ohmic current-voltage behavior.

The dependence of log σ on $1/T$ in GaS samples at temperatures T = 140–238 K is characterized by a monotonic decrease in the activation energy with a decrease in the temperature.This behavior of the dc-conductivity in GaS at low temperatures suggests that charge transfer occurs through the variable-range-hopping mechanism, provided the current is transferred by charge carriers at the states localized in the vicinity of the Fermi level [4]. This is also confirmed by the temperature dependence $\log \sigma \sim T^{-1/4}$. The slope of this curve (T_0) allowed us to estimate the density of localized states near the Fermi level from the formula (N.F. Mott):

$$N_F = 16/T_0 \times ka^3 ,$$

where k is the Boltzmann constant, a is the localization length.

The density of states N_F in GaS was found to be equal to 6.2×10^{19} eV^{-1} cm^{-3}. Estimates are made also for energy spread of localized states near the Fermi level (ΔE = 0.08 eV), the average jump distance (R_{av} = 46 Å), the activation energy of the hopping conductivity (ΔW = 0.07 eV).

The frequency dependence of 300-K conductivity for the GaS crystal has been studied in frequency range from 5×10^4 to 3.5×10^7 Hz. The ac-conductivity of GaS varies as $f^{0.8}$ in the frequency range 5×10^4 to 10^7 Hz and linearly in the range 10^7 to 3.5×10^7 Hz. The $\sigma_{ac} \sim f^{0.8}$ – dependence indicates that the electrical transport in the GaS single crystal is due to carrier hopping between localized states [4]. According to the theory of hopping conduction in alternate electric fields, the parameters of localized states in the forbidden gap of studied crystals have been evaluated from high-frequency electrical measurements.

1. S. N. Mustafaeva, M. M. Asadov, "Currents of isothermal relaxation in gallium sulfide doped by ytterbium", Inorganic Materials, **25,** pp. 212-215, 1989.

2. G. A. Gamal, M.I. Azad, "Photoelectric studies of gallium monosulfide", Eur.Phys.J. Appl. Phys., **32**, pp. 1-5, 2005.

3. S.N. Mustafaeva, " Dispersion of dielectric coefficients and AC-conductivity of $TlGa_{1-x}Co_xS_2$ single crystals in radio-frequency region", Journal of Radioelectronics, **4**, pp. 1-10, 2009.

4. N. Mott and E. Davis, *Electronic Processes in Non-Crystalline materials.* Oxford University Press, 1977.

P2-25: Low energy ion-plasma sputtering of Co and Si. Experiment and modeling

M. Izyumov, A. Kupriaynov, I. Amirov
Valiev Institute of Physics and Technology of Russian Academy of Science, Yaroslavl Branch, Yaroslavl, Russia,
ildamirov@yandex.ru

Low-energy ion-plasma sputtering is a separate stage of the currently intensively developed multistage etching processes of materials with atomic resolution (atomic layer etching) for the purposes of nanoelectronics [1]. This paper presents the results of an experimental and theoretical study of low-energy (<200 eV) sputtering of silicon and cobalt, which is a promising material for the sub-10 nm technology of metallization of integrated circuits. The sputtering coefficients of Co and Si were determined depending on the energy of Ar^+ ions. The molecular dynamics (MD) method was used to determine the dependences of the coefficients of sputtering Co on the angle of incidence of ions at their different energies. Experiments on the sputtering of materials were carried out in a reactor of dense argon plasma of a RF inductive discharge of low pressure. The design of the reactor and the technique of the experiments are given in [2]. The ion energy of variation in the range of 50–200 eV. The experimental conditions were as follows: P = 0.08 Pa, Pw = 800 W, Q = 10 sccm, j_i = 6.4 mA sm^{-2}. Co, Si sputtering with Ar^+ ions was simulated using the LAMMPS software and the NVIDIA Tesla C2075 computer system based on the CUDA architecture. The Si-Si interaction was described by the Stillinger-Weber potential, and Co, Si-Ar, and Ar-Ar by the Ziegler-Biersack-Littmark potential. Co-Co interactions have been described using EAM potential.

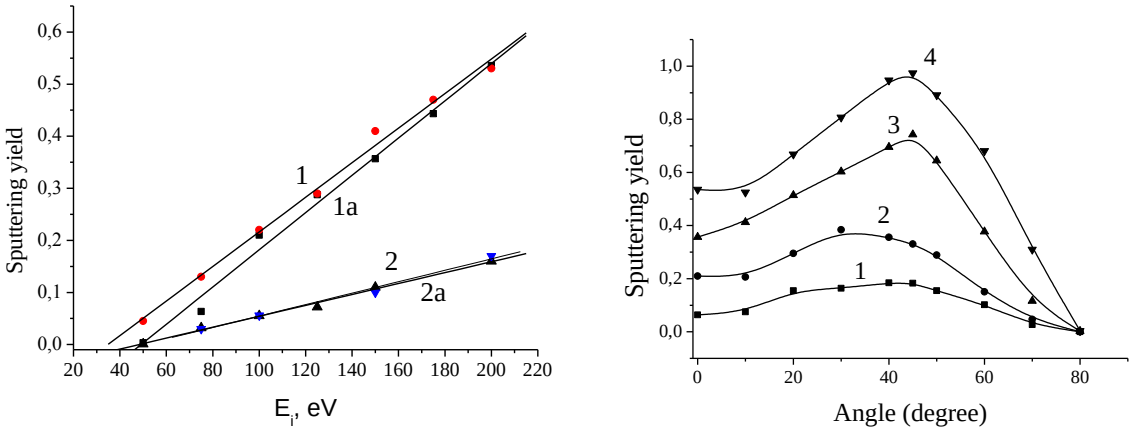

Fig. 1. Dependences of the sputtering yield of Co (1, 1a), Si (2, 2a) atoms from the ion energy - (A) and the angle of incidence of the ions - (B) for Co atoms with different ion energies; 1-75, 2-100, 3-150, 4-200 eV.

The experimental data on the determination of the Co sputtering coefficient depending on the ion energy were in good agreement with the MD data (Fig. 1a, straight lines 1 and 1a). The experimental data on Si were also in good agreement with the calculated data [3]. The yield coefficient of Co atoms, depending on the angle of incidence of the ions, had a maximum value at angles of incidence from 30 to 55 degrees with an ion energy of 75 to 200 eV (Fig.2). A discussion of the data obtained.

The work has been done under State Programs #0066-2019-0002 of the Ministry of Science and Higher Education of Russia.on the equipment of the center for collective use of the scientific equipment «Diagnostics of micro- and nanostructures»

1. L. Berry, K.J. Kanarik, T. Lill, S. Tan, V. Vahedi, R. A.Gottscho. Applying sputtering theory to directional atomic layer etching. J. Vac. Sci. Technol. A 36(1), pp. 01B105, 2018

2. I. I. Amirov, M. O. Izyumov , V. V. Naumov. Low energy selective etching of metal films in oxygen-containing high-density argon plasma. V. 10, pp. 855–859, 2016

3. A.P. Palov, G.G. Balint-Kurti, E.N. Voronina, T.V. Rakhimova. Sputtering of Si by Ar: A binary collision approach based on quantum-mechanical cross sections. J. Vac. Sci. Technol. A 36(4), pp. 041303, 2018

P2-26: Fabrication of silicon structures for 3D All-Solid-State Lithium-Ion batteries using plasma etching

S. Kurbatov[1,2], O. Morozov[1], A. Rudy[1]

1. Valiev Institute of Physics and Technology of Russian Academy of Sciences, Yaroslavl Branch, Russia,
2. Yaroslavl Demidov State University, Yaroslavl, Russia, kurbatov-93@bk.ru

All-solid-state batteries have significantly less specific capacity (>1 $mA \cdot h \cdot cm^{-2}$), in comparison with traditional batteries with the liquid electrolyte. In order to increase the specific capacity, the concept of 3D all-solid-state lithium-ion batteries was proposed [1]. The 3D silicon structures are fabricated by plasma etching of grooves with a positive tapered profile. Due to the conformal deposition of thin-film elements on 3-D structures, the accumulator capacity per surface unit increases. The need for uniform coating of films strongly requires the correct sloped sidewall angle of the grooves. The positively tapered profile may be achieved by adjusting the selectivity between the reflowed photoresist as mask and silicon [2, 3]. Creating a positive taper occurs by the shift of the mask edge during the etching (fig. 1a). Our work demonstrates the implementation of this approach with a modernized silicon Bosch etching process.

Microposit S1813 photoresist layer on the silicon wafer was patterned with line-and-space. The lines were 10 μm wide, with 10 μm space between them. The wafer was hard baked in a drying furnace during 20 minutes at the temperature of 140 °C. The mask profile becomes the spherical shape in these conditions of photoresist reflow. The etching of the grooves was performed with the Plasmalab 100 equipment (ICP 380) from Oxford Instruments. The etching process comprises three steps (fig. 1a): 1) anisotropic plasma etching with SF_6, 2) plasma passivating the side walls of the grooves with C_4F_8, 3) plasma etching of photoresist with Ar/O_2 mixture. The steps 1-3 are repeated the required amount of times.

The steps #1 and #2 (bosch-process) were adjusted to reach the vertical walls of the grooves. The third step duration was calculated according to the measured etching rate of photoresist and mask shape. The time of step #3 is changed from cycle to cycle so that each cycle can provide an equal shift of the mask edge. As a result a sloped sidewall angle ~16° was accomplished (fig. 1b). In presented case, shift of the mask edge was ~10% more than the undercutting due to an isotropic component on the step #1. Strong sidewall roughness (large scallops) can be further eliminated by optimizing the etch recipe.

This work is supported by Program no. 0066-2019-0002 of the Ministry of Science and Higher Education of Russia for Valiev Institute of Physics and Technology of RAS and performed using the equipment of Facilities Sharing Centre “Diagnostics of Micro- and Nanostructures”.

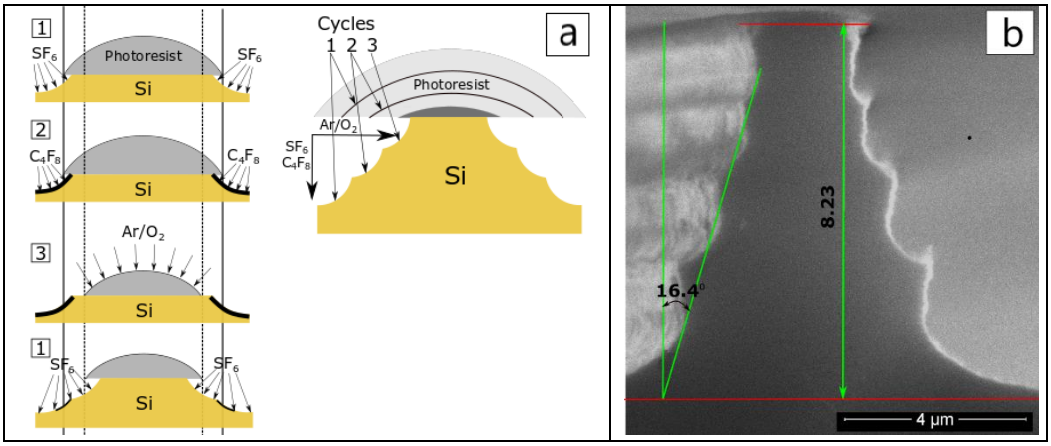

Fig. 1. The etching process of silicon: a) general schemes, b) SEM cross-section image of silicon structure.

1. A. Talin, et al, "Fabrication, Testing, and Simulation of All-Solid-State Three-Dimensional Li-Ion Batteries", ACS Appl. Mater. Interfaces, Vol. 8, p. 32385−32391, 2016

2. M.de Boer, et al, "Guidelines for Etching Silicon MEMS Structures Using Fluorine High-Density Plasmas at Cryogenic Temperatures”, Journal of Microelectromechanical systems, Vol. 11, N. 4, p 385-401, 2002.

3. T. Feidhlim, et al, "Photoresist reflow method of microlens production Part I: Background and Background and experiments" Optic, Vol.113, N.12, p. 1-14, 2002

P2-27: Dynamics of magnetization switching of spin-valve structure

O.S. Trushin[1], A. Rubeikina[2]

1. *Valiev Institute of Physics and Technology of RAS, Yaroslavl branch, Yaroslavl, Russia,, otrushin@gmail.com.*
2. *P.G. Demidov Yaroslavl State University, Yaroslavl, Russia, E-mail address*

Magnetic recording plays an important role in modern technology of information storage. Dynamics of magnetization switching determines rate of bit recording. Controlling speed of those processe is of very important task in development of new generation of magnetic recording. Typically magnetization switching of macroscopic size sample is very fast process, taking about few microseconds. Precise measurements of such rate is challenging problem which requires use of special hight frequency equipment.

This work is devoted to the development of the experimental technique to study dynamics of magnetization swithcing through measurent of magnetoresistance response of spin-valve structure. This kind of technique has already been used for measurements of domain wall speed in magnetic nanowire[1]. Mulatylayer spin-valve structure of the following composition Ta/FeMn/CoFe/Cu?CoFe/Ta/SiO2/Si deposited by magnetron sputtering was used as a test sample for measurement procedure. The sample had rectangular shape with lateral dimensions of 15*10 mm. Mesurements of resistance of the sample as function of time and external magnetic field has been done using home made experimental set up. It included data acqusition board NI PCI 6251 for automatization of the measurement procedure. As the result of measurements magnetization reversal in the external magnetic field parallel to the film surface has been studied. Corresponding curve for resistivity of the structure versus field is shown in Fig,1(A).

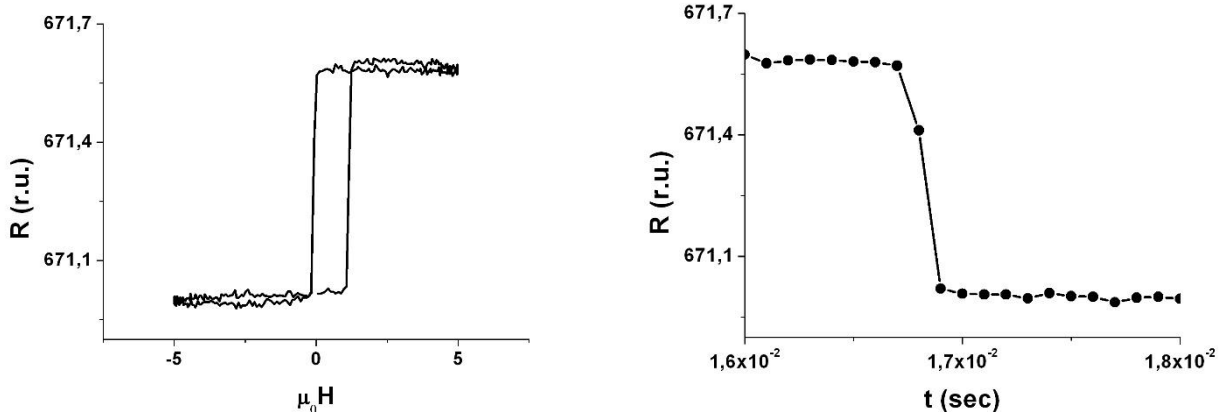

A B

Fig.1 (A) Resistivity versus external magnetic field, (B) Resistyvity versus time during magnetization switching

There is only one hysteresis loop on the curve inspite of the presence of two magnetic layers in the structure. It is due to low magnetude of external magnetic field, which is enough only for magnetization switching of free layer. Fig.1 (B) shows selected part of dependence of the resistance on time, containing magnetization swithcing transition event. Analysis of this figure let us to estimate switching time to be equal to 200 mks. This value is in satisfactory agreement with data of other groups. In summary we developed experimental set up for measurements of fast processes of magnetization swithcing in magnetorestive structures. On the next stage we are planning to increase acquisition rate to improove accuracy of transition times estimates and apply this method for measurements of domain wall speed in magnetic nanowires..

The work has been done under State Programs #0066-2019-0003 of the Ministry of Science and Higher Education of Russia.

1. T. Ono, H. Miyajima, K. Shigeto, and T. Shinjo, “Magnetization reversal in submicron magnetic wire studied by using giant magnetoresistance effect”, Appl. Phys. Lett., **72**, pp.1116-1117, 1998

P2-28: Long-term stability of amorhous Gd-Co films with perpendicular magnetic anisotropy

V.F. Bochkarev, O.S. Trushin, S. Simakin
Valiev Institute of Physics and Technology of RAS, Yaroslavl Branch, Yaroslavl, Russia, otrushin@gmail.com

Development of ultra high density magnetic recording for information storage requires transition to the use of thin films with Perpendicular Magnetic Anisotropy(PMA). Such systems are very rare in nature, becouse strong magnetostatic interaction forces magnetization vector to stay parallel to the film surface. Only materials with very strong magnetocrystalline anisotropy can exibit magnetization perpendicular to plane. One possible example of thin films with PMA are films containing rear-earth elements. Amorphous Gd-Co films were intensively explored in the middle of past century as perspective material for thermomagnetic recording[1]. However it was considered as less stable systems due to degradation of amorhous state with time. This work is devoted to reexamination of amorphous magnetic Gd-Co films being fabricated more than 40 year ago. This Gd-Co film has been deposited on glass substrate using ion-plasma sputtering (with RF and DC discharge) in the earlier eighties of past century and was kept at room temperature and constant moisture during whole that period untill current time. The sample was subjected to complex experimental investigations using several different analytical methods. Magnetic reversal curve of the film in the external field directed perpendicular to the film surface was measured using magnetooptical Fraday rotation method. Corresponding hysteresis loop is shown on Fig.1(A) Analysis of that picture shows that the film is indeed characterized by strong perpendicular magnetic anisotropy. Coercivity of the film was about 7 mT. Structural analysis of the film has been done using X-ray difractometer. It has not revealed any distinct crystal like reflections, thus confirming its amorpous state. Chemical composition of the film was studied using secondary ion mass spectrometry method on the equipment SIMS ION TOF. Corresponding depth profile is shown in Fig.1(B),

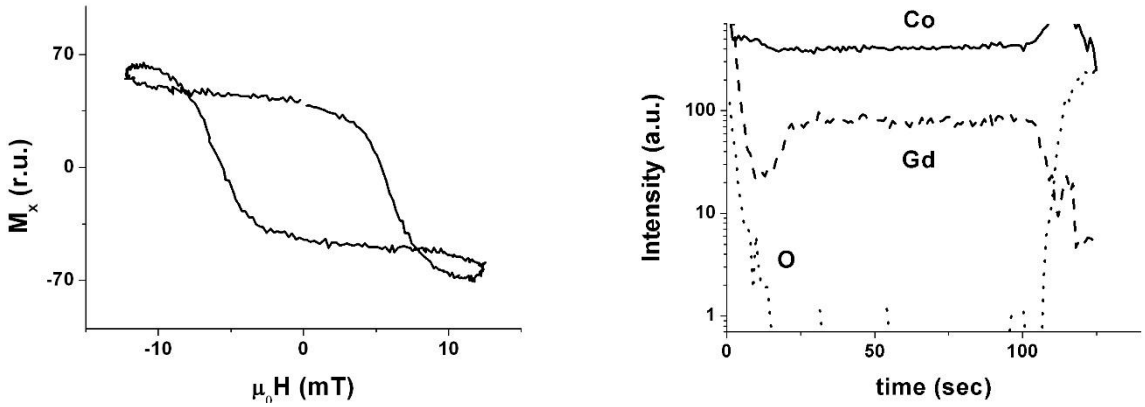

A B

Fig1.(A) Magnetization reversal curve in the field perpendicular to the film surface obtained using magnetooptic Fardey rotation method, (B)SIMS depth profile showing distribution of chemical elements in the film.

In summary, we explored very old samples of amorpous magnetic Gd-Co films on glass substrate, fabricated more than 40 years ago. Our results shows that the system preserved its amorphous state and PMA characteristics during that time. This is due to the formation of thin capsulating oxide layer covering film surface. It means that such systems possess of long-term stability and might be used for information storage applications. The work has been done under State Programs #0066-2019-0003 of the Ministry of Science and Higher Education of Russia.on the equipment of the center for collective use of the scientific equipment «Diagnostics of micro- and nanostructures»

1. Herd S.R.”On the nature of perpendicular anisotropy in sputtered Gd-Co thin films”, J.Appl.Phys.,.-**50**, pp.1645-1647. 1979

P2-29: Obtaining and applications of homogeneous magnetic nanowires

D. Zagorskiy[1] , I. Doludenko[1] , D. Cherkasov[1], S.Bedin[1] , D. Bizyaev[2], A. Bukharaev[2], R. Khaibullin[2]

1. *Center of Crystallography and Photonics of RAS, Moscow, Russia, dzagorskiy@gmail.com.*
2. *Zavoisky Physical-Technical Institute (KPhTI), Kazan, Tatarstan, Russia. 3*

The creation of new types of magnetic materials is an important task. One of the promising approaches here is the synthesis of objects with nanoscale structural units. It is known that magnetic phenomena in various nanoscale materials can be rather specific. This paper is devoted to obtaining one-dimensional magnetic structures-nanowires (NWs).

Such structures can be obtained by the method of matrix synthesis. For this, a growth polymer film is used (the matrix is a PET membrane obtained from JINR, Dubna), in which the pores are filled with the required metal. In our case, the pores are filled with metal by the electrochemical (galvanic) method. We used a polymer film with the pore density of 10 ** 7 - 10 ** 8 pores per square cm and pores diameters of 50–200 nm. Two types of NWs were obtained, from pure metals and from alloys. (In the last case the electectrodeposition process was carried out using electrolyte with the salts of two corresponding metals). The X-ray spectra, magnetic characteristics were studied for obtained samples. There are several promising areas of application of such structures, including in magnetic memory devices and for creating so-called “gradient structures”-some of them

MAGNETIC MEMORY. Initially, it was proposed to use similar structures for planar magnetic memory. Currently, the idea is to create devices with a “deep write”: increasing the recording density is achieved by splitting each NWs in the array into separate domains. In the present work, NWs have been synthesized from magnetic materials — Fe, Ni, Co, or their alloys. To study their magnetic state, magnetometry methods, and AFM were used. Using the method of magnetic force microscopy (MFM), an NWs array in a polymer matrix was investigated — the NWs ends were tested. The character of their magnetization reversal is shown and the mutual influence of NWs on each other is proved. In addition, X-ray diffraction analysis showed that in addition to the solid solution, the second phase, a nickel phase, appears in the iron-nickel sample. The dependence of X-rays parameters on grooving condition and electrolyte composition were investigated. The data of ferromagnetic resonance showed that the direction of magnetization of the NWs lies at an angle of about 20 degrees with respect to their axis.

GRADIENT STRUCTURES. Another features of matrix synthesis include the possibility of obtaining a matrix and, accordingly, NWs with a variable cross section. We have proposed ways to create such structures by etching tracks in ion-irradiated polymer under special conditions. Thus, etching in an alcohol-alkaline solution at a low temperature makes it possible to obtain conical pores and, accordingly, to obtain the replicas of conical shape. Note that by varying the alcohol content and temperature of the processes, one can predictably change the angle at the top of the pores (and, accordingly, the angle at the top of the metal replicas). The possibilities of using such structures for the creation of emitters and for the formation of so-called "Gradient" structures is discussed.

Acknowledgements. Synthesis of NWs was supported by RFBR grant No.18-32-01066, SEM measurements-by the State Task of FNIC “Crystallography and Photonics” of RAS, Part of magnetic measurements were supported by State Task of Zavoisky Physical-Technical Institute of RAS.

P3-1: The nano - structured granular composites as an electromagnetic wave absorber to protect microelectronics devices.

N. Savinski[1], M. Soloviev[2],V. Turov,[3]A. Krenev[3]
1Valiev Institute of Physics & Technology of Russian Academy of Sciences, Savinski1@yandex.ru
2 Yaroslavl State Technical Universities, Russia
3 P G. Demidov Yaroslavl State University. Russia

Electromagnetic interference (EMI) of higher types of harmonics occurs when the power of microwave devices of radio electronics increases and creates interference in electronic equipment and satellite communications, which affects their compatibility and operation. EMI also has a negative impact on biological objects. Moreover, in many countries, screening is used to protect human health and sensitive devices from EMI. Shaping rooms are also necessary to protect against unauthorized removal of information from processing, transmission and storage devices. Therefore, the development of new high-performance broadband radio absorbing materials is an urgent task.

The absorption of electromagnetic energy is due to dielectric, magnetic and conductivity losses, which are trying to maximize to achieve the maximum efficiency of shielding. Recently, as the use of electromagnetic wave absorbers to reduce the strength of radar signals has been growing, research on the use of composite materials to create radar absorbing structures has been actively pursued [1–4]. Composite materials appear to provide the most attractive and promising solution to demands for lightweight, high-performance structures. Since composite materials have high specific strength and stiffness compared with bulk materials, the range of their applications is rapidly expanding from aerospace and military use to commercial activities.

Our work is aimed at a new generation of materials with a wide range of adjustable electrical and magnetic properties: conductive polymers (polyanilines), carbon nanotubes, flaky multilayer graphene, nano - structured granular composites. A portable radar was used to study the absorption properties of electromagnetic radiation. The radar signal was processed using the consistent filtering method. The consistent filtering assumes finding the filter response in the form of convolution of the radar input signal x(t) and the pulse characteristic of the filter h(t 0-t), consistent with the probe radar signal. With this processing in the output signal of the matched filter (SF) z(t), the maximum signal-to-noise ratio is achieved by the accumulation of the useful signal energy and suppression of out-of-band noise. Additional measures may be used to suppress possible interference [5]. It is shown that on the basis of granular nanostructures it is possible to create magnetic materials with close complex magnetic and dielectric permittivity at a magnitude of magnetic losses several times higher than traditional ferrite magnetic materials. These materials can be the basis for the creation of effective broadband electromagnetic wave absorbers with a thickness of hundreds of microns. The work has been done under State Programs #0066-2019-0003 of the Ministry of Science and Higher Education of Russia.on the equipment of the center for collective use of the scientific equipment «Diagnostics of micro- and nanostructures»

1 I. Sadiq “Tunable microwave absorbing nano-material for X-band applications”/Journal of Magnetism and Magnetic Materials v.**401**, p.63–69, 2016
2 Zheng , Shuhua, Xiaolan, Huan, Pei, Qiu “Preparation and microwave-absorbing properties of silver-coated strontium ferrite with polyaniline via in situ polymerization” Journal of Alloys and Compounds v.**621**, p. 194–200, 2015
3 Eiichi Sano, Eiji Akiba “Electromagnetic absorbing materials using nonwoven fabrics coated with multi-walled carbon nanotubes”/ Carbon v.**78**, p. 463 – 468, 2014
4 O. Gohardani, M. Elola, C. Elizetxea «Potential and prospective implementation of carbon nanotubes on next generation aircraft and space vehicles: A review of current and expected applications in aerospace sciences»/Progress in Aerospace Sciences v.**70**, p.42–68, 2014
5 V. E. Turov *Radar fight. Construction and noise protection of basic correlation systems of passive location*: M: University book,p.205, 2011(in Russian)

P3-2: Highly ordered porous alumina membranes for ferromagnetic nanowires fabrication

N. Savinski[1], O. Trushin[1], L.Mazaletski[2], E.Grushevski[2]
1 Valiev Institute of Physics & Technology of Russian Academy of Sciences, Savinski1@yandex.ru
2 P G. Demidov Yaroslavl State University. Russia

Magnetic metal nanowire arrays of variable aspect ratio offer many modern applications such as nanoscale electronic components [1], high-density magnetic memory [2], optoelectronic devices, magnetoresistive sensors [4], etc. In particular, Ni–Fe nanowire arrays being alternated with nonmagnetic Cu layers, which are embedded in porous alumina template, can serve as magnetic storage media with giant magnetic resistance [5]. There are a number of techniques to fabricate high aspect ratio metal nanowires (NW): vacuum evaporation, magnetron sputtering, electroless deposition, electroplating, and wet chemical reduction. Among them, metals are deposited electrochemically into the pores of another material host membrane. The advantage of electrodeposition is strict control of NWs' length and chemical composition (for alloy nanowires), as well as low-cost processing equipment. The choice of suitable template is one of crucial factorsfor NWs' fabrication, because every defect there on is replicated into resulting nanostructure. In general, polycarbonate membranes and anodic alumina membranes (AAMs) are used as templates. Nanoporous anodic alumina is the most used material due to AAMs possesses superior pores density and narrower dispersion of pores diameters; the pores diameter and inter-pores distance could be varied rather simply via anodizing mode control; using two-step anodizing, one can produce AAMs with periodic self-organized pores structure cheaper than with other techniques such a selectron-beam lithography. However, the following factors complicate fabricationof large-area NWs' arrays from multicomponent materials,especially with high aspect ratio (a.r.): chemical composition non-uniformity (variability) along NW length and hydrogen bubbles pores blocking. As regards the nanowires chemical composition uniformity, the determinative processing step is NWs' deposition into membrane pores. The two different deposition techniques are used: constant potential (dc-deposition) and constant current density (galvanic dc-deposition) deposition; .From practical viewpoint, the most suitable are the constant current density deposition. To implement these processes, the two-electrode cells and insoluble inert anodes (graphite, for instance) are used. In the present paper, the fabrication technology for highly ordered through-hole nanoporous anodic alumina (AAO)membranes of aluminum foil is demonstrated. The membranes were synthesized by two-step anodizing in oxalic acid at 50 V and 15 °C with auxiliary technological frame around the perimeter to be mechanically stable enough to handle under the following processing steps. Finally, we present, for the first time, Ni and Co nanowire arrays' fabrication by simple dc galvanostatic electrodeposition into the pores of as-prepared through-hole AAO templates. The thickness uniformity length ~ few μm for MCM NWs' arrays may be achieved over the 1cm2 area. The work has been done under State Programs #0066-2019-0003 of the Ministry of Science and Higher Education of Russia.on the equipment of the center for collective use of the scientific equipment «Diagnostics of micro- and nanostructures»

1. M.V. Puydinger dos Santos, M. Velo, R.D. Domingos, J. Bettini, J.A. Diniz, F. Béron, K.R. Pirota, "Electrodeposited nickel nanowires for magnetic-field effect transistor (MagFET)", J.Integr. Circ. Syst. **11**, 13–18, 2016

2. X. Kou, X. Fan, R.K. Dumas, Q. Lu, Y. Zhang, H. Zhu, X.Zhang, K. Liu, J.Q. Xiao," Memory effects in magnetic nanowire arrays". Adv. Mater **23**, 1393–1397, 2011

3. S. Krimpalis, O.G. Dragos, M. Grigoras, N. Lupu, H. Chiriac, Magnetoresistance and spin transfer torque in electrodeposited NiFe/Cu multilayered nanowires. J. Adv. Res. in Phys **1**(2), 021005, 2010

4 J. Han, X. Qin, Z. Quan, L. Wang, X. Xu, "Perpendiculargiant magnetoresistance and magnetic properties of Co/Cu nanowire arrays affected by period number and copperlayer thickness»". Adv. Cond. Matt. Phys.(2016).

P3-3: Optical properties and conductivity of carbon nanotube networks obtained by deposition on a substrate in the presence of solvent vapor

V. M. Efimov, D. G. Esaev, E. R. Zakirov

Institute of Semiconductor Physics, Russian Academy of Sciences, Novosibirsk, Russia, efimov@isp.nsc.ru

The chemical vapor deposition (CVD) of carbon nanotubes is the most popular method to synthesize single-walled carbon nanotubes (SWCNTs). But in order to use the raw material obtained by this method for the tasks of nanoelectronics, it is necessary to purify it from other carbon inclusions and from particles of a metal catalyst. Besides, it is very desirable to separate CNTs with metallic conductivity from CNTs that possess semiconductor properties. This is especially important when nanotubes are used as active elements of nano-electronics [1]. However, conventional methods developed for the separation of CNTs are, either very expensive, or allow to obtain pure material only in microscopic quantities (for example, the well known method of ultracentrifugation - [2]). In this report we will present the results of a unique experiment of separation, at room temperature, from a raw mixture of carbon nanotubes, CNTs of high purity and low defectiveness. Our SWCNT-films are fabricated as follows: the raw material of nanotubes mixture (the company OCSiAl, Novosibirsk) with the purity of about 85% and with Fe content <1% in amount of 1 mg were dissolved in 10 ml of isopropyl alcohol. The solution is sonicated during two hours to disperse the nanotube bundles. A plastic plate 3x3 cm in size is hung above the CNT solution. The container is not close tightly, so that within a few days about 25% of the solvent is evaporates. Evaporation of the solution occurs at room temperature.

The black film formed on a plastic substrate was investigated by various methods. Fig. 1 shows a part of the Raman spectrum of the raw material and recieved film. The position of the main D and G CNTs-peaks and the ratio of their intensities (G / D) clearly indicate that the film consists of carbon nanotubes of very high purity. While for the raw material this ratio was about 40, for films deposited on the substrate it was about 200. Inset in Fig.1 obtained in the SU8220 scanning electron microscope shows the image of the received CNT material. We obtained the value of the conductivity (600–800 Ω / □) close to those obtained for such CNTs-films in other works (for example 788 Ω / □ in [3]) and the conductivity of multi-layer graphene films. The report will also discuss other optical characteristics of the films – RGB-modes of the Raman spectrum and effect of visible radiation on the electrical conductivity.

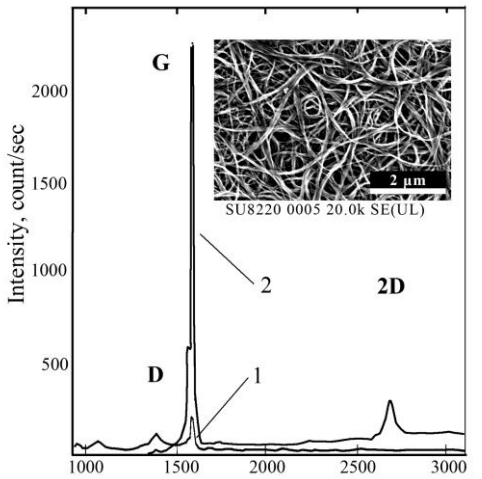

Fig. 1 Рамановский спектр УНТ-пленок: 1,2 - G пики, соответственно, для исходного и полученного нами чистого материала. На вставке СЭМ-изображение чистого материала.

Although the method of the deposition a CNT film on the substrate discovered by us, has such a drowback that it goes very slowly, it has an undoubted advantage in its simplicity and low cost. Our film can be easily transferred to another substrate and therefore it may be effectively used for the development of carbon nanotubes-based nanodevices.

1. A. E. Islam , J. A. Rogers, and M. A. Alam, **"**Recent Progress in Obtaining Semiconducting Single-Walled Carbon Nanotubes for Transistor Applications"**,** Adv. Mater., 27, p. 7908, 2015
2. Sato, Y.; Yanagi et al., "Chiral-angle distribution for separated single-walled carbon nanotubes", Nano Lett., 8, p. 3151, 2008
3. C. Koechlin, S. Maine et al., "Electrical characterization of devices based on carbon nanotube films", Appl. Phys. Lett., 96, p. 103501, 2010

P3-4: Morphology of the polytetrafluoroethylene-like coatings deposited onto the track-etched membrane surface in vacuum

L.I. Kravets[1], R.V. Gainutdinov[2], A.B. Gilman[3], M.Yu. Yablokov[3], V. Satulu[4], B. Mitu[4], G. Dinescu[4]

1. Joint Institute for Nuclear Research, Flerov Laboratory of Nuclear Reactions, Dubna, Russia. 2. Shubnikov Institute of Crystallography of FSRC "Crystallography and Photonics" RAS, Moscow, Russia. 3. Enikolopov Institute of Synthetic Polymer Materials RAS, Moscow, Russia. 4. National Institute for Laser, Plasma and Radiation Physics, Bucharest, Romania. E-mail: kravets@jinr.ru

The surface morphology of the polytetrafluoroethylene-like coatings deposited onto the poly(ethylene terephthalate) track-etched membrane (PET TM) surface by RF-magnetron and electron-beam sputtering of polytetrafluoroethylene (PTFE) in vacuum was investigated by atomic force microscopy. A PET TM with an effective pore diameter of 95 nm (pore density of 1.3×10^9 cm^{-2}) was obtained on the basis of a PET-film (Lavsan, Russia) with a nominal thickness of 10.0 μm according to the procedure described in [1]. The RF-magnetron (MSD) and electron-beam sputter deposition (EBD) of polytetrafluoroethylene were used as techniques to obtain polymer coatings onto the membrane surface [2, 3].

It was shown that the morphology of the PTFE-like coatings formed onto the track-etched membrane surface by the MSD and EBD methods varies considerably. This is due to the size of the deposited polymer nanostructures. The nanostructures produced by the EBD of PTFE under the action of the electron-beam irradiation are usually significantly greater in size than the nanostructures produced by MSD of the polymer. Therefore, unlike MSD, coating formed by EBD of PTFE results in formation of a polymer film with more advanced relief of a surface. Such difference is due to the peculiarities of the impact of the flow of particles falling on the target, leading to the destruction of the polymer and the deposition process itself. The energy impact on the target in the magnetron discharge is more significant. The decomposition at magnetron sputter materials is reached under bombardment with Ar^+ ions. Various atoms, ions and radicals based on C and F atoms from the PTFE target are present in the reaction chamber and after reaching the substrate the film growth is taking place. The decomposition of electron-beam sputter materials is reached under bombardment of electrons. When exposed to the flow of electrons on the surface of the polymer processes are occur, leading to the destruction of macromolecules. As a result, low-molecular fragments are formed in the reaction chamber. The polymer film growth on the membrane surface in this case takes place from polymer fragments as a result the formed nanostructures have more large size.

Determination of a size of the polymer nanostructures by the program SPIP shows that the dimensions of the PTFE-like nanostructures deposited by the MSD varies slightly with the increasing of sputtering time. Whereas at the dispersion of the polymer by EBD the enlargement of nanostructures is observed with an increase in the process time. Thus, the average size of the deposited polymer nanostructures during the process for 6 min is ~300 nm, and their maximum size reaches up to 500 nm. During the process for 15 min, the average size of PTFE-like nanostructures is 400 nm, and their maximum value reaches up to 700 nm. At the same time, the average size of the polymer nanostructures deposited by the MSD during the process for 10 min is ~50 nm, and their maximum size reaches up to 120 nm. During the process for 30 min, the average size of PTFE-like nanostructures is 60 nm, and their maximum value reaches up to 130 nm.

This work was supported by the grant (№ 17-08-00812) from Russian Foundation for Basic Research.

1. P.Yu. Apel and S.N. Dmitriev, "Micro- and Nanoporous Materials Produced Using Accelerated Heavy Ion Beams", Adv. Nat. Sci. Nanosci. Nanotechnol., **2**, no. 013002, 2011.
2. V. Satulu, B. Mitu, V. Altynov, N. Lizunov, L. Kravets and G. Dinescu, "Synthesis and Characterization of Porous Composite Membranes with Hydrophilic/Hydrophobic Sides Based on the PTFE Layers Deposited by Magnetron Sputtering", Thin Solid Films, **630**, pp. 92-99, 2017.
3. L.I. Kravets, A.B. Gilman, M.Yu. Yablokov, A.N. Shchegolikhin, B. Mitu and G. Dinescu, "Properties of Poly(Ethylene Terephthalate) Track Membrane with a Polymer Layer Obtained by Electron Beam Dispersion of Polytetrafluoroethylene in Vacuum", High Temp. Mater. Proc., **19**, pp. 121-139, 2015.

P3-5: Estimation of the share of metal nanotube short-circuits in the sensor structures

V. M. Efimov, D. G. Esaev, E. R. Zakirov
Institute of Semiconductor Physics, Russian Academy of Sciences, Novosibirsk, Russia, efimov@isp.nsc.ru

Interdigital structures (ID), as well as the thin-film transistors (TFTs) structures, are the basis of chemical and biological gas sensors. The random SWCNT- networks are often used for such structures as an active conductive layer. However, such networks contain both metallic (m-CNTs) and semiconducting (s-CNTs) nanotubes. The presence of an electrical paths in CNTs networks affects the sensitivity of the devices. So the modeling and estimation of the metal paths formation by metal-tipe nanotubes is important for the design of the sensors. The main difference of the active layer in TFTs and in the interdigital sensor structures is that in the second case the sensor layer is quasi-one-dimensional: the total length of the interdigital space is several orders of magnitude greater than its width. For example the total interdigital space in our sensors have the length ~ 10^4 μm when the distance between the electrodes is 10-40 μm. For such structures conventional percolation modeling used for TFTs transistors is not applicable [1,2].

In this work we tried to evaluate the quantity of the transverse short-circuits in the quasi one-dimensional (Q1D) bands on the basis of simple model. Then model was used to analyze the experimental data on the conductivity of single-walled CNTs network. The qualitative approach to describing the formation of conductive transverse short-circuits in Q1D bands is illustrated by Fig.1.

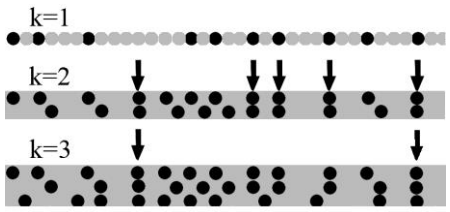

Fig. 1 The model of a quasi one-dimensional bands, consisting of k chains of high-conductivity (black circles) and the low-conductivity (gray circles). The arrows show transverse short-circuits in the Q1D bands (k=1, 2,3 – see text)

Let's a Q1D band consist of k chains of high-conductivity (HCE - blac circles) and low conductivity elements (LCE - gray circles). HCE could be the metal-type and LCE – simiconductor-tipe CNTs. And, in the simplest case, the value of k may be equal to the ratio of the space width in the ID-stnsor to the size of an curved CNT.

The LCE and HCE are randomly distributed in a chane.

If the share of HCE in each chain is ω, then the probability of the formation of an transverse short-circuits in the Q1D band will be ω^3. Then the conductivity of the sensor structure G will be proportional to $\boldsymbol{\omega}^k$ and the value of ω may be determined from the slope of the dependence lgG(k)

For test experimental measurements, we used the circular ID-structures with a distance between concentric gold contacts of 10, 20, 30 and 40 μm. The circular gold interdigital electrodes were formed on silicon wafers thermally oxidized to a SiO_2 thickness of 85 nm. The outer diameter of the circular structures was 2.5 mm. The suspension of purified single-walled carbon nanotubes (average diameter 1.5 nm; average length 10 um) was made with solution of 1 mg of SWCNTs in 10 ml of N-Methyl-2-pyrrolidone and were sonicated for 60 min to dissolve and debundle the nanotubes. A layers of nanotube networks was deposited on the structure in a drop-like manner. DC current-voltage measurements were carried out by Keithley 2450 measuring source with automatic data recording to a computer.

For evaluation of ω from our measurements, the values of distances 10, 20, 30 and 40 μm where corresponded to the values of k = 1,2,3 and 4. The value of ω determined from the slope of the dependence lgG(k) was 0.67. Received values exceed 0.33, which is characteristic of a conventional mixture of nanotubes. It is well known that usually it is very difficult to obtain a suspension from single nanotubes and we assume that the obtained value of ω corresponds not to the single nanotubes, but to CNT nanoclusters. The proposed technique can be used to characterize different layers of nanotubes.

1. V. K. Sangwan, A. Behnam et. al., "Optimizing transistor performance of percolating carbon nanotube networks", Appl. Phys. Lett., 97, p. 043111, 2011
2. H.K.Jang, J.E. Jin, et al., "Electrical percolation threshold of semiconducting single-walled carbon nanotube networks on field-effect transistor", Phys. Chem. Chem. Phys., pp.1-7, 2012

P3-6: Gradient structure of polypropylene composites filled with carbon black

Yablokov M.Yu.[1], Shchegolikhin A.N.[2], Lebedev O.V.[134,] Mukhortov L.A.[3,] Ozerin A.N.[1]

1. Enikolopov Institute of Synthetic Polymer Materials, Russian Academy of Sciences,Moscow, Russia. 2 Institute for Biochemical Physics, Russian Academy of Sciences, Moscow, Russia. 3 Moscow Institute of Physics and Technology (State University), Moscow Region, Russia. 4. Center for Design, Manufacturing and Materials, Skolkovo Institute of Science and Technology, Moscow, Russia. E-mail: yabl1@yandex.ru

Materials with gradient structure, or functionally graded materials are currently in the focus of multidisciplinary research in materials science [1-4]. Polymer composite materials with gradient concentration distribution of filler in the bulk of the material have a number of important practical applications. In particular, polymers filled with carbon blacks (CB) or other forms of carbon, e.g. graphene, carbon nanotubes, globular carbon, nanodiamond of detonation synthesis, are highly desirable in many applications owing to their improved electrical, mechanical and thermal properties. The research of migration of filler to the interface of bicomponent hybrid polymer-carbon systems is of particular importance.

The structure of gradient composites of polypropylene (PP) filled with 7.5-15 wt. % of CB have been studied in present work with the help of Raman spectroscopy. The composites were prepared by mixing of melt PP and CB in the compounder. Subsequent hot pressing gave the composites samples. Surface conductivity of hot-pressed samples was considerably higher than of non-heated composites. This fact may be explained by the enrichment of surface with conducting CB particles. The enrichment of the composites surface with CB may be caused by migration of CB particles from volume toward surface under thermal annealing. This suggestion is supported by the fact of sharp drop of surface conductivity values after mechanical removal of 10-mcm layer from the composite surface.

Raman spectroscopy (λ_{exc} = 785 nm) was used to study of the effect of surface layer enrichment of polymer composites with CB. The Raman spectra of studied samples were completely dominated by the bands G and D of the filler CB particles over PP bands. The increase of the incident laser power above 10 mW has led to corresponding growth in the temperature of the composite resulting in the melting of PP matrix, since CB particles strongly absorb in the NIR spectral region. Therefore only laser powers below 10 mW with laser focusing on the very surface of the sample have been employed during Raman measurements.

Small-sized samples were cut out from hot-pressed composites normally to the pressing surface and flattened using sledge microtome for Raman study. This geometry of samples gives the possibility to characterize concentration gradient of carbon filler in polymer matrix while scanning of laser beam in the direction, perpendicular to pressing surface. The spectra were run in multiple points with an incremental step of 5-10 mcm. It has been found that integral intensity of G and D Raman bands of CB was relatively constant and low in points situated far from the sample surface but showed a gradual increase and growth in close proximity to the surface layer. Thus the growth of CB concentration in the vicinity of the composite surface has been confirmed. Surface concentration of CB was estimated on the basis of calibration dependence. The linear dependence of Raman integral intensity of CB signal on filler concentration was obtained for the samples with constant filler concentration in polymer matrix.

This work was supported by grant № 18-29-19112 from Russian Foundation for Basic Research

1. M. Naebe, K. Shirvanimoghaddam, "Functionally graded materials: A review of fabrication and properties", Applied Materials Today, 5, pp. 223-245, 2016
2. K. Claussen, T. Scheibel, H-W. Schmidt, R. Giesa, "Polymer Gradient Materials: Can Nature Teach Us New Tricks?", Macromol. Mater. Eng., 297, pp. 938-957, 2012
3. D. Almasi, M. Sadeghi, W. Lau, F. Roozbahani, N. Iqbal, "Functionally graded polymeric materials: A brif review of current fabrication methods and introduction of a novel fabrication method", Mater. Sci. Eng., 64, pp. 102-107, 2016
4. R. Parihar, S. Setti, G. Srinivasu R.Sahu, "Recent advances in the manufacturing processes of functionally graded materials: a review", Sci. Eng. Compos. Mater., 25, pp. 309-336, 2018

P3-7: Features of electrophoretic deposition of Al-CuO and Al-Ni-CuO nanosized thermite materials

Larisa Sorokina[1], Egor Lebedev[1], Roman Ryazanov[2], Artem Sysa[2], Dmitry Ignatov[1], Dmitry Gromov[1]

3. National Research University of Electronic Technology, Moscow, Russia. 2. Scientific Manufacturing Complex "Technological Centre", Moscow, Russia

Not so long ago, new unique uses of thermite material have appeared, which continue to develop. One of these new application areas is the use of thermite material as a local heat source for different purposes micro - and nanoelectronics. The energy which is released as a result of the flame front propagation allows connecting various sensitive materials, which is very important in the 3d assembly of microelements [1,2]. Another equally promising application is thermal initiation of secondary reactions [3].

This paper presents the results and features of Al-CuO и Al-Ni-CuO thermite material formation by the electrophoretic deposition method (EPD). The electrophoretic deposition is an experimentally simple technique, that considers the possibility of local and multi-component deposition at room temperature. The obtained Al-CuO samples shows high density of the released energy, flame wave propagation velocity and low energy of reaction initiation. However, the combustion process of the Al-CuO material is characterized by significant gas evolution. In order to reduce gas emission, a three-component Al-Ni-CuO material with new distinctive energy characteristics was produced.

This paper presents the results and features of Al-CuO и Al-Ni-CuO thermite material formation by the electrophoretic deposition method (EPD). The electrophoretic deposition is an experimentally simple technique, that considers the possibility of local and multi-component deposition at room temperature. The obtained Al-CuO samples shows high density of the released energy, flame wave propagation velocity and low energy of reaction initiation. However, the combustion process of the Al-CuO material is characterized by significant gas evolution. In order to reduce gas emission, a three-component Al-Ni-CuO material with new distinctive energy characteristics was produced.

Thermal properties, microstructure, composition and combustion velocity of the formed layers were investigated using simultaneous DSC, SEM, EDX and high-speed video, respectively. The value of the reaction initiation energy in formed materials was determined with a femtosecond Nd:YAG laser. The minimum thickness and the optimum component ratio for the self-propagating reaction realization were determined.

This work was supported by the Russian Federation President's grant (МК-1262.2019.8)

1. J. Braeuer et al "A novel technique for MEMS packaging: Reactive bonding with integrated material systems ". J. Sensors and Actuators A: Physical., **188**, pp. 212-219, 2012.

2. Z. Long et al "Transient liquid phase bonding of copper and ceramic Al_2O_3 by Al/Ni nano multilayers". J. Ceramics International., **43**, pp. 17000–17004, 2017

3. J. J. Granier and M. L. Pantoya, "Laser ignition of nanocomposite thermites," Combustion and Flame., 138(4), pp.373–383, 2004

P3-8: Investigation of the influence of focused ion beam milling parameters on the formation of micro and nanostructure profiles

A. Kotosonova, A. Ballouk, D. Rodriguez, A. Kolomiytsev

Southern Federal University, Institute of Nanotechnologies, Electronics and Equipment Engineering, Taganrog, Russia, alena.kotosonova@gmail.com

Progress in modern micro and nanosystem technology creates a constant demand for the development of new technological processes and methods for the formation of the elements. One of the key technological operations in the production of the element base is the profiling of the surface of solids with a nanometer spatial resolution. One of the most promising methods for nanoscale surface profiling of solids during the formation of elements in micro and nanosystem technology is the method of focused ion beams (FIB) [1, 2].
During the formation of structures by the FIB method, it is important to preliminarily estimate the possible deviation of the profile in the structure being formed from the given one, which will make it possible to more accurately predict the parameters of the surface profile and promptly correct the ion-beam exposure times.
In order to study this deviation, we developed a technique based on a comparison of the AFM profile of the structure formed by FIB milling, depicting a given profile and calculating the ratio of their areas:

$$S_{dev} = 100 - \frac{S_\alpha}{S_\varphi} \cdot 100\%, \quad (1)$$

where S_{dev} is the deviation of the profile of the structure being formed from the given one, S_α is the sectional area of the structure obtained, S_φ is the sectional area of the given structure.
Based on the application of the mentioned technique, the dependences of the profile deviation on the ion beam current (figure 1,a) and the time of exposure of the beam on the surface (figure 1,b) are obtained.

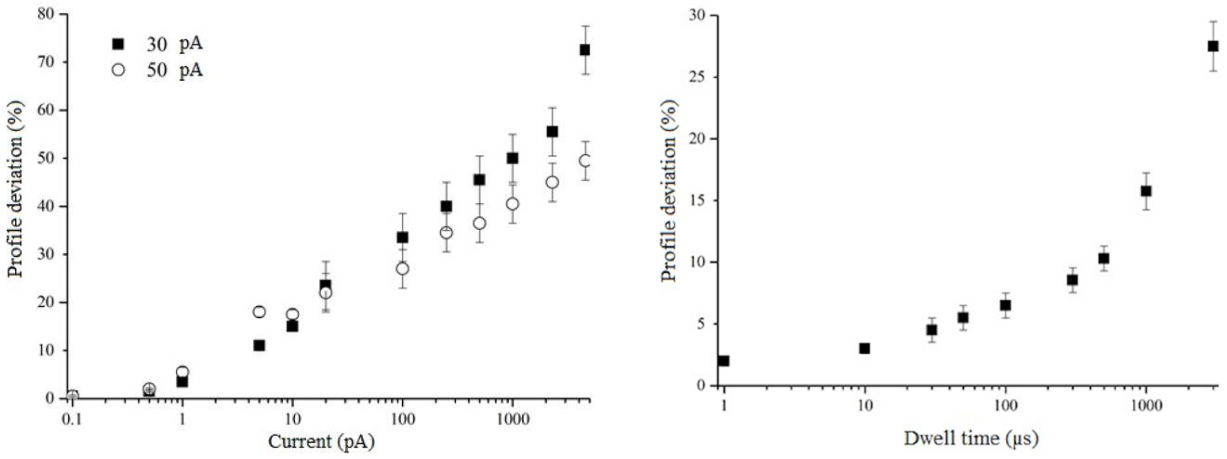

a) b)

Figure 1. Dependence of the deviation on the structure profile on the ion beam current (a) and the FIB dwell time at different currents of the ion beam (b).

The analysis of the obtained dependences shows that the highest accuracy of the formation of structures by the FIB method (deviation of ~ 12%) is achieved at the FIB dwell time at a point from 0.1 to 10 μs and a current of up to 100 pA. A further increase in the exposure time at a point leads to a decrease in the accuracy of the transfer of a given topological pattern to the surface of the substrate. This is explained by the increased influence of the redeposition effect with an increase in the exposure time at a point due to a decrease in the number of FIB passes during milling process.
This work was supported by The Grant of the President of the Russian Federation for State Support of Young Russian Scientists, Candidates of Sciences (project no. MK-1811.2019.8).

1. O.A. Ageev, A.S. Kolomiytsev and A.V. Bykov *Microelectron. Reliab.*,55, pp. 2131–34, 2015.
2. O.A. Ageev, A.S. Kolomiytsev, A.L. Gromov, B.G. Konoplev and S.A. Lisitsyn *Nanotechnol. in Russ.*, 9, 1, pp. 26–30, 2014.

P3-9: Development of thermal sensors by implantation ions P^+ and B^+ in different sides of Si(111)

A. Rysbaev, M. Normuradov, J. Xujaniyozov, Sh. Talipova, B. Ibragimova, A. Rahimov
Tashkent State Technical University, Tashkent, Uzbekistan, E-mail: rysbaev@mail.ru

In the manufacture of semiconductor devices, depending on the type of dopant and technology used, various defects are formed in the structures, which deteriorate the quality of the diodes and their breakdown characteristics. In addition, when using high-temperature technologies, such as epitaxial and diffusion technologies for creating pin-structures, it is possible to activate impurities of the source material, such as Na atoms, which can create fast states, various traps [1], macroscopic fluctuations leading to the appearance of density tails [2], or large inhomogeneities, at least at high concentrations of about $10^{13}cm^{-2}$ [3].

Therefore, to obtain the p-i-n structure, we have chosen the method of ion implantation, which does not subject the sample to high-temperature heating. Our task was to create a thermal sensor that meets the following requirements: small size; high temperature sensitivity; a wide range of measured temperatures; linearity of the temperature characteristics of the output signal of the sensor.

The fig. 1 shows the direct voltage drop across the p-i-n - transition from the heating temperature for Si(111) with a specific resistance ρ = 6000 Ohm·cm (curve 2) and 3000 Ohm·cm (3).

Studying the dependence of the direct voltage drop U_{dir} on temperature during the formation of the p-i-n structure by implanting P and B ions into Si with a gradual decrease in the energy and ion dose showed that the dependence $U_{dir} = f(T)$ turns out to be nonlinear (curve 1). After the initial stage of ion implantation (with E_0 = 80 keV and $D = 0.9 \cdot 10^{16}$ cm^{-2}) and annealing, the dependence $U_{dir} = f(T)$ becomes linear in the low-temperature region of ~ 250 K, and after the final stage of ion implantation (with E_0 = 20 keV and $D = 0.9 \cdot 10^{15}$ cm^{-2} of phosphorus and with E_0 = 10 keV and $D = 0.9 \cdot 10^{15}$ cm^{-2} of boron and subsequent annealing, this dependence becomes linear throughout the entire range of temperature variation.

As can be seen from fig. 1, the sensor performance also depends on the resistivity of the original silicon, i.e. is determined by the processes in the base region of the p-i-n – diode. With a decrease in ρ of the original silicon, the sensitivity of the sensor decreases slightly.

In the method of high-phase ion implantation of P^+ and B^+ to different sides of monocrystal silicon we obtained p-i-n – structure, which has a high thermal sensitivity of 2.3 mV/K in a broad band temperature of (20 ÷ 550) K. We studied the distribution profile P and B atoms implanted in the Si gradually decreasing energy. The effect of the subsequent thermal and annealing IR profile on the distribution of the atoms and the characteristics of the temperature sensor was studied.

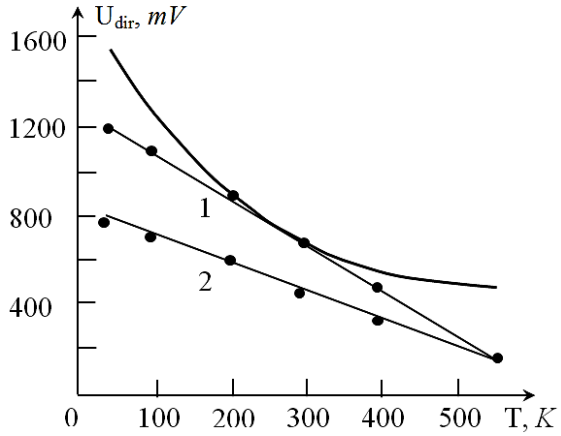

Fig. 1. The dependence of the direct voltage drop on the p-i-n – transition from the heating temperature for the Si (111) with a specific resistance 6000 Ohm·cm (1) and 3000 Ohm·cm (2).

Thus, the above technological modes of ion implantation and pulsed IR annealing are optimal for obtaining a thermal sensor with the following parameters:

1) the range of measured temperatures: from 20 to 500 K. In the whole range, the dependence $U_{dir} = f(T)$ is linear;
2) temperature sensitivity is 2.1 $mV \cdot K^{-1}$;
3) supply current from 100 μA to 1 mA.

1. Di Maria D.J. // J. Appl. Phys. 1981. V. 52. P. 7251.
2. Harstein A. and Fowler A.B. // J. Phys. 1975. V. 8. P. 249.
3. Rysbaev A.S., Normurodov M.T., Nasriddinov S.S. // Technology and Electronics. 2001. T. 46. № 9. p. 1148-1150.

P3-10: Optical properties of indium sulphide films after argon plasma treatment

V.F. Gremenok[1,3], S.P. Zimin[2], A.S. Pipkova[2], V. V. Khoroshko[3]

4. Scientific-Practical Materials Research Center of the National Academy of Sciences of Belarus, Minsk, Belarus, gremenok@physics.by. 2. Microelectronics and General Physics Department, Yaroslavl State University, Yaroslavl, Russia, zimin@uniyar.ac.ru. 3. Belarusian State University of Informatics and Radioelecrtonics, Minsk, Belarus, khoroshko1986@mail.ru

Nanoscale surface modification methods using ion beams are an important instrument in the technology of the fabrication of nanostructured systems. The capabilities of ion-based processes become wider with the transition to the multicomponent materials with complex chemical composition. There are reports on preparation and investigation of CdS and In_2S_3 formed in the nanostructured thin films. All these developments point to a bright future for the application of nanotechnology in film solar cell development.

In this work we report an optical properties of indium sulphide (In_2S_3) thin films after the treatment in high-density low-pressure inductively coupled argon plasma with different regimes.

The investigations were carried out for In_2S_3 films with the thickness of 500–800 nm grown by thermal evaporation technique at a substrate temperature of 300°C on glass substrates using In_2S_3 powder as source material. The as-grown films were annealed in sulfur ambient at a residual pressure of 2×10^{-2} mbar at temperatures in the range of 300°C for 60 min. Plasma treatment of the samples was carried out in the radio-frequency high-density low-pressure inductively coupled argon plasma (RF ICP) reactor: argon flow with a pressure of 0.07 Pa, inductively coupled argon plasma with an argon ion energy of 25–200 eV, the treatment duration was 30–60 s.

As a result of the plasma treatment an array of indium nanostructures appeared on the surface of In_2S_3 films. The nanostructures had a droplet shape; their lateral size was 20–300 nm. The investigations of the optical properties of In_2S_3 films before and after plasma treatment was performed by measuring the optical transmittance and reflection coefficients using a Photon RT spectrophotometer (Essent Optics).

The obtained reflection and transmission spectra of indium sulfide films in the initial state and after treatment in argon plasma are shown on Fig.1. The reduction of transmittance and increase of reflectance for In_2S_3 films after plasma treatment are associated with the appearance of metal indium drops on the surface.

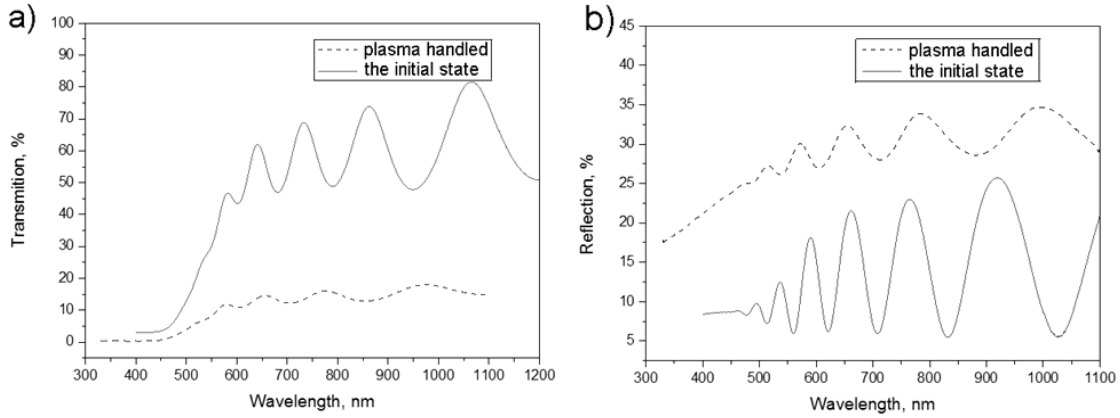

Fig.1. Optical transmission (a) and reflection (b) spectra of In_2S_3 thin films before and after plasma treatment

The band gap E_g of the In_2S_3 films before and after plasma treatment was determined from transmission and refection spectra. The analysis of the E_g value showed that if the films had pre-annealing, the band gap after the plasma treatment is practically not changed (2.6-2.7 eV). For films without pre-annealing, there was a decrease in E_g value from 1.9 to 1.5 eV. Therefore, plasma treatment can serve as an approach for the self-formation of In_2S_3 nanostructure arrays, which can be very prospective for the multilayered device fabrication with active monolithically integrated polycrystalline layers on glass substrates, such as solar cells.

P3-11: Modeling of wavelet transformation algorithms with application to the processing of experimental data

S. Moscovskiy, A. Sergeev, E. Sidorova, A. Marudov
Yaroslavl state University of P. G. Demidov, Yaroslavl, Russia, a.n.sergv@mail.ru

A large multiplicity of events and a high level of noise are characteristic features of tasks that require processing a large amount of data.
The introduction of wavelet analysis methods in data processing algorithms clearly shows their ability to comprehensively approach the solution of problems. One of the methods for processing a noisy signal is tresholding (TSH) [1].
The data of samples of V-O films obtained on an ARL X`TRA diffractometer (Thermo Scientifique - Switzerland, 2009), located in FSC DMNS was processed.
The task is a numerical analysis of the influence of threshold parameters and threshold processing methods on the quality of noise reduction [2]. The main evaluation criterion is the relative standard deviation (RMS) of noise.
Three different algorithms presented in the Wavelet Toolbox expansion package of the MATLAB computer system were considered:
1. The algorithm that uses default parameter selection function;
2. The algorithm for determining the threshold by the Birge-Massart strategy [3];
3. The algorithm that uses an adaptive threshold, which is set by choosing the evaluation criterion [4].
Of all the considered methods for choosing the threshold, the most suitable for our task was an adaptive tresholding algorithm with a minimax estimation criterion and the use of noise rescaling based on the coefficients of the first decomposition level.
Wavelet filtering, as a modern computer data processing method, made it possible to reduce the influence on the shape of the diffraction peaks obtained from thin V-O films of high-frequency noise and inhomogeneous background intensity.
This approach greatly simplifies the further analysis of diffractograms and significantly improves the accuracy of determining the characteristics of the investigated films.

1. N.M. Astaf'eva, “Wavelet analysis: basic theory and some applications”, Physics-Uspekhi, Vol. 166, No. 11, pp. 1145-1170, 1996.
2. M.V. Obidin, A.P. Serebroski, “Wavelets and adaptive thresholding”, Information Processes, Vol. 13, No. 2, pp. 91–99, 2013.
3. L. Birgé, P. Massart, "From model selection to adaptive estimation", Festchrift for L. Le Cam, pp. 55–88, 1997.
4. D.L. Donoho, “De-Noising by Soft Thresholding”, IEEE Transactions on Information Theory, Vol. 41, No. 3, pp. 613-627, 1995.

P3-12: Effect of longitudinal bistability on transfer characteristic of a silicon wafer heated in a lamp-based reactor

Ovcharov V.V., Kurenya A.L., Prigara V.P.

Yaroslavl branch of physics and technological institute of RAS, E-mail: ovcharov.vlad@gmail.com

Temperature and optical bistability in a silicon wafer under the conditions of its heat treatment in a lamp-based reactor were considered for the first time in [1], where the explanation of the phenomenon was put forward and the experimental results revealing it were presented. This phenomenon provides a useful additional control over rapid thermal annealing processes in the interval of the intermediate temperatures (such as $300 \div 900$K, that is the semitransparent region of the silicon wafer) where elements of the semiconductor devices, contact systems, gate structures, and metallization are formed in technological processes of micro- and nanoelectronics. A silicon wafer's transfer characteristic in a steady-state heat mode is determined by balance of heat input to the silicon wafer and heat output from it. A total description of temperature distribution in a silicon wafer which is under heat treatment in a modeled heat system containing a lamp block and a water-cooled pedestal where the silicon wafer is disposed is:

$$\varepsilon_w\left(T_{wup}\right)\left(T_h^4 - T_{wup}^4\right) - \varepsilon_w\left(T_{wdn}\right)\left(T_{wdn}^4 - T_a^4\right) - H_{eff}\left(T_{wdn} - T_a\right) = 0 \ . \qquad (1)$$

Here T_h, T_a are the temperatures of the heater and the absorber; T_{wup} and T_{wdn} are the temperatures of the upper and lower surfaces of the silicon wafer, correspondingly; $\varepsilon_w\left(T_w\right)$ is the hemispherical total emissivity of the silicon wafer; H_{eff} is the effective heat exchange coefficient [1]. It is supposed that for a sufficiently small wafer thickness the temperature of its upper surface is near equal to that of its lower surface; that is $T_{wup} \approx T_{wdn}$. However, the temperature difference between the upper and the lower surfaces of the wafer, $\Delta T_w = T_{wup} - T_{wdn}$, may be as much as 150 K and above, owing to longitudinal bistability as was shown in [2]. In this case, the thin wafer approximation that is usually used for steady-state transfer characteristic's descriptions may result in significant errors. The silicon wafer's total emissivity (on the left in the figure) and its transfer characteristic (on the right in the figure) are corrected by windowing method relative to the temperature T_{wup} with the window width of 150 K. The left curves on the figure correspond to averaging with temperature delay of the wafer in the process of heating of the wafer; the right curves correspond to the averaging with temperature advancing in the process of cooling of the wafer. More rapid switching to a high temperature state which is realized by the upper layers of the wafer to its lower layers under wafer heating is taken into account by averaging with temperature delay. And, on the contrary, later switching of the upper layers relative to the lower ones when the wafer is cooled is taken into account by the averaging ahead of the temperature. The form of the transfer characteristics obtained as a result of simulation corresponds well with the experimental transfer characteristics of [1].

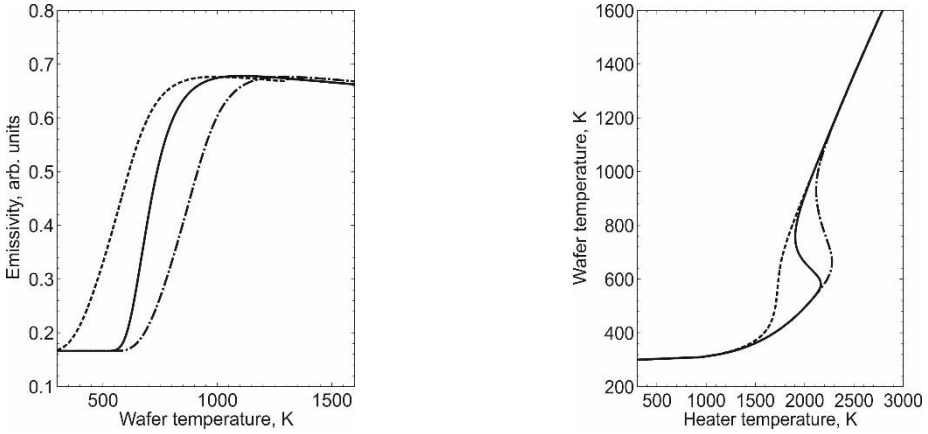

1. V.I. Rudakov, V.V. Ovcharov, A. L. Kurenya, V.P. Prigara, "Bistable behavior of silicon wafer in rapid thermal processing setup," Microelectronic Engineering, 93, pp. 67–73, 2012.
2. N.N. Rosanov. *Spatial Hysteresis and Optical Patterns*, Springer Verlag, Berlin, 2002.

P3-13: Synergistic aspects of the thermal evolution of Si(001)/P^+/O_2^+ defect subsystem induced by preliminary non-isothermal annealing

Yu. Denisenko
Valiev Institute of Physics and Technology, Russian Academy of Sciences, Yaroslavl Branch, Yaroslavl, Russia,E-mail: den-yur55@mail.ru

According to the concept of a deformable solid body as a nonlinear hierarchically organized system [1], the surface layers and internal interfaces are important functional subsystems that determine the development of plastic flow. The goal of this work is the further development of dislocation processes of self-organization of dissipative structures in (100) -oriented *Si* substrate samples, in which this functional subsystem is formed by co-implantation of P^+ and O_2^+ ions and a two-stage annealing process. At the first stage, the substrate was subjected to a 5-minute heat treatment in a non-isothermal reactor at 900 ° C with two signs (directions) of grad *T*. At the second stage, the system evolution process continued in a conventional isothermal furnace. (1150 ˚C, 4 h). Special attention was paid to the phenomena of self-organization of defects and the principle of the synergistic effect of various physicochemical, radiation and deformation effects, since their joint contribution may lead to a qualitatively new beneficial result.

Depending on the sign of grad *T* at the first stage, the process of evolution led to different solid-state reactions and formation of two types of self-organizing dislocation structures, which are mainly dissipative [2]. In the case of grad $T > 0$, a quasi-continuous, non-uniform in thickness and thermo stable layer of the SiP_zO_y phase was synthesized. Visually, the upper part of the layer had no traces of a pitting process. Below this layer, the artifacts of the process of plastic flow are presented as the evolution of an active and supersaturated environment in an open non-equilibrium system. A regular series of mixed dislocations containing hollow nanotubes oriented along the center lines of the screw components was observed. The nanotubes were coated with a SiO_x phase from the inside. According to the concept [3], pores can move along with the dislocation and, depending on the direction of movement, can increase their volume. In this case, the pores are sources for the injection of *Si* atoms, and their combined motion with dislocations is completed by their coagulation with the formation of a cylindrical tube. Since the dislocation core acts as the fastest way for the diffusion of atoms, silicon and excess oxygen atoms (from the forming SiP_zO_y layer) can enter into a chemical reaction. It can explain the occurrence SiO_x phase as a tube shell material.

In the case of grad $T < 0$, no thermally stable layer of *SiPzOy* phase was formed. At the initial stage of deformation (within the range of 0 ÷ 2.5 h in the furnace), dislocations move along the {111} slip planes and <110> directions. Later, slip occurs in other slip systems, and dislocations moving in different systems interact. As soon as a certain critical level of the stored elastic energy is reached, a non-equilibrium phase transition occurs, accompanied by restructuring of the defect structure. Further restructuring of defects (within the range of 2.5 ÷ 4 h) showed an irreversible transition from a quasi-homogeneous plastic flow at a macroscopic level to localization of plastic deformation at a microscopic level through the formation of spatially located dislocation complexes of a round shape. Their formation is initiated by Turing bifurcations in the reaction-diffusion system based on local reactions $Si + xO \rightarrow SiO_x$ and diffusion outflow of oxygen atoms from adjacent areas. It was accompanied by the multiplication of dislocations in the localization of the SiO_x phase and the formation of microcracks in the center of these complexes. Thus, the system selects more efficient channels for dissipating elastic energy through the organization of dislocation multiplication centers based on Frank-Reed sources, and the process of energy dissipation occurs more intensively.

Thus, the obtained experimental results are fully consistent with modern ideas about the self-organization of dissipative structures and the hierarchical structure of defects in a nonlinear system

1. V.E. Panin and L.E. Panin, “Scale levels of homeostasis in deformable solids,” Physical Mesomechanics, **7**(3), pp.5-20, 2004
2. Denisenko Yu.I., “Synergistic effects of deformation and solid-state reactions in Si with buried glass layer initiated by annealing in non-isothermal reactor”, Proc. SPIE 11020, 110221T, 2019
3. Ya.E. Geguzin and M.A Krivoglaz. *Motion of Macroscopic Inclusions in Solids*. Metallurgiya, Moscow, 98-102, 1971 (in Russian)

P3-14: Nanoscale formation of hydrated portland cement structure

A. Guryanov

Samara State Technical University, Samara, Russia, gurjanovam@mail.ru

Cement is one of the main functional construction materials. The hydration of cement is the chemical reaction of cement clinker components with water. During the hydration of anhydrous clinker minerals are converted into the corresponding crystallites (hydro silicates calcium, hydro aluminates calcium, hydro ferrites calcium), which fill the volume of a dense layering of gel particles, causing hardening. As a result of hydration, originally liquid or plastic cement glue turns into cement stone. The stages of this process are the setting and curing. The properties of a formed cement paste depend on the degree and rate of hydration.

The prevalence of Portland cement clinker compounds CaO and SiO_2 leads to the fact that in the process of determining the value of hydration is the formation of hydro silicates calcium (C-S-H). A complex framework of nanoparticles C-S-H formed as a result of hardening of the cement gel. Hydration process of cement depends on the size of grains (fineness), mineralogical composition of clinker, water-cement ratio, temperature hardening, and the introduction of various additives. It is important to understand what kind of structural changes occur in the cement paste or cement stone at the nanolevel.

In this work, the dynamics of changes in the structure of hydrated cement paste and cement stone samples as a function of time (up to 6 months) was investigated by method of small-angle neutron scattering (SANS) [1]. The measurements were performed on a diffractometer "Membrana-2", placed on the WWR-M reactor Petersburg Nuclear Physics Institute. Neutron wavelength λ = 0,3 nm with a line width of $\Delta\lambda/\lambda$ = 0,3. The range of momentum transfers q was from 0.03 nm^{-1} to 0.8 nm^{-1}. The scattered neutrons were recorded of 41-channel ^{3}He-counter in the range of angles of ±2°.

Scattering cross section $\sigma(q)$, per unit volume of the substance and unit solid angle as a function of the transferred neutron momentum q, obtained from the experimental spectra with the background and taking into account the contribution of the beam transmitted through the sample without the interaction of neutrons (transmission) with the normalization of data on the scattering intensity for the standard sample of known cross-section (1 mm H_2O).

For a system of identical scattering objects experimentally determined scattering intensity is averaged over all orientations (directions), the intensity of scattering by one particle in the Born approximation is the Fourier transform of the scattering structure. This allows us to define a number of structural characteristics of the scattering objects [2, 3].

In situ dynamics of changes experimental ranges of sections of dispersion of neutrons on hardening samples of the cement paste is presented over time (up to 6 months).

From the experimental data for neutron-scattering cross-sections using the software GNOM 4.5 [2] the Fourier transform of the distribution of scattering objects recovered in the approximation of homogeneous spheres. When fitting the experimental data varied the maximum radius of the scattering objects in the range from 50 to 100 nm. The scattering data were described quite accurately, if the maximum size of the scattering region was chosen to be 80 nm. The average radius of the scattering structures distributed from 40 to 55 nm. Quantitative relationships that describe the growth dynamics of C-S-H nanoparticles is obtained.

The fractal dimension of the C-S-H nanoparticles is obtained from the experimental SANS data. It is shown that the process of evolution cement paste or cement stone occurs the growth of the fractal dimension structure of C-S-H nanoparticles.

Various additives effect on all the structural parameters of cement paste or cement stone. The mineral and organomineral technogenic and artificial origin additives were considered.

1. L.A. Feigin. D.I. Svergun. *Structure Analysis by Small-Angle X-ray and Neutron Scattering.* Plenum Press, New York, 1987

2. A.M. Guryanov, “Nanoscale investigation by small angle neutron scattering of modified portland cement compositions”, Procedia Engineering, 111, pp.283-289, 2015

3. A. Guryanov, S. Korenkova, Yu. Sidorenko, “Research on the nanolevel influence of surfactants on structure formation of the hydrated portland cement compositions”, MATEC Web of Conference, 86**,** 04011, 2016

P3-15: Investigation of wetting layer in In/GaAs system by X-ray photoelectron spectroscopy

M.M. Eremenko[1] , S.V. Balakirev[1,2] , N.E. Chernenko[1,3] , O.A. Ageev[1] , M.S. Solodovnik[1,2]

1. Research and Education Center "Nanotechnologies", Southern Federal University, Taganrog, Russia, eryomenko@sfedu.ru. 2. Department of Nanotechnologies and Microsystems, Southern Federal University, Taganrog, Russia. 3. Department of Radio Engineering Electronics, Southern Federal University, Taganrog, Russia

Characteristics of grown nanostructures have a significant impact on the improvement of functional parameters of the devices based on semiconductor heterostructures. The separate deposition of components significantly expands the possibilities in the field of control and variation of the parameters of the obtained nanostructures during droplet epitaxy. However, the formation of a wetting layer during the deposition of metal droplets remains little studied.

Previously, we studied the effect of temperature on of In/GaAs(001) system parameters, including the formation of a wetting layer [1]. In this paper we present the results of the experimental investigation of temperature dependence of wetting layer formation during droplet epitaxy using X-ray photoelectron spectroscopy technique.

For our study, we grew a series of samples with In/GaAs(001) nanostructures using droplet epitaxy at various temperatures and deposition thicknesses. Growth temperature varied in the range of 100 – 300°C.

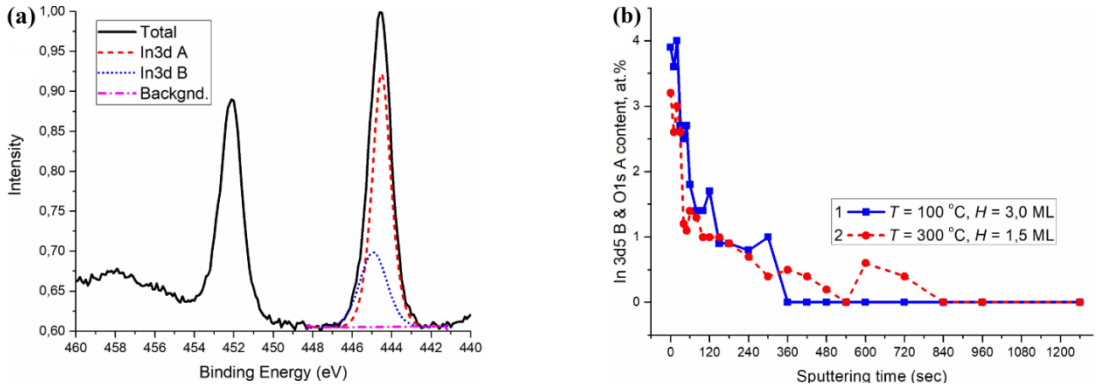

Figure 1(a, b). XPS spectra **(a)** from samples obtained at T = 100ºC, H = 3 ML and T = 300ºC, H = 1.5ML and change of In3d5A line intensity during etching of sample surfaces **(b)**.

Analyzing **Figure 1(a, b)** it becomes clear that the intensity of the In3d5A line on curve 1 (low-temperature sample without droplets) drops to zero much earlier than the lines on curve 2 (high-temperature sample with droplets) – by 360 s and 840 s, respectively. This may indicate a different thickness of the deposited material on the samples (a change of 2 times). At the same time, the lines differ from the different samples qualitatively: curve 1 decreases conventionally monotonously, while curve 2 has two distinct parts: a sharp decline (0 – 120 s) followed by a relatively gentle decrease to zero (120 – 840 s). The conventionally monotonous nature of the decrease in the intensity of the In3d5A spectral line in the first case indirectly indicates the relatively homogeneous structure of the In wetting layer. The complex nature of the intensity curve in the second case is due to the complex structure on the surface.

Thus, the results of X-ray photoelectron spectroscopy of In/GaAs samples formed under different conditions confirm an increase in the wetting layer thickness with a decrease in the formation temperature of the systems.

This work was supported by the Russian Science Foundation Grant No. 15-19-10006. The results were obtained using the equipment of the Research and Education Center and Center for Collective Use "Nanotechnologies" of Southern Federal University.

1. S.V. Balakirev, M.S. Solodovnik, O.A. Ageev, "Hybrid Analytical–Monte Carlo Model of In/GaAs(001) Droplet Epitaxy: Theory and Experiment", Phys. Status Solidi B, **255,** 1700360, 2018

P3-16: Silicene sensitivity to topological defects

N.N. Konobeeva, D.S. Skvortsov, I.N. Staritski, M.B. Belonenko
Volgograd State University, Volgograd, Russia, yana_nn@volsu.ru

Silicene is a set of silicon atoms in a hexagonal lattice [1]. It has attracted significant interest from both academia and electronics industry due to the similarity of electronic properties with graphene. However, silicene is not completely flat, as is graphene. Defects are often the first problem in the practical applications of monolayer structures. It is well-known fact that there are several types of topological defects. Among them is a vacancy, which is almost inevitable in the processing of materials with one layer. Such defects take a place in local changes in the interatomic distances and cause the distortions in the crystal lattice. It should be noted, that sometimes such defects are introduced purposively and can be useful in some applications [2]. In this paper, we offer a technique to defects observation in silicene based on the current-voltage characteristic (CVC) change in the tunneling contact.

We consider two possible configurations for the smaller vacancy clusters with 1–2 missing atoms. The Hamiltonian for electrons in silicene nanoribbon can be written in the following form:

$$H = -t\sum_{\langle ij\rangle s} a_{is}^{+}a_{js} + \frac{i\Delta_{SO}}{3\sqrt{3}}\sum_{\langle\langle ij\rangle\rangle s} s\nu_{ij}a_{is}^{+}a_{js}\,, \qquad (1)$$

here a_{is}^{+}, a_{is} are birth/annihilation operators of electron, Δ_{SO} is the spin-orbit interaction, <<*ij*>> means that the summation goes over all the nearest neighbors, *s*=↑↓ (if *s* as an index), s=± (if *s* as a multiplier). The first term describes the usual electron hopping between the nearest neighboring sites with energy *t*. The second term is the spin-orbit interaction, where ν_{ij}=+1 in the case if jumps between neighbors occur counterclockwise, ν_{ij}=-1 in the case if jumps between neighbors occur clockwise [3].

A two-dimensional array of silicon atoms is renumbered for the further calculations into a one-dimensional one. Further, we calculate the density of tunneling current in the contact of silicene with a metal or a superlattice.

The dependence of the tunneling current (contact with metal and superlattice) for the silicene flakes on the voltage for the vacancy defect is given in Fig. 1.

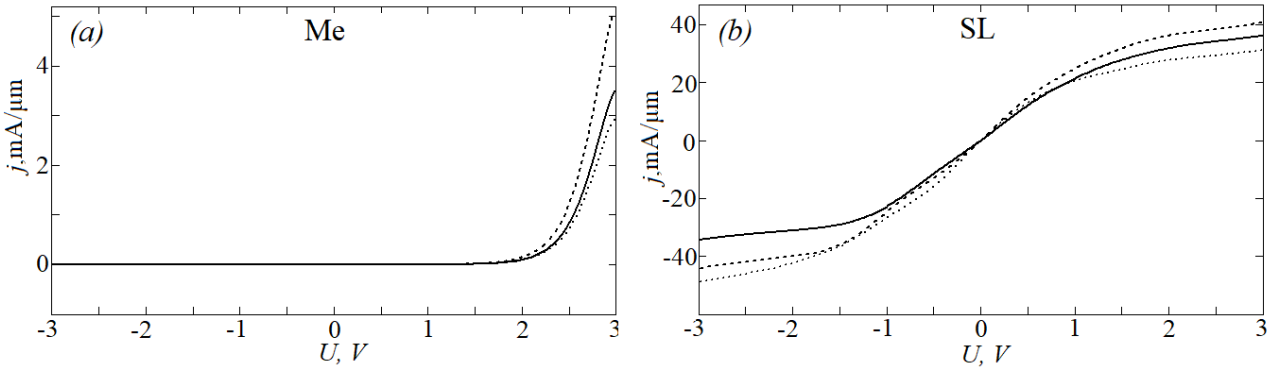

Fig. 1. Dependence of the tunneling current (contact with the metal – figs. a, contact with the superlattice – figs. b) for the silicene flake versus the voltage in the case of the vacancy defects. The solid line – flake without defects; the dashed line – one vacancy; the dotted line – two vacancies.

The reported research was funded by Russian Foundation for Basic Research and the government of Volgograd region, grant № 18-42-343002 and by the Ministry of Education and Science of the Russian Federation (state assignment no. 2.852.2017/4.6).

1. D. Jose and A. Datta, “Structures and chemical properties of silicene: unlike graphene”, Acc. Chem. Res., 47, pp. 593-602, 2014
2. G. Brumfiel, “Sticky problem snares wonder material”, Nature, 495, pp. 152-153, 2013
3. M. Ezawa, “Monolayer topological insulators: silicene, germanene, and stanene”, J. Phys. Soc. Jpn., 84, pp. 121003, 2015

P3-17: The Study of the Evolution of Radiation Defect Profiles during Thermal Annealing by the Rutherford Backscattering Spectroscopy

E. Parshin[1] , N. Melesov[1]

5. *Yaroslavl Branch of the Valiev Institute of Physics and Technology, Russian Academy of Sciences, Yaroslavl, Russia, par1959@yandex.ru, dartnik@mail.ru.*

The study of the evolution of defects in a silicon crystal during thermal annealing was carried out. The defects were formed by the implantation of Ge ions with a dose of $4 \cdot 10^{14}$ atoms/cm^2 at energy of 1 MeV into Si boron-doped [100] wafer with a resistivity of 10 Ω·cm. These structures are supposed to be used as promising light-emitting elements with an emission wave length within the framework of the silicon transparency window. Structures similar to those presented in this work, but with a smaller number of defects, after annealing, showed effective photoluminescence [1]. Luminescence centers are usually associated with certain types of spatial defects in the Si crystal lattice [2]. For this reason, the development of methods for identifying types of defective structures is relevant.

Analysis of the damage to the crystal lattice was carried out by the Rutherford backscattering spectroscopy (RBS) in combination with axial channeling of ions. For scattering on samples ^{4}He ions with energies of 1.3 MeV, 1.8 MeV, 2.6 MeV and 3.6 MeV was used. Figure 1 shows a comparative picture of axial channeling spectra recorded on the sample before and after annealing, as well as the spectra of pure silicon with and without channeling. It was found not only a decrease in the absolute number of defects by the annealing, but also a change in their spatial type. Before annealing, intense scattering of He ions on defects is observed, which indicates their point type (interstitial atoms, Frenkel pairs, amorphous clusters). A subsurface amorphous region is also observed, giving a fragment of the spectrum without channeling. After annealing, direct scattering on defects is not observed. Defects induce only the dechanneling of ion beam. This indicates the extended type of the damage to the crystal lattice (stacking faults, voids, crystal twinning, dislocation lines, dislocation loops). The dependence of the dechanneling ability on the energy of the analyzing ions is specific for each kind of defect, so its analysis can provide information on the predominance of one kind or another [3]. A comparison of the angular dependences of the integral intensity of the spectrum during channeling for annealed samples and for pure Si showed no significant differences. The dependence of the dechanneling cross section on energy was absent. From this we can conclude about the predominance of stacking defects in annealed samples.

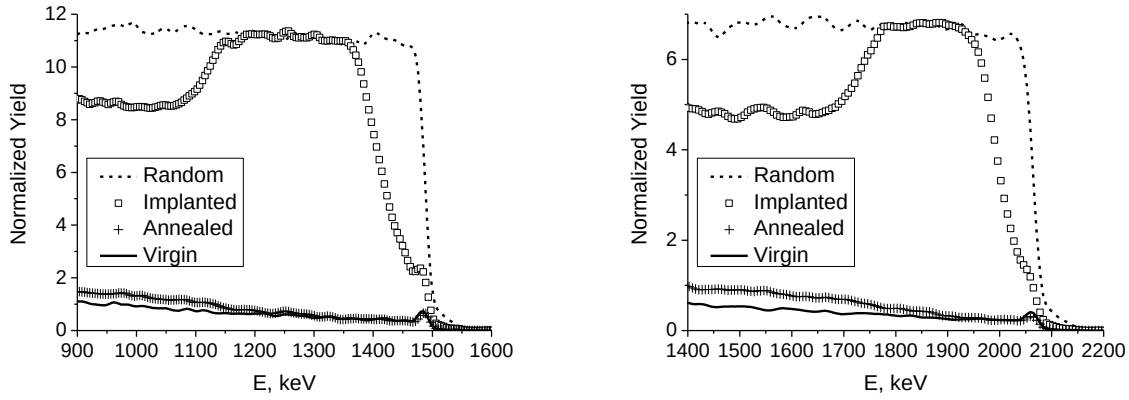

Figure 1. RBS spectra obtained at an ^{4}He energy of 2.6 MeV (left) and 3.6 MeV (right).

Analysis of the signal from Ge showed that during the annealing process, Ge atoms underwent migration. In addition, they are embedded in the nodes of the Si crystal lattice, as evidenced by the absence of a Ge signal on channeling spectra.

1. Соболев Н.А., Калядин А.Е., Сахаров В.И., Серенков И.Т., Шек Е.И., Паршин Е.О., Мелесов Н.С., Симакин С.Г.. ФТП, том 53, вып. 2, с. 165-168, (2019)
2. Соболев Н.А.. ФТП, том. 44, вып. 1, с.3-25 (2010)
3. J.R. Bird and J.S. Williams eds., Ion Beams for Materials Analysis, Academic Press, Sydney, 1989, 719 p.

P3-18: Application of Mössbauer spectroscopy to study the dynamic, structural and mechanical properties of nanofilms of frozen water on the clay surface

A. A. Zalutskii[1], S.A. Krivelevich[2], E.N. Skolnikov[1], A.Yu. Sokolov[1]

1. Yaroslavl Technical State University, Yaroslavl, Russia, E-mail: zalutskii@mail.ru
2. Yaroslavl Branch of the Institute of Physics and Technology, Institution of Russian Academy of Sciences, Yaroslavl, Russia, E-mail: s.krivelevich@mail.ru

Experimental results on the structure and properties of the quasi – liquid water layer in the system "frozen water-clay mineral" are presented using the probe technique developed on the basis of the mössbauer isotope ^{57}Fe in two forms (Fe^{2+} and Fe^{3+}). The problem was solved with the help of the analysis of the temperature behavior messbauerovskoi parameters of experimental spectra in the framework of the physical (quantum and/or classical) nature of the anomalies and properties of water. The temperature transformation of the mössbauer spectra of the system under study was qualitatively explained by the models traditionally described as two types of phase transitions («order-disorder» and «order-order»). If in the three dimensional case, melting always occurs by means of the first kind of transition, then in the two-dimensional case, the melting scenario is established from a variety of options. According to this, the system melts by means of two continuous transitions of Berezinsky – Kosterlitz – Taules with the presence of an intermediate hexatic phase characterized by a quasi-initial order. An attempt of quantitative evaluation of elastic parameters (shear modulus (G) , Poisson's ratio (μ), Gruneisen parameter (γ)) at the surface of the ice. He estimation of the Poisson's ratio gave an unusual result ($\mu = (4/3\gamma - 1)/(2\gamma + 1) = -0{,}699$) because for the overwhelming number of substances $\mu \rangle 0$. Thus, for the first time it is established that quasi-amorphous ice adsorbed on an aluminosilicate surface behaves as an auxetic. It is possible to assume that from the applied and academic point of view such behavior of films of water will help to explain the mechanism of emergence of natural nanotubes. At the same time, its structure was satisfactorily described in the framework of fractal geometry and with a decrease in the layer thickness, the «Menger Sponge → Kantor Dust» transition was established.

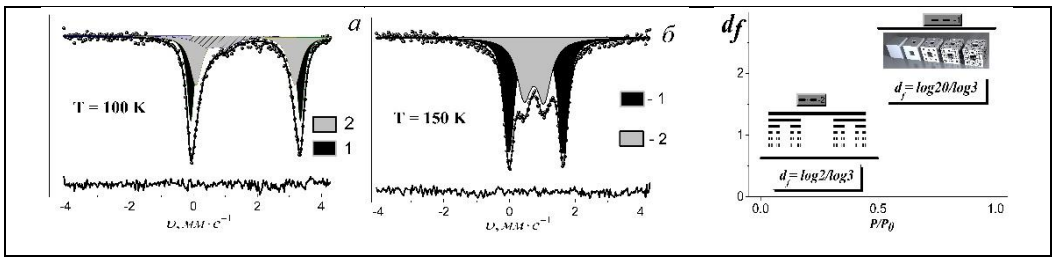

The presented results will be useful in solving the problem of searching for liquid water on Mars, since the diagnosis of the presence of quasi - liquid water layer on the ice surface by the MS method can be a characteristic feature of the presence of «fresh» water on the red planet.

P3-19: Interaction of Electromagnetic *H*-waves with the thin Metal Film in the case of an Anisotropic Fermi Surface, Located on a Dielectric Substrate

D. N. Romanov
P. G. Demidov Yaroslavl State University, Yaroslavl 150003, Russia
E-mail addres: romanov.yar357@mail.ru

The calculation of the interaction of the electromagnetic *H*-wave with a thin metal film taking into account the ellipsoidal Fermi surface and the constancy of the free path of electrons in the case of different angles of incidence of the electromagnetic wave θ. One surface of the film is bordered by a medium with a dielectric permittivity ε_1 and has a mirror coefficient q_1, the other surface of the film is bordered by a medium with a dielectric permittivity ε_2 and has a mirror coefficient q_2. The behavior of reflection coefficients *R*, passage *T* and absorption *A* from the dimensionless effective mass is analyzed. The thickness of the layer is much less than the length of the incident electromagnetic wave, that is, the field inside the film is uniform. The thickness of the film is also less than the thickness of the skin layer, so the skin effect is not taken into account. Quantum effects are neglected. Similar calculations of optical coefficients in the case of a spherical Fermi surface and without taking into account the scattering mechanism were carried out in [1] for the H-wave and [2] for the E-wave.

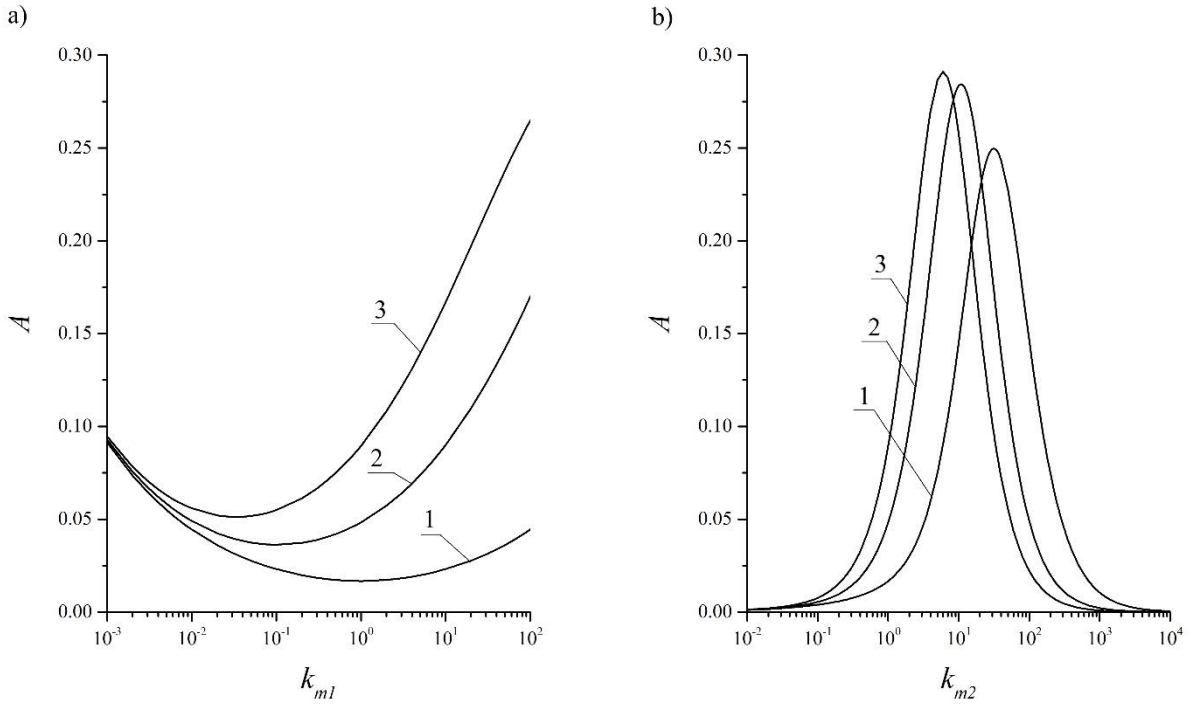

Figure 1. The dependence of the absorption coefficient on the dimensionless effective mass along the X axis (a) and along the Y axis (b). Curves 1 – $q_1=q_2=1$; 2 – $q_1=0.5$, $q_2=0.6$; 3 – $q_1=q_2=0$.

[1] A.I. Utkin, A.A. Yushkanov, "Interaction of Electromagnetic H-wave with the thin Metal Film is Located on the Dielectric Substrate", J. Phys. Chem. Solids., V. 16, № 2, pp. 253-256, 2015, doi 10.15330/pcss.16.2.253-256

[2] A.I. Utkin, A.A. Yushkanov, "The Effect of Specular Reflectances on the Interaction of an Electromagnetic E-wave with a thin Metal Film Placed between two Dielectric Media", Optics and spectroscopy, V. 124, № 2, pp. 247-251, 2018, doi 10.1134/S0030400X18020194

P3-20: Phase transitions on the internal interfaces

V. Sursaeva

Institute of Solid State Physics, Russian Academy of Sciences, Chernogolovka, Russia, sursaeva@issp.ac.ru

More and more attention has been paid to the problem of microstructure management with the help of grain boundaries themselves. Traditional modification of any microstructure is based on deformation and annealing after deformation. This significantly changes the microstructure. But there may be unconventional changes in the microstructure, based only on annealing, during which the microstructure changes due to the properties of the grain boundaries themselves. It is known the grain boundaries at certain temperatures are subjected to phase transitions. Grain boundary phase transitions of faceting-defaceting, coarsening of grain-boundary edges and phase transitions the transformation of the ordered structures in disordered boundary structure can be used to obtain the desired grain boundary structures and properties, as are the possibility of modifying the grain boundary properties not changing crystallogeometry.

The paper presents the results of an experimental study of the thermodynamic properties of grain boundaries with facets and edges by studying the movement of individual tilt $[11\bar{2}0]$ and $[10\bar{1}0]$ boundaries and in zinc [1,2]. Temperature values were determined experimentally:

1. phase transition of coarsening: appearance-disappearance of edges at moving grain boundaries;
2. phase transition of faceting-defaceting on moving grain boundaries;
3. phase transition of transformation of an ordered grain boundary structure in a disordered grain boundary structure.

Kinetic properties of the same boundaries before and after phase transformations on them are investigated. It was found that facets have high mobility. But "weighted" by grain boundary edges, they lose their individuality in the kinetic sense. Therefore, the properties of grain boundary edges affect the movement of the boundaries to a greater extent. An attempt is made to estimate the relative efficiency of the inhibitory effect of facets and grain boundary edges on the grain boundary movement.

Table. Braking performance by grain boundary facets and grain boundary edges.

The braking mechanism,	The braking parameter as a measure of the inhibitory influence of the facets and ridges	Values of the inhibitory effects of Λf facets and edges Λr	References
Grain boundary Facets	$\Lambda_f = \frac{m_f a}{m_b \ell}$	Λ_f= 1-9 при 395-405C	3
Grain boundary ridges	$\Lambda_r = \frac{\theta}{\cos\theta} = \frac{m_r a}{m_b}$	Λ_r= 1-3.6 при 395-405C	4

References

1. Sursaeva V.G., A. B. Straumal. **"**Thermodynamic and Kinetic Properties of Grain-Boundary Ridges on Tilt $[11\bar{2}0]$ Grain Boundaries in Zinc". Bulletin of the Russian Academy of Sciences: Physics, Vol. **82**, No. 9, pp. 1130–1135, 2018. .© Allerton Press, Inc., 2018. Original Russian Text © V.G. Sursaeva, A.B. Straumal, 2018, published in Izvestiya Rossiiskoi Akademii Nauk, Seriya Fizicheskaya, 2018, Vol. 82, No. 9, pp. 1244–1249. ISSN 1062-8738.

2. Сурсаева В.Г. "Термодинамические и кинетические свойства зернограничного ребра на границе наклона $[10\bar{1}0]$ в цинке." Деформация и разрушение материалов. **№ 3.** С. 14-19, 2018.

3.V. G. Sursaeva. S. I. Prokofiev «Faceting of a Moving Grain Boundary and Its Effect on the Kinetic Properties of Grain Boundaries» Bulletin of the Russian Academy of Sciences: Physics, **Vol. 81**, No. 11, pp. 1370–1374. 2017

4. Sursaeva Vera, Alena Gornakova, Faina Muktepavela Grain boundary ridges slow dawn grain boundary motion: In-situ observation. //Materials Letters 124 (2014) 24–27

Acknowledgment

P3-21: Phase transitions at grain boundaries as a cause of temperature hysteresis of grain boundary mobility and shape

V. Sursaeva

Institute of Solid State Physics, Russian Academy of Sciences, Chernogolovka, Russia, sursaeva@issp.ac.ru

A series of experimental studies has recently been devoted to the study of phase transitions at individual grain boundaries in metals. It is known that a phase transition from an unordered grain boundary structure to an ordered grain boundary structure is possible. When changing the structure of the grain boundary, its properties change, so the phase transition should affect the change of material properties. The exact value of the phase transition temperature can not be determined indirectly with high accuracy, since the properties show hysteresis in temperature at phase transitions. When studying the movement of grain boundaries, one can expect the manifestation of hysteresis both on the temperature dependence of mobility and on the temperature dependence of the shape of the moving grain boundary. The hysteresis of the grain boundary mobility and grain boundary hysteresis shape — ambiguous loop-like dependence of grain boundary mobility and shape on the reverse of the temperature, when a cyclic variation. Outside the hysteresis zone, which is limited by the upper and lower closing points of the hysteresis loop, there is a coincidence of the values of grain boundary mobility and shape from the reverse temperature. In [1,2] the experimental results of grain boundary mobility hysteresis and grain boundary shape manifestation in the study of individual boundary motion are presented.Fig.1 and Fig.2. It is assumed that the cause of hysteresis is the phase transformation of the ordered structure of the grain boundary into an unordered grain boundary structure. These papers present indirect evidence of the structural phase transition from the disordered to the ordered grain boundary structure by studying the shape change of the moving individual incoherent twin grain boundary Fig.2, as well as by studying the grain boundary mobility of individual special tilt $[11\bar{2}0]$ grain with angle misorientation 86°Fig.1.

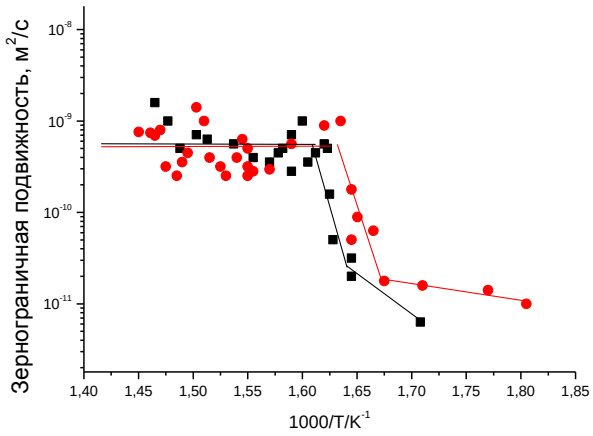

Fig.1. The temperature dependence of the grain boundary mobility of tilt boundaries $[11\bar{2}0]$ with angle of misorientation 86° [1]

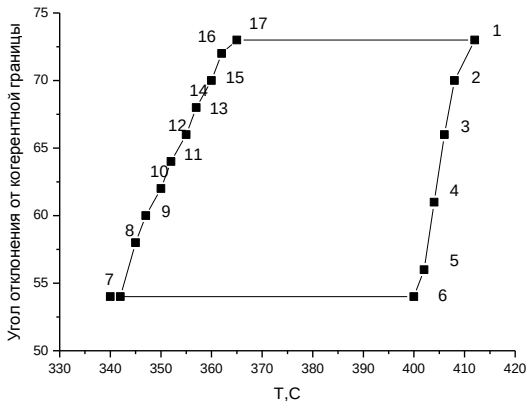

Fig.2. The temperature dependence of the angle between the position of the plane moving and stationary coherent twin boundaries. Twin width 70 μm [2]

References

1. Б.Б. Страумал, В.Г.Сурсаева, Л.С.Швиндлерман, Зависимость скорости безактивационного движения границы зерна от ориентации, ФММ, **49**, вып.5, стр. 1021-1026, 1980.
2. Sursaeva V.G. «Effect of faceting on twin grain boundary motion in zinc». Materials Letters **64,** pp. 105-107, 2010.

Acknowledgment

The research is carried out within the state task of ISSP RAS with the partial support of the RFBR (grant no. 19_03_00168).

P3-22: Sensitivity of the micromachined ring resonator to the point mass perturbation: experimental estimation

O.V. Morozov, I.V. Uvarov, D.E. Pukhov
Valiev Institute of Physics and Technology of Russian Academy of Sciences, Yaroslavl Branch, Yaroslavl, Russia, moleg1967@yandex.ru

Axisymmetric structures such as hemispherical shell, cylindrical shell and a ring has been widely used as the sensing elements of solid-state wave gyroscopes. One of the main advantages of the ring-type design is the suitability to miniaturization using low-cost MEMS production principles. A ring detects angular velocity Ω due to the degenerated pairs of the flexural vibration modes. One mode is located geometrically 45° apart from the other mode. In a perfectly formed ring these pairs have identical natural frequencies. The operation of the sensor is based on the excitation of the primary mode and measurement of the response at the secondary mode, which is directly proportional to Ω [1]. The second order primary mode with four nodes/antinodes is often used as a working mode.

In the micromachined ring resonators, fabrication tolerances lead to geometric distortions that perturb the dynamics of the modes. The imperfections of a ring cause a frequency split between the modes, thereby limiting the sensing accuracy. According to the simplified mass perturbation model for an unsupported ring, any configuration of masses can be represented as a point mass placed at the anti-node of the low frequency mode [2]. Frequency detuning may be eliminated by the removal of the correct amount of mass at this location. Theoretically, a relationship between the frequency detuning (a difference in the modal frequencies Δf) and the trimming mass (m_p) is a linear function. The aim of this work is to measure the resonator sensitivity parameter $rsp = \Delta f / V_p = \Delta f \, \rho_{Si} / m_p$ by mass trimming at the certain points of the ring. It is worth noting that *rsp* can be used for all resonators of a specific design, i.e., it is not necessary to measure this parameter for each sample.

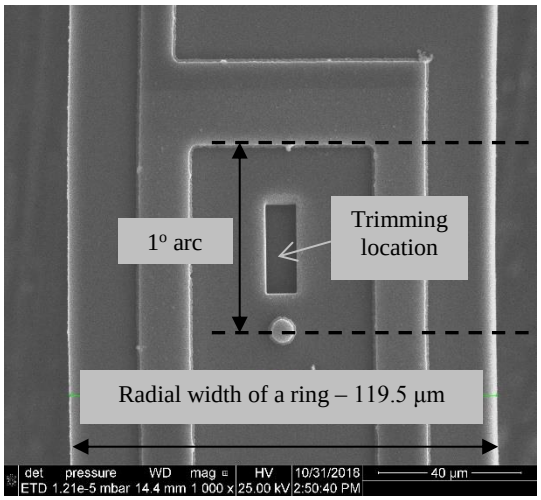

Fig 1. SEM image of the micromachined ring.

The vibration behavior of the micromachined ring resonator was described in our previous paper [3]. The location of anti-nodal axes and Δf were measured by laser vibrometer with the accuracy of ±1° arc and ±0.01 Hz, respectively. In this work, the trimming is performed by focused ion sputtering. An ion column with Ga liquid metal ion source integrated into the SEM Quanta 3D 200i is used as a sputtering tool. The removed point volume is the rectangular prism with dimensions of 25×10×6 mm^3 (Fig. 1). Four symmetrically arranged volumes are removed at each trimming round. For the rounds where the target points are placed near the anti-nodes in a range of ±1° arc, the measured $rsp = 4.34 \cdot 10^{-5}$ Hz/mm^3 is very close to the theoretical prediction ($3.78 \cdot 10^{-5}$ Hz/mm^3). Small error (±2° arc) in positioning of the removed volume on the next round significantly reduces the resonator sensitivity. The experiment confirms the suitability of our technique for the measurement of the anti-node locations. However, at some samples the frequency splitting cannot be reduced. In this case the imperfections of the real resonator cannot be described by the model for an unsupported ring. Probably, the stiffness perturbation of the support springs limits the possibilities of the mass trimming.

This work is supported by Program no. 0066-2019-0002 of the Ministry of Science and Higher Education of Russia for Valiev Institute of Physics and Technology of RAS and performed using the equipment of Facilities Sharing Centre "Diagnostics of Micro- and Nanostructures".

1. A.M. Shkel, "Type I and type II micromachined vibratory gyroscopes", Proc. IEEE/ION Position, Location, And Navigation Symposium, pp.586-593, 2006

2. B.J. Gallacher et.al., "Multimodal tuning of a vibrating ring using laser ablation", Proc. Institution of Mechanical Engineers, Part C: Journal of Mechanical Engineering Science, 217, pp.557-576, 2003

3. O.V. Morozov and I.V. Uvarov, "Determination of vibration axes of the micromachined ring resonator for the modal tuning purposes", Proc. SPIE, 11022, 110220W, 2019

P3-23: Laser interference reflectometry as a method for monitoring DRIE of silicon: useful features of the measurement signal

O.V. Morozov
Valiev Institute of Physics and Technology of Russian Academy of Sciences, Yaroslavl Branch, Yaroslavl, Russia, moleg1967@yandex.ru

Deep reactive ion etching (DRIE) of silicon is key step in MEMS and 3D-IC technologies. DRIE processes provide wide possibilities for creation of high aspect ratio (HAR) structures. The time multiplexed deep etching (TMDE) technique of DRIE, which alternates etching and passivation cycles, is very popular due to high etching rate and high selectivity combined with good anisotropy. Alternating processes of passivation (deposition of a sidewall protecting layer) and etching lead to a sidewall roughness as "scallops". Various applications require a well-defined etch profile of HAR trenches [1]. Details of the profile (depth, a sloped sidewall angle and sidewall scalloping, bottom curvature) need to be monitored to ensure acceptable results.
Laser interference reflectometry (LIR) is successfully used as the end-point detection method in DRIE process [2]. Determination of the trench depth is based on the interference between the waves reflected from the mask and the silicon to be etched. The resultant reflection oscillates during the etching, and the depth of each cycle can be found from the wavelength of the laser. The total depth is found from the sum of the fringes into the measurement trace. This method is extremely useful since it allows following the etching process in real time, and the influence of the TMDE parameters on the etch rate can be determined. This work demonstrates the new ability of the etch profile monitoring using LIR, which is based on the feature of the measurement signal.
Experiments were performed using a laser interferometry tool (λ = 633 nm) with a single-beam scheme from Sofie Instruments. The intensity of the beam reflected from a trench array with a width of 3 μm and a period of 6 μm was registered directly in the TMDE process. The sampling area on the silicon wafer with a chromium mask was about 2 mm. In these conditions the amplitude of the signal depends only on the reflectivity of the trench bottom surface.
Several HAR etch recipes were used. They provide various profiles of the trench sidewalls: from tapered to reentrant. The measurement signal is consistent with the calculation based on the simple description of the two-wave interference assuming that only one beam changes its intensity. Basically, the trench bottom surface becomes less reflective due to the increasing aspect ratio and surface roughness. A situation is exacerbated by the rounding of the bottom section of the narrow trenches. As a result, the amplitude of the interference fringes reduces as the trenches deepen. This effect limits the depth at which the process can be monitored. The deeper trenches may be tracked if the TMDE recipe gives a reentrant profile. SEM images of the cross-section show that the bottom curvature is the smallest in these conditions. A surprising amplitude modulation of measurement signal is also observed. Two diffraction effects are considered as the possible reason of this modulation. The first is the Fresnel diffraction (near field), which explains the similar behavior of a part of the signal with any recipe. The second is the diffraction effect of a sidewall as a grating of the *echelle* type. It explains the correlation between the sidewall angle and the modulation period. Both effects change the reflectivity of the rounded bottom, which depends on the etch profile. Thus, the monitoring of silicon processing directly in TMDE is useful for detection of earlier process deviation, as well as for development of reliable etching recipes.
This work is supported by Program no. 0066-2019-0002 of the Ministry of Science and Higher Education of Russia for Valiev Institute of Physics and Technology of RAS and performed using the equipment of Facilities Sharing Centre "Diagnostics of Micro- and Nanostructures".

1. Banqiu Wu, Ajay Kumar, Sharma Pamarthy, "High aspect ratio silicon etch: A review", J. Appl. Phys., 108, 051101, pp.1-20, 2010
2. Thomas D., "Maximizing power device yield with in situ trench depth measurement", Solid State Technology, April, pp. 48-50, 2007

Р3-24: Разложения воды на поверхности нано-Al_2O_3 под действием γ-излучения

Т.Н.Агаев, С.З.Меликова, С.М.Алиев, Г.Т.Иманова, И.А.Фарадж-заде, В.С.Мирзоев, К.В.Абдуллаева, Э.Р.Велиев, А.М.Алескеров

Институт Радиационных Проблем НАН Азербайджана, Баку, Азербайджан, e-mail:sevinc.m@rambler.ru

Широкое применение нано-оксида алюминия в катализе, а также в радиационной технологии обусловлено наличием у него ярко выраженных кислотно-основных свойств, высокой удельной поверхностью и механической прочностью. Значительная роль в формировании каталитически активных центров в нано-Al_2O_3 принадлежит электроноакцепторным центрам – координационно-ненасыщенным ионам к.н. Al^{3+}. Содержание электроноакцепторных центров в составе нано-оксида алюминия зависит в основном от условий предварительной обработки и различных полиморфных форм. Поэтому одним из путей получения информации о влиянии электроноакцепторных центров в процессе радиационно-каталитического разложения воды является исследование влияние различных полиморфных форм нано-Al_2O_3 на радиационно-каталитическую активность.

Исследована кинетика накопления молекулярного водорода при радиационно-каталитическом разложении воды в присутствии различных полиморфных форм нано-оксида алюминия при различных степенях заполнения поверхности при Т=300К. На основе линейной, кинетической области определено значение скоростей и радиационно-химического выхода молекулярного водорода $G(H_2)$, которые равны 0,9; 1,06 и 1,75 молекул/100эВ соответственно для α-, δ- и γ-Al_2O_3. Разложение воды при Т=300К под действием γ-излучений в присутствии различных полиморфных нано-Al_2O_3 происходит в результате радиационно-каталитического действия нано-оксида алюминия. Радиационно-каталитическое действия нано-Al_2O_3 в процессе разложения воды объясняется передачей дополнительной энергии от катализатора к веществу, подвергающемуся радиолизу, который необходимо наличие сильной адсорбционной связи с поверхностью. Молекула воды является электронодонорной, такая форма адсорбции происходит на сильном центре Al^{3+} (A_S) с образованием поверхностный адсорбционной комплекс (A-H_2O_S):

$$A_S + H_2O \rightarrow A - H_2O_S$$

который является предшественником радиационно-каталитических процессов разложения воды на поверхности нано-Al_2O_3.

Как уже мы отметили, что среди исследованных полиморфных форм нано-Al_2O_3 относительно высокой радиационно-каталитической активностью в процессе разложения воды обладает нано-γ-Al_2O_3. Учитывая этого и влияние температуры на радиационно-каталитическую активность и радиолитических процессов разложения воды при различных температурах проведено на примере нано-γ-Al_2O_3. Исследована кинетика накопления молекулярного водорода при различных температурах (Т=573÷673К) и плотности паров воды (ρ_{H2O}=0,1÷20 мГ/см^3). При этом установлено, что начиная с Т=623К нано-Al_2O_3 обладает термокаталитической активностью в процессе разложения воды и выявлено, что радиационно-каталитическая активность нано-Al_2O_3 растет с температурной в области Т=573÷673К и при Т=673К и ρ_{H2O}=15мГ/см^3 достигает своего значение $G_{общ.}(H_2)$=8,6 молекул/100эВ.

Кроме того исследовано влияние полиморфных форм нано-Al_2O_3 на радиационно-термокаталитическую активность при Т=773К и ρ_{H2O}=10 мГ/см^3. На основе кинетических кривых определены значения скоростей процессов и радиационно-химические выходы молекулярного водорода $G_{общ.}(H_2)$. Значения $G_{общ.}(H_2)$ для α-, и δ- являются одинаковыми и равны $G_{общ.}(H_2)$=7,05 молекул/100эВ, а для γ-Al_2O_3 значение $G_{общ.}(H_2)$=12,4 молекул/100эВ. Это еще раз доказывает, что сравнение скоростей процессов разложения на поверхности полиморфных форм нано-Al_2O_3 растет в ряду α-Al_2O_3, δ-Al_2O_3 и γ-Al_2O_3.

РЗ-25: Получение тонких пленок сплавов кремния

Б.А. Наджафов[1], Х.Ш. Абдуллаев[2], Ф.П. Абасов[1]

[1]Институт Радиационных Проблем НАН Азербайджана
Баку 1143, ул.Б.Вагабзаде 9. [2]Бакинский Государственный Университет
Баку, ул.З.Халилова 23.

Исследованы различные параметры пленок аморфного и нано кристаллического сплава кремния – углерода (а-нк-$Si_{1-x}C_x$:H (x=0-1)) легированного фосфором (PH_3) и бором (B_2H_6). Изучены свойства этих пленок, полученных методом магнетронного распыления на различных подложках из кварца, стекла и кремния с покрытием Fe, Al, Pd, Ni, Ti, Ag,. Наблюдена морфология полученных нано трубок при помощи просвечивающей электронной микроскопии (ПЭМ). Также изучены структурные свойства пленок с помощью инфракрасной спектроскопии и дифракции рентген излучения.
Пленки гидрогенизированного аморфного и нано кристаллического сплава кремния-углерода (*а*-нк-$Si_{1-x}C_x$:H (x=0÷1)) по сравнению с плёнками аморфного кремния и германия имеют большую ширину запрещенной зоны и лучшие оптоэлектронные свойства в видимой части спектра, а также являются терме динамически более стабильными и радиационно-стойкими . Эти свойства позволяют использовать их в ряде направлений нано и микроэлектроники, а также для создания солнечных элементов [1-2].

В работе рассмотрены некоторые параметры тонких пленок аморфного и нано кристаллического кремния – углерода а-нк-($Si_{1-x}C_x$:H, (x=0÷1)) и механизм легирования данной пленки фосфором (PH_3) и бором (B_2H_6). Методом просвечивающей электронной микроскопии (ПЭМ) изучена морфология полученных нано трубок, длина которых в зависимости от условий осаждения, составляет 1÷4 мкм. Структурные свойства пленок анализировались методом ИК спектроскопии и методом рентгеновской дифракции (РД). Замечено, что в зависимости от условий получения пленки, происходит такое изменение параметров, которое характерно для нано кристаллических тонких пленок. Поскольку Al и Ag имеют небольшие диффузионные барьеры и обладают плохим смачиванием поверхности с одностеночными углеродными нанотрубками (ОСУНТ), то они стремятся к агрегации и образованию больших кластеров. С другой стороны, энергия связи между Fe и (ОСУНТ) велика, но из-за большой энергии коррозии и плохого смачивания Fe может образовывать изолированные кластеры. Отметим, что ОСУНТ получается с использованием газовой смеси CH_4 и Ar. Струя ВЧ-микроплазмы генерируется при атмосферном давлении с помощью однотрубчатого электрода и направляется на подложку к-Si покрытой пленкой Fe. Изменяя параметры синтеза в широком диапазоне (внутреннего диаметра сопла электрода, скорости потока метана и температуры подложки), получены такие углеродные микроструктуры, как алмазные частицы, углеродные нанопроволоки, углеродные нанотрубки и конусообразные микрочастицы Si.
Также изучено влияние условий роста, скорости потока метана и типа подложки на распределение структур и свойства двухстеночных углеродных нанотрубок (ДУН). При скорости потока 600 $см^3$/мин. получаются ДУН с преимущественно полупроводниковыми свойствами. При более высокой скорости потока (700 $см^3$/мин) образуются смесь одностенных и двустенных нанотрубок, большинство из которых являются полупроводниковыми. При более низких скоростях (300÷500 $см^3$/мин) преобладают металлические многостенные углеродные нанотрубки. Длина полученных нанотрубок составляет 1÷4 мкм.

1. Получение пленок *а*-$Si_{1-x}Ge_x$:H, изменение ее параметров от состава. // ISIAEE Solar Energy, 2006, № 4, (36), p. 51-55
2. Оптические и электрические свойства аморфных пленок a-$Si_{1-x}C_x$:H films. // Неорганические Материалы, 2010, №,6, т. 46, с. 624-630.

P3-26: SIMS investigations of fundamental properties of clusters

S.E.Maksimov[1,2], Kh.B.Ashurov[1], N.Kh.Dzhemilev[1], S.F.Kovalenko[1], O.F.Tukfatullin[1], Sh.T.Khojiev[1]

[1]Arifov Institute of ion-plasma and laser technologies, Academy of Sciences of the Republic of Uzbekistan;
[2]Institute of Polymer Chemistry and Physics, Academy of Sciences of the Republic of Uzbekistan;
maksimov_s@yahoo.com

One of the most important problems of modern nanotechnologies is the development of the method of production of clusters and nanoparticles having various sizes and stoichiometric composition. Ion sputtering has several advantages over other ways of cluster generation, allowing by selection of the types of bombarding ions and bombarded target material to create the clusters that are difficult to synthesize by other methods. From practical point of view, cluster ion beams are very important in applications of modern secondary ion mass spectrometry (SIMS) [1]. We developed the complex SIMS method of generation of cluster ions and the investigation of their fundamental properties in framework of the same single experiment. This method is based on the study of the processes of the unimolecular fragmentation of sputtered clusters. The investigations are performed on the secondary ion mass spectrometer with reverse geometry [2]. Clusters are generated under ion sputtering of the surfaces of metals, semiconductors or chemical compounds, or (in the case of oxide clusters) under bombardment of surfaces with blowing by O_2. Our type of device [2] has the regions before and after magnet analyzer («field-free zones») where direct observations of the cluster decay processes are possible. A part of the cluster vibrational energy released as a result of decay and converted into translational energy of the fragments. Using the Klots' "evaporation ensemble" model [3], we estimated the dissociation energies E_d of sputtered clusters on the base of the measured energy spectra of fragment ions. The kinetic energies of fragment ions have been measured in the second field-free zone of the mass spectrometer [2] in time range 10^{-5} -10^{-4} s after emission and translated from the laboratory system of coordinates into the center-of-mass system (Kinetic Energy Release (KER) distributions). For the model [3] the KER-distribution is described by the expression:

$$dN/dE \propto E^{l}\cdot\exp[-E/k_bT^{+}], \quad (1)$$

where k_b is the Boltzman constant, parameter l varies from 0 to 1, T^+ is the temperature of an excited cluster, corresponding to the specific energy (to the degrees of freedom). In the frameworks of the theory [3] the dissociation energy E_d can be found basing on the KER-distributions measured in experiments:

$$E_d(T^{+}) = [\gamma(n)k_bT^{+}]/\{1-[\gamma(n)/(2C(n)]+ [\gamma(n)/C(n)]^2/12+\ldots\}, \quad (2)$$

where $\gamma(n)$ is the Gspann parameter [3], n is the number of particles in cluster, $C(n)= 3n-1$ is the thermal capacity of a cluster in the units of the Boltzman constant. The method of estimation of the average rate constant k of clusters' decays is based on the comparison of the numbers of decays in the times Δt_1 and Δt_2 of the flight of clusters through the field-free zones of mass spectrometer [2], where decays occur on timescales of 10^{-6} - 10^{-5} c and 10^{-5}-10^{-4} c after emission, respectively. The numbers ΔN_1 and ΔN_2 of clusters fragmenting in both zones are proportional to the initial numbers N_1 and N_2 of the ions entering in these areas. Decay law:

$$\mathbf{N = N_0 \exp(-k\Delta t),} \quad \mathbf{(3)}$$

where k is the decay rate constant, N is the number of metastable ions having no decays after the time Δt, N_0 is the initial number of metastable ions. After determination of ΔN_1 and ΔN_2 for both zones, the average decay rate constant can be found from their relationship:

$$\mathbf{\Delta N_1/\Delta N_2 = \exp k(t_2-t_1)[1- \exp(-k\Delta t_1)]/[1- \exp(-k\Delta t_2)],} \quad \mathbf{(4)}$$

where t_1 and t_2 are the times before the entering in the respective zones, determined by the geometry of the device. Determining the dissociation energies E_d of clusters from (2) and their average decay rate constants k from (4), we estimate the average excitation energies of clusters by RRK theory [4]. The obtained results allow to make a conclusions about the large abilities of SIMS for the study of basic properties of clusters.

1. *Cluster Secondary Ion Mass Spectrometry: Principles and Applications*, edited by Ch.M. Mahoney. John Wiley & Sons Inc., 2013.

2. A.D. Bekkerman, N.Kh. Dzhemilev, V.M. Rotstein, "Ion Microprobe for Studying Cluster Ion Decay Reactions", Surf. Interf. Anal., 15, pp.587-590, 1990.

3. C.E. Klots, "The Evaporative Ensemle", Z.Phys.D, 5, pp.83-99, 1987; "Kinetics methods for quatifying magic", *ibid.*, 21, pp.335-342, 1991.

4. P.J. Robinson, K.A. Holbrook. *Unimolecular Reactions*. Wiley-Interscience, London, 1972.

P3-27: Template synthesis of the SERS-active substrates

E. Kozhina[1], N.Nechaeva[2], S. Podoinitsyn[2], I. Doludenko[3] , S.Bedin[1,3], V. Kanevsky[3]

1. Moscow state pedagogical university, Moscow, Russia, Liza.kozhina.99@mail.ru.

2. Institute for Biochemical Physics, Moscow, Russia.

3. FSRC "Crystallography and Photonics" RAS, Moscow, Russia, bserg5@gmail.com

Modern technologies often require the instruments for sensing on single molecule (SM) level. It can be realized by detection of fluorescence or Raman scattering signal. Latter has a principal advantage of SM fingerprint chemical analysis, but it is very complicated for experimental realization in usual condition due to extremely weak signal in comparison with fluorescence. To obtain increased Raman spectra (SERS), it is possible to use colloidal solutions consisted of particles of noble metals or use the specially prepared surfaces with plasmon structures on it. Most of the currently known SERS substrates are synthesized of silicon by electron beam deposition, subsequently coated by silver, but one of the disadvantages of this method is poor adhesion of thin films to the substrate due to the low energy of the deposited particles, as well as the complexity of synthesizing and high cost of production. Substrates, obtained by the method of template synthesis, are devoided these disadvantages. Due to the peculiarities of the technology of syntheses, it is possible to obtain substrates of a large area of a given geometry, adjusting the plasmon resonance to the desired experimental range.

In this work, metallic NWs were obtained by the matrix (template) synthesis method in the pores of the track membranes. Polymer films with a thickness of 12 μm and a pore diameter of 100 nm with a surface density of 1,2 $*10^9$ cm^{-2}, respectively, were used as the starting material. Previous to, one of the sides of the sample were covered by silver by spaying in order to obtain the conductive layer. The next step was to fill the pores of the membranes by the copper by the electrochemical deposition. To do that membrane with one side covered by silver was put down in the electrochemical cell as a cathode. The electrolyte used was a commercial electrolyte of the company KLIO and iodide electrolyte. At the end of the electrochemical deposition, the polymer matrix was removed by dissolving in a concentrated alkali solution 25% NaOH (fig.1a).

Further, SERS spectra of the testing substance were obtained on the resulting copper substrates with silver NWs using the BAC151 of the B&WTek company with the instrumental box i-Raman Plus. 4-mercapto-phenylboronic acid (4MPBA) in various concentrations was used as a test substance. Spectra were obtained for two sources of exciting radiation operating at a wavelength of 532 and 785 nm. Examples of spectra are presented in Fig. 1b.

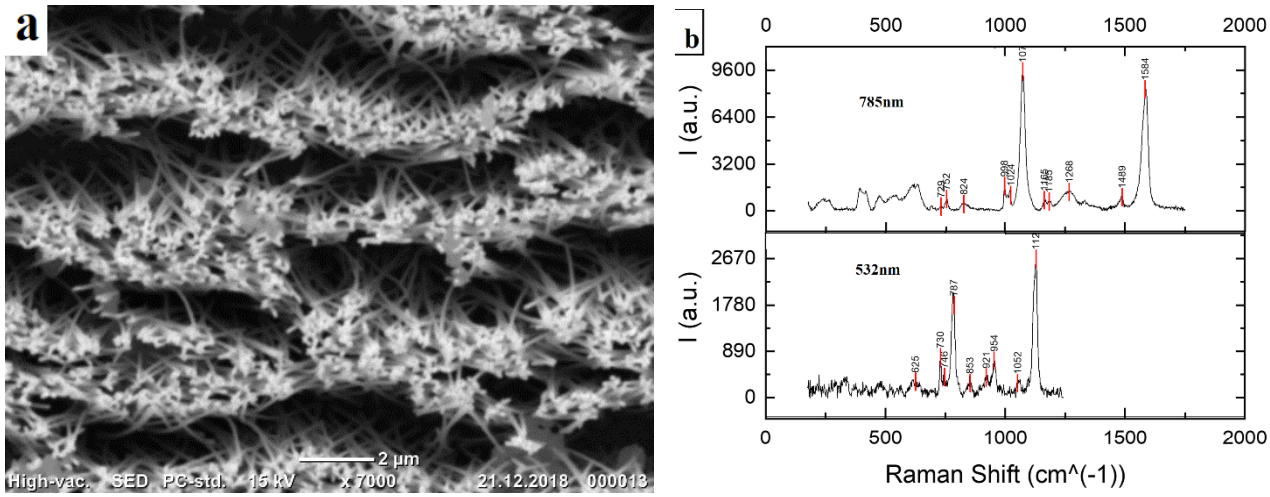

Fig. 1. SEM image of silver NWs(a) and SERS spectra of 4MPBA (b).

Acknowledgment

The work was supported by the Ministry of Science and Higher Education and of the Russian Federation (project 3.7990.2017/8.9) and RFBR according to the research project №16-29-11763.

P3-28: Quartz glass simulation in a lamp-based chamber under a semiconductor heat treatment process

Ovcharov V.V., Kurenya A.L., Prigara V.P.
Valiev Institute of Physics and Technology of RAS, Yaroslavl Branch, E-mail: ovcharov.vlad@gmail.com

Generally, the effect of quartz glass on the heat transfer between a semiconductor wafer and lamp-based chamber elements is evaluated by the restriction of the spectral interval of the radiation incident on a working semiconductor wafer. The restriction corresponds to a spectral window of quartz glass transmission which ranges to 3, 5 mkm [1]. However, in addition to the radiation transmission inside the restricted spectral interval, different brands of real quartz materials have more complex optical properties.

The problem of the description of the radiation heat transfer applied to a system composed of a semitransparent film between two opaque plates was analytically solved in [2]. With an integral assumption, a combined heat transfer has been derived for the closed radiative system [3]. The system included four wafers, two of which were opaque plates with emissivity $\varepsilon_1(T_1)$ and $\varepsilon_2(T_2)$ and modeled a heater and an absorber of lamp-based chamber, and the other two were semitransparent wafers and modeled the quartz glass screen and the working wafer of silicon with emissivity $\varepsilon_q(T_q), \varepsilon_f(T_f)$ and transmissivity $\tau_q(T_q)$, $\tau_f(T_f)$, here T_1, T_q, T_f, T_2 are temperatures of the elements of the system: the heater, the quartz screen, the working plate and the absorber, correspondingly.

The goal of the present work is to consider the heat transfer in spectral approximation for the described heat transfer system. Optical properties of the screen correspond to quartz glass of brand QI by thickness of 5 mm.

The set of equations for the spectral calculation is obtained on the basis of the integral solution of the heat balance equations [3]:

$$\begin{cases} q_{in}(\lambda, T_1, T_q) = q_{out}(\lambda, T_q, T_f) + q_{out}(\lambda, T_q, T_2) + q_{out}(T_q, T_g) \\ q_{in}(\lambda, T_1, T_f) + q_{in}(\lambda, T_q, T_f) = q_{out}(\lambda, T_f, T_2) + q_{out}(T_f, T_2) \end{cases}, \quad (1)$$

where q_{in}, q_{out} are input and exhaust heat fluxes (the index at the first temperature indicates the plate from which the flow enters, the index at the second temperature indicates the plate to which the radiation flux falls), λ is wavelength.

According to the results of the work, an estimate is made of the deviation between the calculation results in the integral and spectral approximations under the same conditions in the thermal system. The obtained results are compared with the results where the cutoff wavelength for the quartz window is taken to be 3,5 mkm. Also, spectral approximation is used to verify the presence of induced bistability effect into quartz glass screen under semiconductor heat treatment process in a lamp-based chamber.

1. R.Singh,"Rapid isothermal processing", Appl.Phys.Lett. **63**, pp.R59-R114, 1988.
2. J.Zeegers, and H.A.L.van Dijk, "A note on the net radiation method applied to a system composed of a semitransparent film between two glazings", Sol. Energy Mater. and Sol. cells, **33**, pp.23-30,1994.
3. V.Prigara and V.Ovcharov, " Induced bistability into quartz glass by silicon wafer heat treatment in lamp-based reactor," *Int.Cond. on micro- and nano-Electronics*, ed. by Lukichev, Rudenko K.V., Proc. of SPIE Vol.11022, 110221U ,2018.

P3-29: Rapid thermal annealing of DLC films on diamond

A. Okhapkin, P. Yunin, M. Drozdov, S. Kraev, E. Arkhipova, V. Shashkin

Institute for Physics of Microstructures, Russian Academy of Sciences, Nizhny Novgorod, Russia,
poa89@ipmras.ru

DLC (diamond-like carbon) is an amorphous carbon phase containing diamond (sp^3) and graphite-like (sp^2) chemical bonds. Active development of diamond electronics arises an interest of using DLC films deposited on semiconducting diamond as insulating and passivating layers. At the same time, the possibility of using ultrathin intermediate layers of DLC in the formation of ohmic contacts to polycrystalline diamond was also shown [1]. An interesting feature of DLC films is that their conductivity can be controlled by external factors — conditions of deposition, annealing, and even bias [2]. This paper is devoted to the study of impact of rapid thermal annealing on the structural and electrophysical properties of DLC films deposited on diamond and silicon from methane using the PECVD method. Rapid thermal annealing (RTA) in argon for 2 minutes below 700°C of DLC films deposited on diamond, didn't lead to significant changes in the properties of the films. This was confirmed by the secondary-ion mass-spectrometry (SIMS) (Fig. 1a), x-ray reflectometry, electron microscopy and atomic force microscopy. An increase of the annealing temperature above 700°C using the same annealing times, led to a drastic changes of the structural and electrophysical properties of the films. According to the SIMS data [3], the fraction of the graphite-like phase increased, which was accompanied by the inversion of the CsC_4 and CsC_8 lines in the mass spectra. The beginning of graphitization was also accompanied by an increase of the thickness (by 9%) and a decrease of the density (by 11%) of the films, which is explained by a larger interatomic distance and a lower density of graphite compared to diamond. At the same time, the DLC/diamond interface didn't not degrade after annealing, which is important for the practical application of the DLC films deposited on diamond.

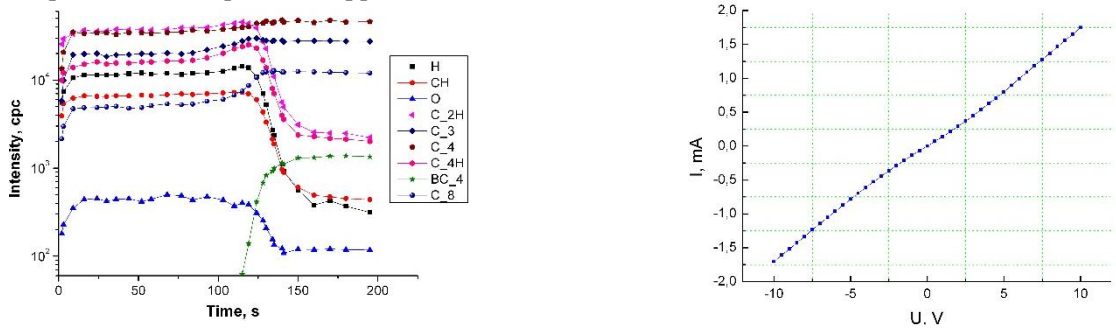

a b

Fig. 1. a – SIMS depth profile of 28 nm thick DLC film deposited on diamond after 700°C RTA; b – I–V curve of 72 nm DLC film deposited on diamond after 900°C RTA.

Also, as a result of RTA, the conductivity of the films changes significantly. The resistivity of films deposited on a single crystal diamond after annealing (900°C) was equal to 4.2 kΩ/□. (Fig. 1b). In this case, the DLC contact resistance measured by the TLM method was $4.7 \cdot 10^{-3}$ Ω·cm^2. Thus, the results of experiments show that as-deposited DLC films can serve as insulating and passivating layers for diamond, while annealed films can be used for the formation of contact layers to diamond. The work was supported by Russian Federation President grant МК-3450.2019.2 and RFBR grant (project 18-02-00565) in the part of the development of SIMS metrology. The research was carried out using the equipment of «Physics and technology of micro- and nanostructures» Center at IPM RAS.

1. A. Galbiati, S Lynn, K. Oliver et. al., "Performance of Monocrystalline Diamond Radiation Detectors Fabricated Using TiW, Cr/Au and a Novel Ohmic DLC/Pt/Au Electrical Contact", IEEE Trans. On Nuc. Sci., **56**, pp.1863-1874, 2009.
2. A.S. Vedeneev, V.A. Luzanov and V.V. Rylkov, "Effects of Monopolar Resistive Switching in Thin Diamond-Like Carbon Layers", JETP Letters, **109**, pp 171-174, 2019.
3. M.N. Drozdov, Y.N. Drozdov, A.I. Okhapkin, et. al. "A New Approach to TOF-SIMS Analysis of the Phase Composition of Carbon-Containing Materials", Technical Physics Letters, **45**, pp 48-52, 2019.

P3-30: SIMS study of the surface layer of silicon, irradiated by gallium ion beam

E. Kozlov[1], D. Pukhov[2], A. Rudy[2], S. Simakin[2]

[1] *P.G. Demidov Yaroslavl State University, Yaroslavl, Russia, E-mail address: eakf@yandex.ru*

[2] *Valiev Institute of Physics and Technology of Russian Academy of Sciences, Yaroslavl Branch , Yaroslavl, Russia*

Surface irradiation by focused gallium ion beams, which was previously used to prepare samples for transmission electron microscopy, is now widely used to analyze the failure of integrated circuits and the formation of nanostructures on the surface of semiconductors. The process of surface sputtering by such beams, featuring the modification of the surface layer by implanted gallium, the redeposition of the sputtered material on the walls of craters with a high aspect ratio, is yet insufficiently studied experimentally. The study of the silicon surface composition irradiated by a gallium beam at various radiation doses and angles of incidence of the ion beam was the goal of this investigation.

The sputtering of silicon samples (KDB (100)) was carried out with a 30-keV Ga^+ ion beam at the QUANTA 3D set up. Rasters with the size of 200x200 μm^2 with radiation doses of 10^{15}, 10^{16}, 10^{17} and 5×10^{17} ions / cm^2 at normal incidence and angles of incidence 0, 30, 45, 60 and 80˚ with an irradiation dose of 5×10^{17} ions /cm^2 were prepared for a SIMS analysis.

Layer-by-layer analysis was performed on a TOF.SIMS[5] installation with a time-of-flight mass analyzer in the registration mode of positive secondary ions. 25 keV Bi_3^+ ions were used as an ion probe. The sputtering of the sample surface during depth profiling was carried out with Cs^+ ions with energy of 1 keV. The area of sputtering beam was 250×250 μm^2. The size of the collection area of secondary ions, was 50×50 μm^2. The concentrations of gallium and silicon in at/cm^3 were obtained after normalization of the intensities of the secondary ions $CsGa^+$ and $CsSi^+$ by the intensity of the reference signal of the ions Cs^+ by multiplying by the coefficient of relative sensitivity. The depth scale of the profiles was transformed from the time scale using the sputtering rate, which was 0.3015 nm/sec under the given analysis conditions.

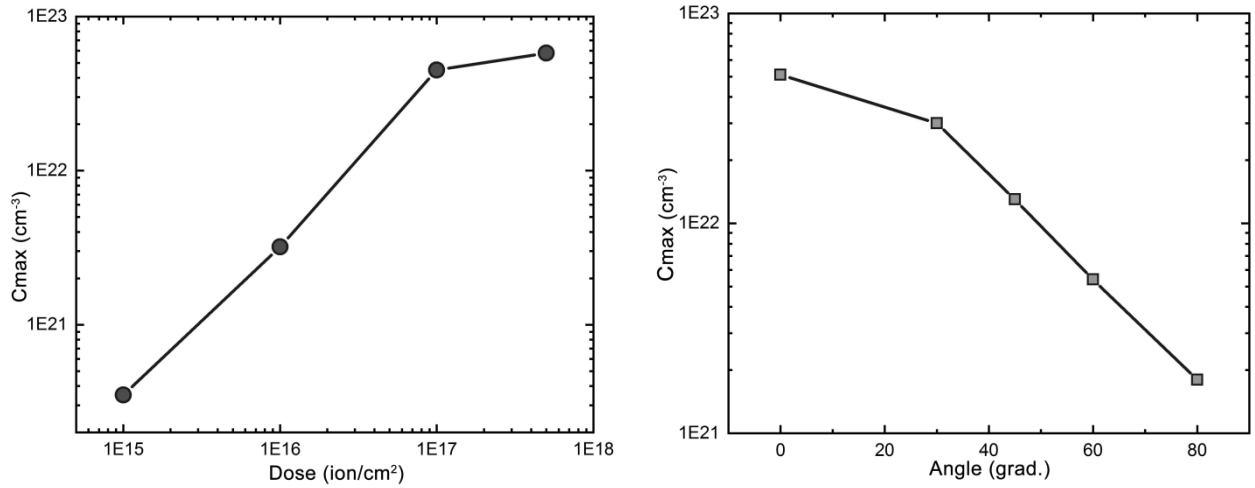

The dependences of the maximum gallium concentration as a function of the radiation dose (left) and the angle of incidence of the ion beam (right) obtained after processing the distribution profiles of silicon and gallium in the surface layer are presented in figure.

The investigation was supported by the Program (№ 0066-2019-0003) of the Ministry of Science and Higher Education of Russia for Yaroslavl Branch of K.A. Valiev Institute of Physics and Technology of RAS and was carried on the equipment of the Facilities Sharing Center “Micro- and Nanostructures Diagnostics”.

THE POSSIBILITY TO USE TRACK MEMBRANES TO CREATE A STABLE METALLIZED COATING OF POLYMER FILM

N. Kovalets, I. Razumovskaya, A. Mironova, S. Bedin
Moscow state pedagogical university, Moscow, Russia, zabalueva_1991@mail.ru

The creation of a metallic coating with high adhesion to the polymer substrate is a promising and rather complicated technological process. In this work, it was supposed to increase the strength of attachment of the metal coating on a polyethylene terephthalate (PET) polymer film in the form of a track etched membrane (TM) by partially filling the pores with TM metal. In this case, the metal in the pores, presumably, serves as the points of attachment of the metal surface film. Silver was selectored as the metallic coating, since it is used for highly reflective surfaces in deep space, in the absence of oxygen. In the work were used TM-based PET with a thickness of 12 μm, manufactured in the Laboratory of Nuclear Reactions. G.N. Flerov JINR (Dubna), with a system of pores perpendicular to the surface. Two TM series were investigated: with a pore density of $1.2 \cdot 10^7$ cm^{-2} and a pore diameter of 0.3 μm (the first series) and with a pore density of $4.41\ 10^7$ cm^{-2} and a diameter of 0.058 μm (the second series). To obtain a metallic coating, initially, a conductive silver layer was applied on one of the TM sides by vacuum deposition: for Series 1 - the layer thickness was 50, 100, and 200 nm, for Series 2 - 50 and 100 nm. Then the pores of the TM were filled by copper with the same electrochemical method, by which we previously obtained polymer/metal composites [1,2]. A potential field regime was used at a voltage of 300 mV and a duration of 360 s (series 1) or 200 s (series 2). The deposition time in both cases was chosen so that the pores filling depth was about 5 μm. The process stopped until the pores were all filled, because the purpose was to create a sufficiently "rooted" metal surface, but without the extraneous technological losses of metal and electricity.

The received metallized films stretched by manual testing device before fracture. The resistance of coating to tensile strain was investigated by the observation it cracking in optical and electron microscopes. For the both series of samples the cracking of the TM coating is accompanied by the formation of cracks system, the appearance of local diamond-shaped exfoliations and peculiar elongated peeling-defects. The breaking deformation $\boldsymbol{\varepsilon}_{fr}$ of metallized TM and deformation ε_{cr} at which cracks appear (so metallized surface functional behaviors are destroyed) were compared (Table 1). It was detected, that the points of «strengthening» the covering to filled by copper pores are originality defects. For the second series of samples the average distance among pores is less its 5 diameters, so the elastic stresses fields interaction is absence [3], what makes the picture of metal surface cracking somewhat simpler. Thus, preliminary consideration, that for obtaining a sufficiently durable metallic coating based on TM is prospective a decrease in coating thickness and pore sizes with an increase in their density was confirmed.

Table 1. Dependence of strain at which surface cracks appear and tensile strain for different series of samples.

	Series 1						Series 2			
	Coating 50 nm		Coating 100 nm		Coating 200 nm		Coating 50 nm		Coating 100 nm	
ε_{cr}, %	7	±3	3	±1	4	±1	9	±1	5	±1,5
ε_{fr}, %	38	±6	47	±16	62	±15	70	±18	71	±14

REFERENCES

1. V. N. Gumirova, G. S. Abdurashidova, S. A. Bedin, N. P. Zabalueva (Kovalets), M. A. Kuvaitseva, I. V. Razumovskaya, «Specific features of the fracture of track membranes and related polymer/metal composites prepared by template synthesis», Physics of the Solid State, Volume 57, N 2, P. 344–348, 2015
2. N. P. Kovalets, I. V. Razumovskaya, A.S. Kechekyan, S. A. Bedin, «The strength of the polymer/metal composites based on track membranes for different orientation pores system», № 4, P. 20-23, 2018
3. L. D. Landau and E. M. Livshitz, Course of Theoretical Physics, Vol. 7: Theory of Elasticity (Nauka, Moscow, 2001; Butterworth–Heinemann, Oxford, 2002).

Acknowledgement
The work was supported by the Ministry of Science and Higher Education and of the Russian Federation (project 3.7990.2017/8.9)